UNIVERSIDAD DE DEUSTO

PEDESTRIAN NAVIGATION USING WRIST-WORN INERTIAL SENSORS

by

Luis Enrique Díez Blanco

A dissertation submitted in partial fulfillment of the requirements for the degree of Doctor of Philosophy, within the PhD. Program in Engineering for the Information Society and Sustainable Development

Supervised by Dr. Alfonso Bahillo Martínez

UNIVERSIDAD DE DEUSTO

PEDESTRIAN NAVIGATION USING WRIST-WORN INERTIAL SENSORS

by

Luis Enrique Díez Blanco

A dissertation submitted in partial fulfillment of the requirements for the degree of Doctor of Philosophy, within the PhD. Program in Engineering for the Information Society and Sustainable Development

Supervised by Dr. Alfonso Bahillo Martínez

The candidate

The supervisor

Bilbao, September 2018

Pedestrian Navigation using Wrist-Worn Inertial Sensors
Author: Luis Enrique Díez Blanco
Supervisor: Alfonso Bahillo Martínez

Text printed in Bilbao
First edition, September 2018

Dedicated to everyone who has ever felt lost

Abstract

Global Navigation Satellite Systems are currently the main source of location information. However, due to the need for Line-Of-Sight with satellites, it is not possible to use them continuously. This represents a limitation to the development of seamless Location-Based Services for pedestrians as they spend most of their time in indoor environments. In this context, the combination of inertial Dead Reckoning systems, which do not need additional infrastructure to be installed in the environment, and wrist-worn wearable devices, such as smartwatches and smartbands, which allow different types of sensors to be carried in a continuous and user-friendly manner, can play a key role in the development of seamless pedestrian localization systems.

However, despite the potential they seem to offer, the upper limbs are a challenging body location and there are few proposals for wrist-worn inertial Pedestrian Dead Reckoning (PDR) systems. Additionally, the existing literature is not enough to provide a complete overview of the operation and performance of this type of localization systems. Therefore, the main goal of this thesis is to contribute to both the understanding and the improvement of the performance of the wrist-worn inertial PDR systems.

To this end, firstly, an in-depth analysis of the characteristics of the signals coming from wrist-worn sensors was carried out, including their variability with respect to factors such as different users, the arm pose or motion, or the walking speed. Then, a complete and systematic review of the step length estimation methods based on inertial sensors aimed to identify the reasons why, despite the many methods proposed, this topic is still in research stage. In relation to the step length

estimation methods, Ultra Wideband (UWB) technology was identified as a possible source of ground truth for calibrating PDR systems, thanks to its balance between accuracy and coverage. Four different step length estimation algorithms using UWB were tested. Later, the performance of a wrist-worn inertial PDR system was evaluated by participating in the IPIN Indoor Localization Competition 2016. Another evaluation stage was also done including multiple users and the simultaneous comparison against other state-of-the-art inertial pedestrian navigation systems. Finally, the improved Heuristic Drift Elimination (iHDE) method, originally designed for foot-mounted inertial navigation systems, was adapted for systems based on the integration of the length and orientation of each step. This simple heading drift reduction heuristic method helps to improve the estimation of the position in most buildings.

The results obtained throughout the thesis indicate that, although clear weaknesses have been identified that still need to be addressed, the performance of inertial PDR systems carried on the wrist is not too far from that of other systems mounted on other parts of the body. Therefore, the main conclusion of this thesis is that work must continue to improve PDR systems on this part of the body, since the advantage offered by the wrist at a level of comfort for the user may be key for achieving that continuous localization systems become real products and reach the mass market.

Resumen

Los sistemas globales de navegación por satélite son actualmente la principal fuente de información de localización. Sin embargo, debido a la necesidad de disponer de línea de visión directa con los satélites, no es posible su uso de forma continuada. Esto representa una limitación para el desarrollo de nuevos servicios basados en la localización, ya que las personas pasamos la mayor parte del día en el interior de edificios. En este contexto, la combinación de sistemas de navegación por estima mediante sensores inerciales, los cuales no necesitan de la instalación de infraestructura adicional en el entorno, junto con dispositivos como relojes o pulseras inteligentes, los cuales permiten llevar diferentes tipos de sensores de una forma cómoda y continua, pueden jugar un papel clave en el desarrollo de sistema de localización continuos para personas.

Sin embargo, a pesar del potencial que parecen ofrecer este tipo de sistemas, las extremidades superiores son una parte del cuerpo desafiante para un sistema de navegación por estima para peatones (PDR) mediante sensores inerciales, por lo que el número de propuestas existentes de este tipo es bajo. Además, la literatura existente no es suficiente para obtener una visión completa del funcionamiento y rendimiento de este tipo de sistemas. Por ello, el objetivo principal de esta tesis es contribuir tanto a la comprensión como a la mejora del rendimiento de los sistemas PDR con sensores inerciales llevados en la muñeca.

Para ello, en primer lugar, se ha realizado un análisis en profundidad de las características de las señales procedentes de sensores llevados en la muñeca y su variabilidad con respecto a factores como diferentes usuarios, movimientos o poses de los brazos, o la velocidad a la que se

camina. A continuación, se realizó una revisión completa y sistemática de los métodos de estimación de la longitud de pasos mediante sensores inerciales con el objetivo de identificar las razones por las que, a pesar de los muchos métodos propuestos existente, este problema aún está en fase de investigación. Además, en relación con los métodos de estimación de la longitud de paso, se identificó que la tecnología Ultra Wideband (UWB), gracias a su equilibrio entre precisión y cobertura, podría ser de utilidad como fuente de referencia para calibrar sistemas PDR. En concreto, se probaron cuatro algoritmos diferentes de estimación de la longitud del paso utilizando UWB. Posteriormente, se evaluó el desempeño de un sistema PDR inercial llevado en la muñeca mediante la participación en la Competición de Localización en Interiores IPIN 2016. También se realizó otra etapa de evaluación que incluyó múltiples usuarios y la comparación simultánea de su rendimiento con respecto a otros sistemas de localización de peatones del estado del arte. Por último, el método improved Heuristic Drift Elimination (iHDE), diseñado originalmente para sistemas de navegación inercial montados sobre el pie, fue adaptado para poder ser usado en sistemas basados en la integración de las longitudes y orientaciones de cada paso. Este sencillo método heurístico de reducción de la deriva de rumbo ayuda a mejorar la estimación de la posición en la mayoría de los edificios.

Los resultados obtenidos a lo largo de la tesis indican que, aunque se han identificado claras debilidades que aún deben ser abordadas, el rendimiento de los sistemas PDR inerciales llevados en la muñeca no está demasiado lejos del de otros sistemas montados en otras partes del cuerpo. Por tanto, la principal conclusión de esta tesis es que se debe seguir trabajando por mejorar los sistemas PDR sobre dicha parte del cuerpo, ya que la ventaja que ofrece la muñeca a nivel de comodidad para el usuario puede ser clave a la hora de conseguir que sistemas de localización continuos se conviertan en productos reales y lleguen al mercado de masas.

Acknowledgements

First of all, I would like to thank my supervisor *Alfonso Bahillo* for the constant trust he has shown in me over the years. Thank you for allowing me to define my own path while guiding and helping me with your ideas, comments and opportunities for my professional and personal development.

Thanks also to *Asier Perallos* and *Pili Elejoste* for giving me the opportunity to be part of DeustoTech Mobility. And, of course, to all the members of the unit, both the current ones (*Aimar, Alex, Amgad, Antonio, Browner, Carlos, Enrique, Florian, Galder, Gentza, Hugo, Iker, Itziar, Jesus, Jon, Juan, Julen, Leire, Nacho, Naia, Natasa, Pablo, Peru, Timothy* and *Unai)* as the former ones (*Alejo, Ander, Bruno, Eneko, Gorka, Idoia, Kevin, Laura, Nikola, Roberto* and *Safaa*). Sharing the day-to-day life with all of them makes that taking the bus every morning to cover the 60 km that separate the capital of the Basque Country from the "capital of the universe" does not require the slightest effort.

To *Antonio Jiménez* and *Fernando Seco*, for hosting me for three months in their group at the CAR-CSIC-UPM in Arganda del Rey, where I was able to learn firsthand how two great researchers work. Thanks also to *Uwe-Carsten Fiebig* and *Stephan Sand* for allowing me to spend three months at the Institute of Communications and Navigation of the German Aerospace Center (DLR) in Munich, to all the members of the Vehicular Applications group for the pleasant stay they put me through, and especially to *Estefanía Muñoz* and *Dina Bousdar* for everything I could learn from you and for all the kilometers we walked around the campus.

Of course, none of this would have been possible without my family: thanks to my parents *Felicitas* and *Félix Ángel* and to my sisters *Laura* and *Elena*. Thanks also to my friends for all these years (and for the years to come) sharing laughter, basketball and life.

And last, but not least, eternal thanks to *Oihana* for accompanying me throughout this change of professional course, for your patience in overcoming the distance that separated us temporarily, for putting up with my boring speeches and recurrent self-justifications, and for your unconditional support and love.

Thank you everyone,

Luis Enrique Díez Blanco

September 2018

Contents

List of Figures

List of Tables

Acronyms

AHE Average Heading Error

AHRS Attitude and Heading Reference System

ANN Artificial Neural Networks

AoA Angle of Arrival

BLE Bluetooth Low Energy

CDF Cumulative Distribution Function

CHAIN Cardinal Heading Aided Inertial Navigation

COM Center of Mass

COTS Commercial Off-The-Shelf

DoA Direction of Arrival

DoP Dilution of Position

DR Dead Reckoning

DTO Distance-to-Origin

EKF Extended Kalman Filter

FE Floor Estimation

FHE Final Heading Error

ACRONYMS

GIS Geographical Information System

GNSS Global Navigation Satellite System

GPR Gaussian Process Regression

GPS Global Positioning System

GTP Ground Truth Point

HDE Heuristic Drift Elimination

HDR Heuristic Drift Reduction

IEC International Electrotechnical Commission

iHDE Improved Heuristic Drift Elimination

IMU Inertial Measurement Unit

INS Inertial Navigation System

IoT Internet of Things

IPIN International Conference on Indoor Positioning and Indoor Navigation

ISO International Organization for Standardization

ITS Intelligent Transportation System

KF Kalman Filter

KNN K-Nearest Neighbors

LBS Location-based Services

LOOCV Leave-One-Out Cross-Validation

LOS Line-Of-Sight

MAE Mean Absolute Error

MC Mode Classification

MEMS Microelectromechanical Systems

NLOS Non-Line-Of-Sight

PDR Pedestrian Dead Reckoning

PF Particle Filter

RLS Regularized Least Squares

RMSE Root Mean Squared Error

RSS Receive Signal Strength

RTK Real Time Kinematic

SD Step Detection

SHE Step Heading Estimation

SHS Step-and-Heading System

SLAM Simultaneous Localization And Mapping

SLE Step Length Estimation

SVM Support Vector Machines

TD Traveled Distance

TDoA Time Difference of Arrival

TDoF Time Difference of Flight

ToA Time of Arrival

ToF Time of Flight

UKF Unscented Kalman Filter

UWB Ultra Wideband

WLAN Wireless Local Area Network

ACRONYMS

WSE Walking Speed Estimation

ZARU Zero-Angular Rate Updates

ZUPT Zero-velocity Updates

We are not lost. We're locationally challenged.

John M. Ford

CHAPTER

1

Introduction

1.1 The General Problem: Seamless Pedestrian Localization

The design of systems capable of adapting their behavior according to the context in which they carry out their work is a goal pursued by different branches of engineering. In addition to the clear advantage of being able to offer highly personalized information and/or services, this ability of adaptation is also key for achieving more efficient systems in the use of resources, an objective that is fully aligned to the current societal challenges [1].

Location is one of the most important types of context [2], especially for new computing paradigms such as ubiquitous computing, in which computing can take place everywhere and anytime.

Today, the *Global Navigation Satellite Systems* (GNSS), such as the GPS (*Global Positioning System*) or Galileo, are the most widespread source of location information, with a large applicability both in mass markets, such as *Location-based Services* (LBS) or *Intelligent Transportation Systems* (ITS), and professional markets, such as aviation, rail, maritime, agriculture, surveying, and timing and synchronization.

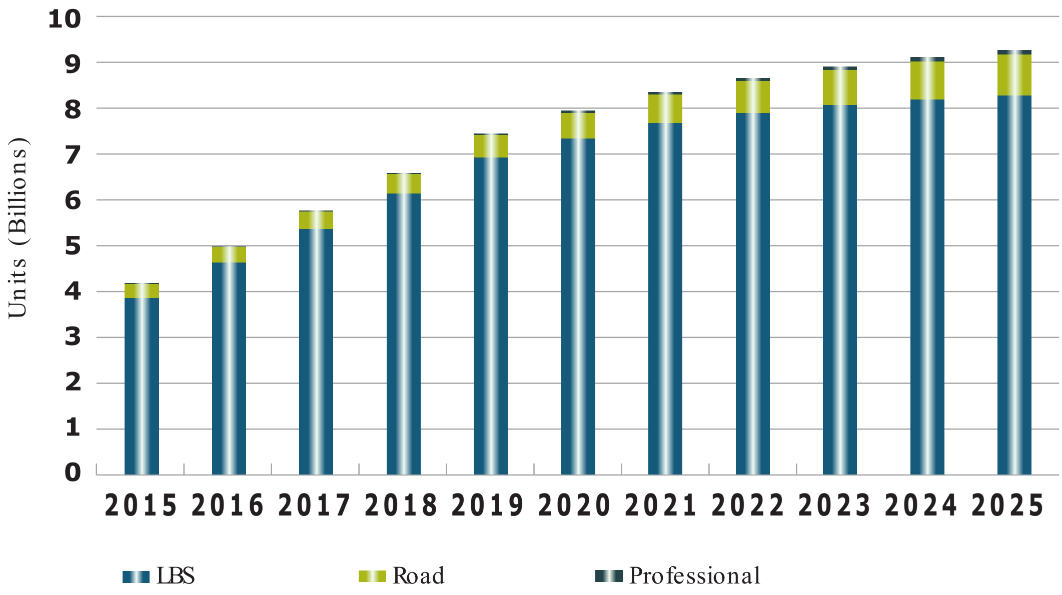

Figure 1.1: Evolution of globally installed GNSS devices grouped by market segment. Source: European GNSS Agency [3].

The importance of GNSS is growing every day due to their crucial role in the technological development of the different implementations of the ubiquitous computing paradigm, such as the *Internet of Things* (IoT), big data, augmented reality, mobile health, smart cities or multimodal logistics. According to the European GNSS Agency [3], it is estimated that 5.8 billion GNSS devices were in use in 2017 and, by 2020, this number is forecasted to grow to almost 8 billions (see Figure 1.1). That means more than one GNSS device per person on the planet.

As can also be seen in that figure, the LBS market segment is currently the most important one. This is due to the great penetration of smartphones and the fact that most of them include GNSS receivers. The inclusion of such functionality in smartphones indicates that, in addition to the lower cost of the hardware, there exists a great interest in LBS for people, with a wide range of applications: from the well-established navigation, geo marketing, sport tracking or social networking applications, to others not so widespread among the general public such as mapping and *Geographical Information Systems* (GIS), ethnography digital tools or platforms for the care of children and dependents.

However, these satellite-based systems are not perfect solutions and it is well

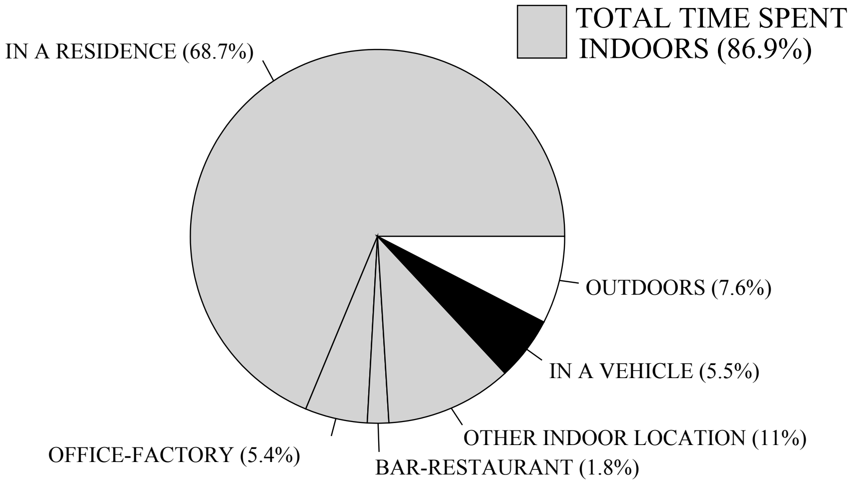

Figure 1.2: Average time people spent in six different locations on the diary day. Percentages in the figure are the average over individual percentages from 9196 respondents of the national human activity pattern survey, sponsored by the U.S. Environmental Protection Agency. Source: N. E. Klepeis *et al.* [5].

known that they perform poorly, or do not even work, in scenarios such as under tree cover, dense urban areas and indoor locations. This GNSS coverage limitation collides head-on with people's current way of life, since those GNSS-denied environments are the places where people spend most of their time:

- On the one hand, according to the United Nations [4], "in 2016, an estimated 54.5 per cent of the world's population lived in urban settlements. By 2030, urban areas are projected to house 60 per cent of people globally".

- On the other hand, studies like [5] or [6] show that people spend more than 80% of their time in enclosed buildings (see Figure 1.2).

Therefore, current satellite-based navigation systems are not enough for providing seamless localization, especially for pedestrians. This prevents developing new and more advanced LBS, so alternative localization systems and technologies are necessary.

1.2 The Base for a General Solution: Inertial PDR

In order to overcome these GNSS limitations, alternative technologies are being proposed for implementing localization systems, such as different radio frequency signals, inertial sensors, cameras, sound waves, magnetic signals or visible light. Some recent survey works that reflect the current state of the art can be found in references [7–12].

At the moment, no single technology offers yet a complete seamless localization solution that meets all the desired requirements, such as long- and short-term accuracy, coverage area, required infrastructure and cost [13, 14]. Given that each technology has its benefits and drawbacks, it is now considered that the solution should be to integrate several of them. For this, the research works in the localization field focus both on the improvement of the individual technologies and on the optimal ways to fuse them. As a proof of the existing ongoing activity in this field, Table 1.1 presents the most important international conferences and competitions around this topic that are organized since 15 years ago.

Among the different proposed alternatives, the systems based on the *Dead Reckoning* (DR) method play a key role. This positioning method is based on updating a known initial position by integrating over time the measurements of speed and direction of the moving object. Since the updates are done relative to the last calculated position, the error accumulates over time, growing unbounded if no external corrections are applied. However, its main strength is that no additional infrastructure needs to be installed in the environment, as all the equipment to measure the displacements can be mounted on the moving object itself. This independence from the scenario is what makes DR-based systems a key actor for providing continuous positioning:

- They can extend the availability of positioning between areas not covered by other infrastructure-based localization systems, such as GNSS, for instance.
- They can also compensate the short-term weaknesses of those infrastructure-based systems, improving the accuracy of the estimation in those areas.

The strengths and weaknesses of the infrastructure-based and infrastructure-free localization systems are usually complementary. Therefore, a logical architecture

Conferences	Since	Editions
Workshop on Positioning, Navigation and Communications (WPNC)	2004	15
IEEE/ION Position, Location and Navigation Symposium (PLANS)	2006	7
International Conference on Indoor Positioning and Indoor Navigation (IPIN)	2010	9
Internation Conference on Ubiquitous Positioning, Indoor Navigation and Location-Based Services (UPINLBS)	2010	5
International Conference on Localization and GNSS (ICL-GNSS)	2011	7
Competitions	**Since**	**Editions**
IPIN Indoor Localization Competition	2014	5
Microsoft Indoor Localization Competition	2014	5
Geo IoT World Indoor Location Testbed	2016	3
Combating Terrorism Technology Startup Challenge - Urban Navigation Challenge	2018	1

Table 1.1: Conferences and competitions on localization technologies.

for a seamless localization system would consist of the continuous use of a DR method and the opportunistic fusion with other infrastructure-based localization methods, whenever these are available.

The DR method can be implemented with different technologies but the use of inertial sensors, i.e., accelerometers and gyroscopes, is the most common one. By integrating the accelerations and angular rates provided by those sensors, it is possible to estimate the three-dimensional position, velocity and attitude of the moving object over time. This concept is known as inertial navigation and it has been used for many years in aviation and maritime navigation [15–17]. However, the inertial sensors used in the professional transport market are usually very large and expensive, which limit their applicability for other use cases, such as pedestrians.

In the last decades, thanks to the development of the *MicroElectroMechanical Systems* (MEMS) technology, inertial sensors have become smaller, lighter and cheaper, so they can be included in multiple electronic devices and easily carried by people. Unfortunately, the performance of the current MEMS-based inertial sensors is still not good enough for implementing *Inertial Navigation Systems* (INS) in an open loop fashion. That is, the position error grows very fast and the localization becomes unfeasible within seconds.

One possible solution is to apply corrections without requiring external information, making use, for instance, of some prior knowledge about the characteristics and constraints of the moving object's motions. In the pedestrian's case, it is possible to apply *Zero-velocity Updates* (ZUPT) when the foot is stationary on the ground, resetting the error after each footstep and making the position error accumulation proportional with the number of steps [18, 19]. This correction technique allows a longer use of the INS systems but requires the sensor to be mounted on the foot, which can be a limitation of usability. In fact, this lack of convenience for the user is one of the reasons why this type of solution has not reached the market yet.

An alternative option for pedestrians is to execute the DR method at the same rate as human gait is performed: updating the position step by step, or stride by stride. The systems that are based on this concept are known as *Pedestrian Dead Reckoning* (PDR) systems or *Step-and-Heading System* (SHS) [1]. For obtaining the step displacement vectors, a PDR is composed of three main blocks: *Step Detection* (SD), *Step Length Estimation* (SLE), and *Step Heading Estimation* (SHE) [20]. These PDR blocks can be implemented using different technologies, including inertial sensors. By decomposing and processing the displacement in steps, the position error is proportional to the number of steps, achieving similar performance results to foot-mounted INS with ZUPT. In addition, since it is possible to adapt the design of the PDR blocks to different mounting points of the sensors, there is no obligation to mount them on the foot. Although this adaptation of the blocks can make PDR systems less generalizable and to require calibration, their larger usability makes them a very attractive option.

[1] Authors such as Harle [20] consider that the term PDR encompasses both SHS and INS systems with ZUPT. Other authors, such as Groves [17], only consider SHS systems as PDRs, since INS with ZUPT can be applied to moving objects other than pedestrians. In this thesis we will follow the latter criterion.

As a summary, DR-based localization systems seem destined to be the basic process on which to build seamless localization systems. And for pedestrians, PDR systems should be one of the first options to consider currently because of their flexibility in choosing the sensor's mounting point, which allows the use of the *Commercial Off-The-Shelf* (COTS) electronic devices that include MEMS-based inertial sensors.

1.3 The Opportunity: Wrist-worn Wearable Devices

The first decision when designing an inertial PDR system is, therefore, where and how to mount the inertial sensors on the user's body. For this purpose, another concept emerged from ubiquitous computing that has gained relevance in the last few years can be useful: the wearable devices. This term includes to any electronic device with sensing, communication and computing capabilities that is integrated into clothes or accessories and that, therefore, can be continuously worn in a comfortable way. They offer a combination of information processing capabilities and convenience for the user that makes them a perfect platform for developing seamless pedestrian localization systems. Furthermore, among the great variety of sensors that wearable devices increasingly incorporate, inertial sensors are the most common ones these days [21]. Therefore, wearable devices are also suitable for implementing inertial PDR systems.

In recent years, the trend has been to use smartphones as platforms to implement inertial PDR systems. These devices have the advantages of being already widely adopted and usually including inertial sensors, as well as high computing power and various communication interfaces. They have proven to be suitable for pedestrian localization, as reported in [7, 9, 10], but, because they are not physically attached to the user's body, they cannot be considered as wearable devices. A study performed by Van Laerhoven *et al.* showed that smartphones are on the user's body 23% of entire day, or 36% considering only daytime [22]. Therefore, they are limited in their ability to execute inertial PDR on a continuous basis. Even when they are carried by a person, their unconstrained freedom regarding the mounting point and orientation makes the PDR process more challenging [23].

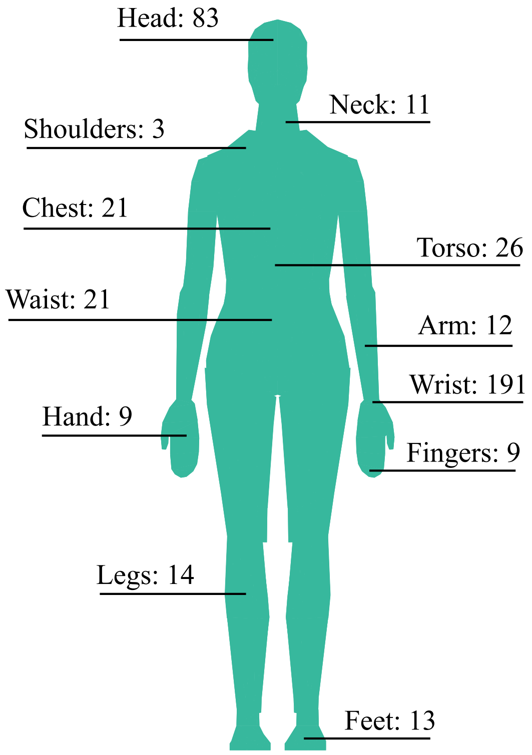

Figure 1.3: Number of wearable devices available in the market for each part of the human body. Source: Vandrico Inc. database [24] queried on 30th March, 2018.

Currently, there are wearable devices designed for many parts of the human body and new proposals are continually being released. According to the Vandrico Wearable Database [24], wrist-worn devices (namely, smartwatches and smartbands) are the most numerous type of wearable devices in the market (see Figure 1.3). The numbers also show the scarcity of foot-oriented wearable devices, confirming the difficulty to make the consumers to find attractive or convenient to buy specific footwear or an additional device for the foot. Subsequently, the use of INS systems with ZUPT seems far from the mass market right now.

Therefore, the current availability of smartwatches and smartbands as COTS products encourages the consideration of wrist-worn devices as candidates to implement inertial PDR with them. And, reflecting both on the reasons for the commercial success of these devices and on their characteristics when used in a localization system, it can be observed that there are several reasons that support their potential:

- It is a convenient sensor location for most users, as evidenced by the fact that we are already used to wearing watches or bands around the wrist, and it offers a level of comfort that allows wearing it continuously. There are some studies that support this idea, such as the previously referenced one by Van Laerhoven *et al.*, in which 51 people wore a smartwatch for 2 weeks continuously and only 5 of them took it off just to sleep [22], or the work of Hassani *et al.*, who obtained an 8% non-consent rate among people over 60 years old when asked to wear a device on their wrist continuously for 9 days [25].

- The fact of being accessories instead of pieces of clothes or footwear makes easier their daily use. That is, it is easier to wear every day the same smartwatch than the same smartshirt.

- It has a fixed location on the user's body, in contrast to the unconstrained freedom of smartphones. This could make the position estimation process slightly less complicated.

- Even in comparison to the case of a handheld smartphone, the dynamics undergone by a sensor worn on the wrist will be simpler than in the hand, because it is not affected by the degrees of freedom that the wrist joint provides.

- Additionally, wearable devices are continually incorporating new kinds of sensors that, although they are not positioning oriented, can be added to the position estimation process, such as the so-called signals of opportunity [21, 26].

- It is also possible to detect different human postures [27], daily user activities [28] or physiological parameters [29] from the wrist, which can be used to add context to the localization process and develop new LBS.

1.4 The Specific Problem: Wrist-worn Inertial PDR

Wrist-worn inertial PDR systems seem to be a great opportunity to make further progress towards seamless pedestrian localization systems. However, there are still no commercial solutions of this kind and even in the scientific literature there are not many proposed PDR systems specifically designed for wrist-worn inertial sensors:

- Kao *et al.* proposed the fusion of a wrist-worn PDR and GPS, but the study was limited to the step length estimation process [30].
- Qian *et al.* described the first complete wrist-worn PDR system [31] – this according to the present author's knowledge. However, both the evaluation and the reporting of results were very limited.
- Duong and Suh proposed a wrist-worn PDR, but it was specifically designed for people moving with the help of a walker [32].
- Jiang *et al.* proposed a method to exclude false positive steps when the user is static and a biomechanical step length estimation method for the specific motion mode of arm swinging, but the rest of the wrist-worn PDR system is not described [33].

It is true that there are available wrist-worn systems, both commercial and in research phase, that implement some of the blocks that make up a PDR system, such as step counters and traveled distance or walking speed estimators. Nevertheless, that information is commonly used for applications whose requirements are less demanding than the ones for localization, such as sport activity monitoring, energy consumption assessment, or prediction of human health status. For example, a 1% error in the step detection process after 1000 steps (i.e., 10 steps) makes little difference if the purpose of the application is to monitor a person's activity level. On the other hand, that same 10 steps error could mean more than 7 meters of error in traveled distance, which for an indoor localization system can lead to missing the room in which a person is and, depending on the application, this could be unacceptable.

This indicates that the development of robust wrist-worn inertial PDR systems is more complex than it may appear at first glance. The first idea that arises as the possible main obstacle is the combination of two factors: the high variability of wrist movements and the difficulty of PDR systems to generalize their performance. However, none of these factors have been analyzed in depth for the wrist-worn case.

1.4.1 Goal and Specific Objectives

Therefore, despite the potential for developing pedestrian LBS, wrist-worn inertial PDR systems remain an open challenge. And the existing literature is not enough to provide a complete overview of the operation and performance of this type of localization systems. This indicates that there is a need to address wrist-worn inertial PDR systems in a specific and comprehensive manner. This is precisely the main goal of this thesis:

> *To contribute to the knowledge and understanding of the design and operation of wrist-worn inertial PDR systems, as well as improving their performance.*

The methodology followed in this dissertation to try to achieve this main goal consists of, firstly, carrying out an exhaustive and in-depth study of the existing literature in order to, subsequently, identify open challenges and opportunities for improving the wrist-worn inertial PDR systems. In this way, a subset of these identified tasks will become the specific objectives of this research work, which will solved or done using the more appropriate methodology for each of them. Obviously, although the main goal is specifically focused on wrist-worn systems, any contribution that covers PDR systems in general will also fall within the scope of this work. As will be described later, the review of the state of the art and the identification of the open points will be carried out in detail in Chapter 3, so that, at this time, only the fundamental definition of the specific objectives is presented:

- Specific Objective 1: *To expand the existing knowledge about the characteristics and variability of the different signals generated from wrist-worn sensors, with the aim of evaluating their suitability for the design and implementation of wrist-worn inertial PDR systems.*

- Specific Objective 2: *To obtain a deep overview of the complete design and evaluation workflow of the SLE methods based on inertial sensors, so that it serves as a starting point for a better methodology in that research topic.*

- Specific Objective 3: *To implement a wrist-worn inertial PDR system and evaluate its performance in real scenarios, as well as comparing it against other state-of-the-art inertial pedestrian navigation systems.*

- Specific Objective 4: *To adapt the method "improved Heuristic Drift Elimination" so that it can be used in PDR systems and evaluate its capacity to reduce the heading drift for the case of a wrist-worn inertial PDR system.*

1.4.2 Structure of the Dissertation

The structure of the remainder of this thesis dissertation is outlined below.

Chapter 2 aims to provide an overview of the problem of localization, presenting the main methods, techniques and technologies that exist in the state of the art for its resolution. In this way, it is intended to reinforce the motivation introduced in the current chapter on the key role of inertial PDR systems for implementing seamless pedestrian localization systems. Therefore, a reader with experience in the field of localization systems may choose to skip this chapter.

Chapter 3 reviews the state of the art of inertial PDR systems in general and those using sensors on the wrist in particular. The aim of this chapter is to identify the open problems and improvement opportunities in the field of wrist-worn PDR systems and, on the basis of these, to define the specific objectives that were finally addressed during this research work and that are described in the following chapters.

Chapter 4 presents an in-depth analysis about the behavior of the wrist-worn inertial signals in relation to different walking speeds, arm movements and different users, and how these variations affect the design of a wrist-worn PDR system. This chapter is therefore aligned with the *specific objective 1*.

Chapter 5 provides a systematic and comprehensive review of the state of the art of SLE methods based on inertial sensors. The work presented in this chapter is therefore directly related to *specific objective 2*. The review includes all the aspects involved in the different phases of the design, testing and evaluation of a SLE method and, based on the results obtained, a reflection is presented on the reasons that hinder the progress of this field.

Chapter 6 presents a first evaluation of the *Ultra Wideband* (UWB) technology as a ground truth source for SLE purposes. Thanks to its combination of accuracy and coverage, under *Line-Of-Sight* (LOS) conditions, it can be an ideal technology for calibrating and evaluating inertial PDR systems. The motivation for doing the work presented in this chapter arises from some of the conclusions of the previous Chapter 5.

Chapters 7 tries to answer the *specific objective 3* by showing the results obtained by a real wrist-worn inertial PDR system in two evaluation stages: an international competition that involved mainly indoor scenarios, and a simultaneous comparison of three different inertial pedestrian navigation systems (foot-mounted, pocket-mounted and wrist-worn). In addition, details on the practical implementation of the system, such as the effect of sampling rate and signal filtering on system performance, are discussed.

Chapter 8 is related to the *specific objective 4* and describes the adaptation of the improved Heuristic Drift Elimination so that it can be used in PDR systems, being evaluated with a wrist-worn inertial PDR.

Chapters 9 revisits the main goal and specific objectives posed earlier in this chapter, outlines possible future research works and summarizes the main contributions of this thesis.

1.4.3 Limitations of Scope

The use cases considered in this thesis assume that:

- Walking forward is the only type of motion considered. Motions such as running, walking backward or sideways are out of scope.

- No fusion of several inertial sensors units or other sources of information is considered. Naturally, the use of multiple sensors provides more information but it also makes the system more complex, so it will be assumed that the user only carries one smart device at a time.

- Low- and medium-cost (i.e., few hundreds or thousands €, respectively) MEMS-based inertial sensors will be used.

1.4.4 Collaborators and Funding

This research work has been made possible thanks to the support of the Mobility research unit of DeustoTech-Fundación Deusto, to the receiving centres in research stays – the Centre for Automation and Robotics of the Spanish National Research Council (CAR, CSIC-UPM) and the Institute of Communications and Navigation of the German Aerospace Center (DLR) – and to the funding in part by the Research Training Grants Programme of the University of Deusto, in part by the Spanish Ministry of Economy, Industry and Competitiveness under the ESPHIA (TIN2014-56042-JIN) and the REPNIN (TEC2015-71426-REDT) projects, in part by the Basque Department of Education under the BLUE project (ref. PI 2016 0010), and in part by the German Aerospace Center (DLR).

I am not young enough to know everything.

Oscar Wilde

CHAPTER

2

Localization Background

The aim of this chapter is to provide an overview of the problem of localization, presenting the main methods, techniques and technologies that exist in the state of the art for its resolution. In this way, it is intended to reinforce the motivation introduced in the previous chapter on the importance of methods based on inertial sensor in achieving seamless positioning solutions for pedestrians. Therefore, a reader with experience in the field of localization systems may choose to skip this chapter.

Section 2.1 presents a brief historical overview of navigation and localization systems and defines several basic concepts. Then, Section 2.2 and Section 2.3 describe the two main localization methods: position fixing and DR. Later, Section 2.4 provides a brief description about the benefits of information fusion and the most common techniques applied for localization. Section 2.5 introduces the Attitude and Heading Reference Systems, a concept closely related to localization systems based on DR that is frequently used. Finally, Section 2.6 summarizes the contents and main conclusions of this chapter.

2.1 Introduction

Since the beginning of time, human beings have had different reasons to move and travel, either to find new sources of food, places with a milder climate or better conditions, or because of the mere desire to explore, driven by their innate curiosity. Subsequently, the expansion of trade and the inevitable wars created the need to record, plan and conduct such journeys in a more efficient and secure manner, as larger distances were being covered. Therefore, the science and art of navigation has been the main application and motivation that has led to the search and design of increasingly more accurate and advanced localization systems, methods and techniques.

Numerous advances have been made in this area throughout history, the following being some of the most notable:

- Celestial Navigation: When traveling on land or in ships close to the shore, the observation of known landmarks allows the navigation. This technique is called piloting or pilotage [34]. However, this is more difficult when traveling around unknown areas or where there are no clear landmarks, such as when moving away from the coast. For more than two thousand years, people like the Polynesians or the Phoenicians began to use the different celestial bodies as a references [15]. The latter used Polaris (now Polar Star) as a reference for the northern direction, as its position in the sky is so close to the Earth's axis of rotation that it appears static every night.

- Compass: The use of the celestial bodies as a reference is subject to clear skies. There is evidence that the Vikings and the Chinese discovered the properties of magnetite more than a thousand years ago, which allowed them to navigate even in situations where the sky was not visible [15]. This discovery allowed the development of the DR technique, by means of which it is possible to obtain the trajectory by updating a known initial position using the measured speeds and orientations [34].

- Sextant and chronometer: The use of astrolabes and then sextants made it possible to measure latitude by observing the elevation of different stars, usually the sun, relative to the horizon. However, calculation of the longitude was a problem for a longer period of time, as it required high precision clocks to know the time in a given reference meridian. It was not until 1761 that John Harrison managed to design a chronometer with an error of 1 second a day, which allowed determining the longitude with an acceptable error [15].

- Radio Navigation: Since the end of the 19th century, the contributions of figures such as Maxwell, Hertz and Marconi, among others, established the electromagnetic theory and the use of radio communications. During the World War II, considerable progress was made in this area, and from that moment on, localization systems based on electromagnetic waves began to emerge. From the first hyperbolic systems such as the Gee, the LORAN, the Omega or the Decca to the current GNSS such as the American GPS (1973), the Russian GLONASS (1976) or the European Galileo (2003) [17].

- Inertial Navigation: In the early 20th century, the first ideas emerged about the possibility of designing a self-contained navigation device that would be capable of tracking the trajectory of an object by detecting changes in its inertia, as indicated by the theory of mechanics established by Isaac Newton three centuries earlier [35]. Once again, with the advances made during the World War II in the technology of inertial sensors for use mainly in missile guidance, it was possible to build the first really useful INS systems, and their use was quickly extended to the navigation of any means of transport. Since the end of the 20th century, and thanks to MEMS technology, it has been possible to manufacture inertial sensors of low cost, size and weight, which allows them to be installed in many portable devices, such as smartphones, and to be used for a wide variety of applications [15, 36, 37].

As can be seen, great advances in the field of localization have come mainly from applications whose cases of use take place mostly in large outdoor spaces. However, as noted in Chapter 1, the new paradigms of ubiquitous computing require location information in a seamless way and in any type of scenario. In addition, the desire to provide such a seamless localization to pedestrians on a massive

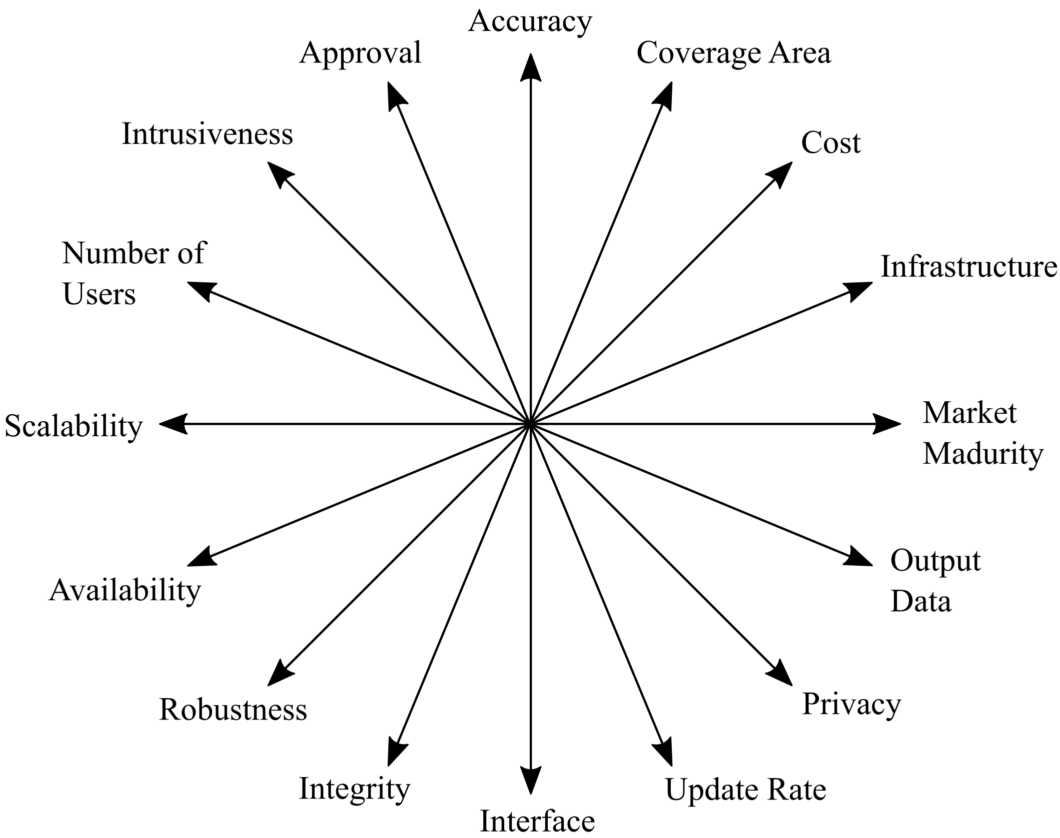

Figure 2.1: User requirements for a localization system. Source: Rainer Mautz [38].

scale implies the use of portable and inexpensive devices, which imposes additional restrictions and requirements that motivate the need to search for new localization methods. A good review of the main requirements that can be asked of a localization system can be found in the work of Rainer Mautz [38], which he summarized in the Figure 2.1.

Before going on, it is convenient to clarify a series of concepts and terms that, although often used as synonyms, have different nuances:

- Localization and Position: In English, to localize and to position are often used interchangeably, but there is a slight nuance. In general, it can be thought that localization is a more abstract concept, which determines the spatial relations between objects. In this way, the localization can be symbolic (I am at home), or physical (latitude and longitude). Therefore, the position could be seen as a type of physical localization, such as the coordinates in a reference system. Thus, all positioning systems are localization systems, but not necessarily the other way around.

- Navigation: This term includes any method of determining and planning the trajectory of an object. Therefore, it requires knowledge of its position, velocity and orientation with respect to a reference frame. Consequently, all navigation systems should include a positioning system and, depending on how the localization information is computed and provided, localization systems can also be navigation systems. For this reason, both terms are sometimes used as synonyms.

- Tracking: It differs from navigation in that the position and speed is obtained by an external agent, without necessarily requiring the installation of equipment on the object being tracked.

As can be deduced from the list of historical milestones seen above, there are five main navigation/localization techniques: pilotage, celestial navigation, DR, radio navigation and inertial navigation [36]. However, all of them can be categorized in two main general localization methods: on the one hand, the so-called position fixing methods, in which the element that calculates the localization uses information received or collected from the environment; and, on the other hand, DR-based methods, in which the element interested in its position is able to calculate it autonomously from changes in its inertia, updating known initial position and orientation. The following Sections 2.2 and 2.3 will review the general concepts of each of these two localization methods, as well as the main techniques and technologies used to implement them.

2.2 Position Fixing Localization Method

The position fixing method is based on using information obtained from the environment to calculate the unknown position of an object. This section will introduce the conceptual model on which this method is based, the type of signals and measurements commonly used, the main estimation strategies and some of the most usual technologies chosen for the actual implementations. There are good references that review in detail the theoretical and mathematical basis of these techniques [8, 39–41] as well as surveys on specific implementations of localization systems [10–12, 38].

In a generic way, the position fixing method assumes the existence of a set of nodes in fixed and known positions, usually called anchors, and a mobile node whose position is to be known. In general, one or more of those nodes may emit signals, which may be received by the rest of them. The basis of position fixing is to consider that the transmitted signals contain some information related to the positions of both the emitter and receiver nodes and that, therefore, they can be used to localize the mobile node. Those signals can be explicitly constructed to contain information about the position of nodes, but it is also possible to use signals that were not previously designed for that purpose, which are often known as signals of opportunity. Additionally, the localization computation can be done in the mobile node, from the information received from the anchors, or in a centralized way by the infrastructure if the signal transmission is produced from the mobile node to the anchors.

Therefore, considering that the resolving node has a set of measurements $\boldsymbol{z} = \{z_i\}$ generated while the mobile node is static at the unknown position $\boldsymbol{x}$, the position fixing method assumes that it is possible to establish a relationship between both variables that can be written as follows:

$$\boldsymbol{z} = \boldsymbol{h}(\boldsymbol{x}) + \boldsymbol{e} \tag{2.1}$$

where $\boldsymbol{h}$ is a function, generally non-linear, that implicitly contains the known positions of the anchors, and $\boldsymbol{e}$ represents any error or noise that is not possible to model and that, in general, will have a random behavior.

2.2.1 Type of Measurements

The most commonly used types of signals are those that do not require physical contact, such as electromagnetic and mechanical (sound) waves, although it is also possible to use static values of magnetic or gravitational field strength, provided that they show some spatial variations. Focusing on the wave-like signals, these are the types of measurements that can be obtained from them and that are useful for localization purposes:

Received Signal Strength

It is known that, in free space situations, electromagnetic waves suffer an attenuation of their power that increases quadratically with the distance to the source, which can be expressed as:

$$P_R = P_T \frac{G_T G_R}{4\pi d^2} \tag{2.2}$$

where P_R is the received power, or *Received Signal Strength* (RSS), P_T is the transmitted power, G_T and G_R are the gains from the transmitting and receiving antennas, respectively, which are separated at a distance of d. Therefore, since the apparent emitted power (i.e. the product $P_T \cdot G_T \cdot G_R$) can be known beforehand, it seems possible to obtain the range between receiver and transmitter from the received power level.

Having the distance or range between an anchor and a mobile node means that the possible positions of the latter are restricted to a circle, or a sphere in the three-dimensional case, which will be centered around the anchor and with a radius equal to that range.

However, the relationship 2.2 is not fulfilled in most real-life scenarios, mainly due to the signal's reflections and refractions with the different elements of the environment, such as the floor, walls, furniture or people. A more realistic model that takes into account this type of effects such as multipath (i.e. fast fading) or shadowing (i.e. slow fading) is the following:

$$P_R = P_T \frac{G_T G_R \gamma h^2}{4\pi d^n} \tag{2.3}$$

where n is the path loss exponent, γ a model parameter for slow fading (log-normal distribution) and h a parameter modeling the fast fading. If the RSS values are averaged over time, the fast fading term h can be approximated with 1 and, expressing the equation 2.3 in logarithmic units, it becomes:

$$P_R(dBm) = \alpha - 10 \cdot n \cdot log(d) + X \tag{2.4}$$

where the X variable models the shadow fading as a zero mean Gaussian random variable and the term α contains the averaged fast fading, the transmitter power P_T and the antenna gains G_T and G_R.

Both the random variable X and the path loss exponent n depend largely on the scenario, this being the main practical difficulty when estimating the ranges between nodes using RSS measurements. To have a notion of this variability, the values of the n loss exponent, which, let's remember, is two in free space conditions, can vary from one, for instance due to the waveguide effect in a corridor, to six in *Non-Line-Of-Sight* (NLOS) situations between transmitter and receiver.

Propagation Delay

If the signal's travel speed (v) in the propagation medium is known and the propagation delay ($\triangle t$) between the emitter and receiver nodes can be measured, it will be possible to know the distance or range (d) between them:

$$d = v \cdot \triangle t \tag{2.5}$$

This measurement, often referred to as *Time of Flight* (ToF) or *Time of Arrival* (ToA), requires the existence of synchronism between the clocks of the emitter and receiver nodes, which is not easy, especially for the mobile node, which usually has greater restrictions on its resources.

An alternative that simplifies the requirements for the mobile node is that it acts as an emitter and its signal is received by a set of anchors. If the anchors are synchronized, it will be possible to measure the difference in arrival times of the signal to each of them, known as *Time Difference of Flight* (TDoF) or *Arrival* (TDoA). In this way, instead of obtaining the ranges between the mobile node and the anchors, differential ranges are obtained, which means that the position of the mobile node will be on a hyperbola, or a hyperboloid in the three-dimensional case, whose foci are the positions of the anchors.

An even simpler alternative is the so-called *Round Trip Time* (RTT), also known as *Two-Way Ranging* (TWR), which consists of measuring the time it takes for the signal to go back and forth between two nodes, assuming the path keeps constant during that period. By subtracting the retransmission delay, the propagation delay will be the average time. It has the advantage that the synchronization between nodes is not necessary, but it forces the measurement of ranges between the mobile node and each anchor to be done sequentially, which may involve some latency in the localization.

The main error sources for this type of measurement are, in addition to the stability of the clocks and their synchronization, the variations in the propagation speed of the wave when passing through different materials and the possibility of receiving multipath signals that can make it difficult to detect the signal corresponding to the direct path. In NLOS situations, obstacles may cause the direct path signal not to be received, so that only multipath signals will be received, incurring in an overestimation of the ranges between the nodes. In LOS situations, problems generated by multipaths can also occur, especially in indoor scenarios where there may be objects so close to the receiver that they produce multipaths that cannot be differentiated from the direct path. The smallest increment of distance traveled by a multipath that can be distinguished from the direct path is defined by the ratio between the signal's bandwidth and propagation speed. Based on the Heisenberg's uncertainty principle, given a certain bandwidth $\triangle f$, the shortest pulse ($\triangle t$) that can be detected will be determined by:

$$\triangle f \triangle t \geqslant \frac{1}{4\pi} \tag{2.6}$$

Multiplying that shortest pulse width by the propagation speed gives the minimum distance to the receiver from which a multipath can be generated and is still distinguishable from the direct path.

Angle of Arrival

Using antenna arrays it is possible to determine the *Angle of Arrival* (AoA) or *Direction of Arrival* (DoA) of the signal. For example, if several receivers are arranged linearly separated by a distance d and the receivers are synchronized in such a way that they are able to detect the phase difference β of the waves they receive, then this relationship can be established:

$$\beta = \frac{2\pi d}{\lambda} \sin\theta \tag{2.7}$$

where θ is the angle of incidence of the wave and λ is the signal's wavelength.

By knowing the angles between an anchor and a moving node it is possible to restrict the positions of the latter to a straight line, or a plane in the three-dimensional case. The main source of errors for this type of measurement is the presence of multipaths, which usually come from different directions than the direct path signal and make detection difficult. Another major drawback of this measure is that more complex and expensive receivers are required.

Proximity

The simple fact of receiving a signal from a node whose position is known provides some information about the location of the mobile node. This measurement, also known as Cell ID, indicates that the mobile node is in the vicinity of the fixed node. Therefore, the localization information that can be provided will be symbolic or, if the anchor coverage area is known, a surface or volume of possible positions is obtained.

2.2.2 Estimation Methods

Given the random nature of the measurements, the position fixing method is basically a statistical problem of parameter estimation. However, as mentioned above, the real scenarios are hardly equivalent to free space condition, since the different elements, such as the floor, the walls, the pieces of furniture or the people passing by, generate NLOS and multipath situations that modify the amplitudes of the signals and produce delayed replicas. This means that errors are not usually Gaussian or that it is difficult even to know their distribution beforehand. This makes it difficult to design unbiased, consistent and efficient estimators.

The following is a brief description of the types of estimators that are commonly used, considering that the mobile node is static. That is, only the measurements associated with the current position of the mobile node are used. In Section 2.4 other estimation techniques will be introduced that allow the use of previous measurements and position estimations, but that require some a priori knowledge of the dynamic characteristics of the mobile node. The current methods can be grouped into three main categories.

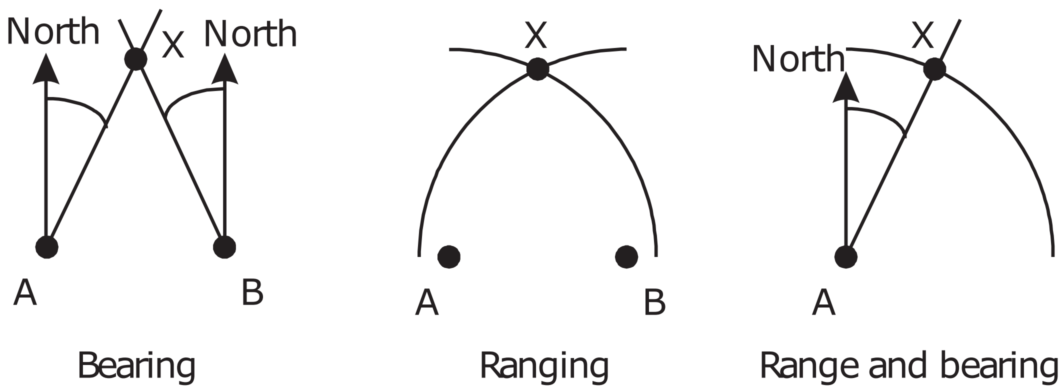

Figure 2.2: Geometric positioning methods: when the measurements obtained correspond to ranges, range differences or direction angles (bearing), in an ideal error free case, the position could be solved by the intersection of different combinations of the geometric elements defined by those these measurements. Source: Paul D. Groves [17].

Geometric Methods

The range, range difference and direction angles values provided by the previously described measurements are not individually enough to know the position of the moving node, as they represent circumferences, hyperboles or lines (spheres, hyperboloids and planes, in the three-dimensional case). However, if several non-redundant measurements are available, a system of equations can be established and the unknown position solved. As can be seen in the Figure 2.2 for the two-dimensional case, there are different combinations of the geometrical constraints that can be combined to solve the unknown position: the intersection of three circumferences, of two lines, or a line and a circumference. In the three-dimensional case there are a greater number of combinations, being the most common one the intersection of four spheres.

If only one type of geometric constraint is used, specific names are usually used: trilateration for ranges (circumferences or spheres intersections); multilateration for range differences (hyperbolas or hyperboloids intersections); and triangulation for angles (lines or planes intersections).

Unfortunately, since measurements are not usually error-free, the problem becomes an over-determined system of non-linear equations, which cannot commonly be solved analytically. If the $\boldsymbol{e}$ error is relatively small compared to the $\boldsymbol{z}$ measurements, iterative methods and approximate closed-form solutions (e.g. least squares) can be applied on linearized functions.

Cost Function Minimization Methods

For cases where the analytical expression of function $\boldsymbol{h}$ is known and the error $\boldsymbol{e}$ is relatively small, one approach is to minimize a cost function such as the following:

$$V(\boldsymbol{x}) = \log p_e(\boldsymbol{z} - \boldsymbol{h}(\boldsymbol{x})) \tag{2.8}$$

where p_e is the probability density function of the error $\boldsymbol{e}$. This optimization process will maximize the conditional probability $p(\boldsymbol{z}|\boldsymbol{x})$, so maximum likelihood estimators can be obtained for arbitrary error distributions. Additionally, it is possible to introduce protections against NLOS situations by converting the optimization problem into a constrained one.

Fingerprinting Methods

When function $\boldsymbol{h}$ has no analytical expression, or it is difficult to obtain, or if the error $\boldsymbol{e}$ is significant compared to the measurements $\boldsymbol{z}$, methods from the machine learning field are commonly used, often known as fingerprinting.

These methods are based on the previous generation of a map or database and convert the localization problem into a problem of inference or classification. Therefore, they consist of two phases: in the first one, known as offline calibration or training, values of the measurements of interest are collected in different positions of the area in which the localization service is to be provided. With these measurements, the database is constructed and, subsequently, during the online estimation phase, based on the specific measurements collected by the mobile node, the database is queried and the nearest or most probable position is returned as the estimated one. Techniques such as *K-Nearest Neighbors* (KNN), Bayesian decision, *Artificial Neural Networks* (ANN) or *Support Vector Machines* (SVM) are usually applied for the estimation.

These methods are based on relying solely on data collected during the offline phase. In this way, they do not need to know more features about the scenario, such as differentiating NLOS and LOS situations, knowing error distributions or even knowing the anchors' positions. This allows them to achieve good levels of accuracy. However, performance depends on the dimensionality and granularity of the data collected during the offline phase and that the scenario is not modified. In addition, that offline calibration phase is often very time-consuming.

2.2.3 Technologies

The characteristics of signals that can be generated by the technology selected to implement a localization system will determine the type of measurements and estimation methods which are more appropriate, and what performance can be achieved in terms of accuracy, coverage and other requirements. The following is a brief review of the main technologies used for position fixing based localization systems, focusing on the main strengths, weaknesses and areas of use of each of them.

Global Navigation Satellite Systems

GNSS is the most widespread type of positioning system, mainly due to its almost global coverage and the availability of receivers integrated in a multitude of devices.

The basis for their operation is the existence of a constellation of satellites whose orbits are known and it is therefore possible to know their position at any given time with good precision. The satellites emit electromagnetic signals in the microwave range, which contain modulated pseudo-random codes specifically designed to facilitate the estimation of the ToF between each satellite and receiver. Synchronization between the satellites is achieved by means of atomic clocks installed on them. On the other hand, the receiver's clock is of poorer quality and contains a certain synchronization error. However, since this error will be common to all satellites that are visible simultaneously, it can be eliminated if at least four satellites are received. By

Source of error	Resulting position error
Satellites' clock and orbits	0.5 m – 1 m
Atmospheric delays	1 m – 3 m
Multipath and NLOS signals	0.1 m – 100 m
Receiver thermal noise	0.1 m

Table 2.1: Order of magnitude of the main position error sources in GNSS systems. Source: SaPPART White paper [42].

obtaining the ranges to at least four satellites, it is possible to compute the three-dimensional position of the receiver by trilateration.

The main weaknesses and disadvantages of these systems are:

- The power of the emitted signals is low, making it difficult to receive them with sufficient quality in, for instance, indoor environments or under trees.
- The troposphere and the ionosphere affect the propagation velocity of the electromagnetic wave, which results in an error in the estimation of the ranges and, hence, of the position.
- The existence of multipaths may also affect the estimation of ranges. This is especially common in NLOS scenarios, such as urban canyons.
- The relative geometry between the satellites and the receiver can generate different accuracies in different directions in space. This is usually known as *Dilution of Position* (DoP).
- The necessary infrastructure, i.e. satellites, is expensive to produce, install and maintain.

In the Table 2.1 it can be seen the orders of magnitude of the effect of the different error sources on the position error. However, depending on the complexity of the receiver and the amount of corrections applied, it is possible to achieve accuracies of the order of 10 meters for basic receivers to centimeter errors with more advanced solutions such as Differential GNSS or *Real Time Kinematic* (RTK), although its use is mainly limited to outdoors scenarios.

Wireless Local Area Networks

Wireless Local Area Networks (WLAN) is a widely used set of wireless communication protocols (mainly IEEE 802.11) that can also be used for localization. It is precisely this availability of already installed anchors in a multitude of environments and receivers in portable devices such as smartphones or laptops that is its main strength when it comes to being chosen as localization technology.

Propagation delay based measurements are often not used because of the poor results obtained. On the one hand, the off-the-shelf WLAN hardware is not usually ready to measure arrival times and, on the other hand, the usual bandwidth of WLAN systems (typically 20 MHz) implies that any multipath that occurs within 1-2 meters around the receiving node can be indistinguible from the direct path signal. This resolution is not enough for indoor environments with many obstacles in that range.

RSS measurements are usually available on devices, but since WLAN anchors installation is usually designed to optimize communication, not positioning, and its coverage typically ranges 50-100 meters, NLOS situations are common. This makes it difficult to use an analytical propagation model, so fingerprinting-based techniques are the most common.

With these techniques, accuracies between 1 and 10 meters are usually obtained, depending on the number of anchors and the density of calibration points. The main disadvantage of using WLAN fingerprinting is the high cost of performing the offline calibration phase, which can be degraded by changes in the environment. In addition, RSS values taken by different receiving devices may vary depending on the hardware and the power control strategies performed during data communications, which will also degrade the accuracy of the estimate.

Ultra Wideband

UWB is a communications technology that is defined as having an absolute bandwidth of at least 500 MHz or a relative bandwidth greater than 20%. It allows short-range communications (less than 100 meters), with high data rate and low power consumption but, thanks to its bandwidth, is especially useful for implementing localization systems based on propagation times. Returning to the equation 2.6, a bandwidth of 500 MHz implies a theoretical 5 centimeters range safe against multipaths. With these characteristics, position estimation with errors of a few tens of centimeters is achieved. However, as this is not a commonly used wireless technology, the systems currently developed are few and more expensive than other adopted technologies such as WLAN.

Sound

In contrast to electromagnetic waves, sound is a mechanical wave associated to a pressure oscillation transmitted through a medium, commonly the air. In general, signals in the ultrasound range are used, although there are also systems in the audible range to take advantage of the sound cards available in many devices.

The characteristics of these signals involve a number of strengths and weaknesses that result in the use of only propagation delay measurements. Regarding their strengths:

- Since the speed of sound propagation in the air is slow (around 343 m/s at 20°C), it is easy to detect and avoid multipaths, so centimeter-level accuracies can be achieved in indoor scenarios.
- This low propagation speed in comparison to the electromagnetic waves also facilitates the synchronization between nodes.
- Its hardware components are simple to implement and low cost.

As for their weaknesses:

- Its main restriction is the low coverage mainly because of the high attenuation of these waves in the air.
- The velocity of sound propagation in the air is highly affected by temperature. This implies the implementation of compensation systems and avoiding environments with large temperature changes, such as outdoors.

- In addition to NLOS and multipath situations, due to the low propagation speed, these systems are also sensitive to the Doppler effect if the nodes are moving at considerable speeds.

These characteristics make sound waves rarely be used outdoors, limiting their use to small spaces, avoiding NLOS situations and especially for applications that require great accuracy. In addition, the availability of high accuracy implies that the positions of the anchors must be known with at least the same accuracy, which complicates the installation process.

Bluetooth Low Energy

Bluetooth Low Energy (BLE) is a wireless communication technology that offers simple devices the ability to exchange small amounts of data with very low power consumption. One of the most common operating modes is advertising, which allows a node to broadcast short messages periodically. These messages and their RSS measurements can be used to detect the proximity to one of these beacons and to estimate the position of a mobile node.

The main advantages of this technology are the availability of receivers in many electronic devices, their high security, low cost and low consumption. The standard allows coverage ranges up to 100 meters but most beacons are usually visible from no more than 10 meters.

This low coverage means that the main estimation technique is proximity and symbolic localization, which may be sufficient for some applications such as shopping centres or museums. However, it is also possible to apply fingerprinting techniques that give similar results to those achieved with WLAN and even to use analytical propagation models, which can achieve good results if the mobile node is about one meter away from the transmitter.

In addition to the low coverage, another of its main disadvantages is that the low frequency of advertising can generate a latency in the estimation of the location, which makes real time applications difficult.

There are many other technologies that can be used to implement localization systems based on position fixing: cameras, infrared, RFID, visible light, magnetic

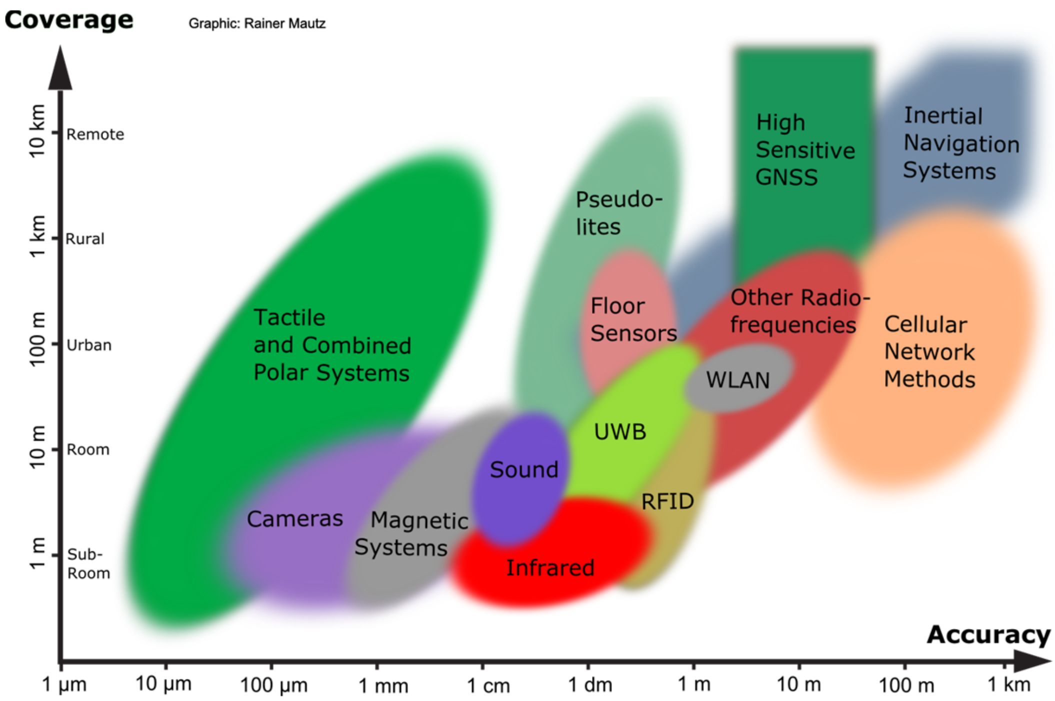

Figure 2.3: Comparison of accuracy and coverage offered by different technologies for position fixing localization method. Source: Rainer Mautz [38].

fields, cellular networks and even television and FM radio signals. When choosing a technology, one of the first features to consider is their balance between accuracy and coverage. In Figure 2.3 can be seen a comparison of the most common technologies. In addition to this compromise between accuracy and coverage, the main characteristic that summarizes the performance of the position fixing localization methods is that they offer better accuracy in the long-term than in the short-term. That is, there may be times when, because of NLOS or multipath situations, or temporary interferences, the position estimation error increases but, on average, it tends to be bounded.

2.3 Dead Reckoning Localization Method

The American Practical Navigator [34] defines DR as “a method for determining the estimated position of a vessel by advancing from a known fix of position along the vessel’s ordered course and speed”. In this way, maintaining a known course by

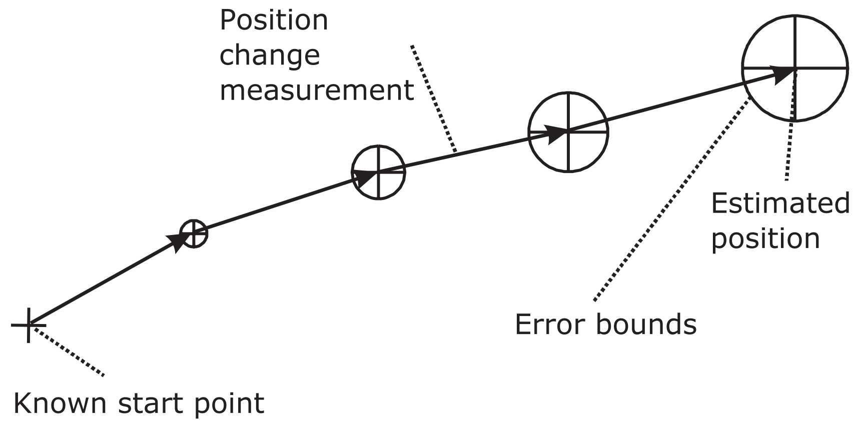

Figure 2.4: The DR method: the estimate of the position is obtained by updating an initial position using the course and distance traveled in that period. Being a relative method, there is an unbounded accumulation of errors. Source: Paul D. Groves [17].

using the compass and periodically measuring the forward speed, the boats were able to update their last known position frequently, without having to wait for the midday sun to calculate latitude and longitude with the sextant and chronometer.

Therefore, the fundamental characteristic of the DR method is that it is self-contained, that is, it does not require the existence of landmarks or reference points in the environment. It is only necessary to know the starting position and the heading and the speed during the integration period. In addition, DR also makes it possible to make future projections of the trajectory and, in this way, plan arrival times or avoid obstacles.

However, its main limitation is that, being a relative positioning method based on the last known position, if no corrective measurements are applied, errors accumulate unbounded over time, as depicted in Figure 2.4. Thus, although the origin of the term is not entirely clear, some theories indicate that "Dead" is due to the dangerousness of such an accumulation of error. Other theories point to the possibility that it was a misspelling from the abbreviation of the term "Deduced" [43].

The DR method is not only limited to maritime navigation and can be applied to any mobile element, such as aircraft, land vehicles or mobile robots. In fact, it is known that many mammals use similar path integration techniques to move around the environment.

Depending on the type of moving object, there exist different techniques and technologies for measuring the displacement, speed and course, so diverse as, for example, using a knotted rope for the measuring a boat's speed or an odometer for cars and bicycles. However, one of the most common technologies nowadays is the use of inertial sensors.

2.3.1 Inertial Navigation Systems

Newton's first law of motion defines inertia as the property of bodies to maintain their state of motion, including both the magnitude and direction of their velocity, if no force is applied to them, or if the net force applied to them is null. Likewise, an inertial reference system is one in which Newton's laws of motion are valid, that is, one that is not accelerated or rotating.

From these concepts arose the idea that, if it were possible to measure the forces acting on a body and trying to change its inertia, it would also be possible to calculate its changes in speed, course and position, regardless of the scenario and condition in which the movement occurs. This would be a major advance in the performance of DR-based navigation since, until then, the displacement, speed and course measurements required different techniques and instruments depending on whether the movement was by land, sea or air.

In the mid-19th century, the first inertial sensors appeared: first, the gyroscopes, capable of measuring angular velocity and, around 70 years later, the accelerometers, capable of measuring linear accelerations. However, it was not after the World War II, when inertial sensors of sufficient quality became available to construct navigation systems that would enable to track the position, speed and orientation of an object in space for a reasonable period of time and with acceptable accuracy. These systems are known as INS.

The early INS used a configuration known as gimbaled INS or stable platform systems: the inertial sensors were mounted on a platform isolated from external rotations by motors that canceled the rotations detected by the gyroscopes, as shown in the Figure 2.5. In this way, the accelerometer reference system was kept aligned with the navigation reference system. After correcting the value of the gravity, the speed and position were obtained by successive integrations of the acceleration

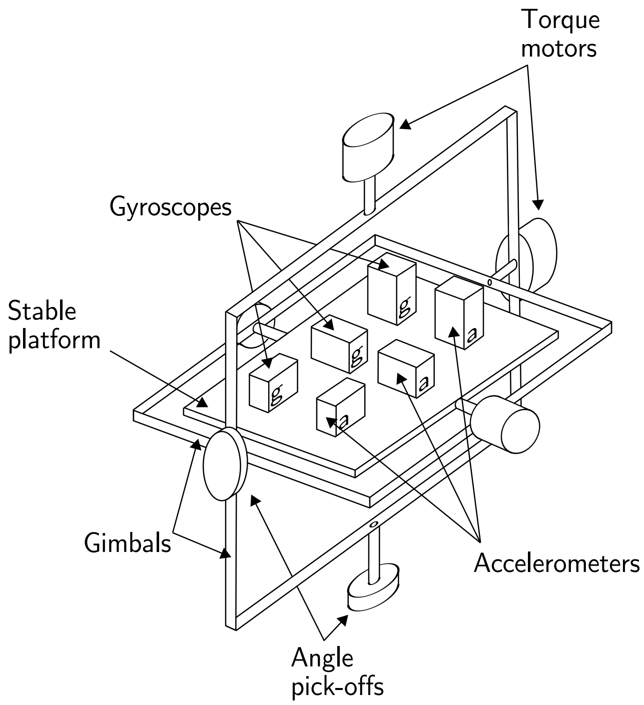

Figure 2.5: Gimbaled INS or stable platform system. Source: Oliver J. Woodman [44].

values. This architecture was determined by the technological limitation of early gyroscopes and by the need to reduce the computational load that the transformation of accelerations from one reference system to another would imply. Subsequently, with the improved performance of gyroscopes and the availability of increased computing power, a configuration in which inertial sensors were rigidly mounted on the moving object was used. This configuration is known as strapdown and, in exchange for greater computational complexity, smaller and mechanically simpler INS are achieved. Currently, strapdown INS is the most widely used configuration.

Next, a general description of the implementation of the strapdown INS is presented, introducing the basic types of inertial sensors, an overview of the algorithm formulation and some cumulative error reduction techniques that can be applied so that the system remains self-contained. There are many references in the literature to these and other aspects of the INS, such as [15–17, 36, 44].

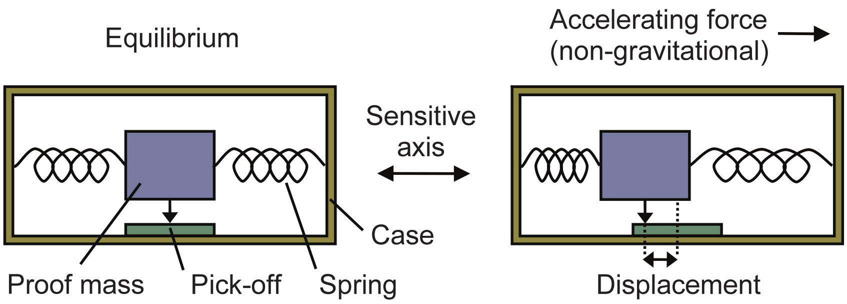

Figure 2.6: Simple mechanical accelerometer. Source: Paul D. Groves [16].

2.3.1.1 Inertial Sensors

Accelerometers

In the Figure 2.6 can be seen the structure of a basic mechanical accelerometer. The basis of its operation is that the relative position between the test mass of the interior and the case is proportional to the force applied in the direction of the measuring axis. That is, when acceleration is applied to this axis, the case moves in relation to the test mass through the springs that connect them. Accelerometers only measure non-gravitational accelerations, known as "specific force". This is because gravity affects the entire sensor and is therefore not distinguishable. This implies that, if the accelerometer is in free fall, the specific force will be zero and so will be the measurement provided by the sensor. On the other hand, if the accelerometer is static and its sensitive axis is parallel to the direction of gravity, the output value of the sensor will be the magnitude of gravity. That is why, when integrating accelerations in an INS, it is necessary to know the local value of gravity in order to correct the measurements offered by the accelerometers. Current accelerometers are based on more advanced designs such as pendulums or vibrating beams, built both mechanically and in solid state [15].

Gyroscopes

The first mechanical gyroscopes were based on a spinning wheel mounted on a gimbaled structure, similar to the one shown in Figure 2.5, which allows it to rotate in all three axes. Due to the conservation of the angular momentum,

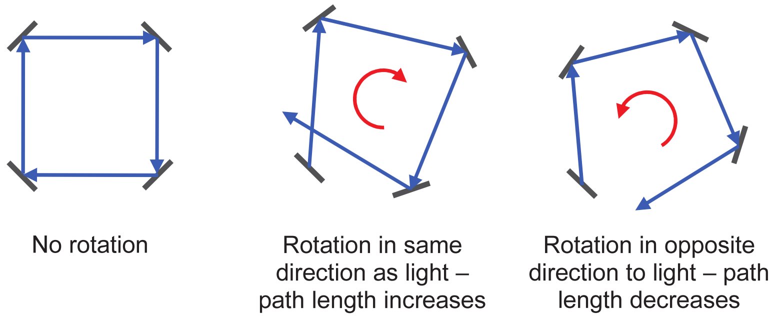

(a) Effect on a ring based gyroscope.

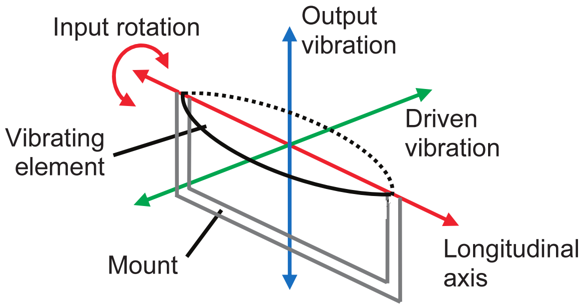

(b) Gyroscope based on a vibrating structure.

Figure 2.7: Working principle of different types of gyroscopes. Source: Paul D. Groves [16].

the spinning wheel resists to change its orientation and, by reading the pick-offs, the orientation angles can be known.

In contrast, modern gyroscopes offer angular rates instead of orientation angles. They are usually built as fiber optic rings or vibrating structures. The former are based on a beam of light emitted through a ring of known length. By measuring the time it takes to go through it, it is possible to know how much the ring turned and in what direction. The latter use vibrating elements to measure the Coriolis acceleration and, from it, the angular velocity. Diagrams of both types of gyroscopes can be seen in Figure 2.7.

Inertial Measurement Units

A body that can move without restrictions in a three-dimensional space has six degrees of freedom: translations along three perpendicular axes (forward/backward, up/down, left/right) and changes in orientation through rotation about three perpendicular axes. Therefore, at least three accelerometers and three gyroscopes will be required to implement an INS in such a scenario.

Accordingly, it is common to group several inertial sensors into a single device, known as *Inertial Measurement Unit* (IMU), which generally contains those three accelerometers and three gyroscopes placed in orthogonal directions. In addition, IMUs may contain additional sensors, such as magnetometers and barometers, and signal matching and calibration capabilities, power supply and communication interfaces.

Inertial Sensors' Errors

Inertial sensors are not perfect devices and have different types of errors. These are some of the most important:

- Bias: It is the offset between the measurement and the actual value. It is usually the biggest source of error.
- Scale-factor: This is the separation between the ratio of actual to estimated values and the unit slope line. That is, it indicates whether the error is proportional to the value of the measured variable.
- Cross-coupling: This occurs when the physical quantities produced in one axis are "felt" on other perpendicular axes of the sensor. This is usually due to misalignment during sensor construction.
- Random errors: They are due to mechanical and electrical sources. Usually known as "random walk" because of the effect of its integration.

The first three types of errors are systematic and are made up of four fundamental components:

- Fixed contribution: Present each time the sensor is used.
- Effect of temperature: Temperature changes affect sensor response.
- Run-to-run variation: It is the variation of each error source between different uses of the sensor.

- In-run variation: It is the variation of each error source during one use of the sensor.

The first two error components can be eliminated or reduced through calibration processes. Not the latter two, which can only be corrected by the use of external information. This way, an error model of the IMU's accelerometers can be written:

$$\hat{\boldsymbol{f}} = \boldsymbol{b_a} + (\boldsymbol{I_3} + \boldsymbol{M_a})\boldsymbol{f} + \boldsymbol{w_a} \tag{2.9}$$

where $\hat{\boldsymbol{f}}$ is the specific force vector measured by the IMU's accelerometers, $\boldsymbol{b_a}$ the accelerometers' bias vector, $\boldsymbol{I_3}$ is the identity matrix, $\boldsymbol{M_a}$ is the matrix of the coefficients of the accelerometers scale-factor (diagonal elements) and cross-coupling errors (off-diagonal elements), $\boldsymbol{f}$ is the true specific force vector and $\boldsymbol{w_a}$ is the random-noise vector. And similarly for gyroscopes:

$$\hat{\boldsymbol{\omega}} = \boldsymbol{b_g} + (\boldsymbol{I_3} + \boldsymbol{M_g})\boldsymbol{\omega} + \boldsymbol{G_g}\boldsymbol{f} + \boldsymbol{w_g} \tag{2.10}$$

where $\boldsymbol{\omega}$ is referred to the angular rate, $\boldsymbol{G_g}$ is the matrix of errors dependent on the accelerations suffered by the gyroscopes, and the rest of symbols are analogous to the accelerometer case.

MEMS Technology

Among the different types of gyroscopes and accelerometers available, the best performances are usually associated with those of greater size and mechanical complexity. This has consequences in terms of usability, as it impacts on their portability and cost, for example.

Since the end of the 20th century, the development of the MEMS technology has made it possible to develop small, lightweight, low-cost inertial sensors. This has allowed them to be included in a multitude of portable devices, such as smartphones or wearable devices, and, therefore, to be available for pedestrian applications. However, although its performance continues to improve, this reduction in size leads to higher levels of error, as shown in Figure 2.8. It is therefore common for inertial sensors to be classified according to their accuracy in categories such as marine, aviation, tactical or consumer.

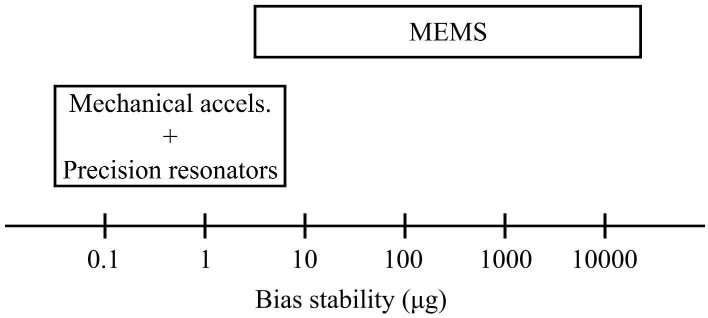

(a) Accelerometers

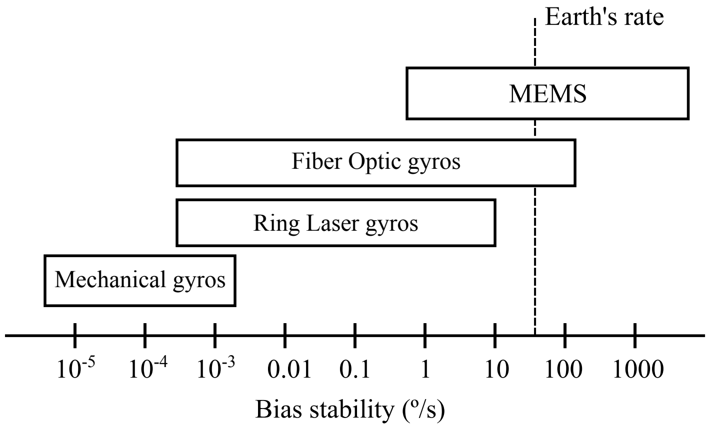

(b) Gyroscopes

Figure 2.8: Performance comparison of different types of inertial sensors. Source: D.H. Titterton and Weston[15].

2.3.1.2 **Strapdown INS Mechanization**

The following will briefly explain the fundamental steps of the strapdown INS algorithm. There are different variants of this method, known as mechanizations, depending on which system is chosen as reference frame. In this case it will be considered that navigation is required with respect to a fixed reference frame. That is, an inertial reference system, which is neither rotating nor accelerated.

A fixed reference system in relation to the Earth is not inertial, as the planet rotates and moves through the universe. Since accelerometers and gyroscopes provide measurements with respect to an inertial system, the rotations and the accelerations associated with the Earth's movement (centripetal, Coriolis and Euler) should be taken into account when navigating with respect to the it. However, if we

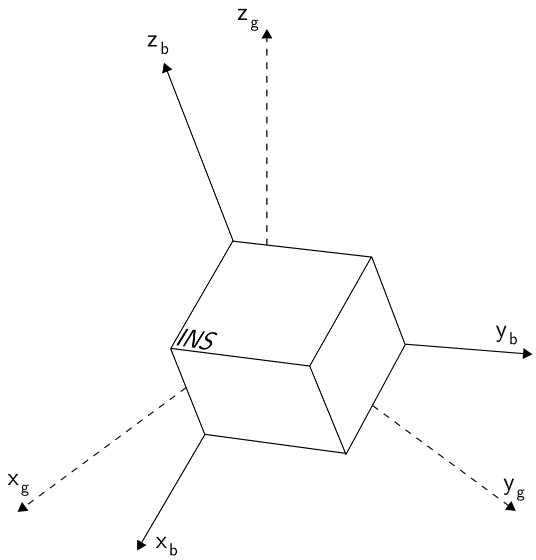

Figure 2.9: The body and global frames of reference. Source: Oliver J. Woodman [44].

limit ourselves to the case of pedestrians and MEMS-based IMUs, the low speed at which we walk and the noise levels of the sensors (as can be seen in the Figure 2.8b) allow to assume that the Earth is a fixed reference frame.

Throughout this section, the subscripts b (body frame) and g (global frame) are used to indicate the frame of reference in which vector quantities are measured, as can be seen in the Figure 2.9.

The strapdown INS mechanization can be divided into 4 basic steps: orientation update, accelerations projection, gravity correction and integration.

Knowing the orientation of the moving object with respect to the global frame is necessary for several reasons. On the one hand, because it is essential for later projecting the accelerations from the body frame to the global frame before integrating them; And, on the other hand, because, in general, orientation cannot be assumed from the direction of traveling. Think, for example, of a person walking sideways: the direction in which he looks does not coincide with that of his displacement.

There are different ways to represent orientations. Some of the most common ones are rotation matrices, Euler angles and quaternions [45]. In this case, we will use rotation matrices. It can be shown that, using the small angle approximation, the variation over time of a rotation matrix can be expressed by the following differential equation ([15, 44]):

$$\dot{\boldsymbol{C}}(t) = \boldsymbol{C}(t)\boldsymbol{\Omega}(t) \tag{2.11}$$

which has the solution:

$$\boldsymbol{C}(t) = \boldsymbol{C}(0) \cdot exp\left(\int_0^t \boldsymbol{\Omega}(t)dt\right) \tag{2.12}$$

where

$$\boldsymbol{\Omega}(t) = \begin{pmatrix} 0 & -\omega_{bz}(t) & \omega_{by}(t) \\ \omega_{bz}(t) & 0 & -\omega_{bx}(t) \\ -\omega_{by}(t) & \omega_{bx}(t) & 0 \end{pmatrix} \tag{2.13}$$

is the skew symmetric form of the angular rate vector $\omega_b(t)$.

Since most gyroscopes are digital and they provide angular rate values periodically ($\triangle t$), it can be shown that the orientation update equation after each successive gyroscope sample has the following form:

$$\boldsymbol{C}(t + \triangle t) = \boldsymbol{C}(t)\left(\boldsymbol{I} + \frac{\sin\sigma}{\sigma}\boldsymbol{B} + \frac{1-\cos\sigma}{\sigma^2}\boldsymbol{B}^2\right) \tag{2.14}$$

where $\sigma = |\omega_b \triangle t|$ and the matrix $\boldsymbol{B}$:

$$\boldsymbol{B} = \begin{pmatrix} 0 & -\omega_{bz}\triangle t & \omega_{by}\triangle t \\ \omega_{bz}\triangle t & 0 & -\omega_{bx}\triangle t \\ -\omega_{by}\triangle t & \omega_{bx}\triangle t & 0 \end{pmatrix} \tag{2.15}$$

These expressions assume infinitesimal rotations and sampling periods. Therefore, the sampling frequency of gyroscopes should, in general, be as high as possible, so that the angular velocity can be considered as constant between each measurement period.

Once the current orientation of the object is obtained, it is possible to project the accelerations from the IMU's body frame to the global frame:

$$\boldsymbol{a}_g(t) = \boldsymbol{C}(t)\boldsymbol{a}_b(t) \tag{2.16}$$

where $\boldsymbol{a}_b(t) = (a_{bx}(t), a_{by}(t), a_{bz}(t))^T$ are the measurements from the accelerometers.

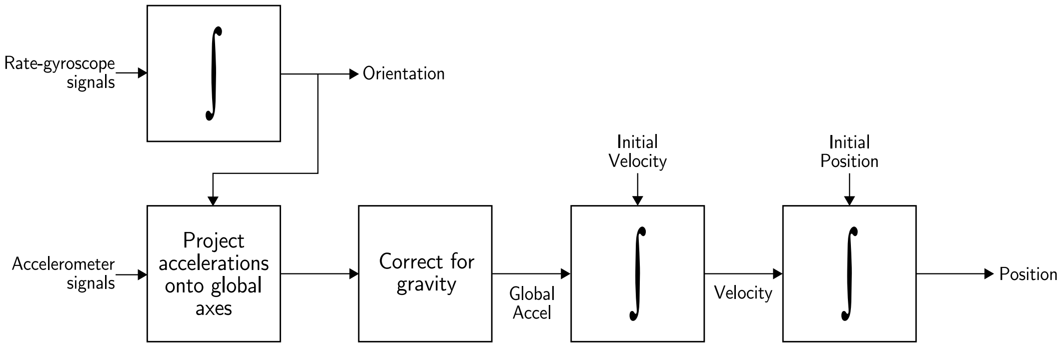

Figure 2.10: Strapdown INS mechanization for a fixed reference frame. Source: Oliver J. Woodman [44].

Finally, the only thing left to do is to correct the gravity, expressed in global frame ($\boldsymbol{g}_g$), and carry out the successive integrations. In a similar way to gyroscopes, the accelerometers deliver their measurements periodically, so integrating by the rectangular rule, the update equations will be:

$$\boldsymbol{v}_g(t + \triangle t) = \boldsymbol{v}_g(t) + \triangle t \cdot (\boldsymbol{a}_g(t + \triangle t) - \boldsymbol{g}_g) \tag{2.17}$$

$$\boldsymbol{s}_g(t + \triangle t) = \boldsymbol{s}_g(t) + \triangle t \cdot (\boldsymbol{v}_g(t + \triangle t)) \tag{2.18}$$

where $\boldsymbol{v}_g(t)$ y $\boldsymbol{s}_g(t)$ are the velocity and position of the moving body, expressed in the global frame, at time t. A general diagram of the algorithm just explained can be seen in the Figure 2.10.

2.3.1.3 **Drift Reduction Techniques**

As discussed in Section 2.3.1.1, inertial sensors contain errors and, since strapdown INS is an integration-based method, those errors will also be integrated and will accumulate unbounded over time. On the one hand, the errors of the gyroscopes will propagate as orientation errors when integrated, which will grow proportionally with time. On the other hand, the errors of the accelerometers will propagate linearly in time as velocity errors and, after the second integration, as position errors in a quadratic rate. However, the orientation error also propagates as position error since it causes that the projection of the accelerations is done wrongly and, therefore, the correction of gravity as well. Therefore, the total position error grows cubically in time. In fact, orientation error is critical: due to the magnitude of the

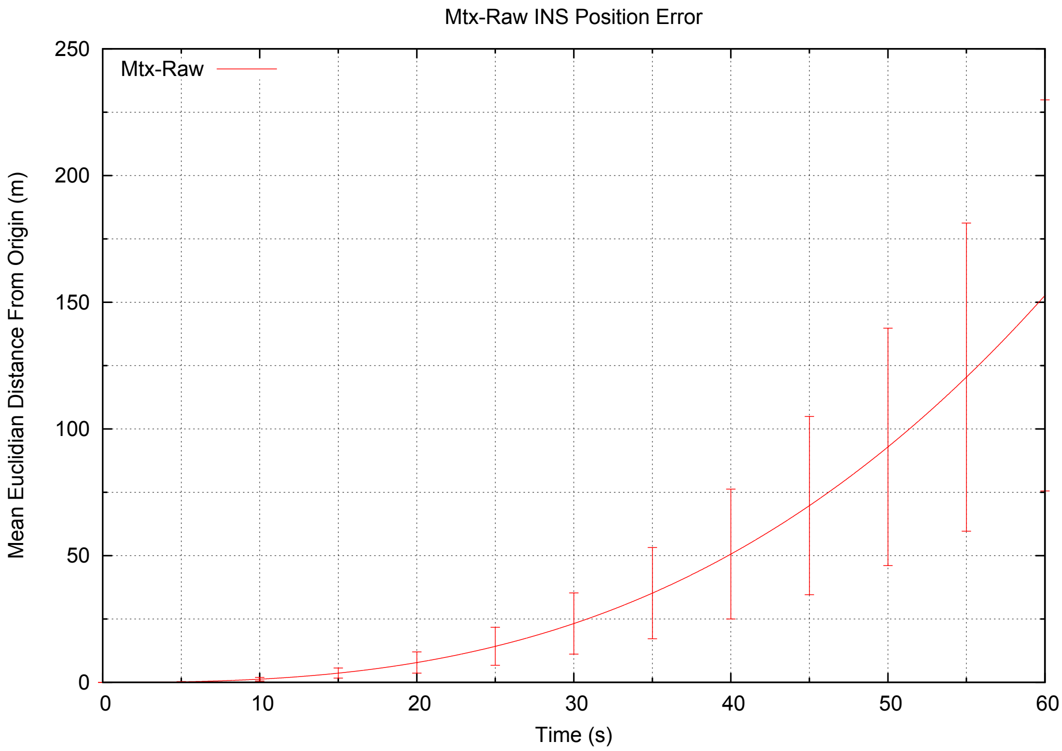

Figure 2.11: Average drift position of a static strapdown INS with a MEMS-based IMU. Source: Oliver J. Woodman [44].

gravity on Earth, any small orientation error will have a great impact in the position error.

The position error accumulation is especially evident if inertial sensors based on MEMS technology are used. In the Figure 2.11 the position error accumulation rate for a static strapdown INS using a medium-low cost IMU is shown. As can be seen, this position error rate makes navigation unfeasible after a few seconds. Therefore, the use of INS systems based on MEMS IMUs, which are the most convenient for pedestrians, seems complicated. And, in general, although high precision inertial sensors are used, the use of INS is limited in time. However, as will be seen in the following Section 2.4, by merging with other technologies and additional information sources, it is possible to use INS systems in such a way that they are useful for navigation. Among the different types of information that can be merged, those that allow the system to remain self-contained are now introduced.

A priori knowledge about object's dynamic

The knowledge about the characteristics of the movement of an object can give the possibility of identifying scenarios in which the value of some of the variables describing its movement is known a priori and, therefore, some corrections can be applied under that assumption.

One of the most common corrections are the ZUPT, which consist in detecting the moments in which it is known that the object is still. This allows correcting the value of the estimated velocity at that moment. In this way, the rate of accumulation of the velocity and position error is reduced, providing a longer operation time the INS.

Another corrective measure is the one known as *Zero-Angular Rate Updates* (ZARU), which, likewise, consists of detecting the static moments of the object but, in this case, to estimate the value of the gyroscopes' bias, since it can be assumed that their output values should be zero at those moments. In this way, the growth rate of the orientation error is reduced, which also impacts the estimation of the velocity and position.

These techniques have been successfully applied to different scenarios, such as underwater navigation [46], oil drilling [47] or geographic mapping [48], and, thanks to the characteristics of the human gait, it can also be applied to pedestrians. Through the use of foot-mounted IMUs, it is possible to detect the moments when the foot is still on the ground, which occurs periodically at each footstep. In this way, it is possible to periodically correct INS errors and reduce the accumulation of the position error to a rate proportional to the number of strides. Furthermore, the detection of the stance periods is possible using only the acceleration and angular rate signals, so the system remains self-contained. With this solution, position errors close to 1% of the traveled distance can be achieved using MEMS IMUs, surpassing even "pure" INS systems with higher performance IMUs. The work of Eric Foxlin is recognized for being the first to use efficiently the ZUPT technique for foot-mounted IMUs [18], and a good explanation can also be found in the work of Jiménez *et al.* [19].

Use of magnetometers

With techniques such as ZUPT and ZARU it is possible to reset velocity and position errors, estimate accelerometer and gyroscope biases and even correct tilt-related orientation errors. However, the heading error is not observable and is therefore currently the main limitation of the INS systems.

One of the most common solutions is the use of magnetometers, by means of which it is possible to calculate the direction of the magnetic north and, in this way, the heading error can be corrected. In addition, it also allows the system to remain self-contained.

Unfortunately, their use is restricted to outdoors scenarios, since the presence of metallic and electrical elements in buildings and different constructions cause distortions in the magnetic field, making the use of magnetometers unreliable as a measurement of the actual heading value.

2.3.2 Pedestrian Dead Reckoning Systems

Walking is the most common form of human locomotion and is based on the continuous repetition of a series of movements of different parts of the body, especially the lower limbs. From the different phases through which the foot passes, a pattern known as gait cycle or stride is defined. As can be seen in the Figure 2.12, a stride is defined between two consecutive moments in which a foot (by convention, the right one) begins the contact with the ground. During the gait cycle, the forward movement basically consists of moving one leg forward while the weight of the body is supported on the opposite leg, which has the foot resting on the ground.

The gait cycle is usually characterized by a set of gait parameters including the stride length and step length. These two gait parameters are close related: the stride length is defined between the positions of two consecutive footfalls of the same foot, while the step length is defined between opposite feet and measured in the forward direction. In fact, when walking straight and without anomalies, the stride lengths of both feet are equal and each stride length is equal to the sum of the last two step lengths.

The basic idea of the PDR technique is to adapt the DR method to the human walking fundamental characteristics, that is, to the gait cycle. Since walking occurs mostly on a usually level plane, PDR systems limit the estimation of the position to

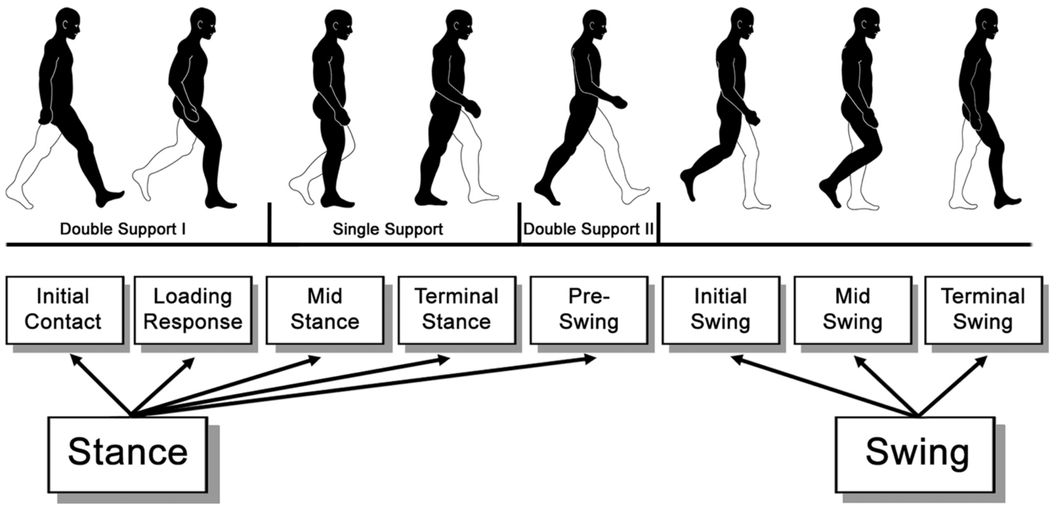

Figure 2.12: Functional divisions of the gait cycle: the gait cycle or stride has two phases. The stance phase is that part during which the reference foot remains in contact with the ground. It constitutes 60 percent of the gait cycle and includes five moments: the initial contact (Heel Strike), the loading response (Foot Flat), the mid and terminal stance, and the pre swing (Toe Off). The swing phase is rest of the gait cycle during which the reference foot swings in the air. Source: T. Stöckel *et .al* [49].

the two-dimensional case, expressing the trajectory of a person as a concatenation of stride lengths, as shown in Figure 2.13. This way, the position update after the k-th stride can be written as follows:

$$\begin{aligned} X(k) &= X(k-1) + SL(k) \cdot \cos(\psi(k)) \\ Y(k) &= Y(k-1) + SL(k) \cdot \sin(\psi(k)) \end{aligned} \tag{2.19}$$

where $SL(k)$ y $\psi(k)$ are the stride's length and heading angle, respectively. Similarly, the position update can also be expressed using steps instead of strides. This formulation based on gait parameters makes the PDR systems to usually be composed of three main blocks: SD, SLE and SHE.

Sometimes, information about the altitude is also necessary. This is the case inside buildings, where knowing the floor may be sufficient. This is usually known as 2.5 dimensional positioning.

Although the definition of many of the gait parameters is based on the position and movement of the feet (including the step length and stride length), the mechanical structure of the human body implies that both the causes and effects of the gait

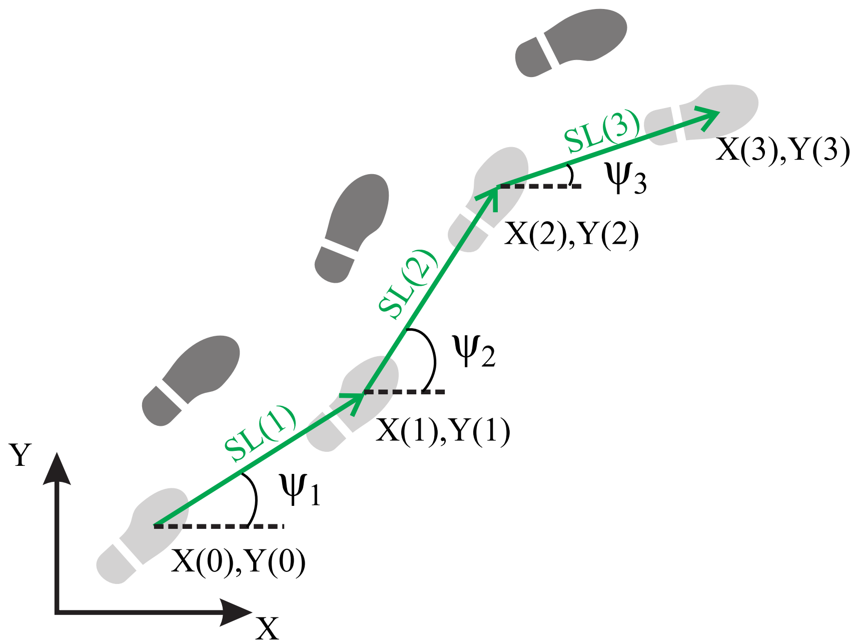

Figure 2.13: A pedestrian trajectory expressed as a concatenation of strides, through their length and orientation. Figure adapted from Francisco Zampella [50].

cycle will be distributed throughout different parts of the body. This means that there must be relationships between the signals observed in different parts of the body and the different gait parameters. Therefore, the knowledge of such models would allow to design the PDR blocks capable of obtaining the length and heading of the steps/strides from specific body parts. This is the main strength of PDR systems: thanks to the mechanical nature of the human body, PDR systems are flexible in relation to the mounting point of the sensors, thus improving their usability.

However, obtaining such models is not easy and usually involves biomechanical models or statistical learning techniques. In both cases, they obtain approximate models from a previous analysis of a reduced set of instances of the gait cycle. Therefore, the main weakness of PDR systems is a lack of generalizability that causes their performance to decrease when the characteristics of the motion or the user differ from the patterns used during model creation.

PDR systems can be implemented using different technologies. Some examples include electromyography sensors attached to the calf [51], ultrasonic ranging between the feet [52] or the combination of force sensor and ultrasonic transceivers

[53]. However, inertial sensors remain the most common technology for the implementation of PDR systems. Especially those based on MEMS technology, thanks to their cost, size, weight and their integration in many electronic devices in the market.

In summary, for the particular case of pedestrians and MEMS-based IMUs, INS is the general and more powerful method but, due to the current quality of that type of sensors, the only feasible implementation requires the use of ZUPT corrections and, therefore, foot-mounted sensors. In contrast, PDR systems offer a compromise between usability and adaptability: they allow greater flexibility in terms of the sensor's mounting point but their operation is usually optimized to a finite set of motions (commonly, forward walking and two-dimensional positioning) and user's characteristics. In addition, for both types of systems, the position error is proportional to the number of steps. For these reasons, as long as the quality of inertial sensors does not increase to allow the use of INS in more situations, PDR systems can be interesting and sufficient for many applications and use cases.

Since inertial PDR systems are the framework for this research work, the following Chapter 3 will focus exclusively on reviewing the state of the art of this type of localization systems.

2.4 Information Fusion

In any estimation process, having information from different sources is always positive. As a general rule, merging several estimates does not always improve the accuracy of the estimate. However, the precision of the estimate will always be better than the precisions of the individual estimates. This may be important for applications that may admit some error in estimation but require certain levels of integrity or confidence in the estimates. The merging of information can be done from various points of view:

Integration of several systems or technologies

When integrating several localization systems, a first strategy may be to use several systems with similar characteristics, in a redundant manner, such as a foot-mounted INS on each foot [54] or to combine a foot-mounted INS with a PDR carried in the pocket of the pants [55]. In this way, the estimation of the position may be improved but the overall system will continue to have the same types of weaknesses.

A fusion strategy that seems more interesting is to combine systems or technologies that have complementary characteristics. A simple example in relation to the coverage requirement could be the use of GNSS for outdoors scenarios and WLAN access points for indoors.

However, the most powerful strategy is to merge localization systems based on different methods, i.e. position fixing and DR. Remembering the main strengths and weaknesses of each type of method, it can be seen that they complement each other perfectly. DR based methods are scenario independent, have a good short-term accuracy but their errors accumulate unbounded over time. Meanwhile, position fixing based methods have bounded errors in the long-term but with a risk of temporary higher errors due to interferences or complicated scenarios. In addition, they depend on the infrastructure installed on the scenario.

The most common example of this strategy is the fusion of GNSS and INS systems. Furthermore, this integration can be done at different levels, depending on whether only the solutions of each systems is fused (loose coupling) or whether the fusion occurs during the estimation process (tight coupling and deep integration). Detailed descriptions can be found in references [15, 17, 36].

Prior knowledge

Another source of information that can be merged to improve estimates is the available a priori knowledge about the use case, which can be of different types:

- Information about movement restrictions: As previously discussed in Section 2.3.1.3, it is possible to use the knowledge about the characteristics of the motion to correct the estimation errors, being two of the best known techniques ZUPT and ZARU, which both make use of the moments when the feet are still on the ground.

  Another technique, known as *Heuristic Drift Reduction* (HDR) [56], is to assume that people usually walk in a straight line, especially inside buildings, which allows to reduce the drift in the heading.

- Information about the navigation scenario: Having information about the spatial distribution of the characteristics of a certain area is not sufficient to localize an object, but it can be useful to improve the estimation obtained by other means. The clearest example is having the map of a building. In addition to assisting in visualization, it can be used to apply corrections to the position estimation, both by using the complete building structure, such as in [57–59], the detection of landmarks of known position such as stairs, elevators, ramps [60], or by the detection of activities performed by the user that may be related to a certain position, such as opening a door.

  Similar to the HDR technique mentioned in the previous point, in addition to assuming straight sections in a building, it is also possible to use the “dominant” directions of the corridors of a building to correct the heading drift [61–64]. Such techniques will be discussed in Chapter 8.

  A more advanced technique is to simultaneously generate a landmark map while locating the object on that map. This technique is known as *Simultaneous Localization And Mapping* (SLAM) and has been widely used in robotics [65].

Dynamic estimation

The estimation methods for position fixing based localization systems seen in Section 2.2.2 assumed that the set of measurements received had been generated when the object was in the same position. This is equivalent to the object being static. When the object is in motion, fewer measurements will generally be available at each position, so the estimate will tend to be worse. However, it is possible to extend the estimation process by trying to use all the measurements received up to that moment. For this, it is necessary to have information about the dynamics of the moving object, so that it allows "linking" the previous measurements and position estimates with the current one, thus improving the estimation of the moving object.

The mathematical tool that is usually used for this type of information fusion is the Bayesian filtering. Given their importance and frequency of use in the field of localization, the following section introduces the main concepts and techniques.

2.4.1 Bayesian Filters

The basic idea is to propose that the probability density function of the estimation of the current position of the object, that is, its uncertainty, can be defined as the probability a posteriori conditioned to all the measurements received up to that moment t:

$$p(\boldsymbol{x}_t) = p(\boldsymbol{x}_t|\boldsymbol{z}_1, \boldsymbol{z}_2, ..., \boldsymbol{z}_t) \tag{2.20}$$

In general, the complexity of computing such posterior densities grows exponentially over time, since more measurements will be available. To reduce that complexity, Bayesian filters assume that the dynamic of the system is a Markov process. Translated to the localization scope, this means that it is possible to make predictions of future positions based solely on the current position, as it contains all the information about its status. In other words, the positions and measurements of the past do not provide additional information.

Under Markov's process condition, it is possible to convert the equation 2.20 into an iterative process, based on two phases. First, the filter predicts the next position from the current estimate of $\boldsymbol{x}_{t-1}$

$$p^-(\boldsymbol{x}_t) = \int p(\boldsymbol{x}_t|\boldsymbol{x}_{t-1})p(\boldsymbol{x}_{t-1})d\boldsymbol{x} \tag{2.21}$$

where $p(\boldsymbol{x}_t|\boldsymbol{x}_{t-1})$ represents the object's dynamic model, that is, how its position varies over time.

The correction phase then merges the newly obtained prediction with the measurements obtained in the period between $t-1$ and t. By applying the Bayes rule, the posterior probability is obtained as:

$$p(\boldsymbol{x}_t) = p(\boldsymbol{x}_t|z_t) = \frac{p(\boldsymbol{z}_t|\boldsymbol{x}_t)p^-(\boldsymbol{x}_t)}{p(\boldsymbol{z}_t)} \tag{2.22}$$

where $p(\boldsymbol{z}_t|\boldsymbol{x}_t)$ is the observation model and the measurement probability $p(\boldsymbol{z}_t)$ normalizes the product for ensuring that the posterior over the entire state space sums up to one:

$$p(\boldsymbol{z}_t) = \int p(\boldsymbol{z}_t|\boldsymbol{x}_t^-)p(\boldsymbol{x}_t^-)d\boldsymbol{x}^- \tag{2.23}$$

In this probabilistic model, $\boldsymbol{x}_t$ represents a state vector, so it may contain additional variables to the position such as velocity, orientation or the inertial sensor biases. In addition, since its formulation is done considering generic probability density functions, it facilitates the fusion of measurements from different types of sensors in a probabilistic way.

The calculation of the different integrals can be difficult to perform in real time. For this reason, there are different simplified implementations of this Bayesian formulation for certain specific cases:

Kalman Filter

The simplest case is the *Kalman Filter* (KF), which is based on a state-space representation of the dynamic system in discrete time, and it can be shown that it is the optimal estimator when the error distributions are Gaussian and the observation and dynamic models are linear function of the state vector. Although the original derivation of the KF used the orthogonality principle and iterative updates to find the best linear unbiased estimator, it can also be derived using a Bayesian approach, where “best” is interpreted in the maximum a posteriori sense, since for Gaussian errors is the same estimate.

So, since a Gaussian distribution is completely described by the mean and the covariance, the prediction stage has the following form:

$$\begin{aligned} \boldsymbol{x}^-(k) &= \boldsymbol{F} \cdot \boldsymbol{x}(k-1) \\ \boldsymbol{P}^-(k) &= \boldsymbol{F} \cdot \boldsymbol{P}(k-1) \cdot \boldsymbol{F}^T + \boldsymbol{Q} \end{aligned} \tag{2.24}$$

where $\boldsymbol{x}^{-}(k)$ and $\boldsymbol{P}^{-}(k)$ are the predicted mean and covariance matrix, respectively, $\boldsymbol{F}$ is the state transition matrix and $\boldsymbol{Q}$ is the covariance matrix of the process noise.

The correction stage will use the observed $\boldsymbol{z}$ measurements with its $\boldsymbol{R}$ covariance matrix for modeling the measurement noise:

$$\begin{aligned} \boldsymbol{x}(k) &= \boldsymbol{x}^{-}(k) + \boldsymbol{K} \cdot (\boldsymbol{z} - \boldsymbol{H} \cdot \boldsymbol{x}^{-}(k)) \\ \boldsymbol{P}(k) &= (\boldsymbol{I} - \boldsymbol{K} \cdot \boldsymbol{H}) \cdot \boldsymbol{P}^{-}(k) \end{aligned} \tag{2.25}$$

where $\boldsymbol{H}$ is the observation matrix and $\boldsymbol{K}$ is the Kalman constant:

$$\boldsymbol{K} = \boldsymbol{H}^{T} \cdot \boldsymbol{P}^{-}(k) \cdot (\boldsymbol{H}^{T} \cdot \boldsymbol{P}^{-}(k) \cdot \boldsymbol{H} + \boldsymbol{R})^{-1} \tag{2.26}$$

Extended and Unscented Kalman Filter

When some of the KF assumptions, i.e. linearity and normality, are not fully met, modified versions of the KF are usually used which, although sub-optimal, achieve good accuracies.

The first of these is the *Extended Kalman Filter* (EKF), which is based on the linearization of the dynamic and observation models, achieving a similar formulation in which the main difference is the use of the Jacobian matrices of those models, in which only the first terms of their Taylor series are taken.

The other variant is known as *Unscented Kalman Filter* (UKF), which is based on propagating over time a sampling of the mean and covariance of the state vector, which are known as "sigma" points. Through this process, states are propagated to the third order terms of their Taylor series, allowing for better estimates and faster convergence.

Particle Filter

When linearity or normality conditions are not significantly met, non-parametric filters, such as *Particle Filters* (PF), are often used. These filters do not assume any dynamic and observational models and are based on propagating a sampling of the probability distribution of the state vector over time. The main objective is to propagate only the most likely points of the sample, eliminating the most unlikely ones in order to reduce the complexity of the calculation. This technique is very flexible in terms of the type of measurements that can be used in the observation model, which is why it is usually the technique chosen to include highly non-linear information, such as map-matching information.

There are good references explaining these techniques in detail (KF/EKF [66, 67]; UKF [68];PF[69]) and their use in localization [40, 70].

2.5 Attitude and Heading Reference Systems

An *Attitude and Heading Reference System* (AHRS) is like a sub-module of an INS: it only tracks the orientation of the object by integrating the angular rates provided by a set of gyroscopes. Therefore, in the same way, the orientation error also accumulates over time and information from other type of sensors is usually fused to reduce or reset the error. Early AHRS designs were based on deterministic fusion strategies and they commonly used accelerometers for resetting the object's tilt, provided that it is static, and magnetometers for the heading [71, 72]. However, since the use of magnetometers to calculate the actual heading can only be reliably performed outdoors, more recent AHRS tend to choose probabilistic fusion strategies and only use such sensors to estimate the bias of the gyroscopes whenever a constant magnetic field is detected [73].

As mentioned in a previous section, the orientation of an object with respect to a reference frame can be represented in several ways: rotation matrix, Euler angles and quaternions. These three representations are equivalent as it is possible to convert each one into the others. However, each one has its pros and cons [45]:

- The rotation matrices, also called direction cosine matrices, are a three-by-three matrix whose columns represent the projection of the body reference vectors on the global reference. Its main advantages are that matrix mathematics is well known and that it is easy to perform transformations such as projections, scaling or translations. On the other hand, its main disadvantages are that it is not intuitive to visualize the orientation from the matrix expression. Additionally, it is a redundant representation, since it uses nine values to represent three degrees of freedom.

- Leonard Euler demonstrated that the orientation of a rigid body with respect to a fixed reference system can be defined as a sequence of three elementary rotations, the so-called Euler angles. The main advantage of this representation is that it is very efficient since only three values are necessary and that, knowing the rotation sequence, it is easy to visualize the orientation. On the other hand, the main problems are that to operate mathematically they must be transformed into rotation matrices and that some rotation sequences can generate a singularity in which a degree of freedom is lost. This situation is called gimbal lock.

- The quaternions are an extension of the complex numbers, defined by four parameters. They allow representing an orientation as a single rotation around a particular axis. Their advantages are their numerical efficiency with respect to the rotation matrices and that they do not suffer from Euler angles' gimbal lock problem. However, it is also not intuitive to visualize the orientation from its values.

For these reasons, during the mathematical formulation of INS strapdown mechanization, rotation matrices were used. In contrast, AHRS systems usually use Euler angles when their estimation is to be shown to the user. So, back to the Euler angles, there are 12 possible rotation sequences, defined with respect to the axes of the body's reference system. One of the most common one is the "ZYX" sequence, whose three angles are usually known as yaw, pitch and roll [74]. As can be seen in the Figure 2.14, yaw is the rotation angle around the vertical "Z" axis of the body. The term heading is sometimes used as a synonym but it is the angle to the north direction, while yaw is with respect to a reference frame which may not be north-facing. Pitch, also called elevation, indicates the rotation around the lateral axis "Y". And, finally, the roll angle, also called bank, is around the anteroposterior axis "X".

PDR systems usually have an AHRS to have a continuous estimation of the heading and, from it, to determine the heading of each step or stride. In addition, there are also systems that use the Euler angles signals as a source of information for detecting the steps or estimating their length. This is because, depending on

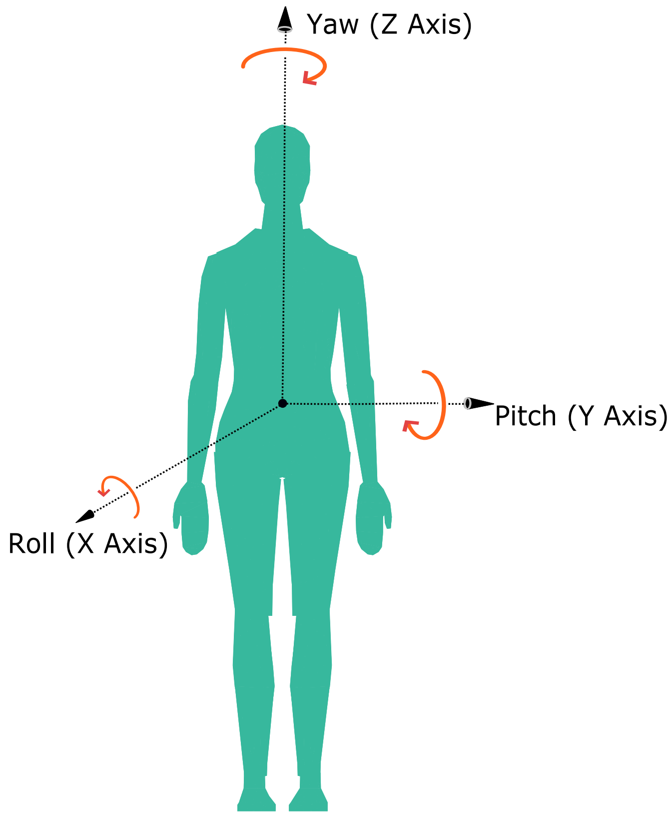

Figure 2.14: Definition of roll, pitch and yaw angles: although there may be variations depending on the definition of the body and global reference systems, in general, the yaw is measured in relation to the vertical axis and indicates the direction that the body faces, the pitch is measured in relation to the lateral axis and indicates the body's elevation, and the roll is measured in relation to the anteroposterior axis.

where the IMU is mounted, these angles can provide a lot of information about the position of some segments of the human body.

2.6 Summary

In this chapter we have reviewed the bases of the two main localization methods: position fixing and dead reckoning. As explained throughout the different sections, neither is able to offer a perfect solution but, fortunately, their strengths and weaknesses are complementary. Position fixing methods offer absolute positioning but require the installation of infrastructure, which limits their coverage, and their ac-

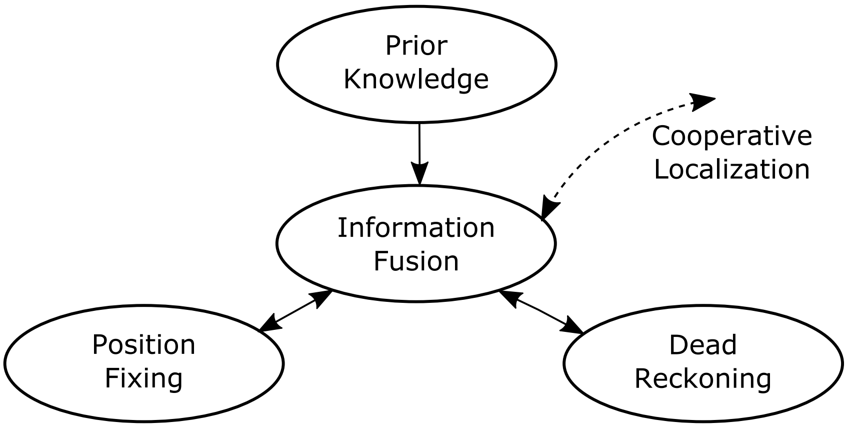

Figure 2.15: Conceptual architecture of a seamless localization system

curacy will be affected by sporadic interference and complex scenarios. The DR method is infrastructure-less, which makes it independent of the scenario. However, it only offers relative positioning and its great limitation is the unbounded accumulation of error over time.

The techniques of information fusion, in addition to allowing both methods of localization to be combined, they also allow merging a priori information about the scenario or the nature of the movements of the object to be positioned. It is even possible to merge the position estimates of other mobile nodes, in what is known as cooperative or network localization [75]. Therefore, it seems logical to think that the architecture of a system capable of providing localization information seamlessly should integrate all these elements, as represented in the Figure 2.15. However, the cooperative localization, the a priori information and the position fixing methods should be considered as opportunistic, as it cannot be assumed that they will always be available. This does not happen with DR based methods, which will work continuously, so they should be considered as the basis of a seamless localization system.

Therefore, when implementing a system with these characteristics for pedestrians, the use of wearable devices that include inertial sensors seems mandatory. Among them, wrist-worn wearables, such as smartwatch and smartbands, stand out for their availability on the market and their convenience for users.

Know how to solve every problem
that has ever been solved.

Richard Feynman

CHAPTER

3

Inertial PDR Systems: State of the Art

In the previous chapter it has been seen that DR-based localization methods are characterized by not requiring the installation of infrastructure in the environment. Among them, INS systems are a very general solution, capable of adapting to any type of motion. However, pedestrians can only carry sensors based on the MEMS technology and, due to their noise levels, the foot is the only recommended mounting point in order to make periodic corrections. PDR is another DR method that is less general than INS but more flexible in relation to the sensor mounting point. Therefore, it seems the right type of implementation to take advantage of the wearable devices available on the market.

The aim of this chapter is to identify the open challenges and improvement opportunities in the field of wrist-worn PDR systems and, on the basis of these, to define the specific objectives that were finally addressed during this research work. First, Section 3.1 presents a high-level review of the current state of the art of inertial PDR systems. Later, Section 3.2 focuses on those PDR systems that use wrist-worn inertial sensors, reviewing in depth each PDR block. However, given the scarcity of wrist-worn inertial PDR systems, a small experiment is carried out beforehand to verify the equivalence between wrist-worn and handheld. Since they

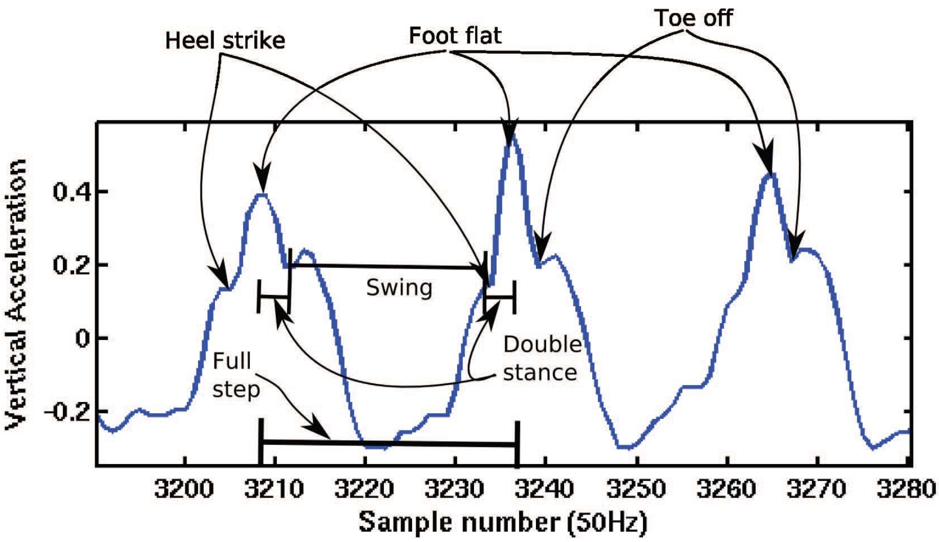

Figure 3.1: Vertical acceleration of the center of mass (COM) of the pedestrian's body while walking. Some gait cycle events defined in the Figure 2.12 can be detected in the COM's vertical acceleration. Source: Diego Álvarez *et al.* [76].

can be considered almost equivalent under some conditions, the review at block level also included handheld PDR systems. Finally, the specific objectives, that are the core of this dissertation, are detailed in Section 3.3.

3.1 Inertial PDR Systems

Since the end of the 20th century, many proposals for PDR systems based on inertial sensors have appeared. Point Research Corporation proposed the first electronic systems that automatically executed the PDR method [77, 78]. An IMU consisting of accelerometers and magnetometers was usually mounted close to the trunk. At this body location, or in any one coupled to user's *Center Of Mass* (COM), the effects from both feet's strides can be experienced. As can be seen in Figure 3.1, the acceleration shows clear patterns associated to the trunk's periodic movements while walking and, in addition, it is possible to identify some of the events that define the gait cycle. Therefore, the step detection from body locations coupled to the COM seems favorable and this led to the design of PDR systems working at a update frequency equal to the step rate. Regarding the step heading, since the position and orientation of the sensor with respect to the body was fixed, these first PDR systems obtained the step headings from the sensor's heading. Finally, the first PDR systems assumed a constant step length value or they estimated it by means of a regression model constructed from the existing relationship with the step rate. Specifically, the first systems from Point Research Corporation detected the steps by looking for the peaks in the magnitude or the vertical component of the acceleration and the heading was obtained by using the magnetometers as a compass, compensating the possible tilt with the accelerometers.

Subsequently, much of the research work has focused on finding better SLE methods, with two types of proposals appearing: on the one hand, methods based on biomechanical models that achieve good accuracy but require calibration for each user and walking speed [76, 79–81]; and, on the other hand, methods based on regression models that usually offer lower accuracy but generalize better to different users and walking paces without the need of an individual calibration [82, 83].

The most common mounting points for these trunk-mounted systems are usually the low back and the waist, with the IMU aligned with the direction of travel, although this is not strictly necessary and there are some techniques robust against the misalignment between the sensor's heading and the travel direction [84]. Also, due to the difficulty of using magnetometers indoors, there are proposals that avoid them and use mainly gyroscopes to estimate the heading [85].

The head is another part of the body strongly coupled to the COM. For this reason, similar PDR systems have also been proposed that mount the IMU on a helmet [86, 87] or use the ones included in smartglasses [88, 89]. There are also proposals that mount the sensor on the ankle [90] or on the feet [91, 92]. For the latter, when comparing the performance of a PDR-based implementation with an INS-based implementation, it is found that similar positioning errors can be achieved but that there is no additional advantage from using PDR. Therefore, it seems clear that, for foot-mounted IMU, INS is the best option.

Despite the favorable conditions offered by the feet or the trunk to install a PDR system, these systems did not find commercial success, possibly because of the need for specific devices, which is often not convenient for users. Undoubtedly, one of the facts that has revitalized the research in the field of PDR systems is the incorporation of inertial sensors into the smartphones. Thanks to their wide adoption by consumers and the fact that they offer more and more features and power, they have become the target device for implementing PDR systems over the past few years.

However, as discussed in Chapter 1, smartphones cannot be considered as wearable devices as they are not physically attached to the body. This means that, in addition to not being possible to claim that they are in constant contact with the pedestrian, their position and orientation with respect to the user's body can change over time [23]. This complicates the detection and estimation of the gait cycle parameters.

As a result, early smartphone-based PDR systems used to limit their use cases to a single pose or carrying mode of the device. Some of them considered that the smartphone was held with the hands in front of the user's face while walking around [93, 94]. This carrying mode, sometimes referred to as "texting", assumes that the user is viewing or using the phone while walking. This assumption may be valid for short periods of time in which the user checks his/her position while navigating but it does not seem likely that a pedestrian will make a long way keeping the smartphone in this pose. The reason why this carrying mode was one of the first ones to be considered is because the phone is quite coupled to the COM, so similar methods as the ones of the trunk-mounted PDR systems can be applied.

Other authors considered that the smartphone is constantly stored in one of the most common places: the front pocket of the trousers. Bylemans *et al.* proposed one of the first PDR systems for this body location [95], basing the stride detection and stride length estimation methods on the ones of the ankle-mounted PDR system proposed by Kim *et al.* [90]. The work of Steinhoff and Schiele [96] proposed a more robust stride detection based on the peaks in the variance of the vertical acceleration and a method for obtaining the direction of travel based on estimating the axis of rotation of the leg. Also noteworthy in this area is the series of works by Díaz [97, 98], in which she uses the variations in the pitch of the thigh (i.e., its angle of elevation) to detect each stride, estimate their length and even estimate the variation in height when going up or down stairs. As can be seen, since the dynamics experienced from the trouser pocket are mainly associated to that same leg, these PDR systems work at the stride rate.

However, considering that the phone is carried in a single way all the time does not seem realistic. For this reason, current proposals of smartphone-based PDR systems try to work robustly for, at least, the most common modes of carrying this device. Namely, handheld while texting, handheld while calling, handheld while swinging the arm as when freely walking, and stored in the front pocket of the trousers. From now on, to keep things short, these carrying modes will be referred to as texting, calling, swinging or pocket, respectively.

Currently, there are two types of strategies on how to achieve this goal. On the one hand, some authors design each PDR block to be able to process all the different carrying modes included in their scope [99, 100]. On the other hand, some authors are opting for including an additional block in the PDR system to detect the way in which the device is being used at any given time. Later, they execute different methods of each PDR block specifically adapted for the detected carrying mode. Some examples of differentiated SD methods can be seen in [101–103], SLE methods in [104, 105] and SHE in [105]. In addition to the device carrying mode, this classifying module can also detect the user's motion mode, such as walking, running, going upstairs/downstairs, and so on, being even capable of detecting moving platforms such as elevators or escalators [106]. From now on, this optional block will be referred to as *Mode Classification* (MC).

While the use of these MC blocks certainly helps to develop more robust smartphone based PDR systems, they are not perfect solutions yet. Like any method that relies on a previous definition of patterns or use cases, the performance will decline significantly when the scenario to be processed differs from that definition. This is, undoubtedly, the big open problem with PDR systems in general: the lack of adaptability to non-seen before scenarios.

The main conclusion of the previous chapter was that, to achieve a seamless pedestrian localization system, it is necessary the fusion of different technologies and information sources, where PDR systems can play the role of base technology. As proof of the validity and interest of this idea, many authors have proposed hybrid systems that include inertial PDR systems. To mention just a few examples: a handheld smartphone plus a GPS receiver [107]; a handheld smartphone with map-matching [105]; a pocket-mounted PDR and a wrist-worn WLAN receiver [108]; or the fusion of foot-mounted INS and pocket-mounted PDR [55].

3.2 Wrist-worn Inertial PDR Systems

As already mentioned in the introduction chapter (1.4), there are few PDR systems specifically designed for wrist-worn inertial sensors:

Kao *et al.* [30]

Kao *et al.*'s work was among the first to explicitly use wrist-worn inertial sensors. However, the aim of their work was not to design a complete wrist-worn PDR system but only a SLE block adaptive to the user's motion mode through integration with a GPS system. To this end, they propose the use of a MC based on a decision tree for differentiating between static, walking and running motion modes. For each motion mode, they define a different set of parameters of a non-linear regression model of the stride length, which uses the step frequency and the acceleration variance over a step as input features. The integration with GPS is carried out by means of an EKF which allows the SLE coefficients to be adjusted to the characteristics of the specific user.

Both the analysis and the experimentation have a limited scope: it seems they only considered the swinging carrying mode, no details are given about the SD, the SHE or how the SLE's input features are obtained, and the performance is reported using only the traveled distance as performance metric.

Qian *et al.* [31]

Qian *et al.* described the first complete wrist-worn PDR system– this according to the present author's knowledge. Similar to Kao *et al.*, they use a tree decision based MC and different SLE models for the walking and running cases. For the SLE they use the same input features, that is, the step frequency and the acceleration variance over a step, but combined in a linear regression model. Their SD method is based on detecting the moments in which the acceleration magnitude crosses a dynamically adapted threshold, together with some validations on the duration of the steps, the sizes of the acceleration peaks and the existence of a periodic behavior of the acceleration signal. As for the SHE block, they use a well-known AHRS for tracking the sensor's orientation and use the periodicity of the arm swinging to get the step heading by querying the AHRS's heading when the arm is always in the same pose.

Again, the analysis and experimentation is limited: on the one hand, they do not make it clear enough whether, as it seems, they only deal with the swinging carrying mode. In addition, they constantly mix the concepts of step and stride, which does not help to clarify the design of the system. On the other hand, the experimentation consists of a single outdoor test on a rectangular circuit. And the performance is reported only as a distribution of the relative position errors without enough details about how it was computed. In future works of the same author ([105, 109, 110]) they use the same PDR design for handheld smartphones in several carrying modes, with a similar experimentation and reporting.

Duong and Suh [32]

Duong and Suh proposed a wrist-worn PDR, but it was specifically designed for people moving with the help of a walker. They considered two styles of using the walker: step-by-step walking, suitable for patients who have an injured leg and use the walker as crutches; or continuous walking, for patients who use the walker for balance only and they keep it always in contact with the floor. For the first style, they implement an INS system, since they are able to detect some moments in which the hand's velocity is zero, so ZUPT can be applied. For the other one, a PDR system is designed including only the SD and SLE blocks.

Although it is not a complete PDR system (it does not include SHE and only evaluates the traveled distance) and its scope is a very specific use case, it is an interesting, well explained and well executed work, which reinforces the motivation about the interest and convenience of wrist-worn devices for positioning purposes.

Jiang *et al.* [33]

Jiang *et al.* agree that the fact that smartphones can be away from the user's body makes it difficult to use them for location purposes and that, on the contrary, wearables represent a great opportunity. Then, they focused on two challenges of the current commercial wrist-worn pedometers: the unreliable step counting and the still in research step length estimation. First, they proposed a method to reduce the false positive steps that can occur when the pedestrian is still and performs any movement similar to the arm swinging. It is not a SD method but an additional validation stage. As for the SLE, they proposed a biomechanical model for the swinging mode. However, some of the assumptions they used for deriving the model are not sufficiently supported by references or experiments. In addition, the calibration method, which seems important for its proper functioning, was omitted and the experimentation and evaluation were rather limited. Although the ideas they proposed seem to have enough potential, again a complete PDR system is not covered and there is room for improvement in the performance evaluation.

As can be seen, the number of PDR systems specifically designed for the wrist is small. However, intuition leads us to believe that a wrist-worn PDR system could perhaps be considered as a sub-case of a smartphone-based PDR system. The first condition for this to be true is, of course, to consider only the carrying modes in which the smartphone is held in the hand, such as texting, calling and swinging. And secondly, it should be checked whether a sensor carried in the hand and one carried on the wrist can be considered equivalents. To this end, this hypothesis is defined: if the wrist joint is fixed, one inertial sensor on the wrist and one on the hand may be considered equivalent. In the following section, a simple experiment is performed to test the validity of this hypothesis and, if so, the smartphone-based PDR systems will be also included in the revision of the different methods for each PDR block.

3.2.1 Equivalence between Handheld and Wrist-worn Inertial Sensors

In order to test the validity of that hypothesis, the following experiment has been designed: an IMU will be installed on the wrist and another one will be handheld. Then, a series of arm movements will be performed. Finally, the accelerations and angular velocities recorded from both inertial sensors will be compared. To

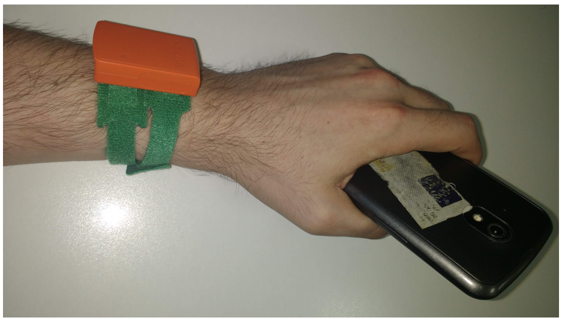

Figure 3.2: Equivalence between handheld and wrist-worn inertial sensors: hardware installation

determine whether equivalence exists, the similarity and synchronization of the signals recorded from both body locations will be visually checked. Given the difficulty of installing both sensors in the same orientation, only the magnitudes of both types of signals will be used.

The hardware and installation, that can be seen in the Figure 3.2, consist of the following:

- On the wrist, a MTw motion tracker, manufactured by Xsens, was mounted. This device includes a 3D-accelerometer, a 3D-gyroscope, a 3D-magnetometer, and a barometer and some velcro straps were used to fix it on the left wrist. For logging the inertial data, the MT Manager software provided by the manufacturer was used.

- A Samsung Galaxy Nexus was held in the left hand. This smartphone includes the same kind of sensors as the MTw motion tracker. For logging, the app called "GetSensorData" provided by the LOPSI-CAR-CSIC-UPM research group was used [111].

The experiment includes three trials and, in each of them, a similar set of arm movements will be performed but allowing different degrees of motion of the wrist joint and forearm:

- In the first trial, with the elbow on a table and keeping the wrist joint fixed, a series of forearm flexion and extension movements are firstly performed and, then, with the forearm in upwards vertical orientation, a series of supination

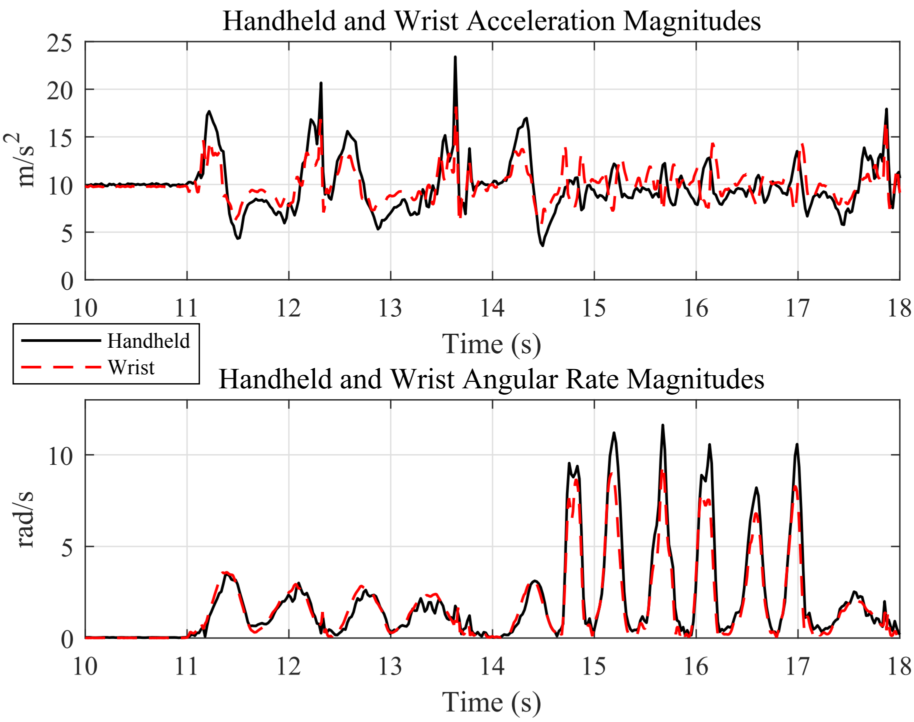

Figure 3.3: Equivalence between handheld and wrist-worn inertial sensors: results of first trial

and pronation turns are performed. By keeping the wrist joint fixed, it is expected that the wrist and hand movements are coupled.

- During the second trial, again with the elbow on the table and the forearm in upwards vertical orientation, the hand performs a series of movements and turns but only from the wrist joint, keeping the forearm as static as possible.

- Finally, in the third trial, and again with the elbow on the table, some elbow flexion, extension, pronation and supination movements are performed simultaneously to hand movements from the wrist joint.

Before each trial, a series of controlled movements are performed to synchronize the signals from both inertial sensors during the post-processing.

In Figures 3.3 and 3.4 the signals obtained at each trial are seen, from which these observations can be made:

- In the first trial, the wrist joint was fixed, so it is expected that the accelerations and angular rates should be quite synchronized. As can be seen in the Figure 3.3, the synchronization is clear for the angular rates. For the accelerations, it seems that they are better synchronized during the first flexion/extension movements than during the next supination/pronation turns. Additionally, in general, the signals from the wrist tend to be slightly smaller.

- The second trial shows that, as can be seen in Figure 3.4a, it is possible to move the hand while keeping the forearm quite static. This effect would be even more evident if, for example, the smartphone were manipulated only with the fingers.

- Finally, in the third trial, as can be seen in Figure 3.4b, it is possible to move the hand and the forearm in a way in which the inertial signals from handheld and wrist-worn sensors seem quite uncoupled, especially the accelerations. This is because the elbow's pronation/supination rotations are always transferred to the hand, so it will be very likely that they will be registered by the handheld sensor.

In summary, the results seem to indicate that it is possible to consider handheld and wrist-worn inertial sensors as equivalents as long as the wrist joint is fixed. However, care should be taken with any method that uses as variables the specific values of peaks or integrated areas since, as have been seen, the values on the wrist tend to be lower because it is not easy to keep the wrist joint completely fixed. Therefore, the following sections will review the different PDR blocks proposed for both wrist-worn and handheld inertial PDR systems.

3.2.2 Step Detection Methods

Most wrist-worn and handheld PDR systems follow the strategy of using a single SD method for several carrying modes. In general, these SD methods are similar to those used in trunk-mounted PDR systems. Therefore, this means that they assume that the IMU is quite coupled to the COM. This assumption may be valid for quasi-static carrying modes such as texting or calling but is not so clear for dynamic modes such as swinging.

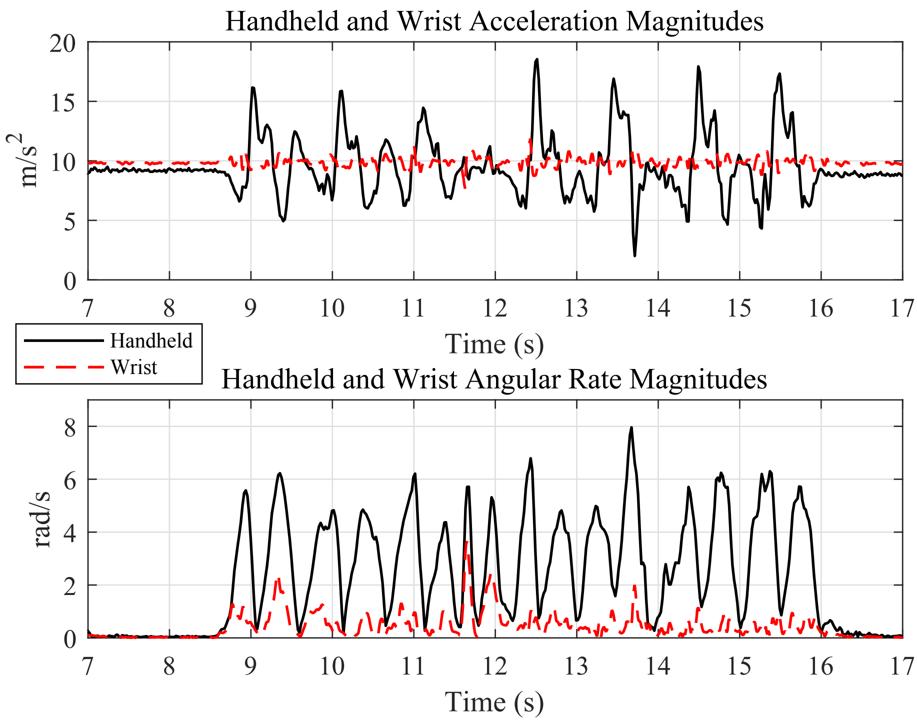

(a) Results of second trial

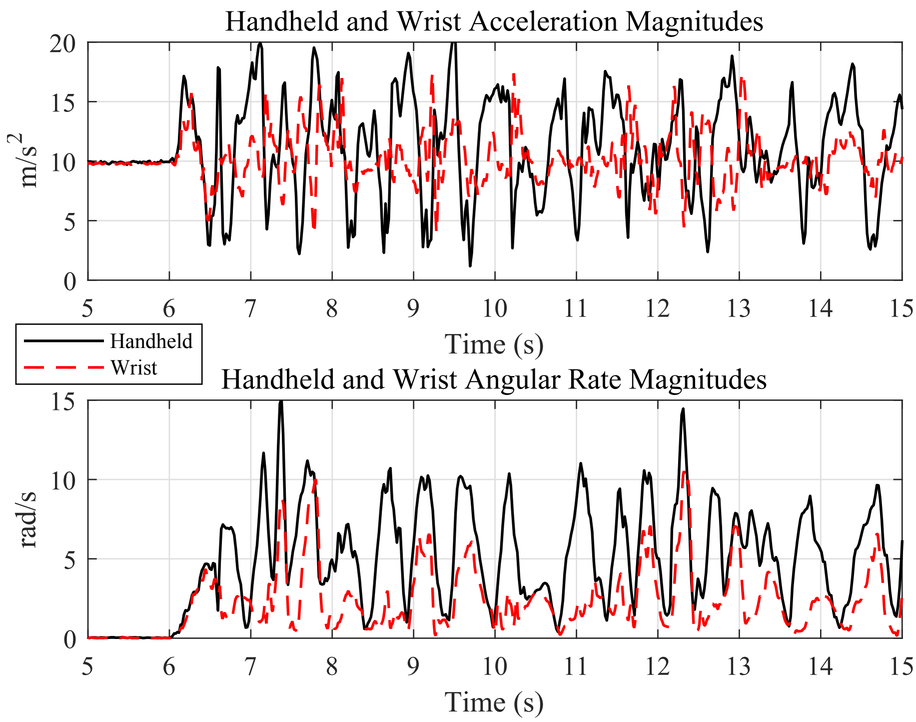

(b) Results of third trial

Figure 3.4: Equivalence between handheld and wrist-worn inertial sensors: results of second and third trials

As stated in the survey on SD methods for smartphones conducted by Brajdic and Harle [112], there are three main types of SD methods: time domain methods, frequency domain methods and statistical learning methods. The time domain methods are the most common ones because of their lower computational load and, in general, they have a common structure: first, a pre-processing stage is applied to the signal, which usually consists of filtering the high frequency components that are far from the step or stride frequencies; then, some technique is applied to detect the events that identify the possible step candidates; and, finally, a set of validations are performed to confirm which candidates are real steps.

Similar to trunk-mounted PDR systems, the ideal seems to use the accelerations expressed in the global or navigation reference frame, especially the vertical component since, as it was seen in Figure 3.1, the step events are reflected quite clearly. However, since this implies having a good estimate of the orientation of the IMU, many authors choose to use the magnitude of the acceleration, which is immune to changes in orientation, and where the vertical component is usually the predominant one.

Regarding the time-domain techniques for detecting step candidates, it can be distinguished two approaches:

- Windowed Peak Detection: As shown in Figure 3.1, each footstep produces a peak in the COM's accelerations. Since it is a periodic event, the detection of such peaks is usually performed within a time window.

- Threshold Crossing: As the acceleration patterns have a sinusoidal shape, the signal will cross the value determined by the average acceleration over a step (usually the local gravity value or zero if it is eliminated), which marks the beginning, the end and, approximately, the midpoint of the step cycle.

The main limitations of the peak detection method are the presence of multiple local peaks from bounces and peaks from movements not associated with real steps. In order to differentiate them, the peaks are usually validated by checking their size. Since different user walking paces produce different peak sizes, that threshold must be adaptive. And also the length of the window used during the detection.

The threshold crossing technique is generally more robust to different walking paces. However, during moments of speed change, the average acceleration over a step can vary, so it is also common to find adaptive threshold crossing [31].

When validating step candidates, a common technique is to check if the time elapsed between consecutive step candidates is valid with respect to the normal range of human walking cadences. Another common validation is to check if the pedestrian was actually walking by measuring the periodicity of the acceleration signal or using a simplified MC that classifies whether the pedestrian is still or walking. Other authors propose comparing the step candidate's signal with a previously known pattern using techniques such as dynamic time warping [113] or fuzzy detectors [114].

Thus, there are many proposals that combine these techniques in different ways for designing SD methods for wrist-worn and handheld PDR systems. A nice review of the main SD methods for smartphones can be found in the Davidson and Piche's survey work [10]. Also, some examples of wrist-worn and handheld SD methods can be found in [31, 93, 94, 99, 100, 104, 105, 109, 110, 113–118].

As mentioned before, other authors choose to use different SD methods depending on the device carrying mode:

- Susi *et al.* designed a decision tree based MC that uses different features of the acceleration and angular rate magnitudes to classify the carrying mode into swinging, quasi-stable (such as texting or calling), irregular or still. It then runs a peak detection SD algorithm for the quasi-stable and swinging modes only, using acceleration and angular rate as input signals, respectively [101].

- Xiao *et al.* summarizes all the possible locations and movements of a sensor on the human body in two: symmetric for those places where both strides are experienced (i.e. steps), such as trunk-mounted, and handheld calling or texting; and asymmetric when the stride from one side is mainly experienced, such as handheld swinging mode or in the pocket. The MC method that differentiates the two modes is based on checking the periodicity of two signals: the vertical acceleration (symmetric mode) or the Euler angle's pitch (asymmetric mode). The steps are then detected by zero-crossing on the corresponding signal [102, 119].

- Tian *et al.* proposes a MC that differentiates between pocket, texting and swinging modes based on the orientation of the device, checking the mode transitions with a finite state machine. Then they use different signals as input to a peak detector. Specifically, the acceleration of the z-axis, the vertical acceleration and the y-axis acceleration respectively for each mode [103].

It should also be noted that there are proposals for techniques that try to reduce the false positives that occur when moving the arms in a similar way to swinging while the pedestrian is really still. Xiao *et al.* proposed to calculate the displacement produced during a step by integrating the accelerations. Although the displacement obtained may not have been correct, it allowed the authors to implement a decision tree to determine the validity of the step [102]. A similar technique is also used in [100]. Jian *et al.* studies the synchronism between the peaks, valleys and crosses of the vertical and anteroposterior accelerations when the pedestrian is still or in motion. By observing that these events are more synchronized when the user is static, it is possible to eliminate false positives in this situation [33].

In general, the performances achieved with all these methods are quite good (errors of less than 3 percent) but none of them is 100% reliable. According to Brajdic's work ([112]), the examined SD methods tend to underestimate the number of steps. This suggests that there could be a tendency to design SD algorithms specially robust against false positives, which could result into slightly overfitted algorithms. In this way, any movement that does not fit the assumptions used during the design could lead to missing steps (i.e., false negatives), which could explain the tendency to underestimate. Thus, the main open problem of the wrist-worn and handheld SD methods is to be more adaptive to different users and scenarios, including some that have not been addressed or resolved yet, such as walking while the arms are moving irregularly, or very short walks, in which there is no time to detect periodicities and the initial and final steps may be significantly different.

3.2.3 Step Length Estimation Methods

The SLE with inertial sensors is a problem that can be considered to be at an earlier research stage than the SD. The main difference between these two PDR blocks is that, while the SD only has to detect whether or not an event has occurred, SLE methods must estimate the value of a characteristic of that event, which is usually more complicated. Firstly, because the length is a continuous variable with infinite possible values and, secondly, because the possible models that define the step's behavior depend directly on each user. Each pedestrian, depending on their anatomical characteristics and other variables such as their physical condition, fatigue, carried weight or the slope of the terrain, chooses different combinations of step length and walking cadence to achieve the desired speed. In this way, SD methods usually obtain similar performances over different users because the existing variability of the inputs has to be reduced to only two possible outcomes: there is a step or not.

The studies and analysis about the step length done by the fields of gait analysis and biomechanics have generated the necessary theoretical basis for the design of SLE methods. On the one hand, through the definition of biomechanical models, such as the one that relates the vertical displacement of the COM with lengths of the stride and the user's leg [120]. And, on the other hand, by identifying the existing relationships between the step length and other features such as the step frequency [121].

PDR systems started to use this knowledge about the step length for designing SLE methods using inertial sensors. In the case of the wrist-worn and handheld PDR systems, some authors take advantage of this knowledge about the COM's mechanical behavior to design SLE methods using the existing geometric relationships [80] or empirical approximations of them [79, 81, 94, 99]. As with the SD methods, this can be valid for use cases in which the IMU is tightly coupled to the COM, such as calling or texting, but it does not seem to be the most suitable option for other carrying modes such as swinging. By contrast, SLE methods implemented as regression models can be better adapted to different carrying modes. Especially those that use features that are independent from the carrying mode, such as using only the step frequency [93, 113] or in combination with the user's height [101]. Other authors prefer to add additional features such as the variance of the acceleration over one step to improve the accuracy of the estimate over different users and walking paces but, as stated before, this makes the SLE less flexible to different carrying modes [31, 116]. For this reason, as was also the case for the SD methods, some authors use different sets of parameters of the regression based SLE methods according to the carrying mode [104] or the user motion mode [30].

The only SLE method based on a biomechanical model specifically designed for the upper limbs is the one recently proposed by Jiang *et al.* for the swinging case [33]. The aim of their method is to estimate the vertical displacement of the COM from the arm displacement during the swinging and, then, use it as input to the already mentioned biomechanical models of the COM. The authors derived a geometric model that relates the COM's vertical displacement (b) from the arm length (m), the horizontal displacement of the hand due to the arm swinging (d) and the vertical displacements during the downward ($h1$) and upward ($h2$) phases. The definition of these variables is shown in Figure 3.5. However, the definition and implementation of the model raises some questions about the performance it will achieve, which are not fully clarified during the experimentation and evaluation. On the one hand, the arm displacements ($d, h1, h2$) are obtained through integration of the accelerations, which is always challenging. On the other hand, some assumptions used to derive the model raise some doubts:

- Does the maximum height of the COM coincide in time with the vertical position of the arm? Does it occur when the arm swings in both directions? No reference or source is provided for this assumption which is basic for the derivation of their model.

- The horizontal displacement of the hand due to the arm swinging (d), when obtained by integration of the accelerations, will also include the effect of the horizontal displacement produced by the step itself. That is, while the vertical displacements ($h1, h2$) include the effects due to both the swinging and the COM, the horizontal one (d) does not include COM's horizontal displacement.

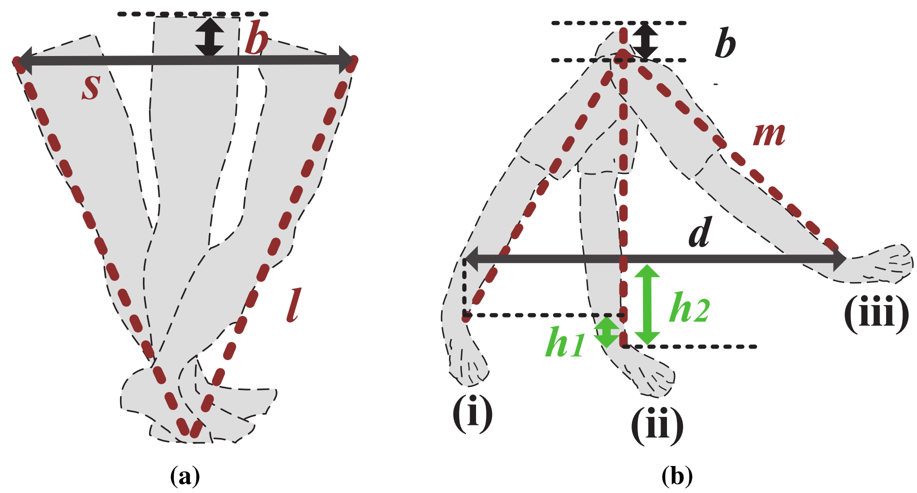

Figure 3.5: There exist SLE methods based on the mechanical relationship between the COM's vertical displacement (bounce b) and the user's leg length (l), as can be seen in figure (a). Jiang *et al.* propose a geometric model to derive that bounce b from the displacements of the wrist or the hand during the swing ($d, h1, h2$) and the user's arm length m, as shown in figure (b). Source: Jiang *et al.* [33]

- The role of the elbow joint, which establishes a second axis of rotation, modifies the effective length of the arm and makes the swinging to occur not only in a vertical plane, was not taken into consideration.

Currently there are many proposals for SLE methods using inertial sensors, both based on biomechanical and regression models, but none have become the gold standard solution. One of the main reasons for this is the lack of a standardized methodology shared by the research community to determine how the procedures of testing, evaluation and comparison of SLE methods should be carried out. This lack of definition means that the quality of those procedures in many works is low and that the reported results are not sufficient to identify the best algorithms. This can be considered as one of the biggest challenges in the current SLE field, as it prevents a reliable comparison of the different proposals and therefore an effective and efficient progress of the research.

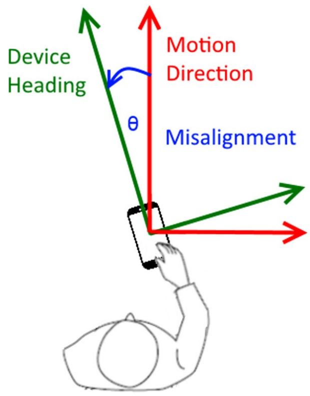

Figure 3.6: Heading offset or misalignment angle between the sensor unit and the walking direction. Reprinted by permission from Springer Nature: Medhat Omr *et al.* [122].

3.2.4 Step Heading Estimation methods

Travel direction estimation is undoubtedly the most critical part of DR-based localization systems because any heading error causes a position error that increases continuously if the translation continues and the error has not been corrected.

In the case of PDR systems, the SHE block have two problems to solve: firstly, to estimate the heading of the inertial sensor unit and, then, to correct the possible offset or misalignment angle between the sensor's heading and the user's walking direction (see Figure 3.6). Because PDR systems integrate steps or strides, the walking direction is defined between consecutive step or stride positions. That is, possible variations in user orientation are ignored while the step is being executed.

Despite its criticality, many works on PDR systems do not pay special attention to the SHE block or even ignore it. This also reflects the difficulty of finding new solutions to existing problems. When reviewing the different difficulties that may affect the SHE and the proposed solutions that exist, different scenarios can be distinguished according to two variables: the variation of the orientation of the IMU with respect to the walking direction and the possibility of using magnetometers to measure the direction of the earth's magnetic field.

First, if it is assumed that the IMU keeps fixed its orientation with respect to the walking direction and there is no magnetic interference, the simplest SHE is to use magnetometers as if it were a compass. It is usually necessary to correct the tilt of the compass, which can be achieved using accelerometers. As discussed at the beginning of this chapter, this type of SHE is used by trunk-mounted PDR systems but could also be used by wrist-worn or handheld PDR systems when the device is in a very fixed orientation. As for the offset between the IMU and the walking direction, since it will be constant, it can be measured beforehand. It is also possible to estimate the walking direction from the principal direction of the horizontal projection of the accelerations [84].

If the Earth's magnetic field cannot be measured reliably, gyroscopes must be used to keep updated over time the known initial walking direction. If the IMU can be mounted with one of its axes parallel to the user's vertical axis, the integration of only one gyroscope will be required [85]. In these magnetometer-free cases, the possible heading offset is eliminated by setting the initial heading value of the IMU with the initial walking direction. Therefore, the heading error will be only due to the accumulation of gyroscope's bias.

Of course, these first two scenarios are too ideal since it is practically impossible to keep a sensor with a perfectly fixed orientation when it is mounted on a pedestrian. If the orientation variation is small, as in the case of the texting mode, it would be possible to continue using the IMU as a compass by averaging the values of the accelerometers and magnetometers, or to project the angular velocity vector onto the vertical navigation axis to obtain the walking direction by integration [94].

However, carrying modes such as swinging imply a continuous and considerable change in the orientation of the IMU. This complicates the two sub-problems of the SHE block. On the one hand, to know the orientation of the IMU, AHRS systems must be implemented, which use the measurements of the accelerometers and, if possible, magnetometers during the static periods of the IMU to reset the accumulated orientation errors due to the gyroscopes integration. Unfortunately, the static moments of upper limbs during swinging walks are rare, which causes a significant error to get accumulated in AHRS systems. Michel *et al.* made an interesting comparison of the performances of different AHRS on handheld devices, including tests under dynamic and magnetic interference conditions [123] . On the other hand, the offset between the IMU and the walking direction varies during the execution of each step, which makes its correction difficult. Some authors choose to take advantage of the periodical nature of human walking and identify the moments when the offset value is constant in order to measure it beforehand. This is the case of Qian *et al.*, who used the gravity crossings of the acceleration for that purpose [31]. If it is not possible to measure the offset value previously, some authors choose to average the values of the IMU heading over the step [99]. This method may be useful in cases where the offset value varies around zero or at least crosses that value. Another option would be, again, to look for the dominant direction of the horizontal projections of accelerations, as proposed by Xiao *et al.* using least squares regression [102]. The problem of this method with dynamic carrying modes is that a good estimation of the orientation of the IMU is required for error-free projection. In addition, if the accelerations due to arm movements are very strong, they may make it difficult to identify the direction of travel.

Logically, heading offset varies according to the carrying mode. Some authors take advantage of the carrying mode transitions in which the offset in the first mode is known, such as the texting mode, to "learn" the offset of the new mode, on the assumption that the walking direction has not changed during that transition [103, 113].

Since the SHE is currently the block that limits the use of PDR systems, it is common to fuse additional information to alleviate heading errors. In this sense, some authors choose to merge several inertial sensors, such as Loh *et al.*'s proposal that implement a smartglasses based PDR system and reduce the SHE error using the headings from a smartwatch [89]. As it was seen in Section 2.4, it is common to use scenario information such as detailed maps buildings or at least their dominant directions. Some PDR systems, such as [85, 99], implement a simpler heuristic known as HDR, which consists of assuming that the pedestrian mainly walks in a straight line.

In summary, in addition to the general difficulties of AHRS systems (namely, gyro error accumulation, optimal fusion with accelerometers and magnetometers, and protection against magnetic disturbances), the main SHE problem concerning handheld or wrist-worn PDR systems focuses on the correction of the variable heading offset in a more general way. In addition, it would also be useful to explore the possibilities offered by the mechanical nature of the upper limbs in order to identify static moments in which to reset AHRS errors.

3.3 Specific Objetives Definition

The main goal of this research work is to contribute to both the understanding and the improvement of the performance of wrist-worn inertial PDR systems. To this end, the purpose of this chapter that reviews the state of the art of inertial PDR systems is to be able to identify open challenges or questions and improvement opportunities whose resolution or fulfillment contributes to the achievement of the main goal. The following is a description of the identified tasks that are addressed in this research work and that, therefore, constitute its specific objectives.

Deep Analysis of Wrist-worn Inertial Signals

In the different reviewed works of handheld and wrist-worn PDR systems it has been noted that the shape and behavior of the inertial signals collected from this part of the body is usually taken for granted. This can be relatively understandable for static carrying modes such as texting or calling, for which it can be assumed that the sensor is coupled to the pedestrian COM. However, for the swinging case, no work has been found that analyzes the characteristics of the inertial signals and whether they vary according to some factors.

It has also been seen that most proposals use mainly acceleration signals. Few use Euler angles or angular velocity signals to implement the different PDR blocks.

For these reasons, before starting to design new methods for wrist-worn PDR systems, it is considered necessary to make a deep analysis of the characteristics of the signals coming from different types of wrist-worn sensors and their variability with respect to factors such as the type of carrying mode, the walking speed or different users. This analysis would allow gaining a better understanding of the existing patterns in the wrist-worn inertial signals, see how far they are from being uniform patterns and, using this information, assess the feasibility of developing robust wrist-worn inertial PDR systems.

Specific Objective 1: *To expand the existing knowledge about the characteristics and variability of the different signals generated from wrist-worn sensors, with the aim of evaluating their suitability for the design and implementation of wrist-worn inertial PDR systems.*

Step Length Estimation Methods based on Inertial Sensors

As indicated in Section 3.2.3, the lack of a clear methodology to guide the design, testing and evaluation of SLE methods is one of the reasons why it is considered that the resolution of this problem is still at the research stage. When defining any methodology, it is necessary to know previously all the aspects that must be taken into account about the process to be standardized and the different alternatives available. However, this general vision does not currently exist in the field of SLE, which leads to the existence of many proposed algorithms, based on different models and methods, tested in different ways and evaluated using different metrics. Of course, this problem is not specific to wrist-worn PDR systems but affects any sensor mounting point and any application using SLE methods. This leads us to define the following specific objective:

Specific Objective 2: *To obtain a deep overview of the complete design and evaluation workflow of the SLE methods based on inertial sensors, so that it serves as a starting point for a better methodology in that research topic.*

Evaluation of wrist-worn inertial PDR systems

The results reported in the limited literature do not provide enough information about the performance of wrist-worn inertial PDR systems, especially in real and large scenarios. In addition to trying to get a better sense of its performance, it is also important to do so in comparison to other state-of-the-art inertial pedestrian navigation systems.

Therefore, an additional specific objective is to implement a real-time wrist-worn inertial PDR system and evaluate its performance against other inertial pedestrian navigation systems that can mount the IMU on other body locations.

Specific Objective 3: *To implement a wrist-worn inertial PDR system and evaluate its performance in real scenarios, as well as comparing it against other state-of-the-art inertial pedestrian navigation systems.*

Heading drift reduction techniques

As mentioned in the review of the different blocks of the inertial PDR systems, the SHE is currently one of the main sources of position error, which can have two origins: the accumulation of error in the estimation of the IMU's heading and the error due to the heading offset between the IMU and the walking direction.

In order to mitigate the first issue, there exists a set of proposals that apply some heuristics using prior information about the building in which the trajectory is taking place. These heuristics assume that the majority of the buildings are composed of parallel and perpendicular straight corridors, oriented towards a small set of directions, known as dominant directions. Among them, the method that presents the best results is the one proposed by Jiménez *et al.* known as *improved Heuristic Drift Elimination* (iHDE). However, their proposal is designed for a foot-mounted INS system and is integrated into the error-state KF. Therefore, an additional specific objective is defined for adapting the improvements proposed by iHDE and implementing them in a PDR system. Specifically, in a wrist-worn inertial PDR system.

Specific Objective 4: *To adapt the method "improved Heuristic Drift Elimination" so that it can be used in PDR systems and evaluate its capacity to reduce the heading drift for the case of a wrist-worn inertial PDR system.*

Logically, there are more problems to be solved or studied, belonging both to PDR systems in general and to wrist-worn systems in particular, but this set of objectives covers most of the inertial PDR architecture (see Figure 3.7), so it is expected that a good overview of this research topic can be obtained. Some of the most important pending challenges, not covered within this thesis dissertation, are listed below:

- Upper limbs' irregular movements: It is quite common for the arms to make movements other than swinging while walking, such as looking at the time on the clock, scratching, waving, or gesturing while speaking. Therefore, despite their unpredictability, it is necessary to design algorithms that are capable of processing them and not simply ignore them.

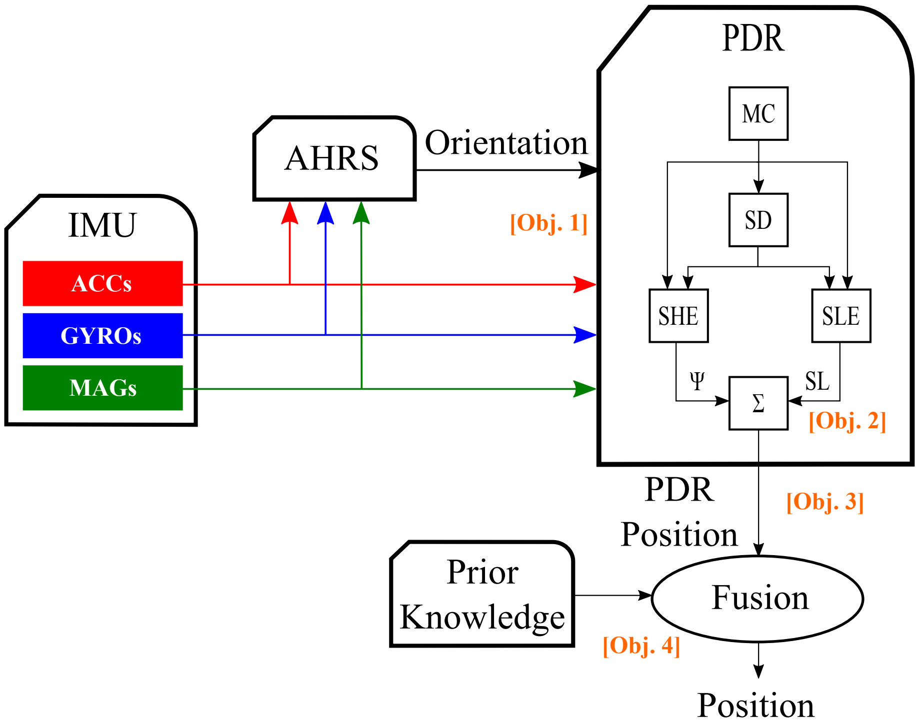

Figure 3.7: Architecture of an inertial PDR system and distribution of the defined specific objectives

- User Calibration: It is necessary to find methods for adjusting the configuration of wrist-worn PDR systems in order to make their performance more user-independent.

- Realistic scenarios: There is a lack of knowledge about the effects on the upper limbs of scenarios such as, non-forward steps (back, lateral, diagonal,...), stairs, non-flat paths, or a sensor loosely attached to the user's wrist.

- Daily activities detection: Take advantage of the possibility offered by the wrist to detect daily activities in order to merge additional information and improve the position estimation.

- PDR systems integration: Address the fusion of several PDR systems mounted on different parts of the body, taking advantage of the availability of different electronic devices such as smartphones, smartwatches or smartglasses.

3.4 Summary

This chapter 3 summarizes the process that has been carried out to define the specific objectives of this research work. First, a high-level review of the different PDR systems in the literature has been conducted. Subsequently, the focus has been on the wrist-worn PDR systems, reviewing the state of the art at the level of each PDR blocks. Previously, a small experiment on the equivalence between wrist-worn and handheld inertial sensors has been explained, leading to the inclusion of the latter ones in the block level review. Finally, based on the vision obtained from the literature, a set of specific objectives have been defined that constitute the content of this work. The following chapters of this dissertation will explain how each of these tasks has been addressed and what results and conclusions have been obtained.

People are not 'well-behaved' mathematical functions.

Admiral Grace Hopper

CHAPTER

4

Suitability Analysis of Wrist-worn Inertial Sensors for PDR Systems

As discussed in the previous chapter, PDR systems that mount the sensor on the upper limbs, either wrist-worn or handheld, often limit their scope to a small set of types of carrying modes: namely, swinging, texting and calling. However, this definition of use cases is not usually accompanied by an in-depth analysis of the characteristics of the different signals, so little is known about the behavior of these signals in relation to factors such as different users or walking speeds.

This chapter presents the work carried out in relation to the *specific objective 1*, the aim of which is to extent the knowledge about the characteristics of the signals coming from different wrist-worn sensors. Specifically, the work presented in this chapter consisted in the installation of several inertial sensors on the body of a group of users, collect the data generated while they walked with different arm movements and, afterwards, analyze the signals' variations over different people, walking speeds and arm motions.

The structure of the chapter is as follows. Section 4.1 reviews the current knowledge in the field of biomechanics about the role and characteristics of the arms while walking. The method adopted to collect the experimental data is described in Section 4.2. Section 4.3 analyzes and describes the obtained data. The implications for implementing wrist-worn PDR systems are discussed in Section 4.4. Finally, a summary of the chapter and the conclusions drawn are presented in Section 4.5.

4.1 Biomechanics: The Arms During the Gait

Usually, biomechanical studies of human gait mainly analyze the role of the lower limbs, considering the rest of the body as one mass. Still, the survey of Meyns *et al.* collects the existing literature on the origin and objective of arm swinging while walking, making it clear that it is a complicated topic with no definitive conclusions as yet [124].

It is well known that swinging the arms is synchronized with the opposite side's foot. That is, the most advanced position of the left hand coincides with the right footstep, and viceversa. However, there are several hypotheses about how arm swinging is really generated:

- Passive origin: By using modeling tools, such as dynamic walking or modeling the arms as an inverted pendulum, it is possible to predict the swinging of the arms without any additional force except gravity and inertia. These models are also able to predict the transition of the oscillation frequency of the arms between the step frequency and the stride frequency, depending on the walking pace.

- Active origin: By using electromiographyc measurements, there has been detected periodic muscular activity in the shoulders accompanying the walking. However, the impossibility of studying the effects of each individual muscle alone makes it difficult to determine whether the aim of the muscle activity is the arm swinging or shoulder stabilization.

Currently, there is no consensus about which hypothesis is right or, as Meyns *et al.* indicate as more probable, whether the origin is really hybrid: part passive and part active. In case there is some active component, then there is an objective reason for swinging the arms. Here, too, there are several different hypotheses:

- Gait stability: Apart from the clear role of the arms in helping recover stability after a large perturbation of the gait, there are contradictory studies as to whether it actually optimizes the stability during steady state walking.

- Energy reduction: Different studies have claimed that arm swinging helps decrease the angular momentum about the vertical and the vertical ground reaction moment. Consequently, there would be a reduction of energy consumption.

- The legacy of the quadrupedal origin of humankind: The robust coupling between the upper and lower limbs in various locomotor activities and the study of inter-limb connections are indirect arguments that support the hard to prove hypothesis that claims that when humans started to walk bipedally, the use of the arms during locomotion did not disappear completely.

Others have studied how the characteristics of arm swinging can change in relation with different parameters: Mirelman *et al.* explained how the arm swinging amplitude, and other walking related parameters, depend on the age of the person, the walking pace, and even the cognitive load during walking [125]. From the results they present it can be observed that the amplitude of the arm swing presents an important variability between different people and a clear asymmetry between the dominant and the non-dominant arm. In another interesting work, Carpinella *et al.* studied the equivalence between walking overground or on a treadmill, since this device is commonly used for gait analysis [126]. Their results indicate that they are not equivalent, especially for slow paces.

In short, the origin and role of the arms during walking is still an open problem. However, results such as those of the last two references clearly indicate that their behavior varies significantly depending on different factors. This reinforces the motivation on the need for a deeper analysis prior to the design of better wrist-worn PDR systems.

4.2 Experimental Method

This section presents the procedure followed for collecting the data. Specifically, it describes the hardware used, how it was installed, the tests performed by the users who participated in the experiment and an introduction to the methodology used to analyze the signals obtained.

4.2.1 Hardware Description

Regarding the sensor units, six new generation MTw motion trackers, manufactured by Xsens, were used. These devices include a 3D-accelerometer, a 3D-gyroscope, a 3D-magnetometer, and a barometer. They were installed on the feet, the right front pants pocket, the chest, the left shoulder, and the left wrist (see Figure 4.1a). This distribution of the motion trackers was chosen for collecting data for several studies about wearable devices. However, in this work only the ones from the wrist and the chest were used, as well as the ones from the feet as additional and assistant information. Therefore, the ones from the pocket and shoulder were not used.

Velcro straps provided by Xsen were used to fix the position of the thigh, feet and wrist motion trackers. A lycra T-shirt from Xsens was used for an easy placement of the sternum and shoulder motion trackers. The wrist-worn motion tracker was installed on the left wrist, as if it were a watch, because the rate of right-handed people is higher, and it is common to wear watches on the non-dominant arm. They were connected by cables to a laptop in a backpack and data were recorded at 100 Hz sampling rate. Figure 4.1b shows the definition of the sensor frame on the left wrist motion tracker. The MTw trackers also include an AHRS that provides the orientation of the sensor.

4.2.2 Experiment description

The experiments took place in the offices of the Institute of Communications and Navigation of the German Aerospace Center (DLR) in Munich, where 11 healthy people participated in the data collection, three women and eight men, whose ages ranged from 25 to 60 years, and height from 1.52 m to 1.91 m. They were asked to walk four times along a straight corridor 65 m long, performing a different carrying mode each time:

- Swinging: This is the more natural way of moving the upper limbs when walking with the hands free. Users were asked to walk this way in two of the

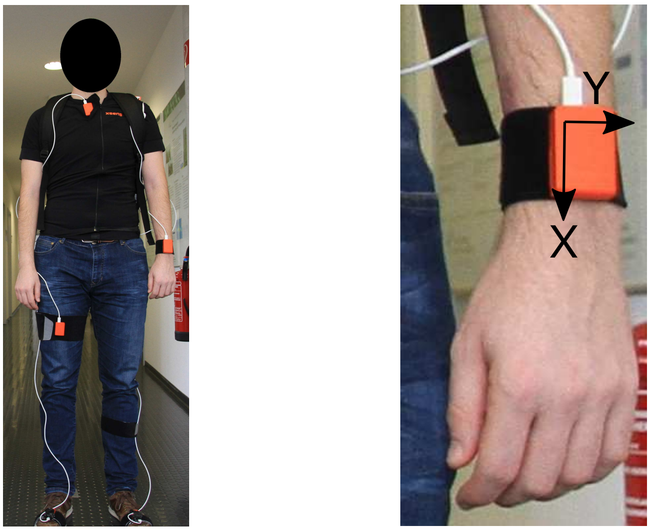

(a) (b)

Figure 4.1: Motion trackers installation: (a) Motion trackers were installed on the feet, the right pocket, the chest, the left shoulder and left wrist. (b) Frame definition of the wrist-worn sensor (Right-hand rule).

four walks.

- Texting: During one walk, users were asked to hold a real smartphone with both hands and pretend to text a message. The exact pose of the wrists was determined by the natural way each user performs that activity while walking.
- Calling: In a similar way, users were asked to put the smartphone close to their left ear, holding it with their left hand, and pretend to speak while walking. They were not given any indication about how to move their heads.

Texting and calling are representative of all the different carrying modes in which the wrist or the hand have a fixed, or almost fixed, pose, such as carrying a weight or having the hands inside the pockets of a jacket, for instance. This kind of carrying mode will be referred to hereafter as "quasi-static modes". Additionally, data from a set of more challenging arm motions were also collected, such as moving the hands while explaining something, waving to somebody, checking the time on a watch, or scratching different parts of the body.

Each participant repeated the set of experiments at three different walking speeds: slow, normal, and fast. The walking speed was determined by a person acting as pacemaker, who adapted his step frequency by following a metronome set at 85, 95 and 115 steps per minute, for the three walking speeds. The participants were asked to follow the pacemaker's walking speed but not necessarily the same step frequency.

In summary, a dataset is available from 11 different people, each of whom walked 12 times a 65 m long straight corridor at three different walking rates and performing three different carrying modes.

4.2.3 Signal Analysis Methodology

The raw measurements of the accelerometers, gyroscopes, and barometer were collected, as well as the Euler angles (as defined in Figure 4.2) provided by the AHRS included in the motion trackers. The measurements from the magnetometers were ignored due to the typical existence of magnetic disturbances in indoor environments.

Due to the mechanical structure of human body, the motion of the wrist can be considered as a combination of two motions: the motion of the trunk and the relative motion of the wrist with respect to the trunk. The trajectories of the trunk while walking present clear step or stride patterns and they have been studied for a long time [85, 120]. Although there exists certain variability of those patterns depending on the users and walking speed, the repertory of patterns is smaller than the one of the upper limbs. For this reason, a lot of trunk-worn PDR systems continue to be proposed [128]. In order to take advantage of that knowledge about the trunk, the analysis performed in this work was especially oriented to check whether the periodic patterns of the signals collected in the wrist are similar to the ones of the trunk, to the ones of the relative motion or they are a combination of the two, as well as to know how they are affected by different users, walking speeds and carrying modes.

Additionally, with the aim of facilitating the understanding of the behavior of the different signals, the measurements from the foot-mounted motion trackers were also processed and a logical signal that represents the landing of the feet

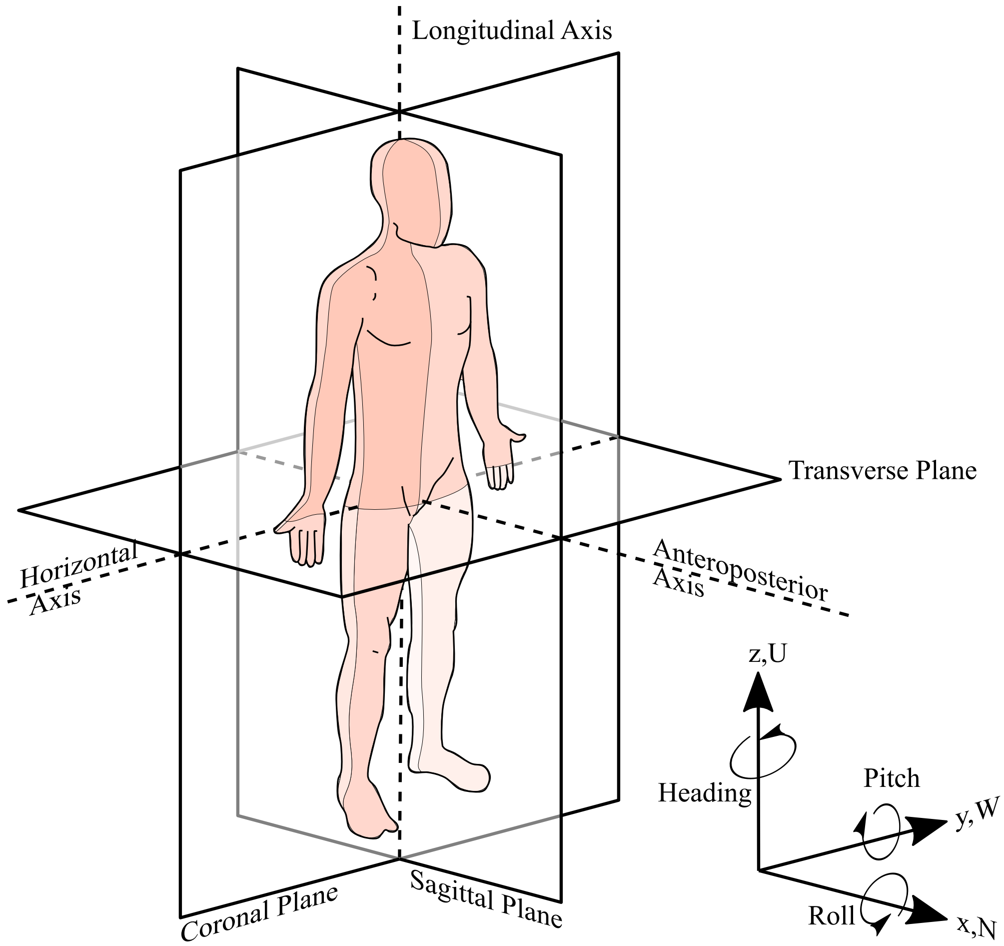

Figure 4.2: Definition of anatomical planes and axes, the North–West–Up navigation frame and the Euler angles. Source: adapted from Edoarado [127]

was generated. This support signal takes the value “high” from the strike of the heel to the moment when the foot is completely flat on the ground and it was plotted in most of the figures throughout the work for helping in the identification of the relationship between the shape of the different signals and the footsteps.

4.2.4 **Limitations**

We are aware that this study has some limitations:

- Only straight walks were considered, so it was not possible to study the behavior of the arms while turning.

- Only flat ground scenarios were considered, so it was not possible to study the behavior of the signals generated in the wrist when there is a change of altitude, such as when climbing stairs, for instance.

4.3 Description of the collected signals

In this section, the characteristics of the signals collected by the different sensors when walking will be described. As mentioned before, one of the aims of this work is to study the variability of those signals over different carrying modes, walking speeds, and users. In order not to extend the length of this chapter too much, a selection of images has been made: only the ones that clearly reflect that variability, or illustrates one observation, have been included. If not stated otherwise, the rest of datasets will behave similarly.

4.3.1 Accelerometers

The raw acceleration values in the sensor frame depend on the sensor's orientation. For this reason they are not used for detecting patterns, unless the orientation of the sensor is known and constant, which is not the case for wrist-worn sensors. Some processed acceleration signals, ideally independent from the sensor's orientation, are commonly chosen instead:

- Magnitude of acceleration: This signal is not affected by the sensor's orientation nor does it accumulate error over time. Its only error is the magnitude of the vector formed by the errors of each accelerometer. However, the only information it provides is the strength of the total effective acceleration experienced by the sensor.

- Navigation frame acceleration: By using an AHRS, the raw accelerations can be projected to a known fixed frame. But since the orientation estimation is not perfect and accumulates error over time, the values of the components of the acceleration in the navigation frame can be wrong. However, the tilt error can be reset whenever the sensor is static and, depending on the quality of the gyroscopes, some AHRS systems manage to maintain a stable tilt estimate for some time even under dynamic situations (about 10-20 seconds maximum for the Xsens MTw). In contrast, the values of the horizontal components will depend on the heading over time, whose error is quite difficult to reset in magnetically disturbed environments. For these reasons, they are not usually chosen for pattern detection.

Therefore, the acceleration signals considered in this work are the magnitude of the acceleration, and the vertical component and the horizontal magnitude in the navigation frame. Accelerometers do in fact provide measurements of the specific force, i.e., the difference between the true acceleration in space and the acceleration due to gravity. On the one hand, for simplicity, the gravity term will be obviated in the equations. On the other hand, for clarity, its effect will be kept in the signals plotted in the figures.

As mentioned before, we can express the chosen signals of the wrist acceleration ($\vec{a_w}$) as a combination of the ones from the trunk acceleration ($\vec{a_t}$) and the relative acceleration ($\vec{a_{wt}}$):

- Vertical component of the wrist acceleration:

$$a_{w_Z} = a_{t_Z} + a_{wt_Z} \tag{4.1}$$

- Magnitude of the horizontal components of the wrist acceleration:

$$||\vec{a_{w_H}}|| = \sqrt{||\vec{a_{t_H}}||^2 + ||\vec{a_{wt_H}}||^2 + \sum_{i=x,y} 2a_{t_i}a_{wt_i}} \tag{4.2}$$

- Magnitude of the wrist acceleration:

$$||\vec{a_w}|| = \sqrt{||\vec{a_{w_H}}||^2 + a_{w_Z}^2} = \tag{4.3}$$

$$= \sqrt{||\vec{a_t}||^2 + ||\vec{a_{wt}}||^2 + \sum_{i=x,y,z} 2a_{t_i}a_{wt_i}} \tag{4.4}$$

Firstly, the step or stride patterns that appear in the trunk's acceleration signals considered in this work will be reviewed. As long as the users have no gait pathologies, all datasets can be considered as equivalent for the purpose of visualizing the patterns in the trunk. Thus, Figure 4.3 shows those signals obtained during one of the walks that *"User 1"* took. The generated patterns are described next:

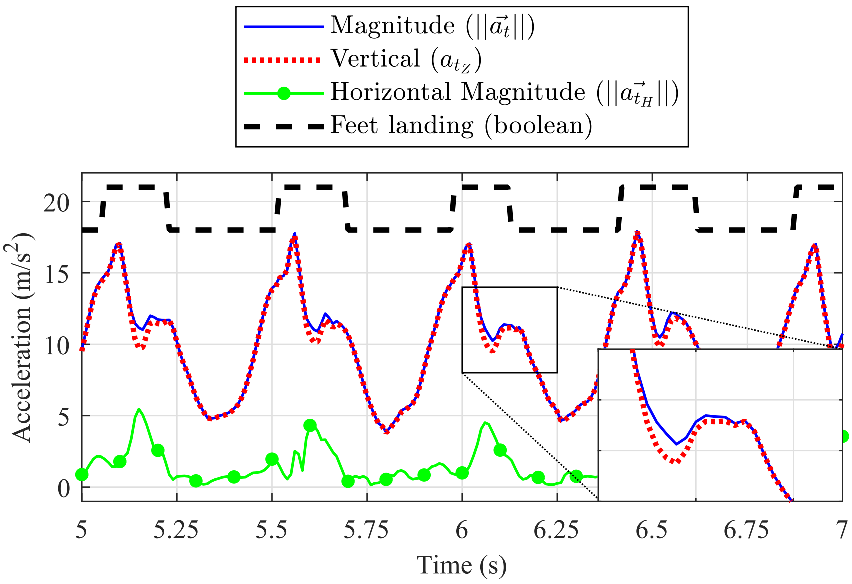

Figure 4.3: Vertical component, magnitude in the horizontal plane, and total magnitude of the trunk's acceleration from *"User 1"* walking fast in texting mode. The accelerometer placed on the chest is considered as representative of the trunk. Additionally, a logical signal that represents the landing of the feet (from heel strike to foot flat) is also plotted. The magnified area shows how the difference between the magnitud and vertical accelerations is bigger during the impacts of the footsteps.

- Horizontal magnitude: Considering the frame defined by the anatomical planes and axes shown in Figure 4.2, it is intuitive to say that the principal frequency of the trunk's acceleration projected on the anteroposterior axis will be periodic with a frequency equal to the step frequency. Meanwhile, the projection on the horizontal axis will be at the stride frequency, due to the alternating swing of the trunk at each footstep. These two axes are generators of both the anatomical transverse plane and the navigation horizontal, since they are parallel. Therefore, the magnitude of the acceleration in the navigation horizontal plane, due to the operation of squaring as part of the computation of the magnitude, will always have the step frequency as its principal one, as can be seen in Figure 4.3. In case there is a clear asymmetry in the footsteps, a stride frequency component can also appear, which will be visible in the temporal domain especially in the different amplitudes of alternating peaks.

- Vertical acceleration: This signal has a sinusoidal shape, as a consequence of the periodic upward and downward motion of the trunk between footsteps, with a transient at each peak generated by the alternating impact of the feet on the ground. This signal has a larger amplitude and power than the horizontal magnitude, and it can also be affected by possible asymmetries when walking.

- Magnitude of the acceleration: This signal is the combination of the two previous ones but, due to the larger values of the vertical acceleration, the magnitude's shape will be similar to the vertical one. Their differences will be more visible especially during the impacts of the footsteps, coinciding with the peaks of the horizontal acceleration's magnitude, as can be seen in the magnified area of Figure 4.3.

According to expressions (4.1)–(4.4), the patterns of the wrist's acceleration signals will depend on both the patterns of the trunk and the relative accelerations, as well as on how they synchronize with each other. Since the trunk's patterns are already known and their variability over different walking speeds and users is smaller than the one of the relative patterns, it could be considered that wrist patterns are the trunk patterns modified by the relative motion patterns and the way they synchronize with each other. Therefore, we could focus the study on the variability of the relative patterns. Unfortunately, the relative accelerations are not available and the subtraction of the wrist and trunk accelerations can be performed with a tolerable error only for the vertical component. In the case of the magnitude signals, this is the expression that is obtained by computing the difference of the horizontal magnitudes (and similarly for the total magnitudes):

$$||\vec{a_{w_H}}|| - ||\vec{a_{t_H}}|| = \frac{||\vec{a_{wt_H}}||^2 + \sum_{i=x,y} 2a_{t_i}a_{wt_i}}{||\vec{a_{w_H}}|| + ||\vec{a_{t_H}}||} \tag{4.5}$$

In both cases, considering that the tilt error of the AHRS should be small for short walks that started in a static pose and that all the motion trackers are equal, gravity will be eliminated when subtracting the signals. Since both the vertical and magnitude differences are proportional to the relative signals, the variability of the latter over different carrying modes, walking speeds and users will be analyzed indirectly, by seeing how the average difference between the wrist accelerations and the trunk accelerations during a walk varies over those parameters. A specific analysis for each carrying mode will be presented next.

4.3.1.1 Quasi-static carrying modes

For quasi-static carrying modes, such as texting or calling, intuition could tell us that the relative acceleration ($\vec{a_{wt}}$) should be virtually zero in all directions. In order to check if this is true, for each experimental dataset, we computed the absolute value of the three differential signals: the vertical relative acceleration, the expression (4.5) for the horizontal magnitude and, analogously, for the total magnitude. Later, they were averaged during the central segment of each dataset (i.e. the initial and final fifth parts of the walks were discarded). Table 4.1 presents the values obtained for each signal of interest, carrying mode and walking speed. In order to summarize the data, the mean, the standard deviation and the coefficient of variation was computed over the 11 users.

The mean and standard deviation values of the quasi-static carrying modes show that the differences between the wrist and trunk signals are clearly different from zero for most of the time and in any direction. This will lead to an alteration of the trunk patterns. Let's see how these differences vary with respect to the walking speed, different users and specific pose of the wrist:

- Walking speed: It can be seen in table 4.1 that these differences increase with the walking speed.
- Different users: The values close to 20% of the coefficient of variation indicate that there is some variation between users but it is not severe. Figure 4.4 shows the patterns of two users walking in texting carrying mode while walking at fast pace. These two users were selected because they are the ones with lowest (*"User 1"*) and highest (*"User 8"*) differences between their wrist and trunk signals in this scenario.
- Wrist pose: It can be seen that the values for texting and calling are very similar. The ones from calling seem a little bit lower, maybe due to the

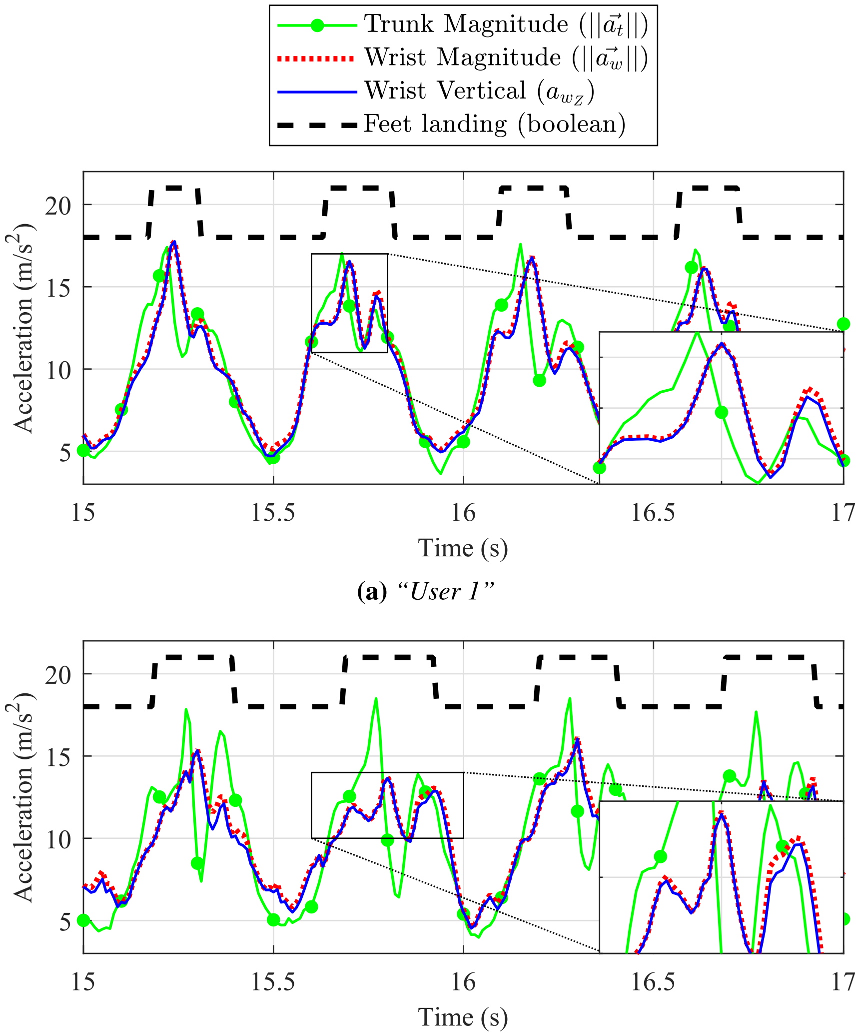

(a) *"User 1"*

(b) *"User 8"*

Figure 4.4: Trunk and wrist accelerations from two users in texting carrying mode while walking at a fast pace. These two users were selected because they are the ones with lowest (*"User 1"*) and highest (*"User 8"*) differences between their wrist and trunk signals.

		Vertical Components (m/s^2) $abs(a_{w_Z} - a_{t_Z})$			Horizontal Magnitudes (m/s^2) $abs(\vec{a_{w_H}} - \vec{a_{t_H}})$			Magnitudes (m/s^2) $abs(\vec{a_w} - \vec{a_t})$		
		Slow	**Normal**	**Fast**	**Slow**	**Normal**	**Fast**	**Slow**	**Normal**	**Fast**
Texting	Mean of users	0.77	0.99	1.58	0.52	0.58	0.77	0.77	0.98	1.58
	Std of users	0.15	0.18	0.27	0.10	0.10	0.31	0.15	0.18	0.28
	CV(%)	20%	18%	17%	19%	17%	40%	19%	18%	18%
Calling	Mean of users	0.79	0.99	1.44	0.44	0.55	0.74	0.77	0.97	1.40
	Std of users	0.17	0.20	0.30	0.10	0.14	0.19	0.17	0.19	0.30
	CV(%)	22%	20%	21%	23%	26%	26%	22%	20%	21%
Swinging	*"User 1"*	0.77	0.86	1.05	0.54	0.77	1.04	0.76	0.86	1.02
	"User 2"	2.68	2.60	5.40	3.31	3.12	5.60	2.53	2.40	4.42
	"User 3"	1.11	1.46	1.41	1.30	1.59	1.91	1.04	1.39	1.35
	"User 4"	1.36	1.57	3.38	1.56	1.81	3.91	1.28	1.50	3.15
	"User 5"	1.25	1.96	3.50	0.96	1.91	3.26	1.19	1.80	3.22
	"User 6"	1.34	2.37	3.56	1.32	2.20	2.67	1.28	2.17	3.25
	"User 7"	0.85	1.45	2.27	1.02	1.62	2.12	0.81	1.39	2.10
	"User 8"	1.00	2.21	4.64	1.13	2.07	3.69	1.00	2.18	4.26
	"User 9"	1.08	1.75	2.90	1.47	1.90	2.62	0.99	1.61	2.60
	"User 10"	1.01	1.73	2.23	1.04	1.37	2.12	0.94	1.62	2.07
	"User 11"	1.32	1.38	3.32	1.41	1.63	3.46	1.30	1.35	3.09
	Mean of users	1.25	1.76	3.06	1.37	1.82	2.94	1.19	1.66	2.77
	Std of users	0.51	0.50	1.29	0.70	0.58	1.23	0.48	0.45	1.08
	CV(%)	41%	28%	42%	51%	32%	42%	40%	27%	39%

Table 4.1: Summary of the absolute differences between the acceleration signals of interest of the wrist and the trunk. For each dataset, the average difference value was computed over the central segment of the walk. Then, the mean, the standard deviation and the coefficient of variation (CV(%)) of the obtained values was computed over the 11 users.

fact that the sensor is closer to the trunk, but data are not enough to draw a conclusion.

Therefore, there is a real relative motion between the wrist and the trunk in both the vertical axis and the horizontal plane, with the former being larger, and whose effect in the three signals of interest has the form of a damping of the trunk's acceleration. That is, the patterns in the wrist will be attenuated and delayed versions of the ones of the trunk, as can be seen in Figure 4.4. Additionally, this alteration can vary according to the walking pace and the users, being not so evident the difference between the texting and calling modes, despite the fact that in the latter mode the sensor is closer to the trunk.

4.3.1.2 **Swinging mode**

This is the natural motion mode when walking with the arms free. Firstly, let's review the theoretical behavior that the relative acceleration signals ($\vec{a_{wt}}$) are expected to show:

- Horizontal magnitude: The accelerations along the anteroposterior and horizontal anatomical axes will oscillate at the stride frequency due to the alternating back and forth motion. However, the magnitude of the acceleration in the horizontal plane defined by those two previous axes will show a combination of stride and step frequency components. The ratio between those two components will depend on the level of symmetry between the back and forth motions of the arm. If the symmetry is perfect, only the step frequency component will be present.

- Vertical component: This will also have a combination of the stride and step frequencies, depending on the symmetry in duration and height reached between the backwards and forwards phases. The stride component will be usually the main one, but if the arm swings as if it were a pendulum, which can happen at slow walking paces, the step frequency can become the main one.

- Magnitude of the acceleration: This signal is the combination of the two previous ones, which are usually well synchronized. Consequently, the ratio between the stride and step frequency components will depend, once again, on the symmetry between the backwards and forwards phases and also on the amplitudes of the accelerations in each direction.

Therefore, the relative acceleration signals are a mixture of the stride and step signals, and its shape will depend on the walking pace and the way each person moves their arms while walking. In addition to this variability of the relative acceleration's shape, the way it is synchronized with the trunk's accelerations will also affect the total wrist acceleration because, as expressions (4.1)–(4.4) suggest, there are interaction terms that can be additive or subtractive. As mentioned in Section 4.1, it is known that the most advanced position of one hand coincides with the opposite side's footstep. This means that at least alternating peaks of the relative acceleration signals will be well synchronized with the peaks of the trunk's accelerations. The synchronization of the other peaks will depend on the rate between the step and stride frequency components of the relative accelerations.

In order to check how the relative acceleration varies with respect to the different users and walking paces, it was followed the same procedure as in Section 4.3.1.1 for the first walk of the swinging mode. Both the individual results of each user and the average values over them are presented in Table 4.1.

Regarding the walking speed, it can be seen that the differential signals increase rapidly their average value for faster walking speeds. When walking at low paces, the arm swinging is mainly passive and its main frequency is close to the step rate, so the behavior is somehow similar to a quasi-static carrying mode. However, as the walking speeds increases, the arm swinging becomes more active and the magnitude of its accelerations will increase.

The values of the coefficient of variation indicate that for the swinging mode there is a larger variation over the users. This variability is determined by the different ways of swinging the arms. To see more clearly this variability, examples from users walking at the same speed but with different arm swinging behavior are now presented:

- Figure 4.5a shows the accelerations for *"User 1"* when swinging while walking at the fast pace. Although the person is actually swinging, the wrist acceleration's behavior is similar to the quasi-static carrying modes. Figure 4.5b shows how the vertical and magnitude wrist accelerations oscillate at the step frequency, while the horizontal magnitude does at the stride frequency but with a lower energy. It can be seen in table 4.1 that this user had the smallest differences between the wrist and trunk signals in all walking speeds. A possible explanation could be that this user's arm swinging is mainly passive, similar to a pendulum.

- The case of *"User 2"*, shown in Figure 4.6, is also an extreme example but opposite to the previous one: this user had the largest values in table 4.1, significantly large even for the slow walking speed. One possible explanation for this is that the user's forward and backward swinging motions are more different between them than in the case of the rest of the users. This

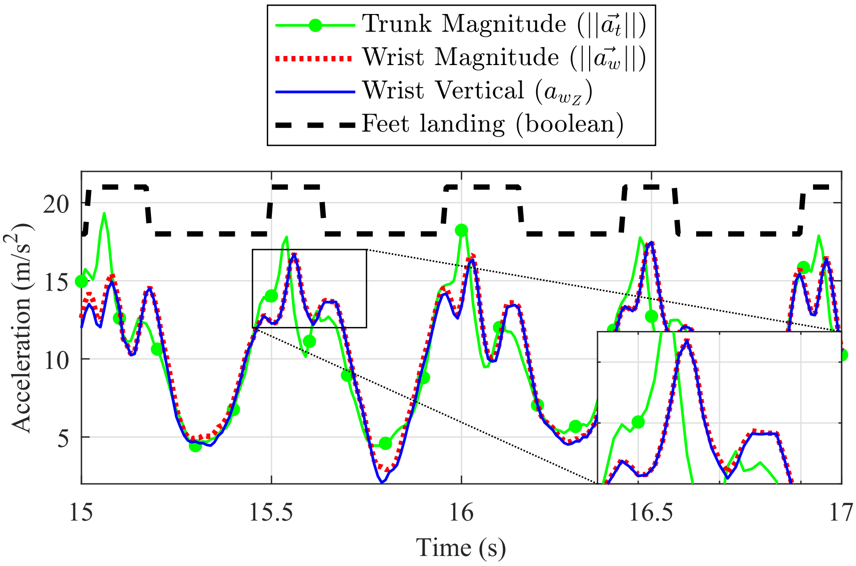

(a) *"User 1"* time domain

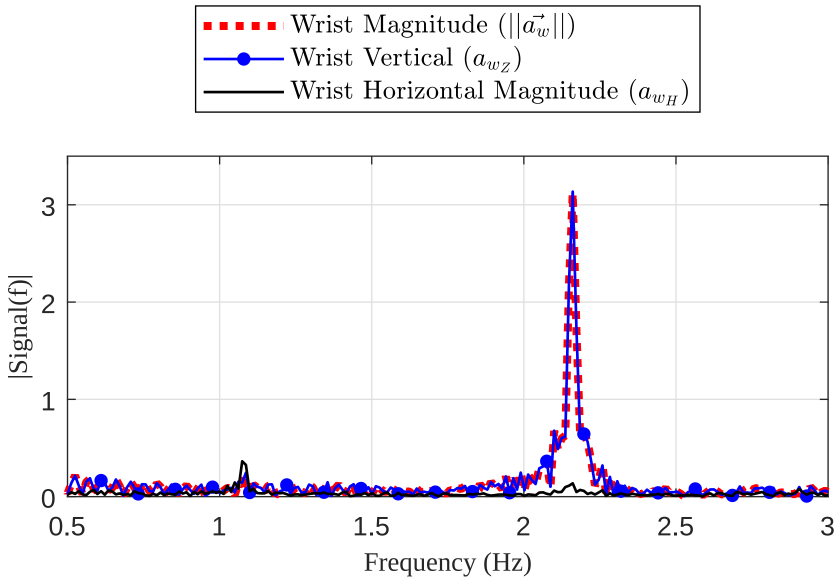

(b) *"User 1"* frequency domain

Figure 4.5: Wrist's vertical, horizontal magnitude and total magnitude accelerations in time and frequency domain, for *"User 1"* in swinging mode while walking at fast pace

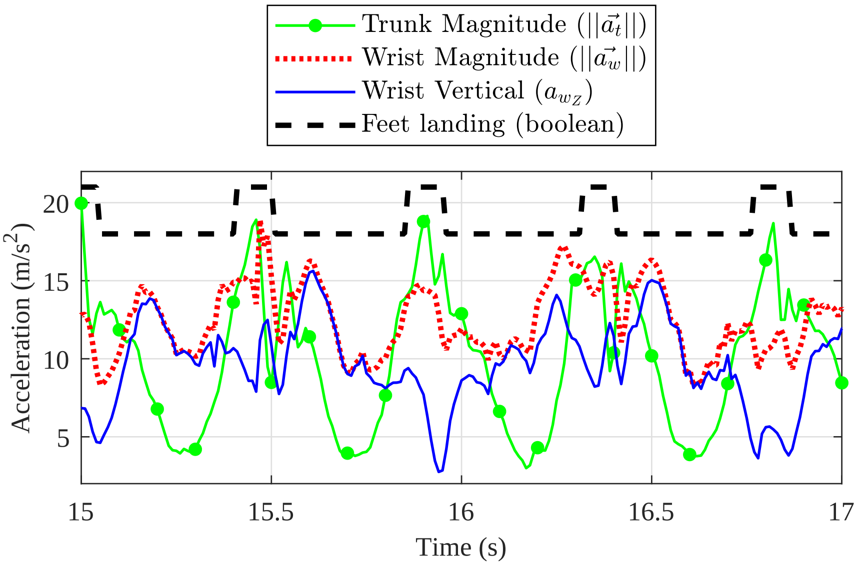

(a) *"User 2"* time domain

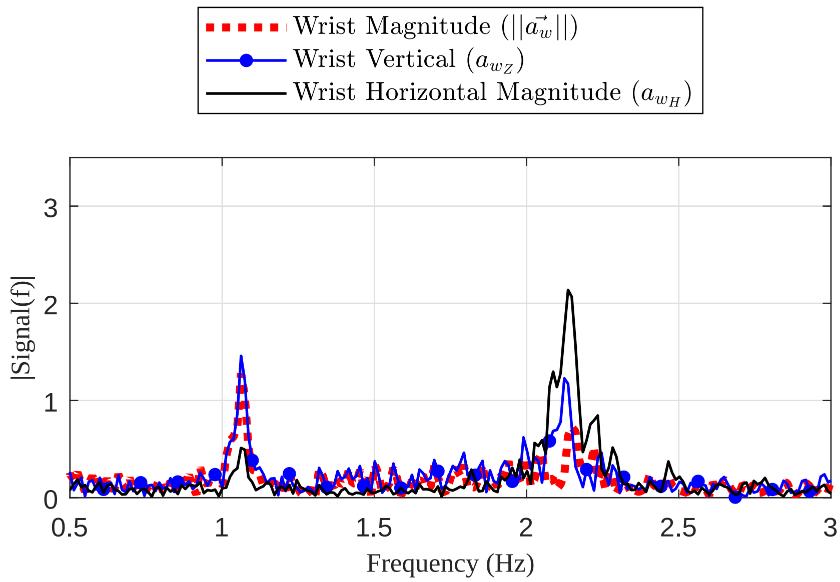

(b) *"User 2"* frequency domain

Figure 4.6: Wrist's vertical, horizontal magnitude and total magnitude accelerations in time and frequency domain, for *"User 2"* in swinging mode while walking at fast pace

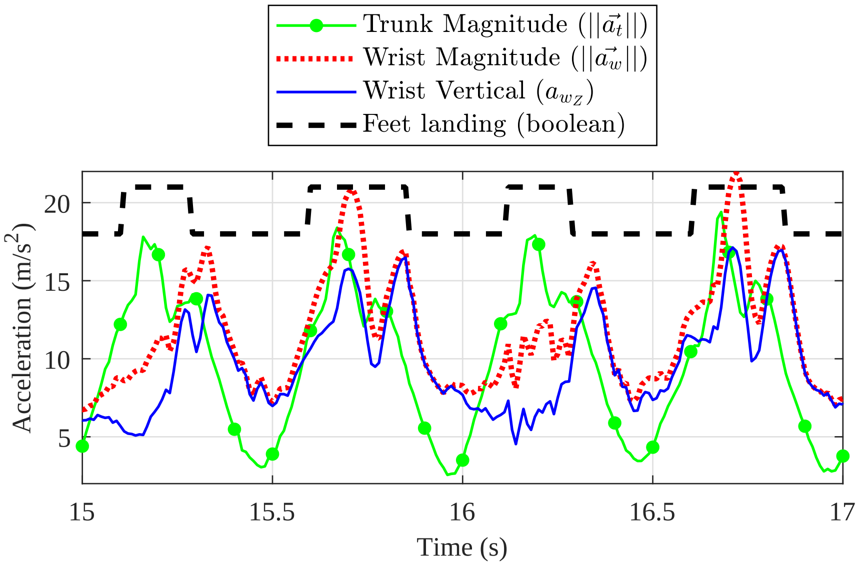

(a) *"User 11"* time domain

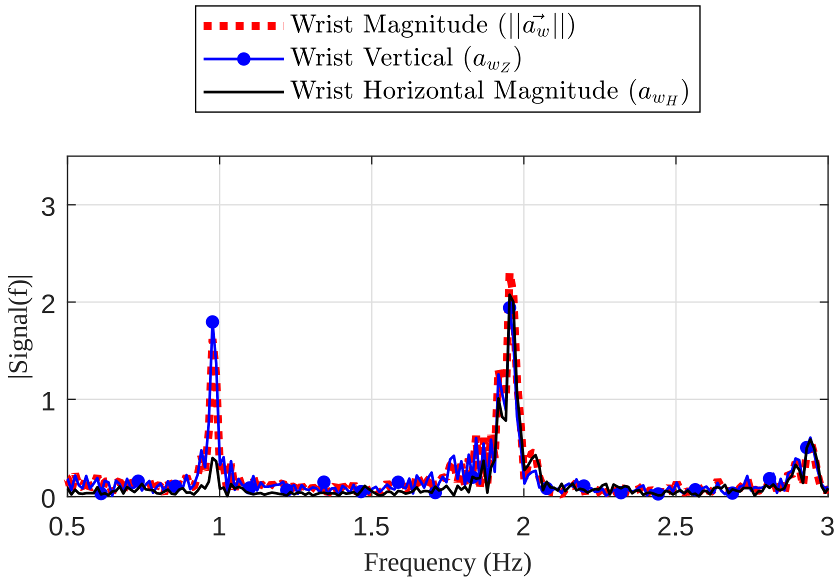

(b) *"User 11"* frequency domain

Figure 4.7: Wrist's vertical, horizontal magnitude and total magnitude accelerations in time and frequency domain, for *"User 11"* in swinging mode while walking at fast pace

is evidenced by the fact that this user's vertical and magnitude accelerations present a stride spectral component stronger than the step one, as can be seen in Figure 4.6b, which makes the wrist acceleration signals differ greatly from those of the trunk.

- Figure 4.7 comes from a user who presents an intermediate behavior: the magnitude of the horizontal acceleration also shows a strong step frequency component but so do the vertical and total magnitude. Therefore, the trunk patterns are still recognizable in the wrist accelerations, although the existence of a stride frequency component can be seen by how the peaks of the wrist acceleration have alternating amplitudes. Additionally, it seems like the lower peaks are more delayed with respect to the trunk's peaks.

4.3.2 Gyroscopes

Gyroscopes measure the instantaneous angular rate vector associated to the change of orientation of the sensor. Due to their design, gyroscopes are also affected by linear accelerations. This effect will be ignored in this work because the accelerations experienced in the wrist when walking are not usually larger than 2 g, in comparison to the up to 10 g experienced in the feet.

The values of the three-axis gyroscope represent the projections of the instantaneous angular rate vector on the sensor frame. As any other vector, it can be expressed in other reference frame but, since the sum of rotations can only be considered commutative for infinitesimal rotations, it makes no sense to analyze its individual components during a period of time. Its global effect has to be studied by analyzing its magnitude and/or three-dimensional direction. The former is the considered signal for this section:

$$||\vec{\omega}|| = \sqrt{\omega_x^2 + \omega_y^2 + \omega_z^2} \tag{4.6}$$

The magnitude provides a measure of how much rotation the sensor experiences over time, it is independent from the sensor's orientation, and, due to the periodic behavior of the human gait, some patterns can be identified.

4.3.2.1 **Quasi-static carrying modes**

At each foot strike, the trunk swings slightly forward and laterally, to each side in alternation. This is reflected in the magnitude of the angular rate as a local minimum whenever the direction of swinging changes. Therefore, the angular rate magnitude of the trunk will be periodic with a frequency equal to the step frequency and with a not very large amplitude. Since there is some damping effect during quasi-static carrying modes, the angular rate magnitude in the wrist will be smaller and, therefore, prone to be hidden by the noise associated to any vibration.

4.3.2.2 **Swinging mode**

For the swinging case, the minimum of the magnitude of the angular rate corresponds to the change of direction of the swinging. The swinging of the arms is more energetic than that of the trunk, so its signal will show clearer patterns. However, similarly to the accelerations, the signal will be a mixture of the stride and step frequency components, in a way that depends on the ratio between the durations of the backwards and forwards phases.

Figure 4.8 shows the magnitude of the angular rate vectors from two of the user cases shown in the acceleration section. These users are again selected because they were the ones with the smallest (*"User 1"*) and largest (*"User 2"*) values in Table 4.1 for the swinging mode. The differences between the users are again visible. The first difference is the smaller magnitude of the angular rate vector of the *"User 1"* (Figure 4.8a). As mentioned before, this user seemed to have a more passive swing. The second difference is the clarity of the generated patterns: *"User 2"* (Figure 4.8b) has a clearer presence of a periodic signal with a frequency equal to the step frequency. Moreover, it can be seen that the minima are perfectly synchronized with the peaks of the trunk's acceleration magnitude signal. In contrast, the patterns of the signal of *"User 1"* are noisier. The fact of its being a less energetic signal makes it weaker against interfering motions. This difference can also be seen in the frequency domain: while *"User 2"* shows a clear step frequency component, *"User 1"* also has a stride frequency component with a power similar to the step component.

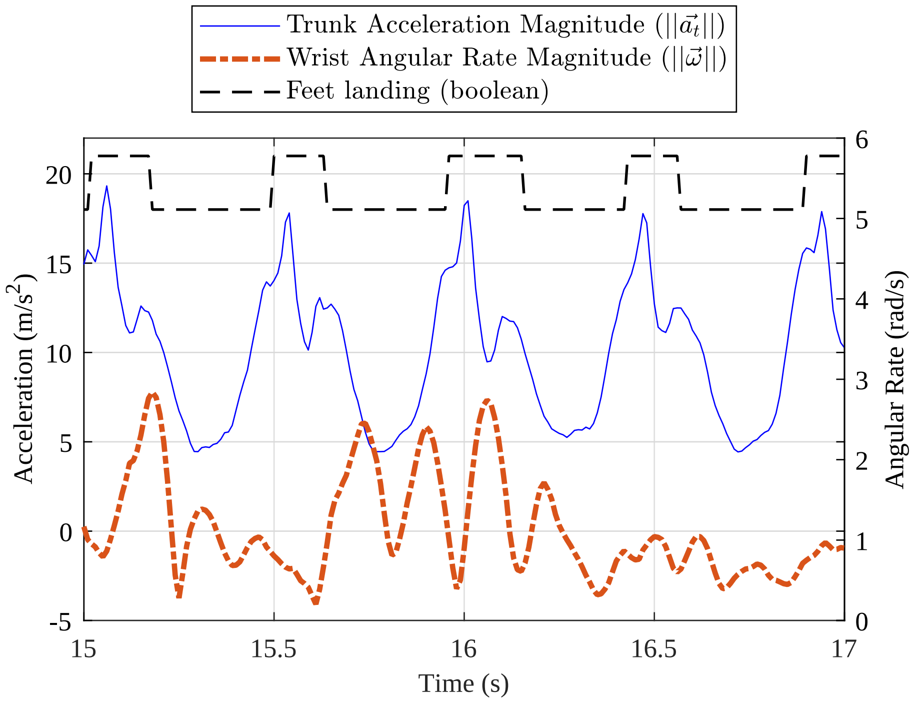

(a) *"User 1"*

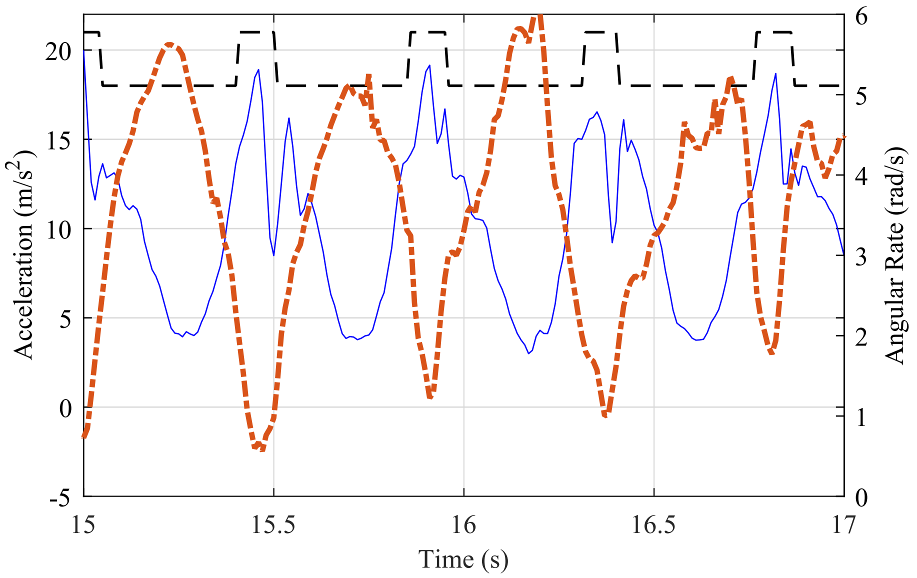

(b) *"User 2"*

Figure 4.8: Magnitudes of the wrist angular rate vectors from two users in swinging mode and fast walking pace.

4.3.3 Orientation

It has just been observed that the patterns produced by the periodic human walk are visible in the angular rate vectors of the wrist. Therefore, it is expectable to find also patterns in the orientation of the wrist. In this section, the Euler angle signals (as defined in Figure 4.2) will be analyzed to check their dependency on different carrying modes, users, and walking paces.

4.3.3.1 Quasi-static carrying modes

During walking, the orientation of the trunk shows step patterns too. The trunk's pitch varies basically at the step frequency, while its roll and heading do so at the stride frequency, even when walking straight.

If we consider the ideal case of no relative motion between the wrist and the trunk, the variation of the trunk's orientation should be transferred to the wrist's orientation. However, the variations of the trunk's roll and pitch angles are not transferred directly: they will depend on the relative heading between the wrist and the traveling direction, that is, the anteroposterior axis. For example, a difference of $90°$ will imply that the trunk's pitch variation becomes the wrist's roll variation. In general, the trunk's roll and pitch variation will be combined to make both the wrist's roll and pitch.

Table 4.2 shows the average orientation of the left wrist for texting and calling poses, collected from the 11 users when they stood still for 2 seconds before starting to walk. The relative heading was computed by comparing the headings provided by the AHRS of the sensors installed on the wrist and the chest, considering the latter as the traveling direction. These heading were computed using magnetometers but it can be considered that they are affected but the same magnetic interference. As can be seen, the heading in texting mode is closer to the traveling direction than

	Roll	Pitch	Relative Heading
Texting	$-96°$	$-6°$	$19°$
Calling	$18°$	$-56°$	$73°$

Table 4.2: Average orientation of the wrist of the 11 users in texting and calling poses

in the calling mode. This kind of misalignment can make the patterns in the wrist's pitch and roll show different mixes of the step and stride frequency components, depending on each carrying mode.

Table 4.3 presents an example of this effect for the case of *"User 1"* walking at normal pace and two quasi-static carrying modes. This table shows the mean peak-to-peak amplitude of the oscillations of the different Euler angles of the trunk and the wrist, for the texting and calling carrying modes, averaged over a walk. Additionally, the principal frequency component of the wrist's Euler angles is also indicated. As can be seen, for similar variations of the trunk's orientation, different patterns are generated in the wrist's orientation signal, depending on the specific carrying mode.

	Texting			**Calling**		
	Trunk	**Wrist**		**Trunk**	**Wrist**	
	p2p	**p2p**	**Freq.**	**p2p**	**p2p**	**Freq.**
Roll	9.4°	4.7°	Stride*	9.1°	6.5°	Step
Pitch	3.4°	2.8°	Stride*	3.5°	2.8°	Stride*
Heading	12.6°	6.8°	Stride	13.4°	7.6°	Stride

Table 4.3: Comparison of the characteristics of the patterns generated in the Euler angle signals for quasi-static carrying modes (*"User 1"*, normal pace). The term "p2p" is for the mean peak-to-peak amplitude and "*" indicates a noisy frequency spectrum.

Anyway, since these orientation variations, although they increase for faster walking paces, are usually small and have a mix of step and stride frequency components, they are prone to suffer noise and vibration, in a similar way as was seen in Section 4.3.2.1 for the magnitude of the angular rates. Only the step patterns of the heading/yaw Euler signal seem a little bit more robust for the quasi-static carrying modes, although this signal can also be altered by non-straight walking or magnetically disturbed environments.

4.3.3.2 **Swinging mode**

Due to the clear periodicity and bigger range of motion of the arms while swinging, the presence of stride patterns in the Euler angles is more evident. An example of this can be observed in Figure 4.11, which contains the data from *"User 3"* for fast walking, and where it can be seen that the Euler angles show a good synchronization with the events of the magnitudes of the acceleration and the angular rate, but with a lower frequency (one-half, actually).

In the same fashion as in previous sections, the characteristics of these stride patterns also depend on the walking pace and the way each user swings their arms. Figure 4.9 shows the range of amplitudes of the oscillations of the Euler angles for three users walking at three different paces. It can be observed that the amplitudes seem to show a linear relation with the walking pace. It is also evident that there is a great variability between users: once again, *"User 1"* shows a very low amplitude of oscillations, while *"User 2"* shows much larger variations of the wrist's orientation, confirming the performance of a stronger swinging.

Regarding the heading misalignment between the wrist and the traveling direction for the case of swinging arms, on the one hand, the variations of the heading are much larger than for the quasi-static carrying modes, and, on the other hand, the way each person swings the arms leads to different values of the misalignment. Figure 4.10 shows the headings of the wrist and the trunk for two different users when walking in swinging mode at a normal pace (these headings were obtained in the same way as in table 4.2). It can be seen that, while the headings of their trunks are similar, the headings of their wrists differ greatly. Apart from the difference in amplitudes, it is remarkable that the heading of the wrist of *"User 1"* never crosses the value of the traveling direction, defined in this case by the trunk's heading. Different individual parameters, such as the rotation axes of the shoulder and elbow or the preferred angle of pronation/supination of the wrist, have a strong influence in the heading misalignment between the wrist and the traveling direction.

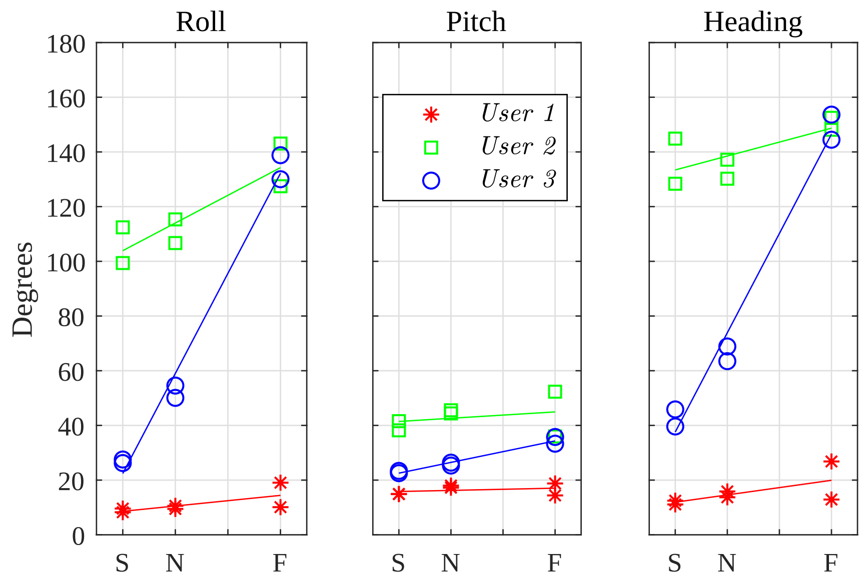

Figure 4.9: Average variations over a walk of the amplitudes of the Euler angles for three different users at three different paces: slow (S), normal (N), fast (F). The straight lines represent the fitted line for each user's data, at each different pace.

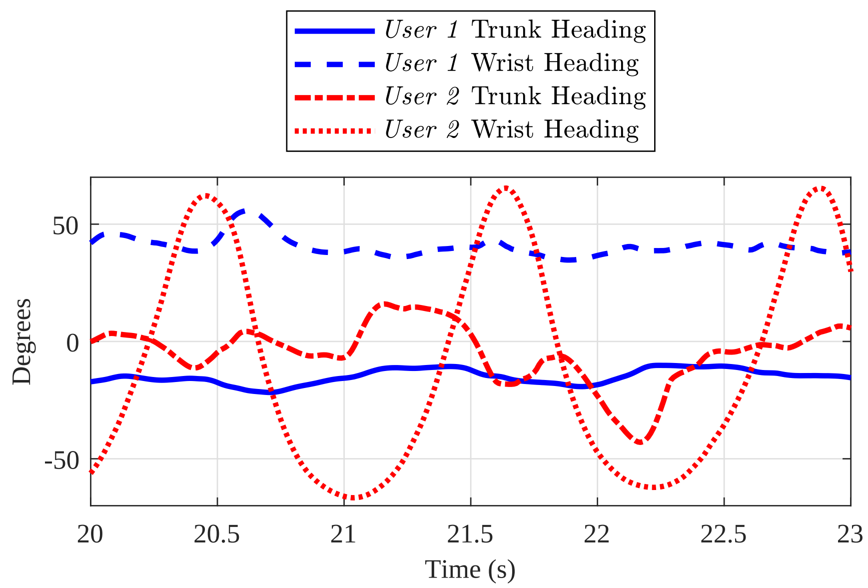

Figure 4.10: Headings of the trunk and wrist from two users while walking in swinging mode at normal pace.

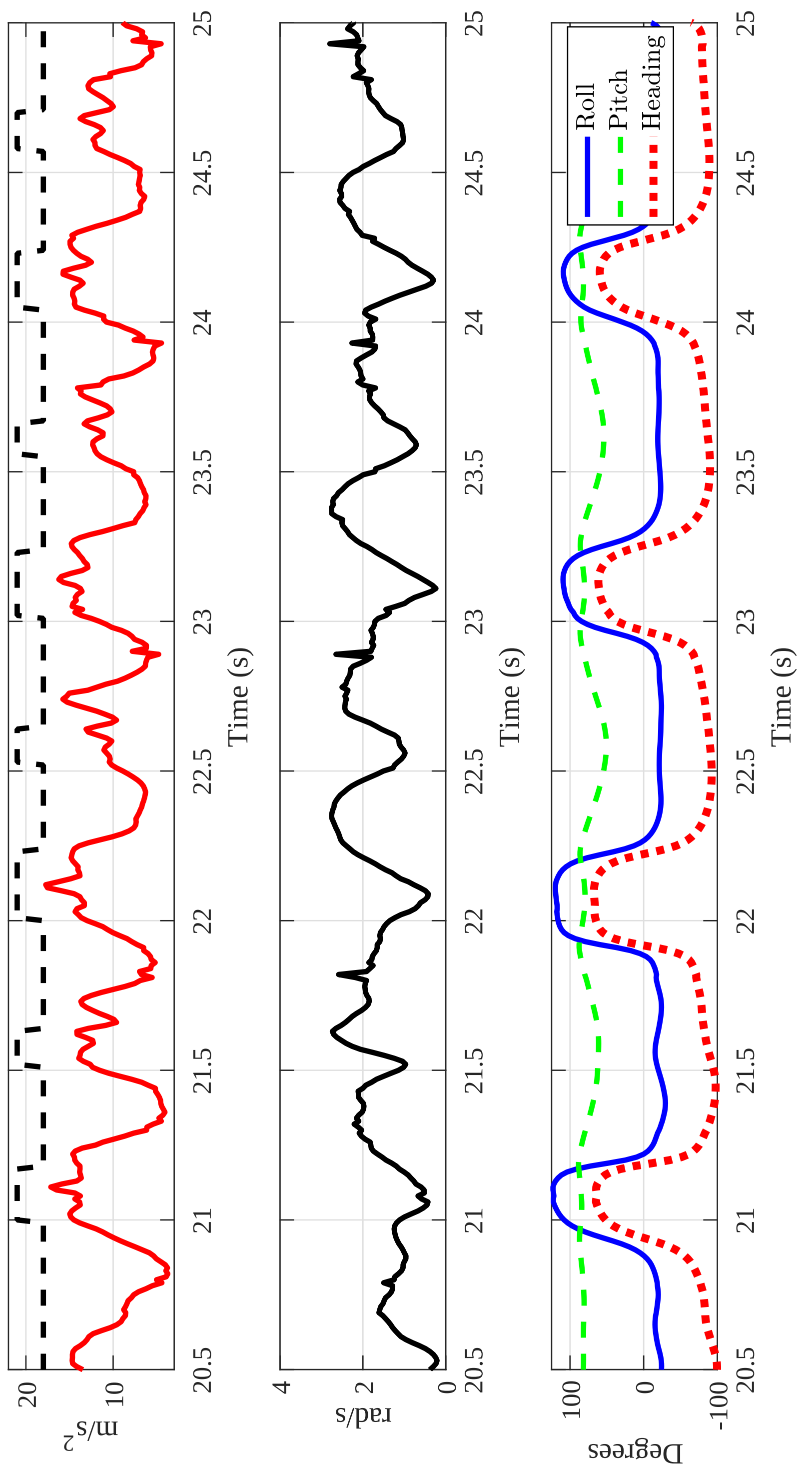

Figure 4.11: Several wrist signals from the *"User 3"* walking fast in swinging mode: magnitude of the acceleration (top), magnitude of the angular rate (middle), and the Euler angles (bottom). The figure in the top includes the binary signal indicating the feet landing.

4.3.4 Barometer

Apart from the variation in the height of the terrain, the wrist also experiences changes in height due to the walking itself, this being more evident in the swinging mode. Since it would be useful to detect this height variation associated to the steps, it has been analyzed whether it is possible to detect them using the kind of barometers included in the smart devices available in the market, that are based on the MEMS technology.

Several barometers were tested: in addition to the one included in the Xsens MTw, one Xsens MTi-300 (4th generation) motion tracker and one Samsung Galaxy S4 smartphone were also used. The Galaxy S4's barometer is a Bosch BMP180 that has an RMS measurement error of 0.5 m in low power mode [129]. The exact model of the barometer of the Xsens devices is not known, but their noise error is 0.85 $\mathrm{Pa}/\sqrt{\mathrm{Hz}}$ and it is similar to that of the Bosch.

The average length of the 11 users' arms is 0.5 m. That would be the change of height of the wrist if it rotated 90°around the shoulder with the arm completely stretched. However, the elbow is usually slightly bent and the rotation angle is smaller, so the variation in the height of the wrist will be smaller than 0.5 m when swinging. Therefore, with such an error noise of the barometers, it will be difficult to detect those variations. This was confirmed by temporal and spectral analysis, although in some cases a very small stride frequency component seemed to be intuited through the noise level.

Some barometers offer configurations with lower noise, such as the BMP180 (0.17 m RMS error) or the DPS310 (0.05 m RMS error) [130]. However, these configurations require higher power consumption, so they are not usually selectable in the commercial devices that include them. Additionally, these configurations also imply a lower sampling rate, around 10 Hz, which can be insufficient for capturing all the dynamics of walking [131].

4.4 Discussion: Implications for a PDR

4.4.1 Step/Stride Detection: What signal to use?

Based on the observations of the previous Section 4.3, different signals can be useful for step or stride detection:

- Accelerations: If the relative motion between the wrist and the trunk is small, that is, quasi-static carrying modes and low swinging mode, the wrist acceleration signals are trustworthy for detecting steps. Since each of the three different acceleration signals provides similar robustness, the total magnitude is the best choice due to its not being degraded over time. In contrast, when swinging modes that are sufficiently energetic are performed, the step patterns will be altered based on the walking pace and the way of swinging the arms of each user. Step detectors can still be used on acceleration signals, but they have to be very adaptive algorithms in order to reduce the number of false negatives and positives in the detected steps.

- Angular Rates: The magnitude of the angular rates is a useful signal to detect steps in any carrying mode. The only risk is that for slow paces, especially in quasi-static carrying modes, the signal is small, so the probability of a wrong detection increases.

- Orientation: The Euler angles signals are mainly useful to detect strides, especially in swinging mode. For quasi-static modes this is more challenging, due to the small amplitude of the signals and because the misalignment between the wrist and the traveling direction can alter the spectral behavior of the roll and pitch.

In the scientific literature there are two main trends: to use just accelerometers for all carrying modes, such as the total magnitude in [31], or to use a different signal for each carrying mode, such as the vertical acceleration and the pitch in [102], or the magnitude of the acceleration and the angular rate in [132][101]. A lot of commercial step counter applications choose the first option so as to reduce the cost and energy consumption, since gyroscopes usually consume more power than accelerometers. However, as was already mentioned, the use of only accelerometers is more problematic in non quasi-static carrying modes.

In summary, it has been observed that the step patterns in the different signals are far from ideal, for several reasons: the person's anatomy, the pose of the arm, as well as the walking speed, for instance. However, they can complement each other, so it seems reasonable that fusion strategies and adaptive algorithms will be necessary for implementing robust step/stride detectors from wrist-worn inertial sensors.

4.4.2 **Classification of Carrying Modes**

Before using specific step/stride detectors based on each carrying mode, a classification stage of the carrying mode is necessary. For this purpose it is usual to collect different temporal and spectral features of the available signals, usually computed within a time window, such as the mean energy, the variance, or the power of the principal frequency components.

Figure 4.12 shows the distribution of the variances of the accelerations and angular rates, averaged over a walk, from all the available data: 11 users, at three walking paces and for three carrying modes.

It can be observed that there are two distinguishable classes that can be classified by using some value of the angular rate variance as a threshold: the larger values will belong to the swinging mode and the lower ones to texting and calling, which can be grouped as quasi-static carrying modes. However, there are also some outliers, that come from users already analyzed in previous sections:

- In the bottom right corner there is a pair of swinging datapoints (blue circles) that have the same characteristics as the quasi-static data points. They belong to *"User 1"*, who, as seen in Section 4.3.1.2, seems to have a pendulum-like swinging.

- In the top left corner there are some swinging datapoints with a large value of angular rate variance but with small acceleration variance. They do not seem to follow the same linear relation that the rest of the swinging datapoints do.

Some of these values belong to *"User 2"*, who has a very energetic swinging, as was seen in previous sections.

Taking into account that this data comes from a small group of people, all of them healthy, from a limited number of carrying modes, and only from straight level walks, it would not be unlikely that the classification would become more difficult when processing more realistic and varied scenarios. In the same way that it seems pretty difficult to classify all people into a finite number of classes by the way they move their arms, it also seems difficult to do so for all the possible carrying modes. If the aim of the classification stage is to select the most appropriate step detector, maybe it would be better to try to identify which signals are the most useful at each moment and use them in the right step detector.

Additionally, this variability in the users' behaviors suggests that a prior calibration stage would be beneficial for the performance of the complete system. The execution of simple and controlled motions could help to capture the characteristics of each user and, this way, adapt the different blocks of the system.

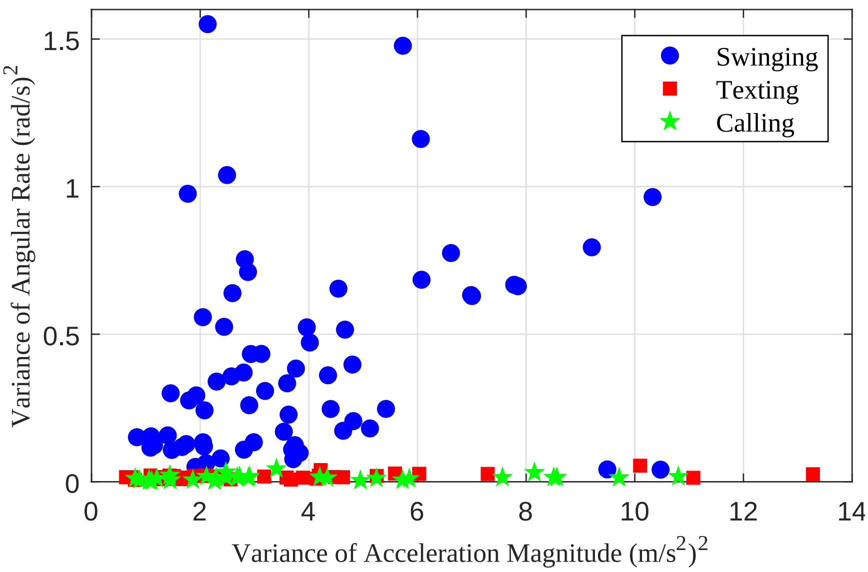

Figure 4.12: Distribution of the variances of the accelerations and angular rates, averaged over a walk, from all the available data: 11 users, at three walking paces and for three carrying modes.

4.4.3 Step Duration Estimation

It is usually interesting to know the duration of the steps (or its inverse, the step frequency) for estimating the length of the step, among other things. This is usually done in the time domain, measuring the distance between the events that identify the steps, because this requires fewer resources and has fewer limitations than in the frequency domain.

As has been seen in previous sections, it is usual that signals that are periodic at the step frequency rate also have a non-negligible stride frequency component, but if the step component is clearly stronger, they can still be used for detecting steps. However, the mixture of frequency components can affect the temporal distribution of the events that mark the steps, modifying the observed step durations. Figure 4.13 contains the distribution of the differences of duration between the steps detected from the magnitude of the acceleration of the wrist and those detected on the feet, for two users walking at a normal pace while swinging. For measuring the duration of the steps from the feet, the ZUPT technique, as explained in [19], was used. Figure 4.13a corresponds to *"User 1"*, for whom the step frequency component was 10 times stronger than the stride one. It can be seen that the differences follow a normal distribution with 0 mean. Meanwhile, Figure 4.13b corresponds to *"User 3"*, who shows a larger mix of frequency components with a step component only three times stronger, but not affecting the step detection process. In contrast, for this case it can be seen that differences in duration follow a bimodal distribution, explained by the unbalanced durations of the forwards and backwards phases of the swinging for this user.

For the same reason, the signals that oscillate at the stride frequency, such as the Euler angles, do not show events at exactly the middle of the period. In other words, the temporal distance between two consecutive peaks of the pitch signal while swinging, for instance, corresponds to the stride period, but the valley (or negative peak) that it is in between, does not take place at the step period. It depends on the balance between the backwards and forwards phases of the swinging.

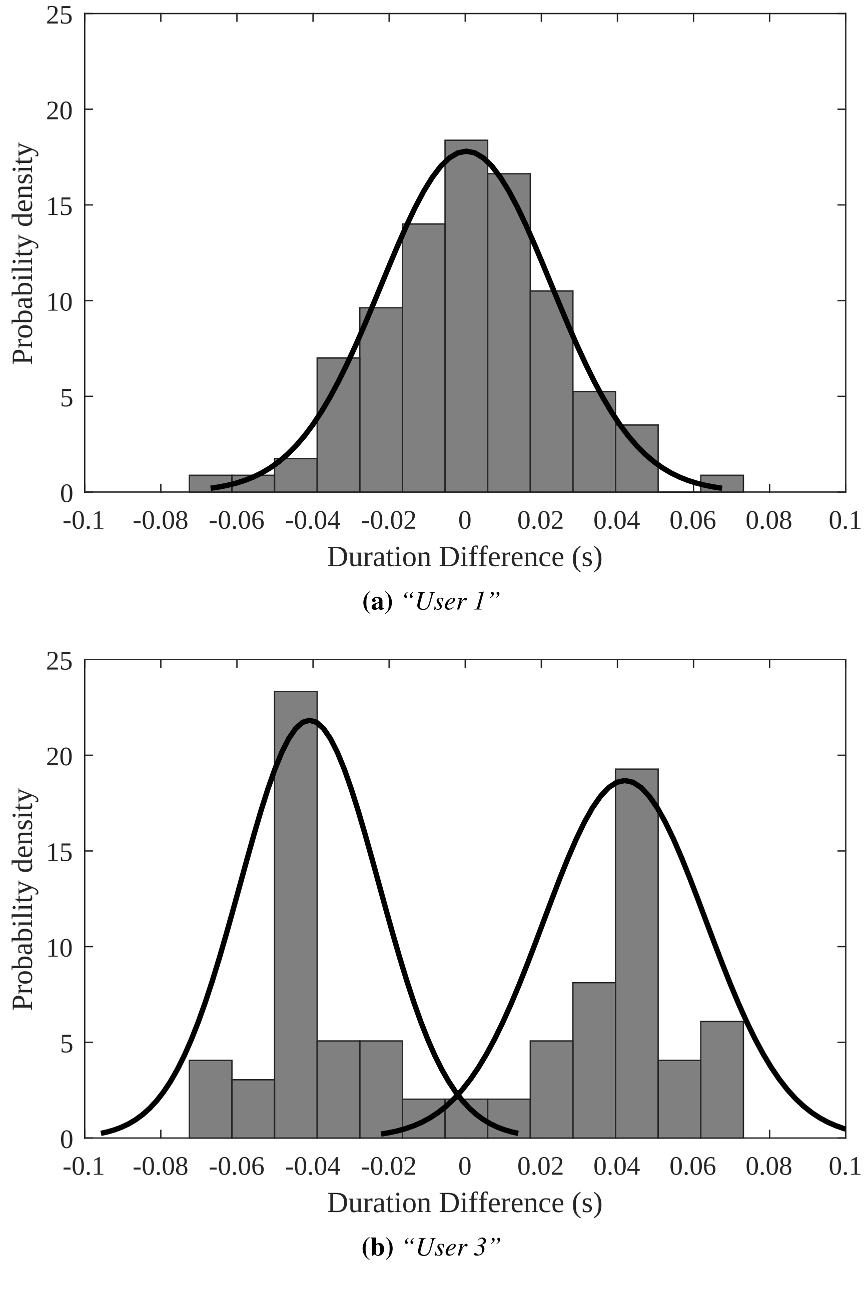

Figure 4.13: Histogram of the differences in duration between the steps detected in the wrist and the steps detected in the feet from two users walking at normal speed in swinging mode.

4.4.4 Step Length Estimation

Step length estimation is usually done by using regression models in which the main predictor variables are usually the step/stride frequency, the variance of the acceleration over a step, or the height of the user. The computation of these predictors is directly influenced by the specific implementation of the step detector algorithm and the way the user moves their arms, especially for the swinging mode.

It has been seen in previous sections that most of the available signals depend on the walking pace, so they can also be considered for being added to the step length regression models. A good example of this is the orientation signal, as was shown in Figure 4.9. To the best knowledge of the authors, no step length regression model has been proposed in the literature that includes the Euler angles as predictors.

Another idea that could be also taken into consideration is to use different step length regression models for each carrying mode, in the same way as is done for the step detection.

Additionally, it is known that there is an asymmetry of motion between the arms of a person. This can affect the performance of the step length estimation because, for the same regression model, the displacement estimate can depend on which arm has had the sensor installed on it.

4.4.5 Traveling Direction Estimation

For the estimation of the step heading, the first option would seem to be to use the sensor's heading signal. However, this involves several difficulties: apart from the usual problems for computing the sensor's heading using low-cost gyroscopes and magnetometers, it is usual that there is some misalignment between the sensor's heading and the actual traveling direction. Moreover, this misalignment can vary over time. Therefore, in order to use the sensor's heading to obtain the traveling direction, it would be necessary to know in which epochs the value of the misalignment is constant, as well as to know the value itself. In some body locations, such as the trousers front pocket or the lower back, this can be done without incurring too much error, because the variation of the misalignment over time is small and this value mainly depends on the installation, so it can be known beforehand. In contrast, for a place such as the wrist, this is more challenging because the misalignment's variation is larger and it depends on the carrying mode, the walking pace, and the way each person moves their arm, as was seen in Figure 4.10.

Therefore, it seems advisable to use different techniques to estimate the traveling direction, such as the identification of the arm's rotation axis [96] or searching for the traveling direction by using principal component analysis on the horizontal projection of the wrist accelerations [84].

4.4.6 Position Integration Rate: Step or Stride?

Strides are defined as two consecutive footfalls of the same foot, while the steps are the same quantity between opposite feet. The real displacement is made stride by stride. Steps are only a relative measurement, which relates the strides from both feet. When walking straight, strides from both feet have to be equal in length. Otherwise the pedestrian will turn. Of course they are not perfectly equal but the differences get compensated for while we walk. In contrast, steps do not have to be equal in length and/or duration. As the strides are the sum of two consecutive steps, the current one and the previous one, their lengths can be different while the strides remain constant. The equality of the steps is just a matter of the balance strategy of the pedestrian, determined by their anatomical characteristics. In Figure 4.14 there is a simple example of the progression of the feet and trunk positions while walking and, as can be seen, if the person stops with the two feet aligned, there can be steps with zero length.

For PDR systems in which the sensor is installed in body locations where only the stride of one side is felt, such as a foot, a leg, or the trousers' front pocket, the integration rate is only possible to be stride by stride. For body locations in which strides from both sides are felt, such as in the trunk or the head, the integration is usually done at the step rate. For this last case, if the regression model for the step length estimation is built using the real feet step displacements, the last step before a stop should be ignored. However, this is not necessary if the average step lengths are used.

In both cases, as can be seen in Figure 4.14, the position of the trunk is not being estimated: when integrating at the stride rate, the position of one specific foot is being estimated; on the other hand, when integrating at the step rate, the estimated position belongs to the last foot that took a step. None of them are the same as the trunk positions, although they can be coincident at the end of the walk.

For a wrist-worn PDR, depending on the carrying mode and the signals used for step detection, it is possible to integrate the position both at the stride rate or step rate. The upper limbs are the only body locations where this happens. If a PDR system is designed to work at different integration rates, depending on the carrying modes (for instance, the step rate for quasi-static modes and the stride rate for swinging), a transition between modes could lead to errors. The reason is that, apart from the possibility of missing or overcounting steps, since the estimated position is different at each integration rate, depending on when the transition takes place, the two position estimates can differ.

Therefore, it seems advisable to try to integrate the positions at a fixed rate. Nevertheless, the errors due to this fact are less severe than, for example, the drift of the heading over time. Nevertheless, it is important to highlight this difficulty inherent to the PDR systems installed in the upper limbs.

4.4.7 Irregular Arm Motions

The arms are used for many activities that can be performed both when the person is still and when walking. These motions can generate signal shapes that can make the step detector over-count (false positive) or miss (false negative) steps, thus reducing the accuracy of the length and heading of the displacements.

Avoiding this is a really challenging problem and the few works that have tried to tackle it are usually limited to identifying the false positive steps when the person is actually still. In contrast, when the person is really walking, any arm motion that does not belong in the defined carrying modes is usually classified as "irregular" and ignored from the position estimation. Unfortunately, these "irregular" arm motions are pretty common: besides the transitions between swinging and quasi-static modes, actions such as checking the time on the wristwatch, waving to somebody, scratching any part of the body, or moving the arms while explaining something, are daily actions that are done while walking.

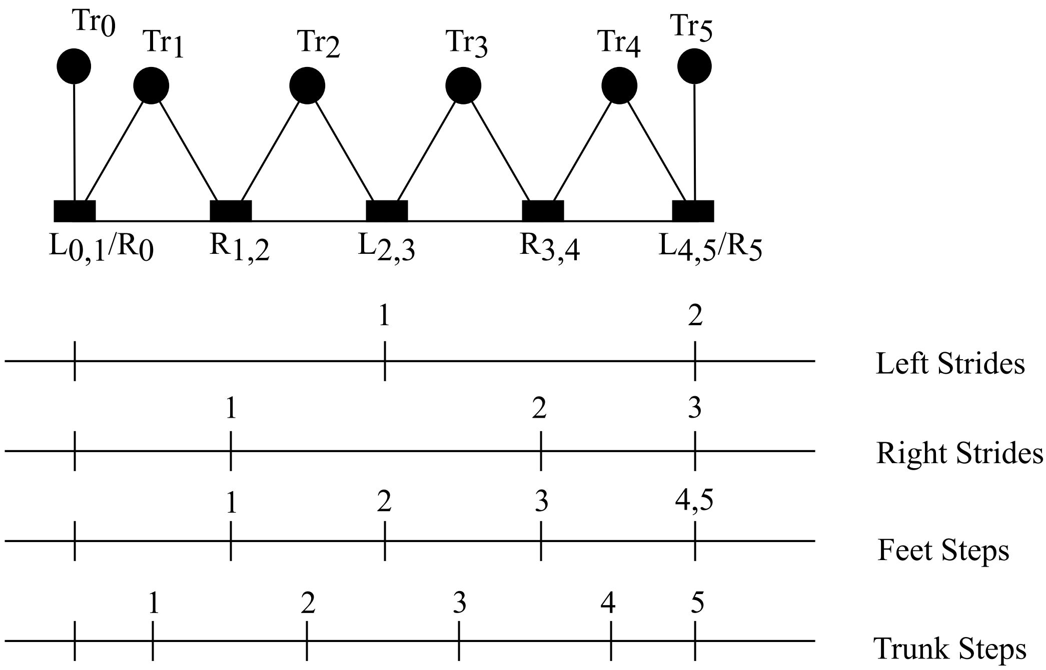

Figure 4.14: Sequence of positions of the trunk (Tr), the left foot (L) and the right foot (R) during a simple walking. It shows how the intermediate positions of the trunk and the feet do not coincide.

Figure 4.15 shows an example of the signals of a wrist-worn inertial sensor for a person who walks swinging their arms, then waves to somebody by oscillating the hand several times, and then resumes the swinging. As can be seen, each signal changes its values, its range of amplitude, and bandwidth, while the trunk's acceleration continues showing the same patterns.

This problem is especially severe for PDRs with sensors installed on the upper limbs, since their motion can be highly uncoupled from the walking. Hence, improving the robustness against false positive and negative steps is key for implementing competitive PDR systems.

4.4.8 **Is a Barometer Useful for Positioning?**

It was mentioned in Section 4.3.4 that it was not possible to detect step or stride patterns with the available MEMS barometers. Nevertheless, if the performance of this kind of sensor continues improving, they should be taken into account for

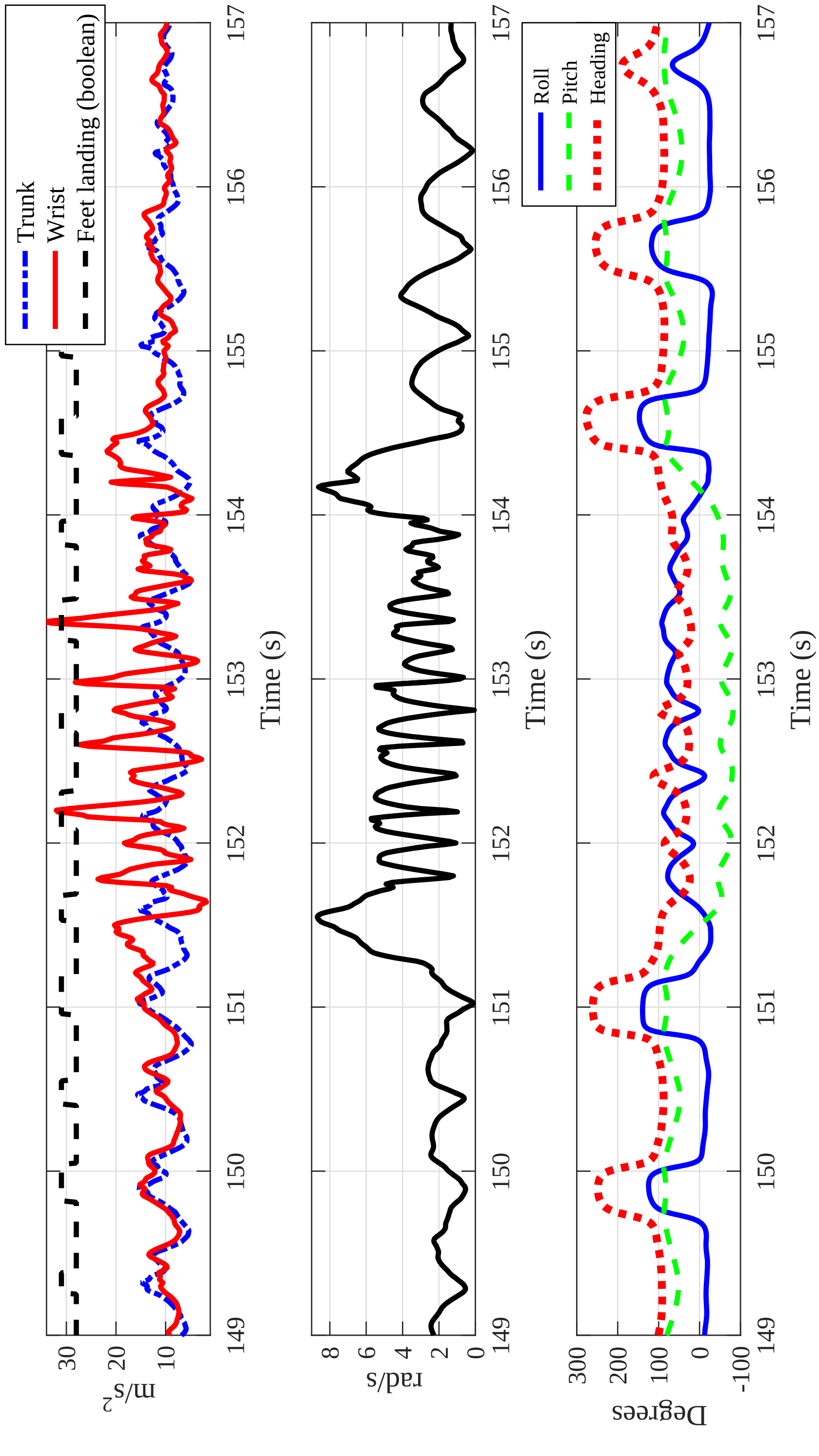

Figure 4.15: Signals from a wrist-worn inertial sensor for a person who walks swinging the arms and waves to somebody while continuing walking: trunk and wrist acceleration magnitude (top), wrist angular rate magnitude (middle) and wrist Euler angles (bottom).

implementing more robust PDR systems. Therefore, their use is currently limited to height estimation, floor change detection, and classification of means of transportation.

4.5 Conclusions

Due to the low number of publications in the scientific literature that specifically study wrist-worn inertial PDR systems, it was considered necessary to perform a deep analysis of the characteristics of the different inertial signals that are generated from the wrist when walking. To this end, data was collected from a series of sensors installed on the bodies of a group of eleven people as they walked at several speeds and with different arm movements.

After analyzing the collected data, the main conclusion is that there are clear step/stride patterns in the different signals taken from the wrist, but their behavior is highly dependent on the carrying mode, the walking speed, and the particular way each individual user moves their arms while walking. In particular, some of the most important observations are the following:

- Swinging mode is, without a doubt, the one with the greatest variability between different users. Both the amplitude and the directions in which the arms swing can vary greatly from person to person. In addition, walking speed also directly influences the amplitude of the swing, which is consistent with the hypothesis that the aim of arm swinging is to compensate for the angular momentum generated in the trunk by the legs when walking. Another interesting observation is that the swing cycle does not have to be perfectly divided by 50% between the forward and backward phases.

- With regard to quasi-static carrying modes, it has been observed that they are not perfectly coupled to the pedestrian's COM because the arms have a damping effect on the motion. This implies that, depending on the person, the carrying mode and the walking speed, the difference with the COM can be significant.

- Steps and stride patterns have been observed on all inertial signals: accelerations, angular velocities and orientation. However, it seems clear that it is advisable to use accelerations for quasi-static carrying modes and angular velocities or orientation for more dynamic modes.

- Current MEMS-based barometers do not currently allow for the detection of changes in wrist height during walking.

All this variability of the patterns makes it difficult to design robust methods for the PDR blocks. Additionally, a lot of daily arm motions do not fit into the usual predefined carrying modes, so they are usually ignored or mis-processed. In comparison to other body locations, it is clear that the upper limbs are the most challenging place for the installation of a PDR system: the further from the feet, the more likely the existence of disturbances.

The viability of implementing robust wrist-worn PDR systems will depend on the design of highly adaptive algorithms, prior calibration stages and the incorporation of more biomechanical knowledge, such as the constraints that the mechanical structure of the upper limbs impose.

All models are wrong.
Some models are useful.

George Box

CHAPTER 5

SLE Methods based on Inertial Sensors: A Review

As mentioned previously in Section 3.3, in order to define a methodology that guides the design, testing and evaluation procedures of the SLE methods, it is necessary to have previously a complete vision of all the aspects and alternatives that must be taken into account during those processes. However, in the scientific literature there are not specific surveys that review the state of the art of this topic. Only a few general positioning surveys [7, 10, 20] and new SLE method proposals [88, 97, 132, 133] include a short and basic review.

This is both the aim and the contribution of this chapter that is, therefore, aligned to the *specific objective 2*: it was conducted a systematic and complete review that covers the whole workflow involved in the design, test, and evaluation of SLE methods based on inertial sensors. Since SLE methods are used in several applications, the work done in this chapter will be useful for the field of PDR systems (not restricted to any particular sensor mounting point) and others such as sport activity monitoring, human gait analysis, energy consumption assessment, or prediction of human health status.

The structure of the rest of this chapter is as follows. Section 5.1 describes the scope of the review and the procedure followed for the selection of the articles.

Section 5.2 presents the methodology used in this review: a set of questions, that are wanted answered, were defined prior to the literature review. The results of the review are described throughout several sections: Section 5.3 presents the different concepts on which the SLE methods are designed; in Section 5.4 the different types of SLE methods are described; Section 5.5 collects all the aspects related to the system requirements and use cases that affect both the design and testing of the SLE methods; and Section 5.6 deals with the reported performances and all aspects of evaluating SLE methods. Then, Section 5.7 presents a series of reflections on the availability of standards and public datasets in this area, whose current lack is considered to be a barrier to progress in this field. Finally, this chapter's conclusions are summarized in Section 5.8.

5.1 Review Definition

5.1.1 Scope of the Review

To make this review tractable, the following set of criteria were established, delimiting the scope of the review:

- The target activity is walking, although some reviewed articles have also dealt with running. Works that estimate the walking speed were also included, as long as the estimation is provided at a rate that is valid for positioning purposes. Although walking speed estimation is quite common in gait analysis applications, they do not usually have the same requirements as positioning. For example, Yang and Li [134] surveyed walking speed estimation methods, and they found that most of them were oriented towards clinical experimentation and foot-mounted inertial sensors were commonly used.

- Strides are defined by the positions of two consecutive footfalls of the same foot, while the steps are defined by the positions of opposite feet (see Figure 5.1). When walking straight, the stride lengths of both feet are equal to each other and equal to the sum of the last two steps. However, this does

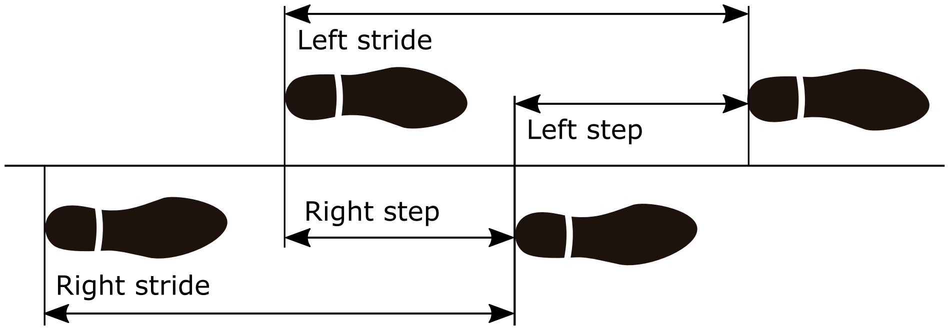

Figure 5.1: Strides are defined by the positions of two consecutive footfalls of the same foot, while the steps are defined by the positions of opposite feet.

not happen when turning, as the foot further from the center of rotation travels a greater distance than the other foot. Additionally, different step length definitions can produce different results [135]. This is something that applications which integrate stride or step lengths must take into account. For this review, both step and stride length estimation methods were considered and no further distinction has been made.

- Only works in which one sensor unit is used were included. Naturally, the use of multiple sensors provides more information but it also makes the system more complex, so it will be assumed that the user only carries one smart device at a time.

- Works with a foot-mounted inertial sensor were not included because it is considered that an implementation based on INS and ZUPT is the best option when the inertial sensor is on that body location, since no training or calibration is needed. However, we are aware that there exists statistical learning based SLE methods for foot-mounted inertial sensors that obtain good results, such as in Hannink *et al.* [136].

- Works in which the performance of the SLE is hidden by the use of additional sources of information, such as map matching or the fusion with other absolute positioning technologies, were not included.

5.1.2 Article Selection

Inspired by the procedure followed by Yang and Li in their survey [134], we searched in the following three popular electronic engines/databases in the fields of engineering and biomechanics: PubMed, ISI Web of Knowledge and IEEE Xplore. The search was made on the first week of May 2018 and the searched keyword string was "(assessment OR estimation OR calculation OR computation OR measurement) AND (inertial sensor OR accelerometer OR gyroscope OR inertial measurement unit) AND (speed OR velocity OR step length OR stride velocity OR stride length) AND (walking)" for appearance in the title (ISI Web of Knowledge) or in any field (PubMed and IEEE Xplore). The results were then refined by selecting only those works that were published from 1990 onwards.

Initially, 987 references were obtained. The title and the abstract of each article was read carefully to exclude any duplicates and works that did not fit in the defined scope. A total of 49 works were ultimately included, as follows: [30–33, 76, 77, 79–83, 87, 88, 90, 93, 95, 97, 99, 103, 107, 128, 132, 133, 137–162].

5.2 Defining the Review Questions

To make a complete and systematic review of the state of the art of a given field, it is advisable to identify in advance the questions, concepts, or criteria on which the focus will be placed when reviewing the selected literature. In this work, to make this identification as exhaustive as possible, a hypothetical workflow to design and validate a new SLE method was defined, as can be seen in Figure 5.2. Reflecting on each of the tasks that make up this workflow, the questions wanted answered during the review of the selected literature were identified. Positioning was selected as the possible target application because it imposes high performance requirements on the SLE method.

5.2.1 SLE Method Design

The design of a SLE method will be the result of a certain compromise between the characteristics of the system in which the SLE method will be included, the use cases to be addressed and the previously available knowledge on the behavior

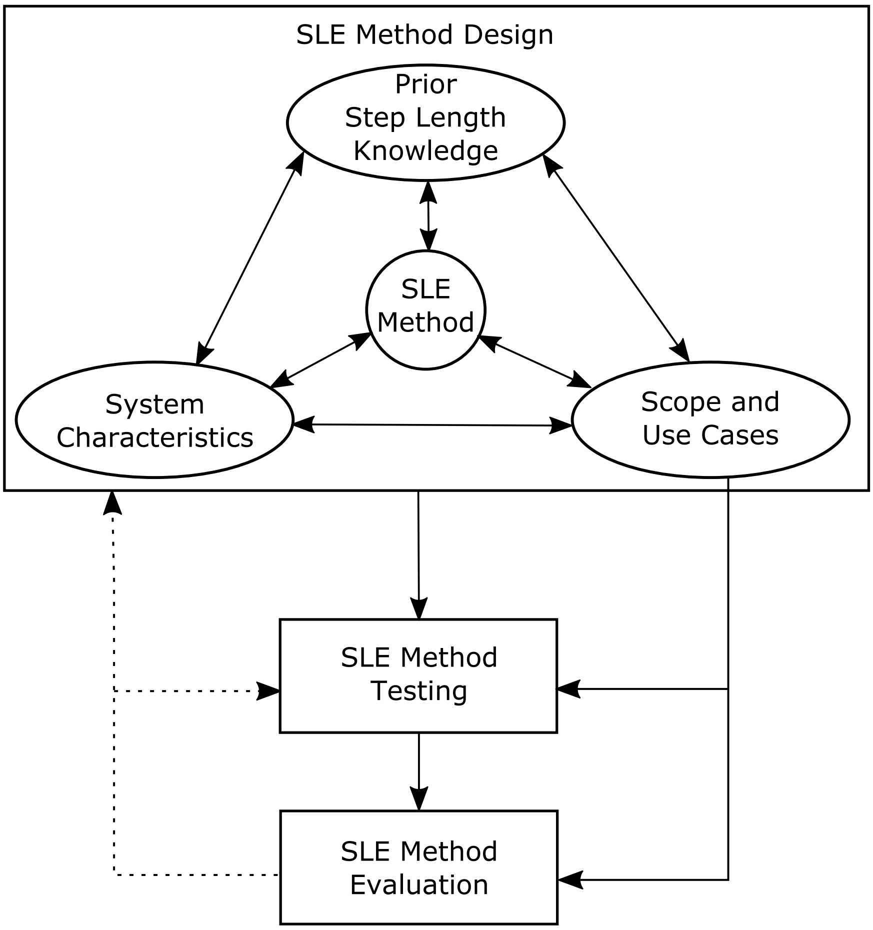

Figure 5.2: Hypothetical workflow that could be followed during the design, testing, and evaluation of a new SLE method that is part of a higher level system. It can be seen that definition of use cases can affect all phases: design, test and evaluation. The dotted arrows mean that, after a SLE method is evaluated, it can be decided to loop back iteratively for improving its performance.

of the step length. The review questions that may arise in each of these individual areas will be presented below, without analyzing the possible inter-dependencies between them.

5.2.1.1 **Prior Step Length Knowledge**

To design an SLE method, it is necessary to have certain knowledge about the process that will be estimated. The following questions may arise from this task:

- What knowledge or observations are used as a basis for the different SLE methods?
- What fields do they come from?
- Do they come from proven and recent sources? (e.g. journals, conferences, books, etc.)

5.2.1.2 System Characteristics

Most of the system characteristics that can be involved in the SLE method's design are related to the hardware used, so the following questions arise:

- What types of sensors are used? Accelerometers? Gyroscopes? Others?
- What are the technical characteristics of the sensors? For example, what is the number of axes, sampling rate, measuring range?

5.2.1.3 Scope and Use Cases

Given the great variability in users, activities and configurations, it is common that systems that deal with human activities are designed for a limited number of use cases. The following questions can be stated:

- Where on the body is the sensor unit placed?
- What are the target users' characteristics? Will age or anatomical restrictions be used? Will only healthy people be used or will people with gait pathologies be included?
- What kind of movements and activities are contemplated?
- In which scenarios will the system be used? Indoors or outdoors? Leveled or with slopes? Stairs?

As can be seen in Figure 5.2, the definition of the use cases can influence both the experimentation and evaluation processes, since they all have to be aligned.

5.2.1.4 SLE Method

The combination of the prior knowledge about step length, the system characteristics and the use cases will lead to the design or choice of a particular SLE method, which can be described from different criteria:

- What types of SLE methods exist? What kind of model or assumption is each type of SLE method based on?
- How many input parameters does each type of SLE method need? Of what kind? And, how are these inputs obtained?
- Is it necessary a calibration of the SLE method for each specific user? If so, will it be an offline or an online calibration?

5.2.2 SLE Method Testing

Once a SLE method has been implemented, it must be tested to validate its operation. This experimentation process can be described according to different parameters, as follows:

- Are the experimentation's trials aligned with the use cases defined by the scope?
- Is the test data sufficient in volume and variability?
- What information source is taken as a reference or ground truth?

5.2.3 SLE Method Evaluation

The aim of the evaluation is to extract enough information from the data obtained during the experimentation to decide whether the performance of the SLE method is valid or to loop back iteratively to improve it. For this purpose, the evaluation can be broken down into several phases: the definition of the performance metrics, the calculation of the value of these metrics and the decision about the validity of the SLE method by comparing its performance with some predefined thresholds or other SLE methods' performances. Thus, the following questions arise:

- What different performance metrics are commonly used?
- Assuming that the estimation error is the most common performance metric, what definitions of estimation error are commonly used?
- Since experimentation only provides a sample of the performance of the SLE method, how is the process of estimating the SLE error? What descriptive statistics are commonly used to describe the SLE error?
- What is the performance of the different SLE methods of the state of the art? Is it possible to compare them from the reported SLE errors?

5.2.4 Results of the review

The following sections will present the results obtained after reviewing the selected literature through the points of view defined by the identified review questions. To do this, the workflow shown in Figure 5.2 will be followed downwards:

- Section 5.3. Prior Knowledge about Step Length
- Section 5.4. Step Length Estimation Methods
- Section 5.5. System, Use Cases and Experimentation: All aspects related to the characteristics of the final system, the definition of the use cases and the experimentation will be grouped in the same section, because all of them must be aligned.
- Section 5.6. SLE Methods Evaluation

5.3 Prior Knowledge about Step Length

It is possible to design SLE methods using simple ideas, such as the relationship between the stride length, the user's leg length, and the opening angle of the leg during each stride. However, most of the SLE methods are based on not so evident patterns that have been observed thanks to the study of the human gait over many years, especially in the field of biomechanics.

5.3.1 Displacement of the Pelvis During Human Walking

Given that the COM of the body lies within the pelvis, it is very interesting to know the trajectories of that part of the body during locomotion (see Figure 5.3). To study the fluctuations of the potential and kinetic energies of the body during walking, Cavagna *et al.* [163] proposed a model in which the COM rotates as an inverted pendulum over the stance foot during the single support phase, followed by a forward horizontal displacement during the double support phase; that is, when both feet are on the ground. Later, Zijlstra and Hof [120] used this model to study how the spatio-temporal gait parameters affect the pelvis' displacement and they derived a geometrical expression that relates the vertical displacement of the pelvis, the leg's length and the step length. This geometrical expression has been used many times by different SLE method proposals.

More complex models have been proposed including other features such as the use of a percentage of the foot length for the longitudinal displacement during the double-stance phase [164, 165], the rotation of the pelvis or the flexion of the ankle and the knee [166, 167].

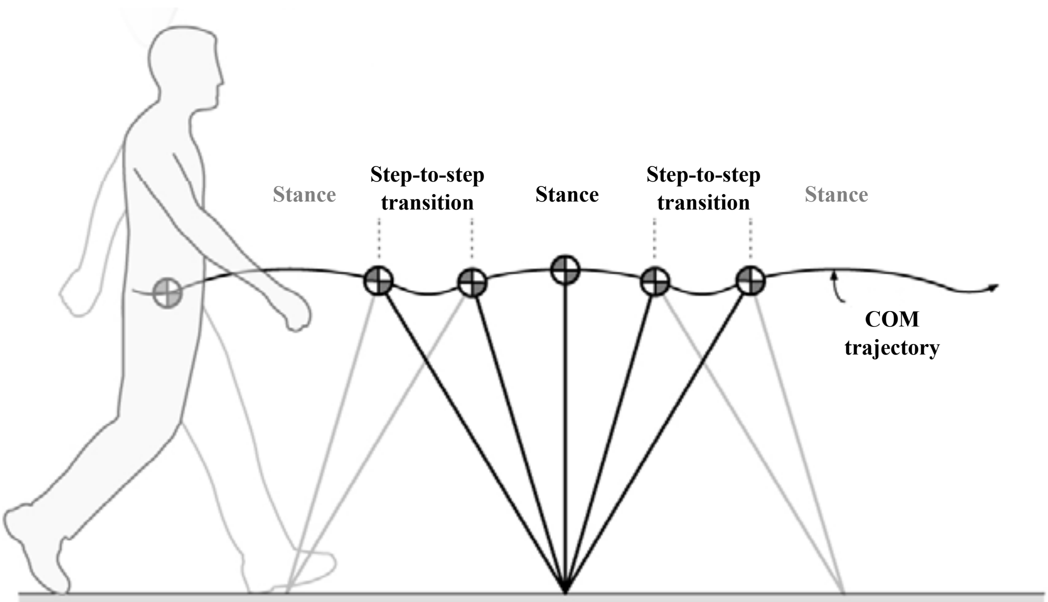

Figure 5.3: COM trajectory during walking. Figure adapted from Steven Collins [168].

5.3.2 Spatio-temporal Gait Parameters

The human gait has been analyzed in depth for many years. Spatio-temporal parameters, such as step length, step frequency, walking speed or gait asymmetry, are used as one of the main tools to describe gait operation and to detect anomalies. The behavior of the step length, as one of these spatio-temporal parameters, has been studied in relation to different parameters, such as its variation over time, between alternative footsteps, age or gender [169].

One topic that has attracted a lot of interest is the relationship between walking speed, step length and step rate. A faster walking speed implies an increase in both the step rate and the step length, but each person implements that mechanism in a different way. The works of Kuo [170], and Bertram and Ruina [121] proposed a model for this relationship and they suggested that it is due to an optimization strategy, in which each person optimizes an underlying objective function that has a minimum at the preferred gait. However, works such as Sun *et al.* [171] have shown that this relationship is also affected by other external factors, such as the slope of the terrain.

5.4 Step Length Estimation Methods

Methods for computing the step length can be divided in two main classes: the first are direct methods, based on the integration of the accelerations; and the second are indirect methods, which use a model to compute the step length. For the latter, there is a large variety of proposals that can be divided again according to whether they are based on geometric models or if they use statistical methods of prediction.

Next, each type of method will be described in more detail. This is supported by Figure 5.4, which shows the distribution of the reviewed references over the main body locations, and Table 5.1, which presents the main characteristics of the indirect methods. In addition, the different types of calibration that are usually applied to SLE methods to adjust their performance to the characteristics of each user and/or scenario will be described.

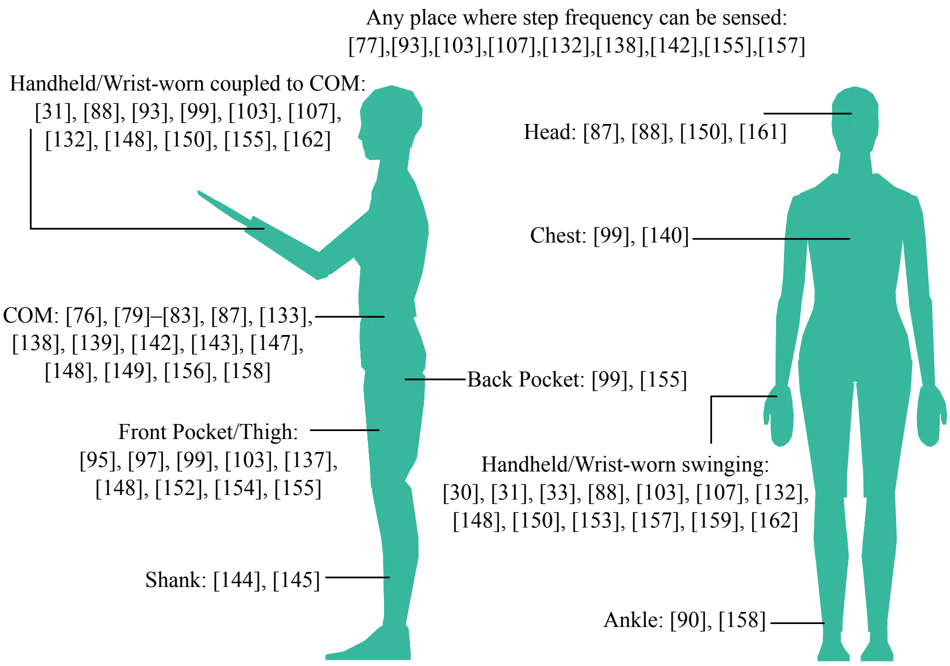

Figure 5.4: Distribution of the different body locations of the SLE methods from the reviewed references. The SLE methods that only depend on the step frequency can be used on any body location in which that feature is sensed. For those SLE methods, the body location on which they were tested in the original reference is also indicated.

5.4.1 Integration Methods

The double integration of the acceleration in the forward direction is the best method in theory to compute the length of the steps because it is not based on any model or assumption and it does not require training stages or user specific calibration. However, as for any INS, the non-negligible bias and noise of the MEMS accelerometers and gyroscopes make the distance error grow boundless cubically in time. Several assumptions and heuristics have been used to reduce this error rate.

However, the first difficulty of these methods is how to obtain the acceleration in the forward direction from the sensor's measurements. Because each part of the body moves in different directions during walking, it is not easy to constantly maintain a sensor parallel to the direction of travel. It is, therefore, necessary to continuously know the orientation of the sensor, which will involve the use of several accelerometers and gyroscopes to transform the sensors accelerations into the navigation reference system. Of course, this process is also not error-free.

Li *et al.* [144] and Yang and Li [145] proposed mounting a 2-axis accelerometer and a 1-axis gyroscope on the lateral side of the mid-shank. Both the segmentation into strides and the transformation of the accelerations into the navigation frame are obtained by using the angle obtained by integrating the gyroscope's angular rate. They use the vertical position of the shank to divide the stride segments and they assume that the initial velocity in that moment is zero. After integration, they also assume that the net acceleration during one stride was zero to correct the error of the accelerometers.

Köse *et al.* [133] proposed a system that requires a 3-axis accelerometer and a 2-axis gyroscope that are placed on one side of the pelvis. They are able to detect and differentiate the steps of each foot by using wavelet decomposition. They then compute the length of each step using a combination of direct and reverse integrations of high-pass filtered accelerations.

The fact that only these two works have been found and that both are focused on gait analysis, where the environment is usually more controlled and the time of use is shorter than in positioning applications, highlights that these integration techniques are less suitable for positioning than ZUPT for foot-mounted sensors.

5.4.2 **Biomechanical Models**

Due to the mechanical nature of the human body, it is possible to define analytical expressions of the step length based on geometrical relations between some dimensions, angles, and displacements of different parts of the body. The advantage of using biomechanical models is that it allows a good understanding of the relationships on which the estimation of the step length is built. However, due to the complexity of the human body and the great variability of people and scenarios, these models are usually simplifications and approximations that require calibration phases to adjust their performance to each specific user and walking pace.

Miyazaki [137] used a simple geometric model in which he estimated the stride length using the leg length and the opening angle during the stride. To measure this angle, he used a 1-axis gyroscope mounted on the thigh. Miyazaki found that the error in the estimation of this model depends on the walking speed, so he introduced an adaptive correction parameter to address this issue.

Several SLE method proposals have emerged from the relationship between the vertical displacement of the pelvis and step length, as described in Section 5.3.1. Using the inverted COM pendulum model, Zijlstra and Hof [80] derived the geometric expression (5.1) that relates the step length, the length of the user's leg (L), and the vertical displacement of the COM during the stance phase (H), which is obtained by double integration of the high-pass filtered vertical acceleration of a sensor placed on the low back. However, they found that this model tends to underestimate the step length and that a calibration parameter is needed to adjust the performance to each user.

$$SL = 2\sqrt{2LH - H^2} \tag{5.1}$$

Álvarez and González proposed several modifications of Zijlstra's model, such as the use of heuristics to reduce the integration drift error in [76] or the inclusion of the length of the user's foot as a predictor of the forward displacement during the double-stance phase in [139].

There are also works that are based on the same biomechanical observation but which propose empirically simplified expressions to avoid the integration: Weinberg proposed in [79] the expression (5.2), which is proportional to the amplitude of the vertical acceleration during a step.

$$SL = K\sqrt[4]{A_{max} - A_{min}} \tag{5.2}$$

Later, Scarlett [81] proposed the expression (5.3) that is an improvement of Weinberg's expression which looks for a better adaptation to different users through the inclusion of the dispersion of the vertical acceleration during the step. Neither expression contained a parameter related to the user's physical characteristics and, therefore, they need to be calibrated for each user and each walking pace.

$$SL = K\sqrt{\frac{(A_{max} - A_{min})}{(A_{avg} - A_{min})}\sum_{n=1}^{M}\sum_{n=1}^{M}(A_n(t) - A_{avg})} \tag{5.3}$$

In an attempt to simplify the calibration process at different paces, Mikov *et al.* [99] substituted the calibration parameter in Weinberg's expression by the time duration of the step. In a more general way, Zhu *et al.* [87] substituted this with a linear regression model of the step frequency and the acceleration variance during a step.

More complex biomechanical models have also been used, such as in Hu *et al.* [149], where the authors used a pelvic displacement model that takes into account the knee and ankle flexion during the stance phase, which is often known as rolling-feet. They derived a dynamic model of the pelvis and they estimated the walking speed using an unscented Kalman filter.

Although the inverted pendulum model offers simplicity and acceptable performance, it requires the accelerometers to be as coupled to the COM as possible. As was described in Section 3.2.3, Jiang *et al.* [33] proposed a geometric model in which they estimated the COM's vertical displacement from a wrist-worn sensor during arm swinging. They used some assumptions about the synchronization between the vertical movements of the trunk and the hand, which have not been referenced or demonstrated. However, this is a novel proposal that reflects the potential of using knowledge about the body's mechanical structure. Also for a wrist-worn sensor, Bertstchi *et al.* [153] proposed a walking speed estimation method that is based on one of the hypothetical objectives of arm swinging seen in Section 4.1: the compensation of the torque generated by the legs in the trunk. They claimed that walking speed is proportional to both the step frequency and to this torque, which they modeled as a non-linear function whose expression is not described because the patent is pending.

5.4.3 **Statistical Regression Methods**

Statistical regression methods seek to estimate the relationships among variables, which is useful for predicting the value of a variable that is difficult to obtain from the values of other variables that are easier to measure. These latter variables are known as features or predictors. As seen in Section 5.3.2, there is a clear relationship between step frequency and step length, and also with other variables. Therefore, they can be used as predictors of the step length and, thanks to the periodicity of human gait and the mechanical nature of the human body, some of them can be measured from different body locations, and by using different techniques and sensors. This flexibility is one of the main reasons to use statistical models for SLE.

SLE Method	References	Features	Gait parameters			User			Signal			Other features
			SF	VD	ANG	H	L	W	σ^2_{acc}	$\triangle$	FFT	
Biomechanical	[33]	4					X					Hand's vertical displacement Hand's forward displacement User's arm length
	[149]	6					X					User's pelvis width Rolling-foot radius to leg length ratio Navigation frame accelerations
	[80]	2		X			X					
	[76, 139]	3		X			X					User's foot length
	[79]	1								X		
	[81]	3										Mean, max, min of vertical acceleration
	[99]	2	X							X		
	[87]	3	X						X	X		
	[137]	2			X		X					
	[153]	6	X			X		X				Navigation frame accelerations
Linear regression	[162]	5	X			X			X			Variation of altitude in the terrain Mean of acceleration norm
	[103, 107, 132]	2	X			X						[103] uses square root of step freq.
	[30, 31, 82, 83, 147]	2	X						X			[30] also square and product of features
	[77, 93, 138, 142, 157]	1	X									[138] quadratic model
	[97, 152]	1			X							
Lasso regression	[158, 159]	50				X		X	X		X	Temporal statistics of acceleration
Logistic regression	[155]	1	X									
FOS	[88, 150]	14	X						X			Delayed versions and all inter-products
FIS	[156]	2	X									Area of acceleration norm
	[154]	2	X						X			
GPR	[143]	6144									X	
	[158, 159, 161]	50				X		X	X		X	Temporal statistics of acceleration
RLS	[148]	61									X	Energy
ANN	[140]	5				X		X		X		
Empirical	[90]	1										Mean absolute acceleration
	[95]	3	X							X		Mean absolute acceleration

Table 5.1: Proposed SLE indirect methods in the reviewed literature and the main features that they use. Acronyms: step frequency (SF); vertical displacement of the COM (VD); angular amplitude of the leg (ANG); users' height (H), leg length (L) and weight (W); moving variance of the acceleration (σ^2_{acc}); range of the acceleration ($\triangle$); FFT coefficients of the acceleration (FFT); fast orthogonal search (FOS); fuzzy inference system (FIS); Gaussian process regression (GPR); regularized least squares (RLS); artificial neural networks (ANN).

The features used in the SLE methods of the reviewed articles can be observed in Table 5.1.

The task of estimating the relationship between the variables of interest is usually known as training. The data and the model estimation techniques used during this task will affect the accuracy and the generalizability of the subsequent estimation of the step length. There are two types of model estimation techniques: parametric and non-parametric.

Parametric techniques assume an a priori type of model. Generally, they are simple models with a low number of predictors, which can provide a certain insight about the real relationship. However, if the selected a priori model is very different from the real one, then the prediction accuracy will be low. The simplest and most commonly used parametric technique is the linear regression (or ordinary least squares). It is assumed that step length is a linear combination of the features, using as fitting criteria the minimization of the quadratic error. Many works use this technique with the step frequency as the only feature ([77, 93, 142, 157]), or they also add the variance of the acceleration over a step ([31, 82, 83, 147]), or a greater number of features, such as Fasel *et al.* [162]. Although the step frequency is the most common predictor, there are works that are based on other features. For example, Díaz *et al.* proposed to use an inertial sensor mounted on the thigh and they built a linear regression model using the amplitude of the variation of the leg's pitch as the only predictor [97, 152]. The linearity criterion refers to the parameters that fit the model and it does not refer to the predictors. Consequently, it is also common to find proposals that use transformed versions of the features and/or products of several features.

In general, using more predictors helps to get better predictions but there is a higher risk of overfitting the model to the training data. To reduce this, Zihajehzadeh and Park [158, 159] used the Lasso regression, in which the linear model is fitted by minimizing a penalized version of the least squares loss function. This makes it possible to include a large number of features into the training, but the model is fitted by using only a selection of them. Some proposals have used non-linear models. For example, the logistic regression used in [155], or system identification techniques, such as the fast orthogonal search used in [88, 150], in which the feature selection is made from a set that also includes values of features of previous taken steps. Fuzzy inference systems could also be considered as a parametric method because they allow us to build a prediction method in the cases where the model is vaguely known, or fuzzy defined. The works of Li *et al.* [154] and Lai *et al.* [156] used this approach.

Non-parametric techniques do not assume an a priori model and are fitted to the training data in a flexible way. In general, they achieve better prediction accuracy than parametric techniques but they require larger training datasets, need more features, are more prone to overfitting, and they provide less information about the actual relationship. In the revised literature, we have found works that have used non-parametric methods such as *Gaussian Process Regression* (GPR) in [143, 158, 159, 161], *Regularized Least Squares* (RLS) in [148] and ANN in [140]. Non-parametric methods can include works that propose expressions obtained by empirical manual fitting, such as the works of Kim *et al.* [90] or Bylemans *et al.* [95].

5.4.4 **Calibration Procedures**

All SLE methods, except those based on direct integration, require the execution of a calibration procedure to adjust the accuracy of the SLE. Three main types have been identified, as will be described in the following subsections.

5.4.4.1 **Universal Calibration**

This refers to the training phase that is typical of the SLE methods based on statistical regression. This type of calibration is very convenient for the end users because they do not need to participate in the training phase and, therefore, they can start using the SLE method immediately. At most, they will have to inform some parameters about their anatomy, such as the height. However, the accuracy of the SLE method will also depend on its generalizability. As mentioned in Section 5.4.3, this is affected by both the model estimation technique and the training data.

5.4.4.2 **Offline Individual Calibration**

This type of calibration is common in SLE methods based on biomechanical models, since it is necessary to previously adjust certain parameters of the model to the characteristics of each user in order to improve the accuracy. These procedures usually consist of walking a known distance and then adjusting a scaling parameter to improve the estimation result. Although this is a simple task, this is not always convenient for the final user. For instance, some SLE methods, such as the one proposed by Scarlett [81], require each user to perform that calibration procedure for each different walking pace. Qian *et al.* [151] proposed a more comfortable procedure in which the optical flow captured by the camera of a smartphone is used to compute the traveled distance and to automatically perform the individual calibration .

5.4.4.3 **Online Individual Calibration**

This type of calibration attempts to combine the advantages of the two previous types of calibration. A universally calibrated regression model is progressively modified, as long as the SLE method is used, to find a better fit to the characteristics of the active user. GNSSs are usually used as the necessary source of ground truth. In this way, when walking outdoors, it is possible to adjust the SLE method so that, when entering a zone without GNSS coverage, the SLE method will yield a better accuracy than using the initial universal calibration. Several authors have proposed different iterative techniques for implementing online calibration, such as the EKF [30, 107], an adaptive KF [82], and recursive least squares [132]. In a similar way to the training phase in statistical learning, these recursive methods need to process sufficiently varied data to estimate the closest model for the user and to avoid obtaining just a local optimization. This could happen, for instance, if the calibration is performed using data from a small range of walking speeds.

5.5 System, Use Cases and Experimentation

5.5.1 Sensor Mounting Point

As can be observed in Figure 5.4, several SLE methods are available for many parts of the body. The first proposed SLE methods were designed for mounting the sensor in just one possible body location, preferably involving as little change of orientation as possible. Therefore, the pelvis and the low back were the first places chosen. In the case of gait analysis applications, because the experimentation is usually carried out in a controlled environment, other body locations such as thigh or shank were also proposed. In both cases, these body locations are ideal for SLE methods based on biomechanical models.

Many researchers have begun to use smartphones for SLE. This has led to the design and validation of SLE methods for the body locations where smartphones are usually carried, including the possibility that the device may change its position and orientation during the estimation process. In the experimentation, only a limited number of places where the smartphone can be carried are usually considered. The most common places are in the trouser pocket, handheld (in several poses), or inside a bag [88, 132, 148]. Finally, the recent appearance of wearable devices, such as smartwatches or smartglasses, has again generated the opportunity to design SLE methods for specific body locations because it can be assumed that the wearable device will not change its mounting point [33, 153, 159, 161, 162].

5.5.2 Characteristics of the Sensors

Accelerometers are the most commonly used inertial sensor for SLE, either alone or with gyroscopes. Miyazaki's proposal is the only one that has been found that estimates the step length using only a gyroscope [137]. Regarding other types of sensors, Fasel *et al.* [162] also included a barometer to measure changes in the terrain's altitude and added that information into the SLE.

The number of axes of the sensors should be differentiated between those available in the sensor unit and those that are actually used for SLE. The latter depends on both the type of SLE method and the body location where the sensor is mounted. Works that use only accelerometers usually choose 3-axis accelerometers and they compute the norm of the vector composed by the measurements of the three axes. This signal has the advantage of being immune to the change of the sensor's orientation. If the sensor is placed in a body position where its orientation is almost constant, then it is possible to dispense with some of the axes. This is the case of some trunk-mounted SLE methods that process only the vertical axis [79, 81, 138]. Regarding the SLE methods using both accelerometers and gyroscopes, it is common that both sensors have three axes because they are necessary for continuously estimating the sensor unit's three dimensional orientation and, later, transforming the sensor's accelerations to the navigation reference frame. In some cases, when it is known that the motion of interest occurs only in one plane, it is possible to use fewer measuring axes, as Yang and Li [144, 145], who only used a 2-axis accelerometer and a 1-axis gyroscope for measuring the swinging of the shank.

The measuring range and sampling rate are also important characteristics of inertial sensors. Both values have to be suitable for the dynamic range of motion to be measured. Regarding the measuring range, although many authors do not indicate this value in their works, values between ± 2 g and ± 16 g have been found for accelerometers, the lowest is the most common, and 150 $^{\circ}/$s, 300 $^{\circ}/$s and 1000 $^{\circ}/$s is used for the gyroscopes' measuring range. It should be noted that the larger measuring ranges were found in works with wrist-worn sensors [31, 153, 162], which is one of the body areas that experiences greater range of motion during walking. For the sampling rate, the reported values range from 10 Hz to 200 Hz, and 100 Hz is the most used value. A person's step rate does not usually exceed 3 Hz, so a 10 Hz sampling rate may be enough to sample the signals. It is common that both the accelerometers and gyroscopes work at the same rate.

5.5.3 User Typology

Most of the reviewed works present a good user gender balance in the experimentation. However, their scope is limited mainly to young people, excluding children and the elderly. It is also common to include in the experimentation only users without gait pathologies. Some exceptions are found in Miyazaki [137], in which tests were performed on patients with above knee prostheses or hemiplegia, and in Duong and Suh [32], whose work was specifically designed for people that needed a walker to move around. For the physical description of the users included in the experimentation, some works describe their physical characteristics, such as their height or weight, but they are never values too far from the average and it is not usual to perform a specific analysis of their influence on the SLE. For the number of users whose data is collected, there exists a wide variety, from data acquired in works which limit experimentation to a single user, to data acquired from experiments that exceed 20 different users, such as in [80, 82, 137, 149, 155, 157, 162].

5.5.4 Scenario Typology

Most measurement campaigns take place indoors and there are two types of trials. The most common trial is to walk a certain route inside a building, usually taking advantage of straight corridors whose length is 20–30 meters. The other type of trial is to use a treadmill, which offers the possibility of setting different walking speeds and slopes, and which can collect data over long periods while staying in a reduced and controlled environment. Works such as [80, 140, 145, 153] have used these treadmills during their experiments, setting different configurations of walking speed (from 0.5 m/s till 4.28 m/s) and slope (between -20% and +21%). For each combination of speed and slope, the trials usually lasted between 30 seconds and 2–3 minutes. Some disadvantages of using a treadmill are that it is no possible to make a turn and the equivalence with overground walking is not exact [126].

Some studies have carried out their experimentation outdoors, with the advantage of more varied scenarios in terms of slope and soil types, and longer duration. For example, in Fasel *et al.* [162] each user walks up to 4.7km, while in Song *et al.* [140] they walk up to 10 kilometers.

5.5.5 Motion Typology

As mentioned in Section 5.1.1, walking is the only activity considered in the scope of this review paper. However, some of the revised SLE methods are also reported to be valid for running [30, 83, 88, 150, 153]. As for the direction of travel, all works assume that the user only moves forward and they do not consider lateral or backward movements. It is worth noting the work of Díaz [97], who is able to estimate the displacement on the vertical axis when climbing up or down stairs from only an inertial sensor placed in the thigh.

Virtually all of the works consider and test various walking speeds and there are many different ways of implementing them. As discussed in the previous section, works that use a treadmill can easily configure different walking speeds. In the case of performing the experiments over ground, most authors set the speed in a fuzzy and user-dependent way: using each user's normal or preferred speed as a reference and then instructing them to walk faster or slower. Some authors try to establish a specific pace, using a metronome, such as Yang and Li [145], or a specific speed, with an additional person controlling a wheel speed sensor and acting as pacemaker, such as Renaudin *et al.* [132].

When the sensor is mounted on the upper limbs, it is necessary to indicate what kind of movements are performed by them during walking, either swinging naturally, in a quasi-static pose (coupled to the COM), or totally uncoupled to the walking. The latter option is not considered by any SLE method and some are only designed for just one of the other two, as can be seen in Figure 5.4.

5.5.6 Ground Truth

The source of ground truth is an important characteristic of the experimentation and it can affect other stages, such as the calibration and evaluation of the SLE method. However, its impact is not usually discussed. There are two types of ground truth sources regarding the level of resolution provided. The first type, which is usually simpler and cheaper, is based on knowing the traveled distance by using maps, blueprints, measuring tapes or laser rangers, and then dividing this measurement by the number of taken steps or the elapsed time, which can be obtained from a stopwatch, as in [76, 148, 158, 159, 161], or with infrared sensors, as in [149]. However, these methods are only able to provide the actual value of the average step length or walking speed.

The other type of ground truth sources seeks to provide a reference value for each taken step, and there are several proposals with different costs and accuracies. Some works use foot-mounted inertial sensor and perform INS integration to compute the displacement of each step [32, 157]. Although this method is not error free, its accuracy is better than the one of any SLE method on a body location different from the feet. González *et al.* [139] installed centimeter level marks on the floor and then recorded the path using two camcorders. Köse *et al.* [133] used an optical motion capture system that provides a very high precision. However, these systems are expensive and they operate in reduced areas, such as the 4 meter long segment in the study by Köse *et al.*. When using a treadmill for the experimentation, the step length can computed from the configured walking speed and the duration of each step. However, Díaz and González [152] combined both a treadmill and an optical motion capture system, and they then found that the speeds reported from both systems were unequal.

When the experimentation is carried out outdoors, it is usual to use GNSS systems as reference. However, the basic GNSS receivers, such as the ones included in most smartphones, are not accurate enough to provide step level reference [82].

Renaudin *et al.* have used more complex GNSS techniques, such as the interpolation of post-processed GPS positions over each identified step [132] or HGNSS Doppler measurements [107].

In relation to the technologies that can be used as ground truth of the length of each individual step, an exploratory study on the possibility of using UWB technology for this task will be presented in Chapter 6. This RF communication technology achieves worse accuracy than optical or ultrasonic systems but reaches wider ranges and coverage areas. Therefore, it seems to be an interesting technology to use as ground truth in experiments and scenarios that require larger areas.

5.6 SLE Methods Evaluation

The aim of the evaluation is to provide enough information about the performance of the SLE method to decide if it is valid or it is necessary to loop back iteratively to improve it. The estimation error is the most common performance metric. Only in the work of Renaudin *et al.* [132], another performance criterion was briefly evaluated: the number of iterations required until the online calibration method converged.

Focusing on the estimation error, it is first necessary to define the error metric and the ways to compute it, characterize it and compare it with reference values. Different ways of doing this have been found in the literature, as will be described in the following.

5.6.1 Error Metric

When evaluating the performance of an SLE method, the estimation error is the main analyzed parameter. Depending on the type of estimation method, experimentation and ground truth source, different definitions of the error metric can be found, as follows:

- Step length error/Walking speed error: These are the most appropriate metrics because they evaluate the same variable that is estimated. Ideally, the ground truth should be available at the same rate as the estimations are generated. However, some works, especially those that develop their experimentation in indoor and overground scenarios, only have the average walking speed or step length as ground truth. This limitation can be better assumed by works interested only in walking speed. Therefore, this error metric is common in walking speed estimation, such as in [137, 140, 145, 148, 149, 158, 159, 161, 162]. In contrast, the difficulty of having ground truth at step level makes few authors to choose this metric for SLE purposes [33, 133, 151].

- Traveled distance error: This is the most used metric in the revised literature because the ground truth is easily obtainable. However, this metric is affected by the performance of both the step length and the step detection, and not all works describe the performance of the latter.
- Position error: This error depends on the performance of the step detector, the step length estimation and the step heading estimation. Therefore, it is difficult to use it to gain an insight of the SLE method's performance. However, works that use the position error as a metric can be found in [31, 142, 154].

The values of these error metrics can also be found relative to the real values of walking speed, step length, or traveled distance. This allows us to aggregate error samples from trials with different characteristics.

5.6.2 Generalization Assessment

The statistical regression methods that rely on a training phase should assess how their estimations generalize to new "first seen" datasets, in order to have a more realistic performance metric. The simplest way to do this is by dividing the available data in training and test datasets (around 70%–30% commonly). Despite its simplicity, it has been found that some works do not follow this procedure.

To get a significant conclusion from this practice, it is necessary to use a large amount of available data. Given that data is always expensive to obtain, cross-validation techniques are used to get a more significant assessment of the performance. Zihajehzadeh *et al.* [158, 159] and Park *et al.* [148] used a 10-fold cross-validation technique, while the *Leave-One-Out Cross-Validation* (LOOCV) technique is used by Fasel *et al.* [162] and Zihajehzadeh *et al.* [161].

SLE methods based on biomechanical models, which usually rely on individually calibrated parameters, should also evaluate how the calibration phase affects the estimation performance, especially those works in which the calibration has to be repeated for each user and walking pace. However, we have not found any work of this kind that has used cross-validation techniques.

5.6.3 Statistical Description

The estimation error is, in general, a random variable, and the results obtained during the experimentation are only a sample. Therefore, it is common to use different statistics to describe the distribution of the estimation error. Some works only report errors obtained from individual trials, or the maximum and minimum errors obtained in a set of them. Meanwhile, other authors give more details about the error distribution like the mean values, for instance in [79, 81], and the standard deviation, such as in [132, 133, 157]. There are several ways of describing the whole error distribution. Histograms provide information about the shape of the distribution. Cumulative distribution functions are useful for the analysis of the frequency of occurrence of a phenomenon with relation to a reference value;. Box-and-whisker diagrams provide a fast and easy way for visualizing the mean and the main percentiles, identifying outliers and comparing several datasets. The latter is the most commonly used tool, such as in [76, 139, 141, 146, 153, 162].

Many times the distributions of estimation errors are quite centered on 0, indicating that such SLE methods can both underestimate and overestimate. In such cases, it is usually interesting to analyze only the magnitude of the error, ignoring its sign. To do this, it is common to find authors who use cost functions to describe the overall performance of the estimate, such as the *Root Mean Squared Error* (RMSE) or the *Mean Absolute Error* (MAE). These cost functions summarize both the bias and variance of the signed error, so they are useful for comparing in a better way overlapped signed error distributions. The main difference between RMSE and MAE is that the former penalizes the higher values more. In the case of positioning applications, it is important that both the bias and the variance are as close to zero as possible; consequently, RMSE seems more appropriate. Some authors sometimes report both, such as Zihajehzadeh *et al.* in [158, 159, 161].

Finally, a scatter diagram has also been used to study the relationship between the estimated and the actual values, such as in [137, 140, 143, 145, 159]. If the estimation were error-free, then all points should be on the line $Y = X$. To numerically evaluate the performance of the estimation, the linear regression of the cloud of points can be computed. A correlation coefficient close to 1 indicates that the SLE method works similarly across the entire range of scenarios in which it has been tested. In this case, the difference between the regression line and the line $Y = X$ could be compensated by applying a scale factor and an offset value.

5.6.4 Performance Comparison

Due to the existing variety of error metrics, statistics, and experimental procedures and datasets, it is very difficult to summarize the performances obtained by each type of SLE method in an aggregated way or to make a fair comparison between them. In other works that addressed briefly this task, such as [7, 10, 20], or the walking speed survey of Yang and Li [134], the performances of the different surveyed methods were presented only by reproducing textually the reported performances. This way does not facilitate the always difficult task of drawing conclusions from such heterogeneous data. In our case, we have decided to present the results of only those studies that showed sufficient experimental evidence and reported their results using relative metrics, along with their trend and dispersion statistics. With this filtering it is sought to select those works that favor the comparison of their performance. The results are presented in Table 5.2, in which they are grouped by type of SLE method and sensor's mounting point in order to gain some additional insight.

As can be seen, it is not easy to make a comparison of the performance of different SLE methods from the reported results. The ideal way would be to process the same dataset with different SLE methods. In fact, this task should be done in all works that propose a new SLE method: to compare the new proposal against some reference SLE methods from the state of the art. Otherwise, it is difficult to know if there is any performance improvement. Besides the works whose aim was to compare various methods, such as [76, 139, 141, 146], there are few additional works that compared their proposed SLE method to some existing one. When this is done, the SLE methods most commonly taken as reference are the lineal regression model of the step frequency, for instance in [88, 97, 143, 148, 150, 155], and the Weinberg's method [79], such as in [103, 148, 156].

After processing the same dataset with several SLE methods, it should be verified if the observed performance differences are statistically significant, in order to assure a fair comparison. Statistical tests, such as ANOVA, can be used for this task. Only the works of Lopez *et al.* [141], Vathsangam *et al.* [143] and Zihajehzadeh and Park [159] performed these and similar statistical verifications.

Implementing, testing and evaluating different SLE methods in order to have a fair comparison of their performances can be considered as a whole project on its own. Therefore, it is beyond the scope of this review. However, some observations can be highlighted from the analysis of the summary of the reported results presented in Table 5.2 and the conclusions of those works of the literature whose aim was to compare various methods:

- General accuracy: As can be seen in Table 5.2, the values of the central tendency statistic (median, mean) of the relative estimation errors of traveled distance or walking speed are in the $\pm 2\%$ range. Considering just the magnitude of the errors, the RMSE/MAE statistics are around 5%. Therefore, new proposals for SLE methods should set their accuracy targets at least for these values.

- Universal vs. Individual calibration: Using a specific calibration or training for each user has its reflection in a better accuracy and precision of the estimation in comparison to using a configuration that tries to be universal. In the results reported by Hu *et al.* [149] (COM), Renaudin *et al.* [132] or Suh *et al.* [157] (both for upper limbs) it can be seen the order of magnitude of the improvement that is achieved.

- Complexity of biomechanical models: The use of more advanced biomechanical models leads to better accuracies. This can be clearly seen when

Mounting	SLE Method Types			
Point	Integration	Biomechanical	Parametric Regression	Non-parametric Regression
Ankle				[158] WSE $4.9 \pm 4\%$ (MAE)
Shank	[144] TD 4%, WSE 7% (RMSE) [145] WSE 5.6% (RMSE)			
Thigh		[137] WSE $\pm 15\%$ ($\triangle$)	[152] TD $0.15 \pm 1.58\%$	
COM	[133] TD $[-1.6\%, 1.7\%]$	[80] WSE $\pm 15\%$ ($\triangle$) [76](M1) TD 2.5% (Median), $[-15\%, 22\%]$ (M2) TD 2% (Median), $[-12\%, 12\%]$ (M2 in [141]) TD $0 \pm 2.8\%$, 20.15% ($\triangle$) (M3) TD 5%, $[-23\%, 22\%]$ [139] TD $0 \pm 2.1\%$, $[-5.5\%, 6\%]$ [149] WSE $0.58 \pm 0.76\%$ (abs error, univ.) $3.36 \pm 2.33\%$ (abs error, ind.) [79] TD $\pm 8\%$ ($\triangle$) In [76] TD 2% (Median), $[-13\%, 8\%]$ In [141] TD $0.88 \pm 2.6\%$, 17.3% ($\triangle$) [81] TD $\pm 6\%$ ($\triangle$)	[76] TD -2% (Median), $[-17\%, 10\%]$ [88] TD 5.4% (Mean) [128] TD 5.2% (RMSE)	[148] WSE 12% (MAE) [158] WSE $4.5 \pm 4.3\%$ (MAE)
Chest				[140] TD 0.9968 (correlation) WSE 0.9874 (correlation)

— Continued on next page —

— Continued from previous page —

Mounting Point	SLE Method Types: Integration	Biomechanical	Parametric Regression	Non-parametric Regression
Head			[88] TD 5.19% (Mean)	
Upper limbs		[153] TD $[-1.2\%, 1.4\%]$ WSE $\pm 5\%$ (Interquartile range) (swinging)	[132] TD $5.7 \pm 1.6\%$ (univ.) $4.26 \pm 0.7\%$ (ind.) [88] TD 4% (Mean) (texting) 6.5% (Mean) (swinging, univ.) [159] WSE $12.7 + 7.7\%$ (swinging, univ.) [157] TD $0.2 + 7.8\%$ (univ.) $0.2 + 3.8\%$ (ind.) [162] WSE -0.67% (median) $[-6.52\%, 6.23\%]$ (Interquartile range)	[148] WSE 12% (MAE) [159] WSE $5.9 \pm 4.7\%$ (MAE) (swinging)

Table 5.2: Accuracy reported by a set of representative works, grouped by type of SLE method and sensor's mounting point. Clarifications: *Traveled Distance* (TD); *Walking Speed Estimation* (WSE); Brackets indicate minimum and maximum error values ([min,max]); $\triangle$ indicates the length of the range of error values, i.e., $max - min$; The terms "ind." and "univ." refer to individual or universal calibration; For the upper limbs case, static and swinging refer to the results differentiated by arm motion; Reference [76] from Álvarez *et al.* tested several methods, indicated as M1-3; Whenever a method has been tested in another work is annotated as "in [ref]".

using different models of the displacement of the COM during gait: the estimation of walking speed using the inverted pendulum model of Zijlstra and Hof [80] is clearly exceeded by the Hu *et al.* [149] method which uses a more complex model of the pelvic movement. Another example is the different accuracies of the distance traveled estimations obtained by Álvarez and González [139] using first a model similar to that of Zijlstra (M1 in [76]) or a more advanced model that also includes the length of the foot as a feature. An example of the opposite case, that is, using a biomechanical model that is too simple, can be found by comparing the works of Miyazaki [137] and Díaz [152]. Both use the opening angle of the leg when walking, but Miyazaki used a too simple model that seems to be surpassed by the SLE method based on a linear regression of that angle, proposed by Díaz.

- Signal integration: Some SLE methods use as input parameters some feature that are obtained by integration of inertial signals. Since these signals contain errors, the way in which the integration is performed can affect the accuracy of the SLE method. For example, the difference in precision between the M1 and M2 methods of Álvarez *et al.* [76] is due only to different ways of integrating the vertical acceleration. In the case of Köse *et al.* [133], they achieve very good results through more advanced integration techniques. On the other hand, given the difficulty of achieving a precise integration, some authors prefer to use empirical expressions that approximate this integration, such as Weinberg [79], who is able to get similar results to Álvarez.

- Effect of the sensor mounting point on the performance: Observing the data presented in Table 5.2, the swinging upper limbs seem one of the most challenging scenarios for step length estimation. In the works of Zihajehzadeh and Parks [158, 159] it can be seen how the same SLE method gets worse performances when the sensor is on the wrist than on waist and ankle. Omr's work [88] seems to indicate the same idea, showing the clear difference in performance when the arms are coupled to the COM or when they swing.

- Type of regression method: In general, non-parametric regression methods achieve better accuracy, although they may be more prone to over-fitting.

Zihajehzadeh and Parks compared in [159] a parametric regression method (LASSO regression) to a non-parametric one (GPR) for a wrist-worn sensor, achieving significantly better results with the latter. Compared to other non-parametric methods, GPR seems to obtain better walking speed estimation results when applied on a waist-worn sensor [158] than the ones obtained by Park *et al.* [148] using RLS for the same body location.

- Correspondence between traveled distance error and walking speed error: Although there is a clear physical relationship between the two magnitudes, the estimation errors do not seem to be directly comparable between them. In the works of Li *et al.*[144], Bertschi *et al.* [153] and Song *et al.* [140], which report both error metrics, there are clear differences between them for the same datasets.

- An example of the difficulty of comparison: To illustrate the difficulty of comparing the performance of different SLE methods from their reported results, we can look at the works of Renaudin *et al.* [132] and Suh *et al.* [157]. In both cases they used wrist-worn sensors and evaluated SLE methods based on a linear regression of the step frequency. In the case of Renaudin *et al.* they also used the user's height, which leads one to believe that better results should be obtained. However, the reported mean and standard deviation values of Suh *et al.* seem significantly better, which does not seem convincing. Therefore, with the available information, we are not able to compare them reliably.

5.7 The Problem of the Performance Comparison

As seen throughout this work, there is a wide variety of SLE methods based on different assumptions and for different parts of the body. Therefore, it is necessary to evaluate them and compare their performances in a fair and robust way, in order to choose the most appropriate option for each case of use and continue advancing in the development of new SLE methods. However, it is currently very complicated to make such a comparison from the results that are reported in each work due to two main reasons: the lack of public datasets and the lack of a standard methodology for testing and evaluation. In this section we will review the current status of both issues and reflect on the different aspects that need to be taken into account in order to move towards their achievement.

5.7.1 Public Datasets Availability

The availability of public datasets can determine the successful future of a research field. Especially in those where it is difficult to generate data in a synthetic way, as is the case here due to the great variability of human bodies and the difficulty of modeling the human gait. In addition to the obvious optimization of resources and efforts, the existence of shared datasets is essential to ensure the reproducibility of the results of the different methods and to make a fair comparison between them. This has been shown to be very useful in different fields, some of which are close to the estimation of the length of the step, such as the classification of human activities [172], the detection of steps [112, 173, 174] or pedestrian positioning [96, 175–178]. Some of these datasets can be found in online repositories, such as the well-known UCI machine learning repository [179–183].

However, no SLE-oriented datasets have been found and, after reviewing the mentioned datasets found, it has been checked that none of them are suitable for the task of evaluating SLE methods. The most common limitation is the lack of ground truth information at the required level of accuracy and resolution.

5.7.2 Standardization

The definition of standards that establish a testing and evaluation methodology and that are shared and accepted by the scientific community and the industry, provides a common language and practice that can greatly benefit the pace of progress in a field. Through its use, the aim is to establish minimum criteria for experimentation and evaluation, ensure the reproducibility of experiments and, therefore, increase confidence in the results obtained and reported by the different members of the research community.

No standards have been found that fit perfectly within the scope of SLE but, as with public datasets, there are some standards and initiatives underway in nearby areas, which may serve as a reference for the drafting of new standards or which could be modified to include SLE-related cases.

- The Biomathics and Canadian Gait Consortiums Initiative: Since 2015, two consortia of international researchers have joined forces with the aim of providing a certain consensus on gait analysis for older people. Given that changes in gait are a very powerful indicator of health status, this initiative has developed a guideline on how to perform experimentation and published a set of reference values of different gait parameters [184]. This guideline indicates which parameters should be included to characterize the subjects participating in the experiments and to describe their gait. It is interesting that it was indicated which of those parameters should be taken as mandatory and which as optional (minimum and full dataset). They also give advice on how the data collection and analysis procedure should be. The guideline does not fit with SLE because it is oriented to the analysis of the distribution of gait parameters across several subjects groups. That is, its objective is not to estimate those parameters in a indirect way. They assume that the data are accurately obtained in a clinical laboratory environment. In addition, it should be noted that they do not use the step length concept. They only refer to the stride length, which is marked as an optional parameter. This reflects the differences imposed by the final application.

- ISO/IEC 18305:2016: The *International Organization for Standardization* (ISO) and the *International Electrotechnical Commission* (IEC) identified that the lack of a standard test and evaluation methodology slows down the growth of the localization systems market, as it makes it difficult to compare the different existing systems and easily determine their performance. At the end of 2016 they released the standard ISO/IEC 18305, entitled "Test and evaluation of localization and tracking systems" [185], which aims to provide instructions on how to develop test scenarios and performance metrics, and how to report the obtained results. This standard is really exhaustive but it is also not suitable for assessing SLE methods because it is mainly focused on RF-based localization systems, which are tested only at system level considering a "black-box" approach. If this standard was someday updated to include DR based localization methods and/or component level evaluation, it could be valid for SLE purposes.

Other ongoing initiatives in this area include the standard ISO 17438-1:2016 "Indoor navigation for personal and vehicle ITS station" or the activities held at the 2017 edition of IPIN conference, which held specific sessions on localization system evaluation and the announcement of the creation of the International Standards Committee of the IPIN.

5.7.3 The Role of the Competitions

The holding of competitions is another opportunity to advance in the development of methodologies, the comparison of different systems and the generation of datasets. Again, no competition specifically designed for SLE has been found. The closest ones are the different localization system competitions that are held, many of which usually publish articles summarizing the results obtained and lessons learned: the Microsoft Indoor Localization Competition at the International Conference on Information Processing in Sensor Networks [14]; the EvAAL initiative that organizes international competitions on indoor localization and indoor activity recognition since 2011 [186]; the IPIN Indoor Localization Competition, that has formally adopted the EvAAL framework since 2016 [187, 188]; the PerfLoc, organized by the US National Institute of Standards and Technology [189]; and the indoor location testbed organized by Geo IoT World conference [190].

However, similar to ISO/IEC 18305, most of these competitions are aimed at evaluating location systems based on signals coming from the environment. Inertial sensors are often used only as an additional source of information, so their specific performance is not evaluated. Even in competitions with a specific category for inertial PDR systems, as in the IPIN competition, they are evaluated in the same way as the positioning systems based on beacons or other signals from the environment. We believe that, because of the accumulation of error over time, positioning systems based on DR should be evaluated in a way that allows characterizing their performance in terms of elapsed time, traveled distance or number of steps walked. In such a case, positioning system competitions could become valid for evaluating SLE methods.

5.7.4 Reflections on Testing and Evaluating SLE Methods

In the process of developing standards that are suitable for testing and evaluating SLE methods, it would be appropriate to take as an example the existing experiences in related fields, such as those mentioned above, and adapt them to the specific needs of SLE methods. Next, we will present a series of aspects that the authors consider important to be reflected in those possible future standards.

5.7.4.1 Final application agnostic

Since the knowledge of step lengths can be useful for different applications, the possible future methodologies and datasets should try not to be biased towards a particular final application. To this end, users from different applications of step length must be involved during the definition. In this way, efforts can be pooled and resources optimized.

5.7.4.2 Experimental considerations

The design of the experiments should aim to facilitate their repetition and try to capture as much variability as possible for the problem at hand. The choice of the source of ground truth is crucial as it determines where the experiments can be conducted and the characteristics they may have at that location. This and other aspects that should be taken into account during the design of the experiments will be briefly discussed:

- Ground truth source: Ideally, the ground truth source should provide the length of each of the steps or strides and, to do this, it is necessary to know the positions of the feet when they rest on the ground. There are different positioning technologies that offer different combinations of accuracy and coverage area, which are often inversely related. As mentioned before, Chapter 6 will present an exploratory study on the using of UWB technology as ground truth source in order to exploit its balanced combination of ranging accuracy and coverage. If it is not possible to have ground truth for each individual step, it could be considered to use the average step length from the traveled distance and the number of steps, although it would be necessary to study how this affects the performance assessment. On the other hand, in our opinion, it should always be avoided to evaluate an SLE method by means of the position errors at different evaluation points.

- Experimental scenario: As mentioned above, the choice of the ground truth source will determine whether the experiments can be done outdoors or indoors and the size of the experimental area. Therefore, ground truth ends up also influencing the characteristics of the scenarios where the experiments will be carried out and their duration. For example, when the coverage area of ground truth is very small, many authors choose to use a treadmill to increase the duration of experiments. In our opinion, the use of this tool should be avoided, since the way of walking can be altered by its use [126], and the walk tests should be attempted over ground.

- Features of the experimental scenario: In general, straight and flat paths are tested, as these are the most common situations in real life. When assessing which other features of the scenarios should be taken into account in the evaluation of SLE methods, we think that they could be prioritized according to their effect on the step length and their likelihood of occurrence and duration in real situations. For example, the incorporation of different slopes seems almost mandatory, since they affect the size of the steps, are common in real scenarios and their duration can be considerable. In the case of stairs, the step length is determined by the own design of the stairs, not so much by the person or their speed, and their dimensions usually follow certain design rules. In addition, the stairs sections are not usually very long, so it seems to us to be less of a priority than the slopes. Finally, turns usually only occur when the person wants to change the heading. As we tend to walk in straight segments, the duration of the turns does not usually last more than two or three steps. Therefore, we can consider them to be of very low priority.

- Walk tests size: The size of the walk tests can be measured in distance, time duration or number of steps. For the first two options, the problem is that the number of steps will depend on the user and the speed, so if the same distance or time is always used, unbalanced datasets can be generated. The problem with indicating the size by the number of steps is that it is necessary to count the steps while walking, which may be inaccurate and inconvenient for the user over long distances. One possible solution would be to use different distances or temporal durations depending on the walking speed of each trial. Obviously, the more data, the better, but from a minimum number of steps that allows the user to achieve a steady state walking speed and ensure some statistical evidence, it may be sufficient. Anyhow, short routes are ideal for evaluating SLE methods under predictable difficulties, as they are more controllable. On the other hand, a long path can be a more realistic trial because there are more chances of unforeseen events to occur. For example, even if the users are asked to walk naturally, on a short path they may unconsciously modify their gait if they are too focused on the trial, while on a sufficiently long path they may relax and perform more natural movements and gestures. Therefore, long walk tests may be more suitable for advanced stages of SLE method testing, when basic cases have already been tested and obvious errors corrected. They can also be interesting for collecting training datasets including different use cases in a single run.

- Users' motions: Users can move in different ways, such as walking, running, backward walking or sidestepping. And they can do it at different step rates or speeds. Therefore, it is also important to define if the step rate or walking speed will be self-selected by the user or established by an external tool or person. In addition, it may be desirable to define what other activities the users will be doing while walking, especially if the sensors are mounted on the upper limbs or if the effect of the cognitive load on the walking is going to be assessed.

- Sensors: In order to generate the most useful datasets possible, it would be ideal to install as many inertial sensors as possible on the user, on different parts of the body, and to store their output data in a synchronized way. This would require a standard definition for the mounting points on the body. In addition, it would be appropriate to define minimum requirements or quality categories for the inertial sensors.

- Users' characteristics: It is important to include in the experiments subjects of different genre, age and anthropometric measurements. For the latter, it should also be defined which body dimensions should always be collected and the procedure to do it. Additionally, the characterization of gait anomalies also would deserve special attention.

5.7.4.3 **Evaluation**

The evaluation process also contains several aspects that merit some reflection:

- Step length definition: While the stride length definition is unique, for the step length there are different definitions that mainly differ in their results when the walking is not straight [135].

- Effect of the step/stride segmentation: When designing an SLE method, it is usually assumed that the segmentation of the dataset in steps is given and is perfect. Since this may not be true, mechanisms must be sought to decouple the performance of the segmentation from that of the SLE. These can be achieved by using a single segmentation method in each body location or by eliminating the steps that have not been correctly segmented.

- Estimation error: A future standard for evaluating SLE methods should establish how to perform the entire process related to the accuracy assessment: the error metric definition, its calculation, the statistics to be used for its reporting and how to perform the comparison with other methods' errors. In our opinion, the estimation error should be calculated at the level of each step, using both signed and unsigned errors (absolute error or squared error). The former is useful to detect if a method has a tendency to overestimate or underestimate, and the latter ones allow having a better perception of the magnitude of the errors. For the error calculation, whenever the SLE method requires a training or calibration phase, techniques that provide a better estimation of the error, such as cross-validation, should be applied. When reporting the obtained errors, it should be established which trend and dispersion statistics should be mandatory, as well as which statistical tests should be performed for analyzing how the error values are affected by variables such as the sex of the subject or the walking speed, and for assessing the statistical significance of the differences between the errors obtained by different SLE methods.

- Other performance metrics: In addition to the estimation error, it should be established what other performance metrics it would be interesting to evaluate, such as the cost of the system, the difficulty of installation, the latency in the estimation process, or the user's acceptance.

5.7.4.4 **Generation of public datasets**

A dataset consists of two elements: the data and the associated documentation. As for the data, since the aim is to share them with the scientific community, they should be coded using open file formats and made available online. They must include, at least, the raw measurements of the inertial sensors and the ground truth information. Ideally, both data should be synchronized over time and, if not, it must be provided the tools and information to synchronize them. In addition to the raw measurements, processed data can also be provided (segmented, cleaned, filtered, and so on), as well as software tools for their manipulation and processing. Such actions would improve the reproducibility of the reported results.

With regard to the documentation, it should describe in detail how these datasets were generated and collected. In addition to describing the format of the datasets, the users who have participated in the experiments, the hardware that has been used and the experiments that have been performed must be described. Regarding the information about the users, it must be anonymized beforehand. One of the best ways to ensure a good documentation is to write and publish a dataset paper in a scientific journal. In this way, the peer-review process ensures its quality, gives visibility to the dataset and the authors, and the document gets a normalized reference.

5.8 Conclusions

The work presented in this chapter has reviewed the state of the art of the SLE methods based on inertial sensors. The whole workflow of design and development of a SLE method has been taken as a guide to perform a systematic and deep review. The main conclusion of this work is the corroboration that this field is still in the research stage, which is supported by two reasons. On the one hand, there is a wide repertory of available SLE methods, based on different models, assumptions and techniques, whose sensor units can be placed on different locations over the body. On the other hand, there is a lack of public datasets and standard methodology for the experimentation and the evaluation. This second reason makes it very difficult to have a fair and robust comparison between the available SLE methods and, as yet, there is no gold standard solution. For this reason, in addition to having reviewed the existing initiatives regarding standardization and available datasets in the SLE field and others close to it, a reflection has been made on which aspects should be taken into account in future advances in this field.

The research stage is also reflected in the greater proportion of papers published in congresses with respect to impact journals. The 49 papers that we reviewed are distributed in 28 conference papers, 17 journal articles, two applications notes, one patent and one doctoral thesis. Many SLE methods are only available as conference papers and they have a limited experimentation and a poor evaluation, which makes them not robust enough to serve as evidence.

Regarding the different types of SLE methods, in Table 5.3 can be seen a summary of the strengths, weaknesses and suitable application case of each of them. It has been observed that, because integration methods are limited to very controlled scenarios, most SLE methods are based on biomechanical models and statistical regression. The latter have gained popularity in recent years due to the flexibility that they offer in terms of supporting multiple mounting points, various types of user movements and the possibility of not requiring an end-user calibration phase. Moreover, there is a tendency towards a more frequent use of non-parametric techniques. This can also be further evidence of the research stage of this field—the focus is mainly on the improvement of the accuracy, not on the understanding of the underlying model.

Apart from the necessary progress in terms of standardization of testing and evaluation and the availability of public datasets, there are other open issues in the field of SLE methods:

Integration methods	
Strengths	- It is a direct method, theoretically perfect, that does no assume any model. - No training or calibration is needed.
Weaknesses	- In practice, it is limited by sensor's noise and bias. - It is usually necessary to transform accelerations from sensor frame to navigation frame. This adds another source of possible errors.
Suitable application case	- It is feasible for gait analysis through short walks performed in clinical laboratories.
Biomechanical methods	
Strengths	- They are based on known models about human gait's mechanics. - Good accuracies can be achieved for calibrated cases and users.
Weaknesses	- Human body mechanics is complex, so simplified models get worse accuracies. - They usually requiere a calibration stage for each user and walking pace. - It is necessary to know the length of different body segments. - They require to mount the inertial sensor on specific body locations.
Suitable application case	- For well defined use cases: a known user, sensor mounting point and kind of motion.
Statistical regression methods	
Strengths	- They offer a balance of accuracy and generalizability. - Any signal that shows correlation with the step length can be used as feature. - Some regression models allow several sensor mounting points. - They do not require a calibration for each user. Parametric models: - They provide some insight about the mechanics of human gait. - They are usually simple and light enough to be executed in real-time. Non-parametric models: - They can achieve higher accuracy than the parametric ones.
Weaknesses	- They require a previous training stage with a great variety of users and motion. Therefore, it can be time consuming. Parametric models: - The accuracy can be not very good. Non-parametric models: - Black-box nature, no explanation about the working principle.. - Higher risk of over-fitting.
Suitable application case	- Use cases in which flexibility is more important than accuracy. That is, consistent performance for different users, paces or sensor mounting point.

Table 5.3: Summary of strengths, weaknesses and suitable application cases of each type of SLE method

- Validity of the SLE methods: Each SLE method is based on certain assumptions, such as geometrical models, linear relationships or a constant variance of the error (known as homoscedasticity). However, the validity of these assumptions are rarely completely checked. Similarly, an analysis of the theoretical limits of the performance of the estimators, such as the error analysis done by Jahn *et al.* in [146], would be also useful to gain further insight.

- Impact of the features' quality: This can be seen from two levels. First, regarding the quality of the sensors, some authors do not indicate which sensors they used in their experimentation and, therefore, little is known about the impact of the sensors' characteristics, such as the sampling rate, the measuring range or the noise, on the performance of the SLE. Consequently, questions such "Can similar performance be expected if different sensors are used?" could provide interesting findings. Second, little is known about how much the computation method of a feature affects the estimation performance. For instance, the step frequency can be obtained using temporal or spectral tools, which do not always have the same requirements or accuracy. In addition, the kind of filtering applied to the signals or the type of step detector can also be an important investigation to undertake, in addition to how to measure some anatomical dimensions needed as input parameters in some SLE methods, whose procedure is seldom described.

We shape our tools, and then our tools shape us.

Marshall McLuhan

CHAPTER

6

SLE using UWB Technology: A Preliminary Evaluation

The survey conducted in the previous Chapter 5 was intended to serve as a starting point for better development of SLE methods. One of the conclusions drawn in it is the important role that the ground truth source plays in the calibration, testing and evaluation of SLE methods based on inertial sensors. Nevertheless, the technologies that are commonly used as ground truth do not offer a good balance between accuracy and coverage area. On the one hand, technologies such as optical systems can achieve millimeter accuracies of the lengths of each step or stride. Unfortunately, due to LOS requirements, its use is limited to very small areas, which leads a lot of researchers to choose to perform experiments on treadmills, which makes it difficult to collect data associated with realistic day-to-day activities. On the other hand, other technologies that can be used in larger and outdoor areas are not able to measure the length of each individual step but the average after a walk.

Motivated by these facts, the UWB technology was identified as a possible candidate to be used as a ground truth source in the field of SLE. This technology offers only decimeter-level ranging accuracy but provides larger coverage areas than optical or ultrasound systems, which can be useful for the training and evaluating PDR systems. Therefore, in this chapter, a preliminary evaluation of the accuracy of UWB technology as a ground truth source for SLE related tasks is presented.

The structure of the chapter is as follows: Section 6.1 introduces the work and existing related literature. The experimental setup and the method adopted to collect the experimental data is described in Section 6.2. Section 6.3 describes the SLE methods that are implemented and tested. Section 6.4 presents and analyzes the results obtained by the different implemented SLE methods. Finally, in the last Section 6.5, we give some conclusions and future work.

6.1 Introduction

The step length is a gait parameter defined by the consecutive relative positions between both feet when they are still on the ground. To obtain the feet positions, technologies such as optical systems, ground reaction force sensors and ultrasound beacons have traditionally been used, achieving centimeter accuracies and even better, especially with some optical systems [191]. However, all of the aforementioned methods have limitations such as the coverage range (about 10 meters in LOS conditions) or, in the specific case of ultrasound, the sensitivity to the temperature variations, which restrict their use to dedicated indoor laboratories. This makes it difficult to collect data belonging to day-to-day activities.

In the field of inertial PDR systems, most of them need to perform a training or calibration stage of the SLE block. Therefore, a reference or ground truth step length is necessary during that training stage. The space restrictions of the measurement systems based on optical or ultrasound technologies can alter the subject's normal gait, limiting, for example, the speed that can be reached or the number of consecutive steps that can be taken. For this reason, despite their high precision, these systems are not usually used during the PDR systems calibration.

Some of the most common sources of step length reference in that PDR field are GNSS or the computation of the average step length after traveling a known distance. Although these ground truth sources allow operating in large coverage areas, they do not provide sufficient precision to estimate the length of each individual step. They are only able to provide average step length values. On the one hand, this implies having to repeat the data collection at different speeds. On the other hand, although the subject tries to walk at a constant speed, it is not usually evaluated how representative the average step length is in such walks. Therefore, finding a technology that allows combining the estimation of the length of each individual step, with an acceptable accuracy and in a large coverage area, would improve the training stage as it would include more realistic scenarios and would require less data collection repetitions.

UWB is a communication radio technology that offers low-power consumption and, thanks to its high-bandwidth and high ranging accuracies even in severe multipath environments. In recent years, there has been a great deal of interest in its use for positioning [192–196]. UWB offers decimeter-level ranging accuracies, worse than optical (millimeter-level) or ultrasound (centimeter-level) systems, but with coverages of several tens of meters (see Figure 2.3). Therefore, it could be considered as a candidate technology for SLE purposes in larger testing scenarios.

No work has been found in the literature that uses only UWB technology to perform SLE. The use of this technology in people is usually oriented to track their position by mounting a single UWB node in parts of the body away from the floor [197–199] or to perform motion capture by installing several nodes along the body for tracking the position of the different segments that define the user's skeleton [200]. In the case of the ultrasound technology, some works do use it for SLE purposes [52, 53, 201, 202], possibly because of its precision and low cost, although, as mentioned above, with a limitation in terms of coverage. In addition, there are also works that combine IMUs with different wireless technologies such as custom-made RF links [203], cameras [204], UWB [193] or ultrasound [205]. In this way it is possible to compensate for the weakness of each technology but at the expense of increasing the cost and complexity of the system.

This work pretends to provide an initial assessment of the accuracy that UWB technology used standalone can offer for SLE purposes. To this end, a set of UWB nodes will be installed as anchors and on the feet of a person, and several state-of-the-art SLE methods based on wireless anchors will be implemented, tested and evaluated. Depending on the results obtained, a more extensive future evaluation will include larger spaces, more complex trajectories in terms of direction and speed changes, and the assessment of the benefit of its use for training SLE methods in comparison to the using of the average step length.

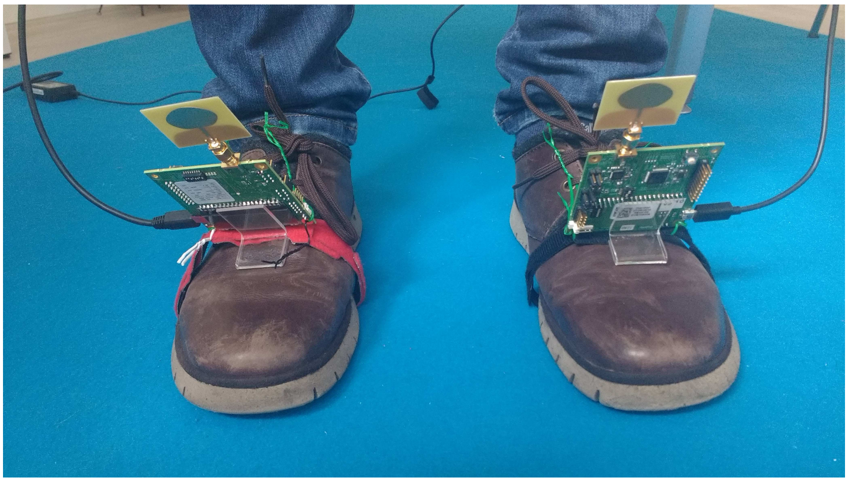

Figure 6.1: Decawave UWB nodes mounted on the feet.

6.2 Experimental Setup

6.2.1 Hardware description

Regarding the UWB nodes, several TREK1000 development kits manufactured by Decawave were used. They are fully compliant with the IEEE 802.15.4-2011 UWB standard. According to the manufacturer, it is possible to achieve ranging errors of ± 10 cm with measurable ranges larger than 100 m, depending on the specific antenna, frequency channel and conditions of the scenario. Therefore, a real time localization system with an accuracy of about ± 30 cm should be possible to implement.

For our experiments, the nodes were configured to work in the channel 2 (3.99 GHz) and with a 6.8 MB/s data rate, the so-called S2 mode. Five nodes were used, three of them configured as anchors and the other two as tags. However, due to the operation of the software provided by the manufacturer, the nodes configured as anchors A1 and A2 are placed on the feet and the nodes configured as T0, T1 and A0 are placed in fixed positions. In this way, in addition to the ranges from the feet to the fixed nodes, the inter-feet ranges can also be obtained. Figure 6.1 presents how the nodes were mounted on the feet using velcro straps and wires. They were mounted as rigidly as possible in order to avoid vibrations of the UWB node. Additionally, the software provided by the manufacturer was modified to reduce the size of the time frame and adjust it to the specific quantity of nodes used in these experiments. In this way, and together with the configuration indicated above, it is possible to increase the ranging frequency up to 25 Hz.

6.2.2 Environment description

The UWB nodes that act as anchors were mounted on tripods in the positions indicated in Table 6.1. The small difference in height is due to the use of different tripod models. A laptop is connected to the A0 anchor to store all measurements. Sixteen ground marks of tape were installed on the floor, representing the foot positions for 14 steps of different lengths. That is to say, these tape marks are the reference of the potential ground truth system. Table 6.2 presents the coordinates of these ground marks. The positions of the tripods and ground marks were determined by using a laser rangefinder. The experiments were carried out in a 8 m $\times$ 10 m room and the origin of the reference system was defined in one of its corners. In Figure 6.2 a diagram of the complete installation can be seen.

6.2.3 Walks description

Using the installed ground marks, a series of walks are taken following this procedure:

- The walks start with the feet on the ground marks with the index 1 indicated in the Table 6.2, i.e. the furthest away from the anchor A0.
- The walks always start with the right foot, walking at normal speed and, at each footstep, the foot is landed trying to leave the ground mark under the instep area.
- When the subject reaches the end, he waits 10 seconds standstill, turn around, wait another 10 seconds and walk back to the starting position in the same way.

In a first session, this procedure is repeated 18 times and in a second, 21 times. Therefore, there are 39 walks, in two directions, and each one composed of 14 steps, which makes a total of 1092 steps.

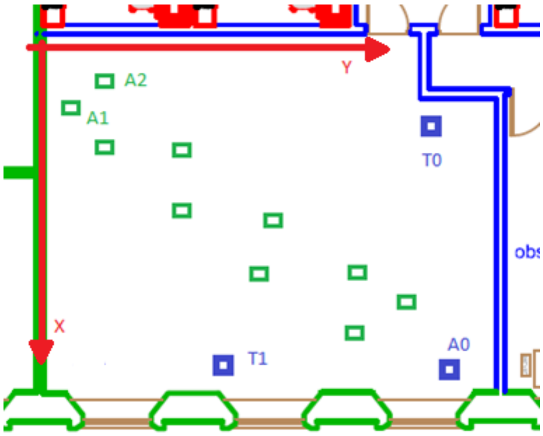

Figure 6.2: Map of the room and the installation.

	X(cm)	Y(cm)	Z(cm)
Tripod T0	186	794	156
Tripod A0	661	818	158
Tripod T1	651	420	158

Table 6.1: Coordinates of the fixed position UWB nodes.

A1	X(cm)	Y(cm)	A2	X(cm)	Y(cm)
1	124	71	1	98	92
2	157	118	2	160	171
3	218	201	3	221	260
4	289	295	4	299	366
5	354	386	5	383	472
6	447	508	6	450	557
7	507	589	7	513	649
8	589	692	8	565	708

Table 6.2: Coordinates of the ground marks, grouped by each side's footsteps. That is, A1 would be the right foot and A2 the left foot if the user walks toward anchor A0.

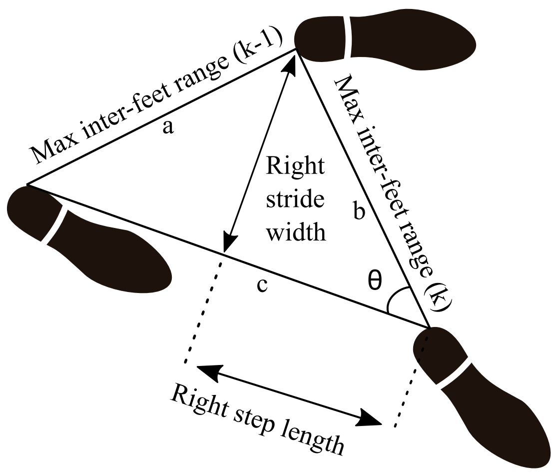

Figure 6.3: Step length definition based on the triangle formed by the consecutive footsteps, as described by Huxham *et al.* [135]. It can be seen as the inter-feet range presents a periodic behavior with consecutive local maxima.

Using ground marks can change the way the subject walks, but since the aim of this paper is to evaluate the accuracy of the step length estimation, it is not relevant that the gait is not entirely natural. In addition, the size of the ground marks (approximately 25 cm^2) is enough to make it easy to step on them when walking at a normal speed.

Taking into account the installation of ground marks and tripods, the realization of walks in both directions, forward and backward, provides two scenarios with different characteristics. In the case of forward walks, the NLOS situations are few. They will only appear when the swinging leg stands between the node of the foot that is still on the ground and the anchor of the opposite side. On the other hand, in the backward walk, NLOS situations will be more frequent as the legs themselves produce a shadow effect. In addition, in both cases, the proximity of the feet nodes to the ground produce multipaths that can affect the time of flight estimates.

6.2.4 **Step Length Definition**

To calculate the step length, we use the definition from Huxham *et al.* [135], which exploits the triangle defined by the positions of the feet when resting on the ground, as shown in Figure 6.3. By applying the cosine rule, these expressions can be obtained:

$$\text{Right step length} = b\cos\theta = \frac{b^2 + c^2 - a^2}{2c} \tag{6.1}$$

$$\text{Right stride width} = \sqrt{b^2 - SL^2} \tag{6.2}$$

The advantage of this definition is that it is not necessary to walk in a straight line, which is to say that the width of the steps can vary between successive steps. As mentioned previously, it is not necessary to know the positions of the feet in a global reference system but only their relative positions, since only the dimensions of the triangle defined by the footsteps are necessary.

6.3 Description of SLE Methods Based on UWB

As explained in the previous section, the infrastructure of the experiments consists of one UWB node mounted on each foot and three UWB nodes in fixed and known positions, acting as anchors. In addition to the ranges from each foot to each anchor, the inter-feet range is also obtained. With these signals available, it is possible to implement different methods to estimate step lengths, which are explained next.

6.3.1 SLE Based on the Direct Approach to a Fixed Point

This method was proposed by Huitema *et al.* in [201] and is based on using the variations of the range from each foot to a fixed point while they approach to it. In their work they used ultrasound as ranging technology.

We implemented this method using the ranges between each feet (A1 and A2) and the central anchor A0. In the case some sample is missing, its value was recovered by interpolating the previous and following ones. The difference of height between the nodes on the feet and the one on the tripod was taken into account for correcting the ranges. Additionally, the ranges were smoothed by applying an fifth-order Butterworth low pass filter, with a cut-off frequency at 2 Hz, which should be enough to keep the stride frequency.

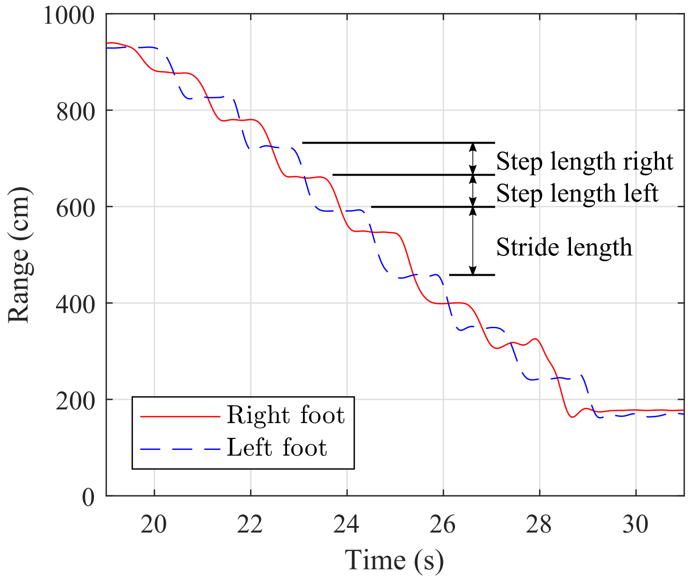

(a) Ranges from each foot to the fixed point

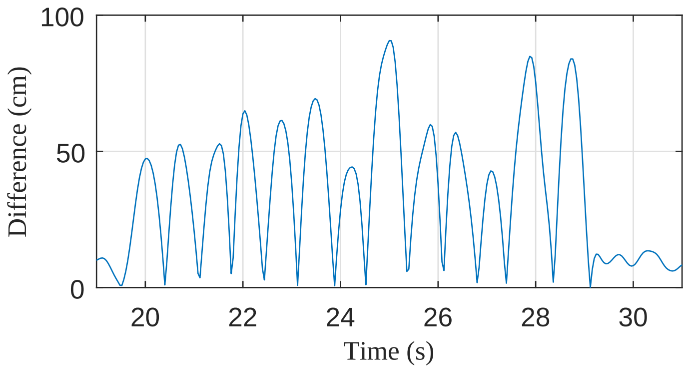

(b) Absolute difference the ranges from each foot to the fixed point

Figure 6.4: Example of the signals involved in the SLE Based on the Direct Approach to a Fixed Point

The variations of one foot's range corresponds to the length of its strides. Similarly, the periodic peaks of the difference between the ranges of both feet corresponds to the length of each step. An example can be seen in Figure 6.4. For that reason, in order to obtain the step lengths, the absolute value of the difference between both feet's range signals is computed, a peak detection algorithm is executed and the value of each peak is considered as the different step lengths. This method has the advantage that little infrastructure is needed, only three nodes. However, this method is a biased estimator: using the ranges from both feet to a single fixed point means that, as the pedestrian approaches to it, the stride width will be progressively reduced, which is unrealistic. If two fixed points separated by a distance equal to the stride width are used, an unbiased estimator would be obtained, provided that the stride width is constant during the walking.

From now on, this method will be referred to as **method 1**.

6.3.2 SLE Based on Inter-feet Ranges

This method was proposed by Saarinen *et al.* in [52] and is based on using the periodicity nature of the inter-feet range to estimate the step length using the expression (6.2). In their work they also used ultrasound as ranging technology.

Specifically, they associate the last local maximum of the inter-feet range with the b segment and the last local minimum with the stride width, as defined in Figure 6.3. However, this method is also approximate, as it assumes that the swinging foot has actually followed the path marked by the horizontal segment c, which implies that:

- The swinging foot advances in a straight line between its two consecutive footsteps and therefore the minimum occurs when the swinging foot exceeds the stance foot. This may not be the case in reality.
- They use the three-dimensionally calculated minimum inter-feet range, rather than its projection on the horizontal plane. This introduces an error proportional to the height of the foot as it passes the other foot.

In our implementation, we used the ranges between the nodes mounted on the feet, i.e. A1 and A2. Again, missing samples were recovered by interpolation and a fifth-order Butterworth lowpass filter was applied, but with a cut-off frequency at 2.75 Hz. For this method the filter has a higher cut-off frequency because the inter-feet range varies at the step rate. To obtain the step lengths, the peaks and valleys are detected and then the expression (6.2) is applied. An example can be seen in Figure 6.5.

From now on, this method will be referred to as **method 2**.

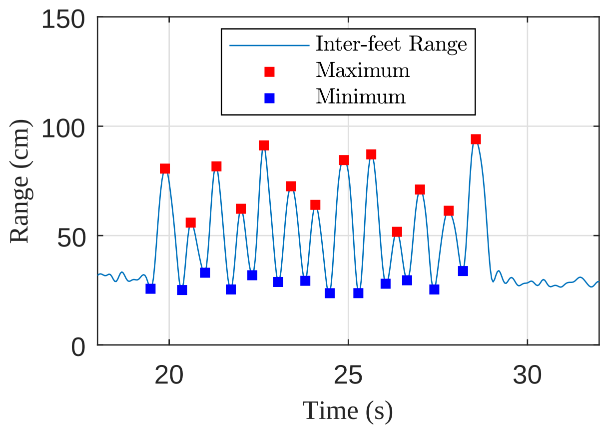

Figure 6.5: Example of the peaks and valleys in the inter-feet range signal

6.3.3 SLE Based on Feet Positions

In order to apply expression (6.1), it is necessary to know the positions of the feet when they are resting on the ground. So, firstly, the positions of the feet over time will be obtained using the ranges between the UWB nodes. For this purpose, a localization algorithm based on the KF is designed, with a discrete time white noise acceleration driven model as dynamic model and the ranges between the feet and the anchors as measurements. Due to the nonlinearities in the measurement model, an EKF will be implemented, in the same fashion as described in [199].

The state vector $\boldsymbol{x}_k$ is defined by the three-dimensional position ($\boldsymbol{p}$) and velocity ($\boldsymbol{v}$) estimates for right and left foot, indicated with subscripts r and l, respectively:

$$\boldsymbol{x}_{k|k} = \boldsymbol{x}_k = \left(\boldsymbol{p}_{r,k}\ \boldsymbol{v}_{r,k}\ \boldsymbol{p}_{l,k}\ \boldsymbol{v}_{l,k}\right)^T \tag{6.3}$$

As mentioned before, to model our system, we will use a discrete time white noise acceleration model for $\boldsymbol{x}_k$:

$$\boldsymbol{x}_{k|k-1} = \boldsymbol{F}_k \boldsymbol{x}_{k-1|k-1} + \boldsymbol{w}_k \tag{6.4}$$

$$\boldsymbol{F}_k = \begin{pmatrix} \boldsymbol{F}_{r,k} & 0_{6x6} \\ 0_{6x6} & \boldsymbol{F}_{l,k} \end{pmatrix} \tag{6.5}$$

$$\boldsymbol{F}_{r,k} = \boldsymbol{F}_{l,k} = \begin{pmatrix} 1 & 0 & 0 & \Delta T & 0 & 0 \\ 0 & 1 & 0 & 0 & \Delta T & 0 \\ 0 & 0 & 1 & 0 & 0 & \Delta T \\ 0 & 0 & 0 & 1 & 0 & 0 \\ 0 & 0 & 0 & 0 & 1 & 0 \\ 0 & 0 & 0 & 0 & 0 & 1 \end{pmatrix} \tag{6.6}$$

where $\boldsymbol{F}_k$ is the state transition matrix, ΔT is equal to the time difference between timestamps k and $k-1$, and $\boldsymbol{w}_k$ is the process noise, modeled as a white noise acceleration with covariance matrix $\boldsymbol{Q}_k$:

$$\boldsymbol{Q}_k = \begin{pmatrix} \boldsymbol{Q}_{r,k} & 0_{6x6} \\ 0_{6x6} & \boldsymbol{Q}_{l,k} \end{pmatrix} \tag{6.7}$$

$$\boldsymbol{Q}_{r,k} = \boldsymbol{Q}_{l,k} = \sigma_a^2 \begin{pmatrix} \Delta T^2/2 & 0 & 0 & 0 & 0 & 0 \\ 0 & \Delta T^2/2 & 0 & 0 & 0 & 0 \\ 0 & 0 & \Delta T^2/2 & 0 & 0 & 0 \\ 0 & 0 & 0 & \Delta T & 0 & 0 \\ 0 & 0 & 0 & 0 & \Delta T & 0 \\ 0 & 0 & 0 & 0 & 0 & \Delta T \end{pmatrix} \tag{6.8}$$

The state vector $\boldsymbol{x}_k$ is initialized with the coordinates of the first ground marks and a zero velocity, giving their initial standard deviations as 10 cm and 5 cm/s, respectively. Regarding the uncertainty of the dynamic model, the standard deviation that models the acceleration driving noise σ_a is set to 5 m/s^2.

The measurement model has the form:

$$\boldsymbol{z}_k = \boldsymbol{h}(\boldsymbol{x}_{k|k}) + \boldsymbol{n}_k \tag{6.9}$$

where $\boldsymbol{z}_k$ is the measurements vector, $\boldsymbol{h}$ is the measurement non-linear function, and $\boldsymbol{n}_k$ is the measurement noise with covariance matrix $\boldsymbol{R}_k$. By using UWB ranges from different anchors to update the estimate of the state $\boldsymbol{x}_{k|k}$, these measurements have the following form:

$$\begin{aligned} z_{i,k} = h_i(\boldsymbol{x}_{k|k}) = \\ = \sqrt{(p_x - a_{x,i})^2 + (p_y - a_{y,i})^2 + (p_z - a_{z,i})^2} \end{aligned} \tag{6.10}$$

where $z_{i,k}$ is the measured range between the ith anchor at the position $a_{x,i}, a_{y,i}$, $a_{z,i}$, and a tag with current position estimates at p_x, p_y and p_z.

Regarding the uncertainty of the measurement model, a standard deviation of 4.5 cm is set, value obtained from a set of preliminary measurements to characterize the UWB nodes.

Since the EKF filter provides a continuous estimation of the position of both feet, it is necessary to detect when the feet are still so that the position of the footsteps can be determined. In addition to estimating the position of the feet over time, the performance of this stance detection algorithm determines the performance of the whole SLE. In this work we have implemented it as a three-step process:

- Smoothing: first, a moving average filter was applied to the three components of the estimated positions of both feet. The length of the window was empirically set as 120 ms.

- Filtering: in order to reduce the number of outliers in the position estimation, a moving variance was computed over the horizontal module of position estimation of each foot. A window length of 120 ms is used and, afterwards, the samples whose variance exceeds a 500 cm^2 threshold are eliminated. The values of both parameters were set empirically.

- Determination of the footsteps positions: the k-means clustering algorithm is applied on the horizontal coordinates of the filtered estimates. The obtained centroids are taken as the positions of the footsteps. Since k-means is an algorithm with a certain random component, it is re-run if the result differs significantly from the correct footsteps.

An example of the whole process of obtaining the footsteps positions from the continuous foot position estimation is shown in Figure 6.6.

From now on, this method will be referred to as **method 3**.

In addition, a variation of the method 3 is implemented in which the inter-feet ranges are also included as measurements. The model of these measurements has the same shape as in (6.10) but using the range between the estimated positions for both feet. From now on, this method will be referred to as **method 4**.

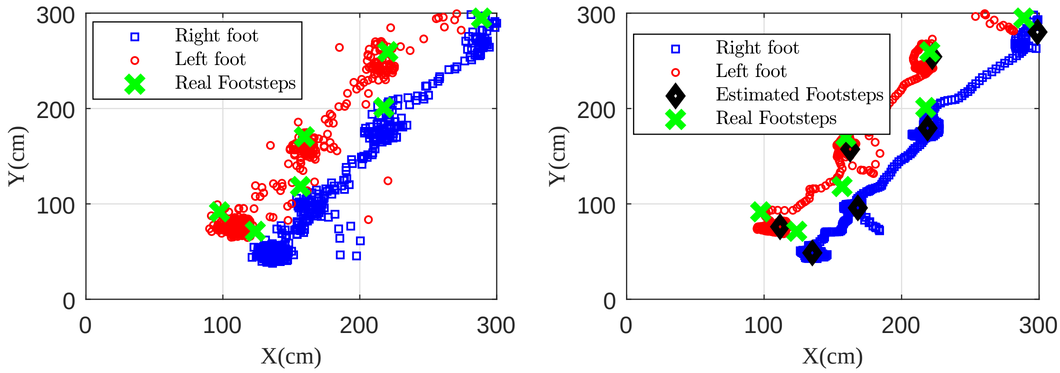

Figure 6.6: Example of the application of the algorithm designed for obtaining the position coordinates of the feet when they are resting on the ground. The image on the left shows the estimates provided by the EKF and the one on the right shows the estimated footsteps after applying smoothing, filtering and clustering techniques, as described in Section 6.3.3.

6.4 Results and Discussion

To compare the performance of the different methods implemented, the absolute value of the difference between the real step lengths (calculated using the equation (6.1) and the ground mark positions) and the values estimated by each method is used as error metric. In order to better see these SLE results, the empirical *Cumulative Distribution Function* (CDF) of each SLE method are shown in the Figure 6.7 and their main statistics are presented in the Table 6.3. In a first analysis, it can be observed that method 4 provides the best performance up to the 75th percentile. However, at the 90th percentile, the methods 1 and 2 outperform it. Observing the CDF and the mean and standard deviation of method 4, it seems that this method

Method	Median	P75	P90	Mean	Std	Median(%)
1	10.1	16.8	22.8	11.9	9.4	19.1
2	8.6	14.5	20.1	9.9	7.1	15
3	10.7	18.2	31.1	15.5	19.4	19.4
4	7.4	13.6	24.8	11.9	16.3	13.2

Table 6.3: Statistics of the absolute errors (in centimeters) and the relative errors (only median) for each SLE method.

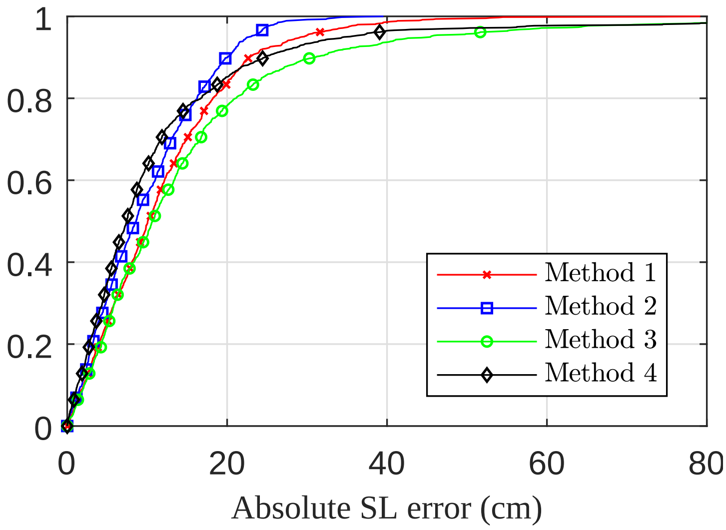

Figure 6.7: CDF of the empirical errors obtained from the implemented SLE methods.

suffers a higher effect of larger errors and outliers.

For a more detailed analysis of the performance of the different methods, the results will be analyzed grouped by the direction of the walk. That is, forward when the feet are approaching the anchor A0, or backward when they return to the initial ground marks. As it was mentioned in Section 6.2.3, due to the configuration of the experimental setup, when walking backward the NLOS situations are more frequent than when walking forward, as the legs interpose between the mobile nodes and the anchors. Therefore, by splitting the results according to the direction of the walk, the effects of the NLOS situations and the robustness of each method against them might be better observed.

The CDF of the grouped results for each SLE method are shown in Figure 6.8 and their main statistics are presented in the Table 6.4. On the basis of these, the following observations are made:

- Method 4 obtains the lowest errors up to the 90th percentile in the forward walks case. However, it is clear that its performance depends to a large extent on the absence of NLOS situations. This is seen in the large difference in its performance between forward and backward walks, which is reflected in mean and standard deviation values higher than, for example, the ones of method 2.

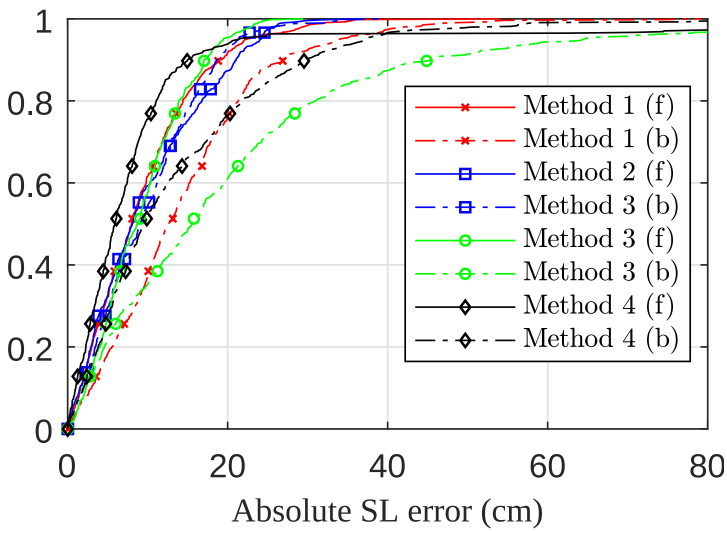

Figure 6.8: CDF of the empirical errors obtained from the implemented SLE methods, grouped by the direction of the walks: forward walks (f) and backward walks (b).

- Comparing the results from method 4 and method 3, it can be seen that the introduction of inter-feet ranges as measurements in the EKF has a positive effect. This effect is more evident in the backward walks, since those additional measurements help to reduce the errors induced by the NLOS situations and to maintain a better estimate of the relative feet position.

- Regarding the method 2, its results show that the performance of this SLE method is similar in both directions, which can be also seen in its lowest standard deviation. This makes sense since it only uses the inter-feet ranges, so it is not affected by the NLOS situations with respect to the anchors. Although its estimator is biased, it gets the good accuracy along with good variance, and with the additional advantage of needing very little infrastructure (only two nodes).

- With respect to the method 1, it seems clear that it can be discarded since one of its advantages was the reduced need for infrastructure, which is overcome by method 2, which also achieves better results and does not have the limitation of straight paths or the weakness against NLOS situations.

Forward						
Method	**Median**	**P75**	**P90**	**Mean**	**Std**	**Median(%)**
1	8	13	19.3	9.4	7.3	13.6
2	8.1	15	21.1	9.8	7.4	13.9
3	8.8	13.2	17.1	9.2	5.7	14.9
4	5.9	9.8	15	10	18.6	10.2
Backward						
1	12.6	19.8	26.9	14.5	10.5	23.1
2	9.1	14.3	18.7	9.9	6.8	16.1
3	15.5	27.1	45.5	21.7	25.3	28.8
4	9.7	19.4	29.7	13.8	13.3	18.4

Table 6.4: SLE errors (in centimeters) and relative errors (only median) grouped by walk direction

In addition to comparing the different methods, we must also assess the accuracy obtained:

- Few state-of-the-art works report the statistical characterization of the individual errors of each step length. It is more common to report errors at the distance traveled level, which can compensate for errors of different signs. Among the works which report errors at individual step level, we could find only hybrid systems, such as the work of Hung and Shu [204], which integrates IMUs and a camera for the inter-feet range and gets an average error of 2.2 cm, and the work of Weenk *et al.* [205], which integrates IMUs and ultrasound to obtain an average error of 1.7 cm. In our work, method 2 obtained a global average error of 9.9 cm ($\pm$7.1 cm), and the method 4 showed 11.9 cm ($\pm$16.3 cm). Therefore, it can be seen that hybrid systems achieve better performance in terms of accuracy.

- As it can be seen from the Table 6.3, the relative errors are between 13% and 19%, which may not be sufficient for some applications. Further research is needed in order to evaluate if the combination of this accuracy level and coverage level is worth it for SLE training of pedestrian navigation systems.

- It should be noted that the ground truth source used in this work is ground marks of a size of approximately 25 cm^2 on which the foot has landed during walking. Therefore, there is some margin for error in the numerical evaluation of the methods' performances.

6.5 Conclusions

In this chapter we have presented a preliminary evaluation of the accuracy of the UWB technology for SLE purposes. Four different methods have been tested in a reduced experimental environment as a previous step to a more extensive future evaluation that will include larger spaces, more complex trajectories and the assessment of the benefit of using UWB for training SLE methods in comparison to the using of the average step length.

After analyzing the performances of the different SLE methods, a first observation can be highlighted: since the step is a relative measure between the foot positions, the use of inter-feet ranges has proven to be essential when it comes to reducing the estimation error. In this sense, two of SLE methods should be highlighted:

- Method 2, despite being an approximate method, achieves good accuracy and low variance, with the additional advantage of requiring little infrastructure. In addition, the no need to install anchors eliminates restrictions on types of routing and makes it robust against NLOS situations. These features fully support the choice of this method when low cost solutions are sought, which also leads to choose ultrasound as the suitable technology for inter-feet ranging, since it offers greater accuracy than UWB.

- Method 4 achieves better accuracy in LOS scenarios but is weaker against NLOS situations. Therefore, this would be the indicated method if there are no cost limitations and it is possible to install enough anchors to minimize the risk of NLOS.

The first results indicate that it is possible to obtain errors below 10 cm for more than 50% of the steps, which makes us optimistic about the use of UWB as step length ground truth since it is possible to improve those results easily by installing a greater number of anchors to minimize NLOS situations and the use of filtering techniques for outliers ranges. This exploratory work therefore supports future work on assessing whether the combination of the accuracy and coverage provided by UWB is really useful for SLE training of inertial PDR systems, especially in comparison to the use of the average step length as ground truth.

The bare truth of science: Nobody believes a computational model except the person who built it. Everybody believes an experimental measurement except the person who made it.

Ash Jogalekar

CHAPTER

7

Evaluation of a Wrist-worn Inertial PDR System in Real Scenarios

The existing literature offers limited insight into the performance that wrist-worn inertial PDR systems can achieve. Typically, experiments consist of short and simple paths and few users are usually involved. In addition, their results are not usually compared to those of other pedestrian navigation systems worn on different body locations. This led to the definition of *specific objective 3*, which is addressed in this chapter.

In particular, this chapter presents the results obtained by a state-of-the-art wrist-worn inertial PDR system during two different evaluation stages. The first one corresponds to the IPIN Indoor Localization Competition 2016 held during that year's IPIN conference. One of the main characteristics of the IPIN competition is that it is usually held in big challenging multi-floor environments with significant path lengths and duration. However, the different participating navigation systems were not evaluated simultaneously and were carried by only one user, who was different for each system. A fair comparison of systems must be performed under the same conditions, i.e. same sensors, paths and users. For this reason, the second evaluation stage focuses on the comparison of different inertial pedestrian navigation systems simultaneously carried and evaluated for a set of pedestrians. In both evaluation stages, only the swinging mode is evaluated, as it is considered to be the most common carrying mode during long walks in which no other activities are carried out in parallel.

The chapter has the following structure: Section 7.1 describes some details about the implementation of the wrist-worn inertial PDR system used in both evaluations. Section 7.2 describes the IPIN competition, while Section 7.3 focuses on the simultaneous evaluation campaign of several systems. Finally, Section 7.4 summarizes the conclusions from these evaluation processes.

7.1 Wrist-worn Inertial PDR System Description

The system that was chosen to be implemented is the proposal of Qian *et al.* [31] as it is the only specific wrist-worn system that is fully described in the literature. Based on this proposal, some modifications were made to meet the requirements of the IPIN competition. Specifically, the system was extended to operate over several floors of a building, calibrated to the characteristics of the person who carried the system during the competition and implemented in such a way that the position estimation was provided in real time. This real time requirement was imposed by the competition, as the trajectory estimate had to be handed over to the judges immediately after the end of the path, and any type of post-processing was prohibited.

Figure 7.1 shows the block diagram of the implemented system. Qian *et al.* described the different algorithms of their wrist-worn PDR system but they did not give any detail about the configuration or values of the different parameters involved in those algorithms. Therefore, in addition to a brief description of each PDR block, the configuration and calibration processes that were carried out are described below.

7.1.1 Mode Classification Block

As mentioned previously, only the swinging carrying mode was considered during these two evaluation processes. However, given that the IPIN 2016 competition

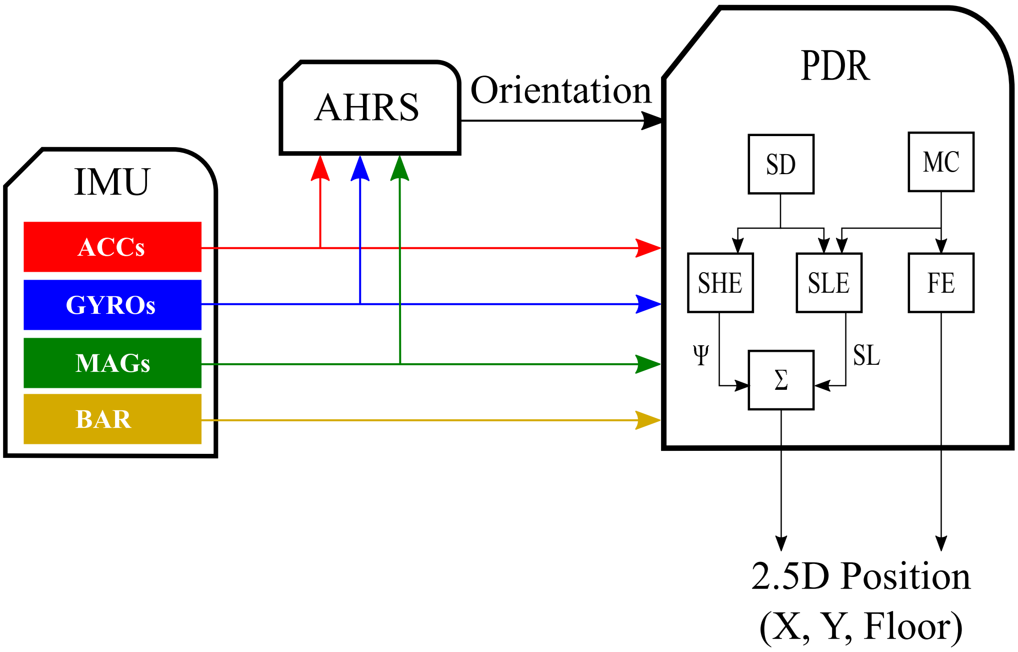

Figure 7.1: Block diagram of the implemented wrist-worn inertial PDR system. In order to provide 2.5D position estimation, a barometer and a *Floor Estimation* (FE) block were included.

could include stairs, ramps or elevators, an MC block was included whose mission is to detect those segments in order to subsequently adjust the behavior of the SLE block and, as will be explained later, use this information to estimate the change of floor inside the building. Specifically, the objective of the MC block is to classify the type of motion into the following five classes: stairs (up and down), elevator (up and down) or leveled walking. For this purpose, a very simple classification algorithm was designed using the barometer available in the XSens IMUs.

Since barometers provide measurements of the atmospheric pressure, they have to be firstly converted into altitude. The barometric formula [206] adjusted to provide the altitude with respect to the sea level was used:

$$h = 44330 \cdot \left(1 - \left(\frac{p}{1013.25}\right)^{1/5.255}\right) \tag{7.1}$$

where p is the pressure measured in hPa and h is the altitude in meters (above sea level) corresponding to that pressure. This model is not exact because it assumes some variables as constants, and it does not take into account other factors such as humidity, weather, or the presence of air conditioning systems. However, the MC does not use the absolute altitude but the relative altitude changes over the time, so this approximate expression can be enough.

As the signal from the barometer is usually quite noisy, the altitude signal is softened by a three-second moving average filter. The vertical velocity is then obtained by differentiating the altitude signal. And, again, smoothing is applied by means of a five-second moving median filter. The reason for using a longer filter is the possible presence of landings during the stair sections. Next, from each vertical speed sample, the type of motion is determined by applying a tree decision classification algorithm, that can be seen in Figure 7.2. Finally, to avoid transients in the motion estimation, a two-second moving median filter is applied on the motion estimation samples. The lengths of these smoothing filters and the tree decision thresholds were defined empirically from real data collected in the building of the engineering faculty of the University of Deusto. An example of this data and the output produced by the MC block can be seen in Figure 7.3. The route taken in this example consisted of descending four floors down the stairs, stopping for 10 seconds between each floor. Then, returned to the starting point by elevator, waited 10 seconds, got down to the bottom floor by elevator and climbed to the initial floor by stairs. As can be seen, the leveled walks, stairs and elevators are associated to different vertical speeds and, therefore, that signal can be used to classify the type of motion.

7.1.2 Step Detection Configuration

The SD algorithm proposed by Qian *et al.* uses the basic structure of pre-processing, detection of candidate steps and validation of steps. In the pre-processing stage, they calculate the magnitude of the acceleration from the measurements provided by the IMU's three accelerometers. This way, the SD algorithm is not affected by the orientation of the sensor unit.

In our case, we have also added a filtering stage to remove the frequency components higher than those associated with the human walking. In Qian's later works this filtering stage was also included.

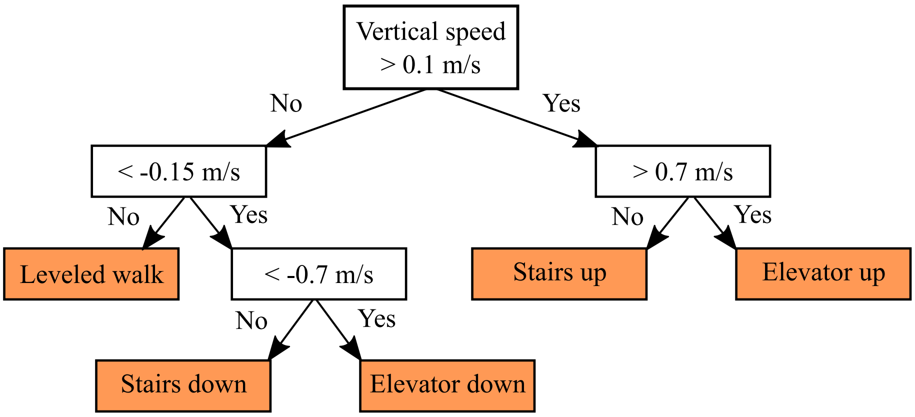

Figure 7.2: Tree decision algorithm that classifies the current motion mode from the vertical speed estimation

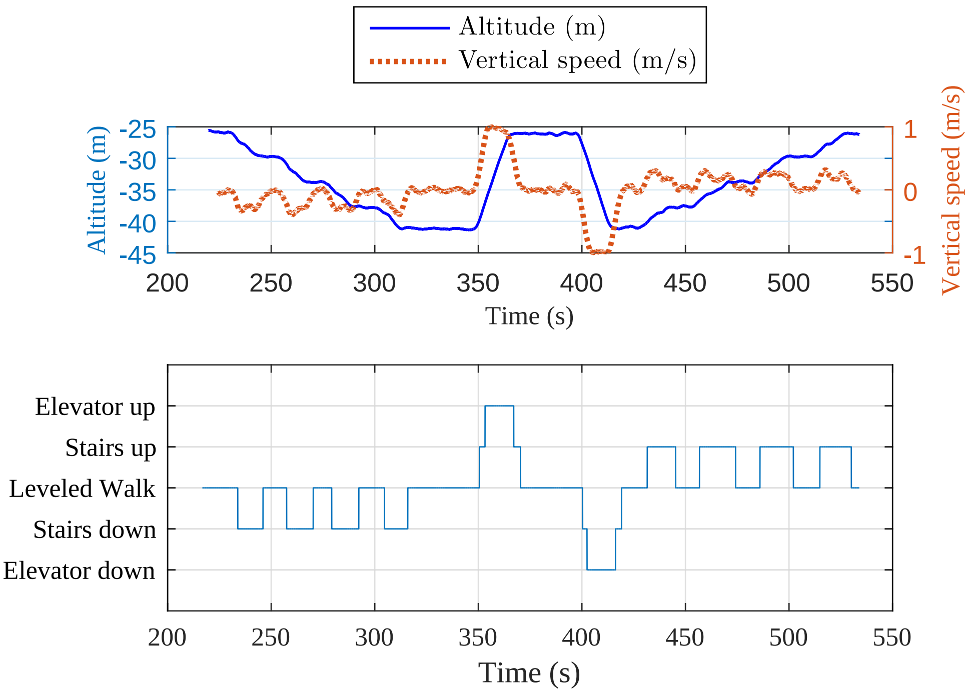

Figure 7.3: Visualization of the altitude and vertical speed signals (top) and the motion mode estimation (bottom) during an example that consisted of descending four floors down the stairs, stopping for 10 seconds between each floor. Then, returned to the starting point by elevator, waited 10 seconds, got down to the bottom floor by elevator and climbed to the initial floor by stairs.

The candidate step detection stage is based on threshold crossing and the subsequent validations that are applied to check that the temporary duration of the candidate step is compatible with normal walking cadences, that the acceleration peak over a step does not correspond to a perturbation and that there is a certain level of periodicity in the signal, in order to assure that the pedestrian is walking. In addition, the threshold value is dynamically updated using the average acceleration over the last candidate step. This makes the SD algorithm more robust to speed changes. In the Figure 7.4 can be seen the workflow of this SD algorithm.

As can be seen, there exists a set of parameters that will determine the performance of the SD algorithm and for which there is no indication of which values should be used. To find a good configuration of the SD algorithm, it was decided to define a range of possible values for each parameter and to look for the combination that maximizes the accuracy of the detector when processing a training or calibration dataset. The Table 7.1 shows the values included into the search of the configuration for each parameter.

Parameters	Values
Min step duration (t_{min})	[0.25, 0.33, 0.4, 0.5] (s)
Max step duration (t_{max})	[0.667, 0.8, 1, 1.333, 1.667] (s)
Min peak-to-threshold (a_{min})	[0.5:0.5:2] (m/s^2)
Max peak-to-threshold (a_{max})	[4:1:7] (m/s^2)
Sliding window size	[1.5:0.5:7] (s)
Autocorrelation threshold	[0.1:0.1:0.6]

Table 7.1: Considered values for searching the SD's configuration. The expressions [a:b:c] indicate the set of values between "a" and "b", separated by an increment "c".

In addition to the SD parameters it was also decided to evaluate the effect of different IMU sampling rates and different cutoff frequencies of the low pass filter during the pre-processing. As the datasets were collected with the IMU's sampling frequency set to 100 Hz, different sampling rates were obtained by downsampling the collected data. This way, the following sampling rates were obtained: 100 Hz, 50 Hz, 25 Hz, 20 Hz, 10 Hz and 5 Hz. Regarding the low pass filter, a 7^{th} order Butterworth filter was used with cutoff frequencies between 1.5 Hz and 7.5 Hz.

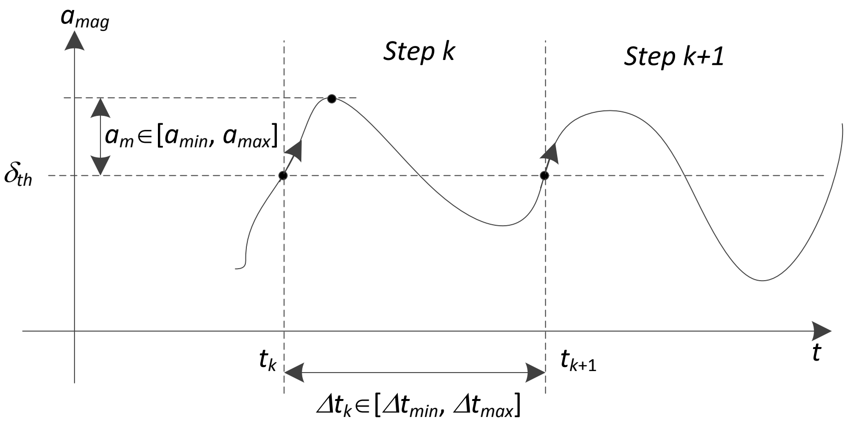

(a) Detection of step candidates. Source: Qian *et al.* [31]

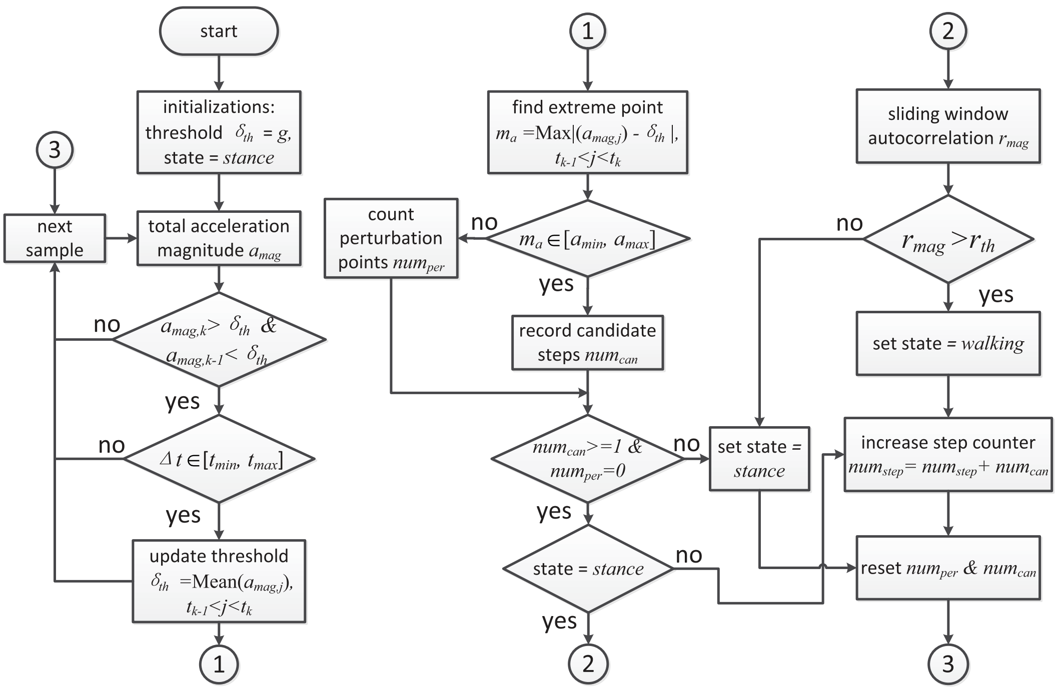

(b) Complete workflow of the step detection algorithm. Source: Qian *et al.* [110]

Figure 7.4: Step detection algorithm proposed by Qian *et al.*

The calibration dataset was generated by a subject who took 30-step long straight walks at different step rates. The pedestrian walked with the arms freely swinging and a metronome was used as a step rate reference, covering the usual range of walking step frequencies: from 1.5 Hz to 2.1 Hz, with increments of 0.1 Hz. For every different step frequency, five walks were taken. Therefore, 35 different registered walks were available to be processed.

The complete dataset was processed by each different possible combination of the previously defined values of sampling frequency, low pass filters and values of the algorithm's parameters. The accuracy of each combination was determined by the RMSE over the whole dataset, defined the error as the normalized difference between the detected and actual number of steps of each walk.

7.1.2.1 **Effect of the Sampling Rate**

The Figure 7.5 shows the results of the 100 best configurations at each sampling rate. First of all, it is observed that, since the usual step frequency is usually around 2 Hz, a sampling rate of 5 Hz does not seem enough to collect all the variability of the acceleration signal. Although with 10 Hz the accuracy improves significantly, the results seem to indicate that a sampling rate of at least 20 Hz is recommended. Secondly, it can be seen that from this frequency onwards the improvement in step detection is minimal or practically non-existent, which must be taken into account when developing PDR systems with low energy consumption requirements.

However, since the IMU will also be used to implement an AHRS and the orientation tracking requires a high update rate, a 100 Hz sampling rate will be used from now on.

7.1.2.2 **Effect of the Filtering**

Figure 7.6 shows the distribution of errors obtained by the 100 best configurations for each cutoff frequency of the low pass filter, as well as the option of not applying any filtering. These results are for the 100 Hz sampling rate only.

It can be seen that applying a low pass filtering to the signal makes it easier to find configurations of the SD algorithm that obtain better performances. However, the cutoff frequency of the low pass filter must be higher than the walking rate, otherwise the information needed to perform the step detection is removed, as it is indicated by the performance degradation for cutoff frequencies below 2 Hz. On the other hand, the results also indicate that it is not so crucial to perfectly adjust this cutoff frequency to the walking cadence, as there is a certain upper margin in which the performance degrades slowly.

7.1.2.3 Final Configuration

The Table 7.2 shows the selected configuration for the SD algorithm after the optimization process.

Parameter	Value
Sampling rate	100 Hz
Butterworth low pass filter cutoff frequency	2.5 Hz
Min step duration (t_{min})	0.33 s
Max step duration (t_{max})	1.667 s
Min peak-to-threshold (a_{min})	1 m/s^2
Max peak-to-threshold (a_{max})	7 m/s^2
Sliding window size	2.5 s
Autocorrelation threshold	0.1

Table 7.2: Configuration of the SD algorithm.

As can be seen in the Figure 7.5, the best found configurations offer step detection errors close to 2%, over the entire range of walking cadences considered. In the Figure 7.7 it can be seen an example of one of the calibration walks processed with the selected configuration of the SD algorithm. In this example, only 29 of the 30 steps taken are detected, since the first step candidate was not counted because the validation of periodicity in the signal had not yet been completed (white circle in the second 11).

7.1.3 Step Length Estimation Block Calibration

As shown in Figure 7.1, the SLE block makes use of information provided by the SD and MC blocks. Specifically, depending on the type of motion detected by the

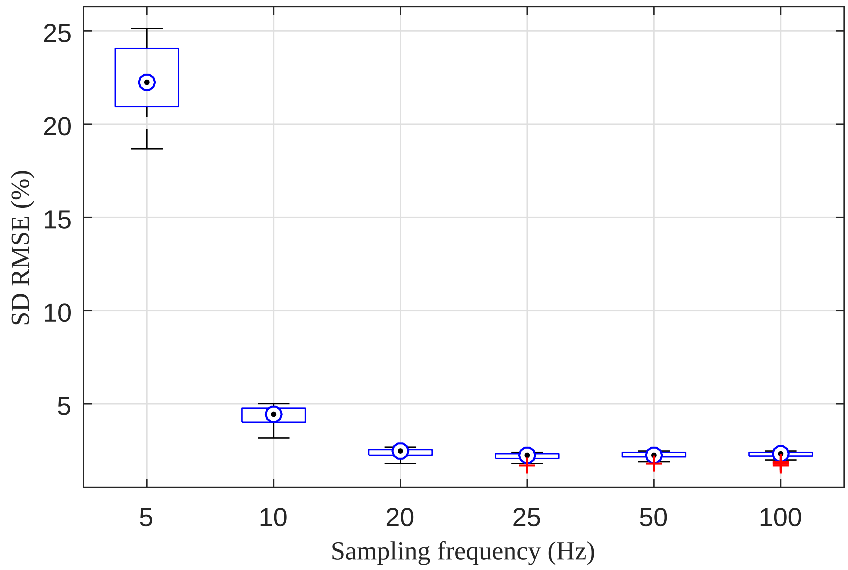

Figure 7.5: Distribution of the SD errors obtained by the tested configurations, grouped by sampling frequency.

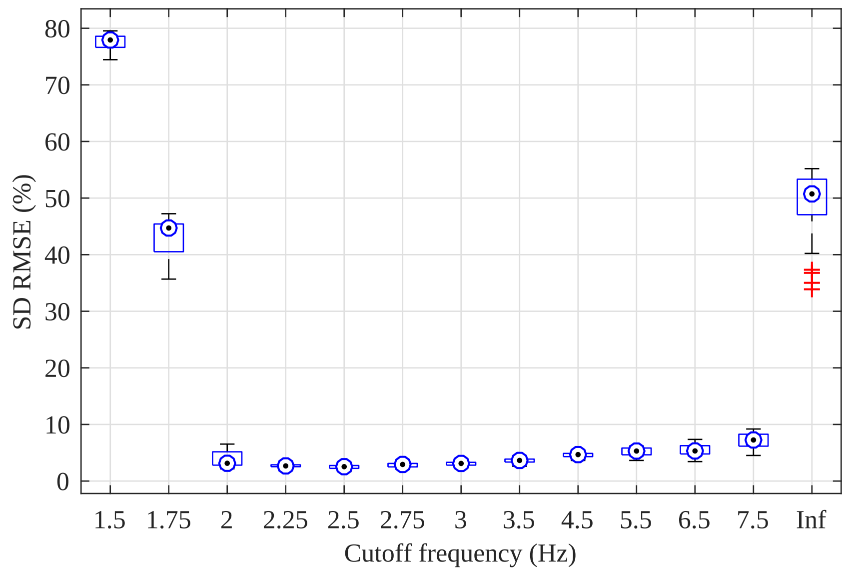

Figure 7.6: Distribution of the SD errors obtained by the tested configurations, grouped by cutoff frequency of the low pass filter. The "Inf" cutoff frequency refers to no low pass filter.

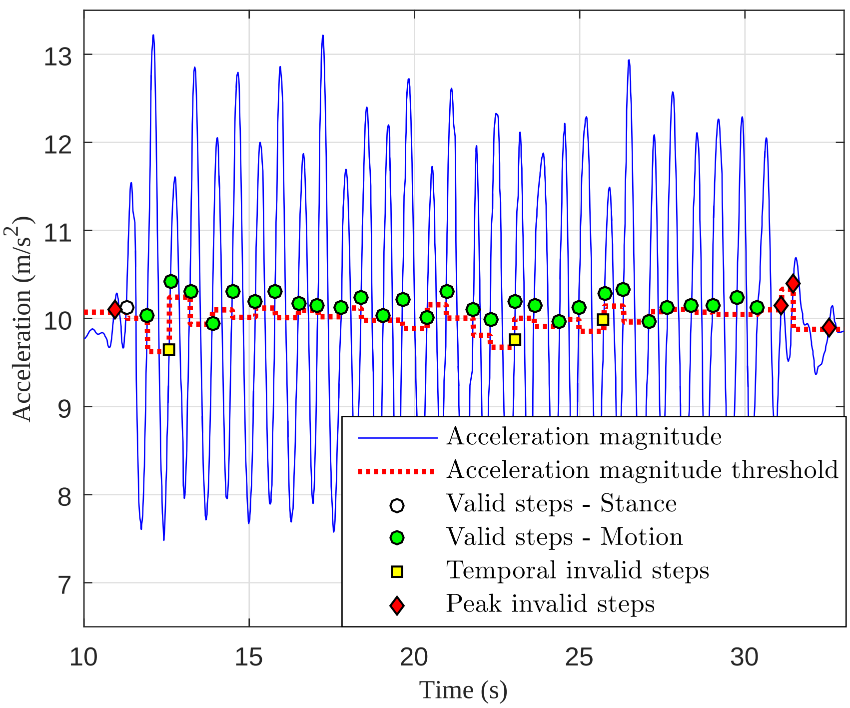

Figure 7.7: One of the calibration walks processed with the selected configuration of the SD algorithm. In this example, only 29 of the 30 steps taken are detected, since the first step candidate was not counted because the validation of periodicity in the signal had not yet been completed (white circle in the second 11).

MC block, a different SLE model is applied. When the user is inside an elevator, any detected step is assumed to be zero length. For the moments when the user is climbing or descending a flight of stairs, each detected step is assigned with a constant length that will depend on the dimensions of each building's stairs. It is assumed that the steps are climbed one at a time and, for the case of the IPIN 2016 competition, this value was set at 30 centimeters. In the case where the pedestrian is walking on a level surface, the same SLE method originally proposed by Qian is applied, that is, a linear regression model based on the step frequency and the acceleration variance over the step.

The training of that regression model was done using the same dataset as for the SD configuration: for each 30-step walk, the traveled distance was measured with a measuring tape and the average step length was computed. Also, from the steps detected by the SD, the averages of the step frequency and the acceleration variance were also computed for each walk. Therefore, the training dataset was composed by the average values of the step length, step frequency and step acceleration variance over the whole set of walks. With the step frequency and the acceleration variance as features and the average step length as response, the following linear regression model was obtained:

$$\text{SL} = 0.15 + 0.36 \cdot \text{SF} - 0.01 \cdot \text{VA} \tag{7.2}$$

where SL is the step length, SF the step frequency and VA the acceleration variance. As can be seen, the acceleration variance has very little weight in this model. This is because the model has been generated for a single user (the one who participated in the competition) and therefore the step frequency is sufficient to collect most of the variability of the step length. If the model had been generated from data from multiple users, the advantage of including acceleration variance in the regression model would be more evident.

7.1.4 Step Heading Estimation Block Configuration

The Qian *et al.* SHE algorithm uses an AHRS for tracking the orientation of the wrist. In particular, they used the AHRS proposed by Sebastian Madgwick [72]. Then, as was already mentioned in Section 3.2.4, they estimate the step heading by reading the wrist heading at the periodic gravity crossings of the wrist acceleration. This way, since they use magnetometers in the AHRS for computing the wrist's heading, the wrist's heading is read at times in which the heading misalignment with the traveling direction is constant and can be measured beforehand.

In our case, the system implemented for the IPIN 2016 competition implements the same SHE algorithm but uses the AHRS included in the XSens IMU instead of the Madgwick's one. The choice of this AHRS, in addition to the convenience of being already included in the IMU, is due to the fact that, a priori, it offers a more robust implementation, based on a KF that incorporates techniques against transient accelerations and magnetic disturbances [207]. Finally, the misalignment error was calculated empirically and fixed at a value of 20°.

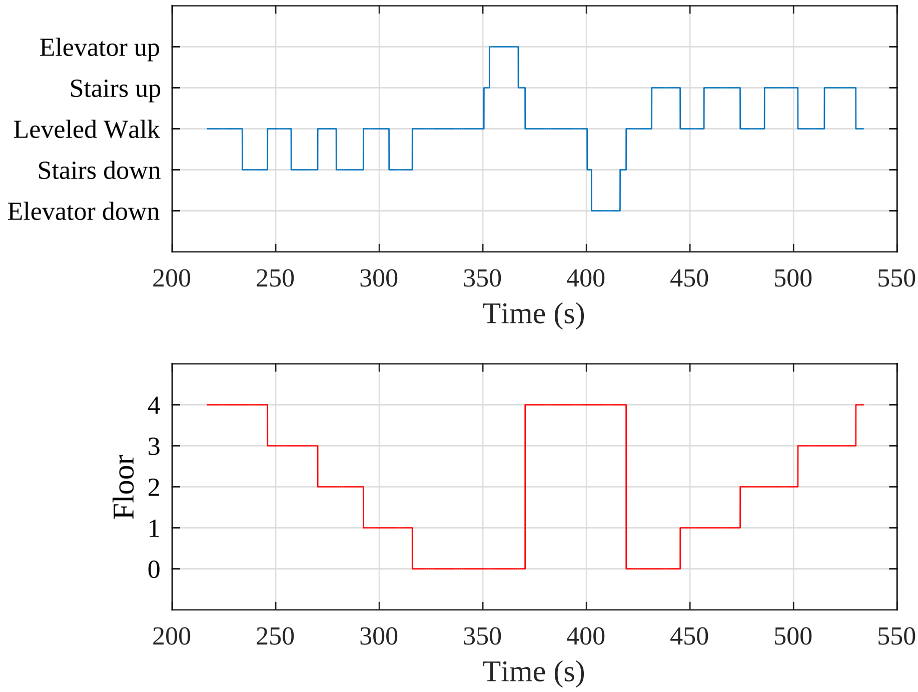

Figure 7.8: Example of FE block operation. For the same example path as in Figure 7.3, it can be seen how the floor where the pedestrian is can be tracked from the type of motion estimate.

7.1.5 Floor Estimation Block

As mentioned before, the IPIN 2016 competition took place in a multi-storey building and, therefore, it was necessary to include the floor where the pedestrian was located in the position estimation, which is known as 2.5D positioning. For this purpose, a FE block was included which, as shown in Figure 7.1, makes use of the information provided by the MC module. Specifically, the implemented FE algorithm looks for the changes in the motion type transitions detected by the MC block and, when the new type of motion is leveled walking, calculates the difference in altitude with respect to the previous period in which the pedestrian performed the same type of motion. Based on this value and knowing the initial floor number and the height between floors of the building, it is possible to track the floor where the user is located with good accuracy.

Therefore, since this FE algorithm requires the initial floor, it can be considered a DR-based method. And, in addition, it needs to know certain a priori environmental information regarding the height between floors in the building. An example of the floor estimation for the same path shown in Section 7.1.1 can be seen in Figure 7.8.

7.2 Indoor Localization Competition IPIN 2016

The IPIN conference is one of the oldest in the specific field of indoor positioning and, since 2014, they are organizing a competition with the aim of promoting the definition and standardization of evaluation metrics and procedures for comparing positioning systems in realistic indoor scenarios. To this end, it is worth noting the complexity of the paths of IPIN competitions, as they are usually held in big challenging multi-floor environments with significant path lengths and duration, instead of evaluating competitors in small single-floor environments. In addition, measurements are taken while naturally moving through a predefined trajectory unknown to competitors, instead of evaluating the competitors by standing still at evaluation points.

The 2016 edition sought to cover three different use cases: positioning of people in real time, positioning of people off-line and robotic positioning in real time. Four different tracks were defined for this purpose:

- Track 1: Smartphone-based (on-site)
- Track 2: PDR positioning (on-site)
- Track 3: Smartphone-based (off-site)
- Track 4: Indoor mobile robot positioning (on-site)

Smartphone-based tracks (1 and 3) differ from the PDR track 2 in that they allow to use any sensor available on a smartphone and do not impose any restrictions on how the device should be carried. Therefore, most of the teams that competed in those tracks proposed hybrid positioning systems combining the inertial sensors and RF interfaces included in smartphones, and the device was carried always in texting mode. In contrast, track 2 only allowed the use of MEMS sensors (inertial, magnetometers and barometers), whether off-the-shelf or self-developed, without any limit concerning the number of sensors and the mounting positions on the body.

The competition was held at the Polytechnic School of the University of Alcalá de Henares (Spain) and the evaluation path for tracks 1-3 traversed four floors, including the patio and stairs for moving between floors. The path started from the ground level, went up to floors 1, 2 and 3 by means of stairs, then went to a terrace about 50 meters long, went back to the ground level, then to the patio and back indoors to the initial point. A total of 56 evaluation points were marked on the floor, with a evaluation length of 674 meters (accumulated distance between evaluation points). The pedestrians moved at a natural pace, typically at a speed of around 1 m/s, so each trial lasted around 10 minutes.

The wrist-worn inertial PDR system described in Section 7.1 was implemented to participate in the track 2. The hardware that was used for this competition consisted of an IMU MTi-300 from XSens mounted on the left wrist and connected by a cable to a laptop carried in a backpack. A Matlab implementation of the PDR system was executed in the laptop, processing the measurements provided by the IMU and estimating in real time the position of the pedestrian. The evaluation points were recorded by clicking a wireless mouse held in the right hand, which also can start and stop the execution of the PDR system. Since the laptop was inside the backpack, a beep-based interface was designed to know if the evaluation points had been recorded correctly. Figure 7.9 shows the installation of the system and one of the evaluation points.

A total of eight teams were admitted in the track 2 but finally six of them competed. Most of the teams used foot-mounted PDR systems (Seoul National University, Xiamen University, Tianjin University), even using several IMUs mounted on both feet, like the team from the University of Parma and the two teams that did not compete finally. It is worth noting the proposal from the Sysnav team: a magneto-inertial INS system that used a magnetometer array to exploit the variations of the magnetic field with respect to time and space to indirectly estimate the velocity.

A more detailed description about the competition can be found in the conference website [186, 208] and the related paper [188].

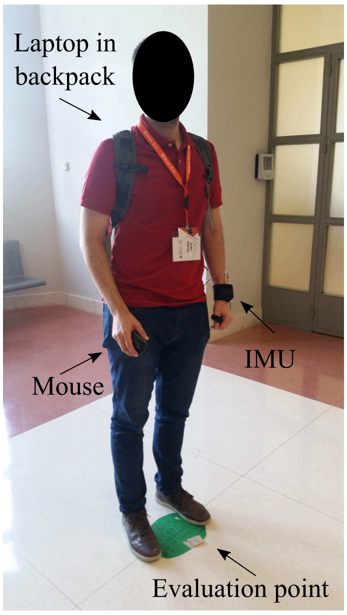

Figure 7.9: Installation of the wrist-worn inertial PDR system used to participate in the track 2 of the IPIN 2016 competition

7.2.1 Results of the Competition

At the end of each trial, the competitors had to submit to the organizing committee a log file with the estimated trajectories and positions of each evaluation point. To evaluate the performance, the error was calculated as the Euclidean distance between the estimated and actual XY coordinates at each evaluation point. In addition, a penalty of 15 meters is added for each floor error. The final score metrics is the third quartile of the positioning errors over the whole set of evaluation points, which makes the accuracy results less prone to the influence of outliers. Two trials were given for each team, and the best result was selected for the competition. Figure 7.10 shows the official results of the track 2 of the competition.

As can be seen, the Seoul National University team was the clear winner. Their proposal consisted of a foot-mounted INS in which they are able to estimate the velocity of the IMU during the stance phase, achieving a better correction than assuming that the velocity is zero, as is done with ZUPT. To do this, they need to know very precisely the position of the IMU on the foot and the dimensions of the footwear, which leads them to use a specific pair of shoes.

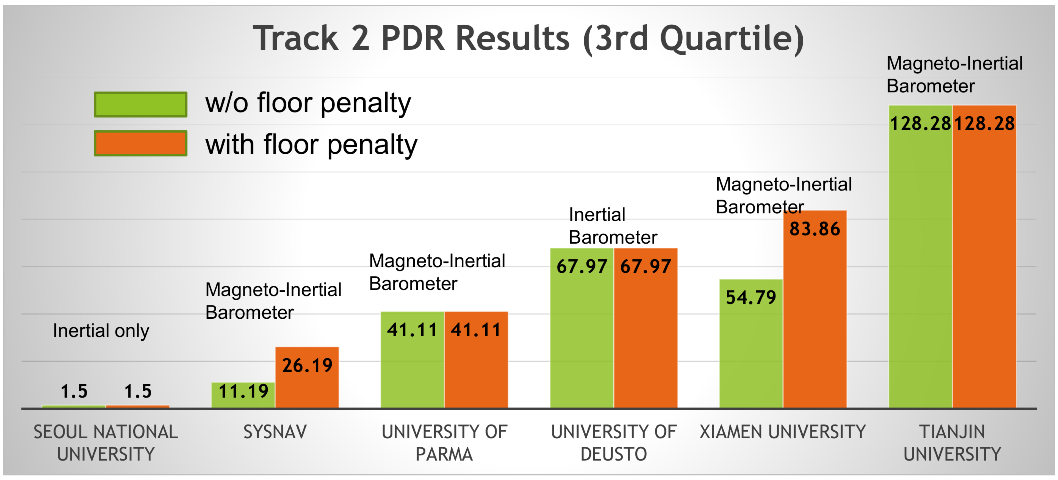

Figure 7.10: Official results of the track 2 of the IPIN 2016 competition. Source: EvAAL [186].

As the judges indicated, the biggest source of position error was the heading error, especially for the three teams that came in last place, possibly due to over-utilization of the magnetometers. On the other hand, the errors due to the estimation of the building's floor plan did not have much impact on the results obtained.

With respect to our wrist-worn inertial PDR system, although its performance is one of those affected by the magnetic disturbances of the building (team University of Deusto), it achieved close and even better results than other systems that used one or more foot-mounted IMUs, which a priori should be more accurate than a wrist-worn PDR system. This indicates, on the one hand, that the performance of wrist-worn systems is not too far from that of other a priori more accurate systems and, on the other hand, the difficulty of both developing reliable real systems and processing realistic scenarios. Any error or problem in the system or the presence of unforeseen situations can seriously affect the estimation of the position or, as happened to one of the teams, be unable to participate due to technical problems.

In the following section, more details about the performance of our wrist-worn inertial PDR system and the effect of the magnetic disturbances on its performance will be presented.

7.2.2 Effect of Magnetic Disturbances

As the judges of the competition indicated, several teams suffered important position errors due to the magnetic disturbances existing in the building. In the case of our systems, we relied on the AHRS included in the XSens IMU, which makes use of magnetometers, because the previous tests performed in our facilities had been quite satisfactory. However, the building in which the competition took place had larger magnetic disturbances that made it practically impossible to use these sensors.

To check the impact of these disturbances on the position error, after the competition, the AHRS of XSens was replaced by the one proposed by Madgwick [72], which was the one initially used by Qian *et al.*. This AHRS has a version without magnetometers, which computes the orientation by fusing the accelerometers and gyroscopes measurements. Since this version is purely inertial, the initial traveling direction should be known. In addition, the heading of the first step detected is assumed to be equal to that initial traveling direction. This corrects the possible initial offset generated by the integration of the gyroscopes' angular rates. Therefore, using that AHRS with a gain parameter value $\beta = 0.033$, the sensor's raw measurements corresponding to the two trials of the competition were reprocessed.

	Trial 1			**Trial 2**		
	Official	**Unofficial**	**Unofficial no MAG**	**Official**	**Unofficial**	**Unofficial no MAG**
3rd quartile	82.16	63.03	27.77	67.97	52.73	12.53
Mean	70.71	55.01	20.13	60.13	46.21	7.82
Median	76.4	58.98	22.02	59.88	45.92	5.82
Std	18.75	16.19	12.23	18.93	14.66	6.71
Final error	96.44	72.80	30.75	126.78	95.84	19.89
Max error	-	106.60	56.41	-	95.84	22.81
TD	975.41	738.41	738.41	962.33	728.30	728.30

Table 7.3: Statistics of the position errors (meters) obtained by our wrist-worn PDR system in the IPIN 2016 competition, both the official results and those obtained by ourselves with the original and the modified system.

In the Table 7.3 can be seen the statistics of the errors obtained by the system used in the competition and by the new version without magnetometers. This table presents three columns for each trial: the official results of the competition and those computed by ourselves for the original system and for the modified system. As can be seen, the two results for the original system do not coincide. The ones computed by ourselves have been obtained by calculating the Euclidean distance between the real and estimated positions of the evaluation points, expressed in UTM coordinates, which is how the PDR system works internally. The official errors have not been reproduced even though it was tried other ways such as using the WGS84 coordinates (i.e., latitude, longitude) and different formulas to calculate distances on spherical surfaces (the "haversine" formula and spherical law of cosines [209]). The most likely reason, although not fully confirmed, is that the organizing committee appears to have used EPSG:3857 coordinates [210, 211], which is a projection widely used to represent maps in web applications because it generates square projections but is not suitable for distance measurements [212].

Anyhow, the aim of this section is to check the variation of the system's performance when removing the magnetometers and, as can be seen from the data shown in the table, it improves significantly. Figure 7.11 shows the estimated trajectories by both versions of the system for the second trial, which was the best one, where it can be clearly seen how the original system suffers an important heading drift from the very first moment. In contrast, the system without magnetometers accumulates heading drift more slowly. Therefore, these even better results, although still far from those obtained by foot-mounted systems, indicate that wrist-worn PDR systems are an option to consider and encourage further work on their improvement.

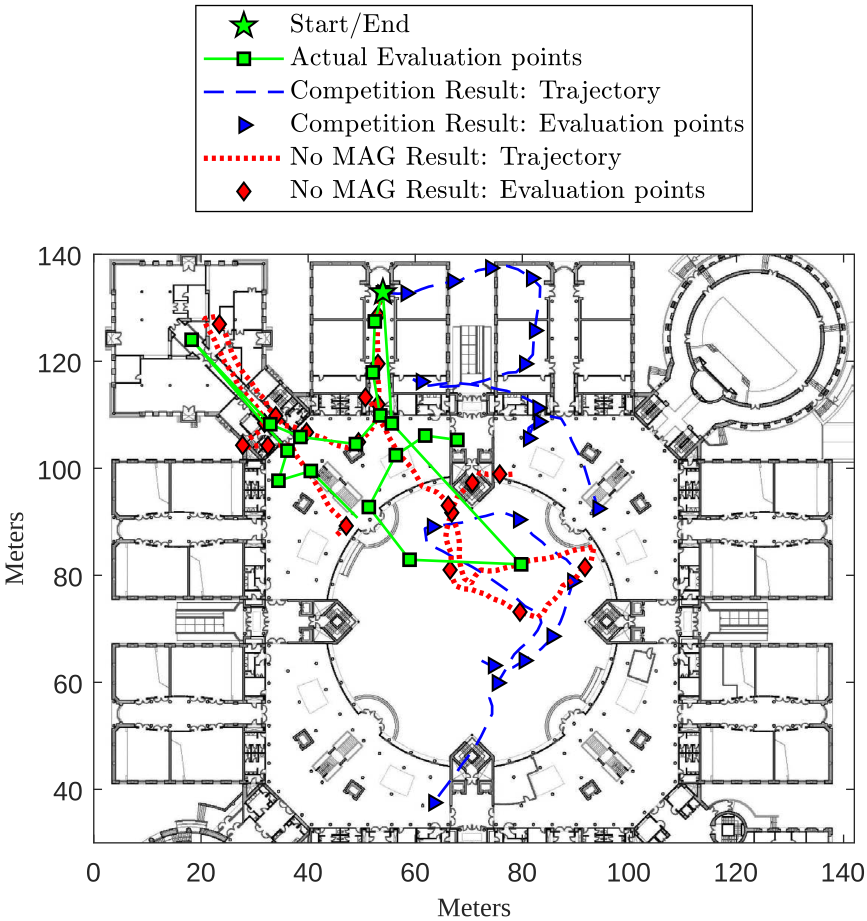

(a) Ground level

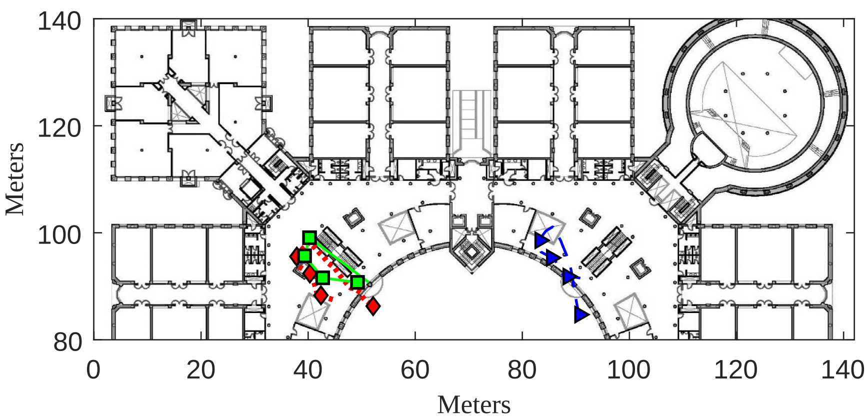

(b) Floor 1

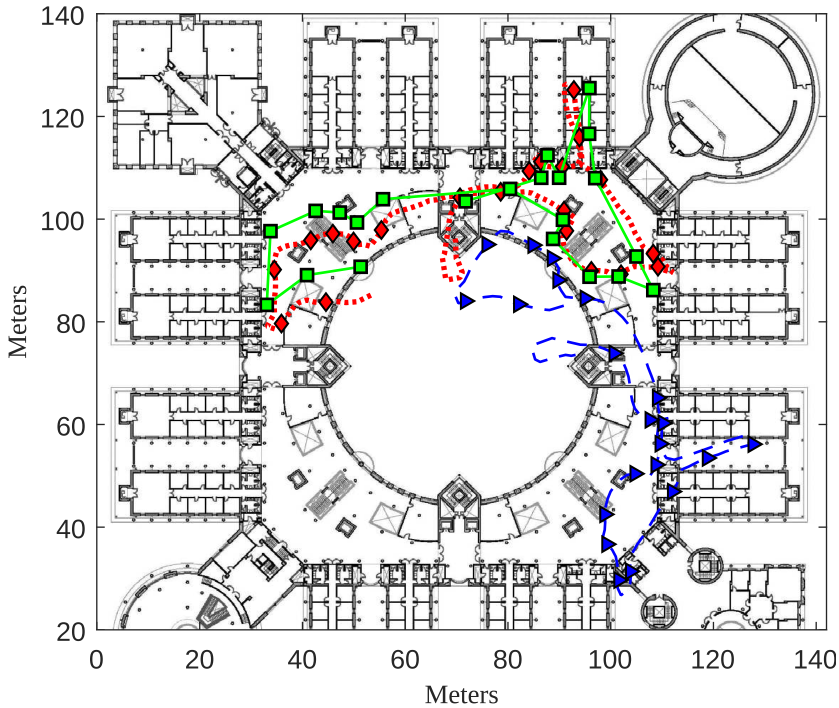

(c) Floor 2

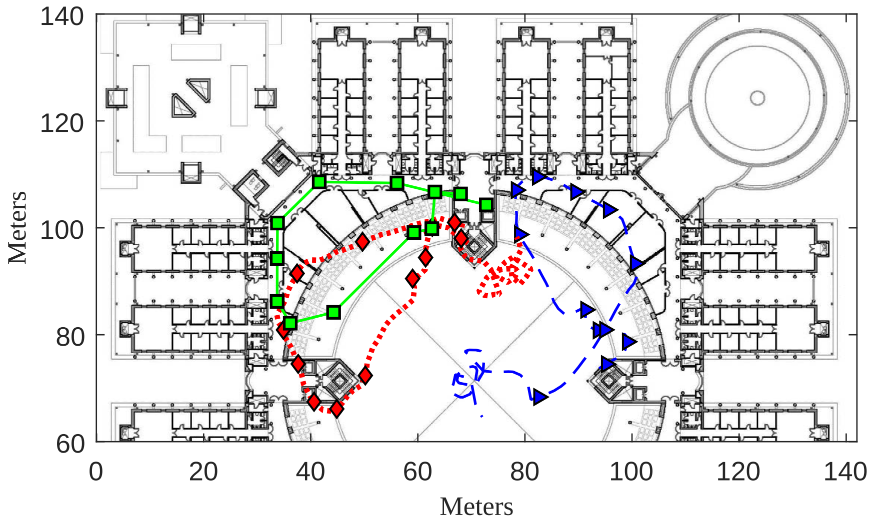

(d) Floor 3

Figure 7.11: The evaluation path starts from ground level, goes up to floors 1, 2 and 3 by means of stairs, then goes to a terrace about 50 m long and proceeds to the ground level, goes to the patio and indoors again, ending at the initial point. The trajectories estimated by the wrist-worn inertial PDR system in the competition and after removing the magnetometers are also shown.

7.3 Simultaneous Evaluation of Pedestrian Navigation Systems

Thanks to smartphones and wearable devices, each body location is an opportunity to develop a new pedestrian navigation system. This has led to the existence of a great diversity of proposals and, in order to identify the advantages offered by each of them, systems need to be tested under the same conditions, similarly to [213, 214]. Given the large number of variables that can affect the performance of a navigation system, such as the sensors, paths and users, one fair option is to test them simultaneously.

Since in the IPIN 2016 competition each pedestrian navigation system was evaluated individually, in this section the performance of the wrist-worn system will be evaluated simultaneously with two other pedestrian navigation systems: one foot-mounted and the other pocket-mounted. In addition, in that competition each system was tested by only one user, who was different for each system, so it was not possible to draw conclusions on how different users affect the performance of the pedestrian navigation systems. Therefore, in this section the experiments will be repeated with different users, analyzing the effect on the wrist-worn PDR system.

The experiments were carried out on a large outdoor area (more than 14000 m^2) in which 69 *Ground Truth Points* (GTP) were placed, whose coordinates were determined with centimeter precision. The aim of this is to be able to define multiple evaluation paths of different shapes and lengths, instead of repeating several times only one path, as was the case in the IPIN 2016 competition. However, in this case, only 2D positioning will be evaluated.

Furthermore, it is frequently the case that the datasets used in the experiments are not available for public use. Therefore, besides the final results and conclusions, there is little benefit for the scientific community from the experimental work done by other peers. In this case, the datasets used in the experiments, as well as the GTPs, are available in [215].

7.3.1 Pedestrian Navigation Systems Description

The wrist-worn inertial PDR systems used during these experiments is the one described in Section 7.1 but with the magnetometers-free AHRS proposed by Madgwick. That is, the corrected version after the IPIN competition that was also used in Section 7.2.2. The other two inertial pedestrian navigation systems are described below.

Foot-mounted Navigation System

As is already known, the foot is a very convenient body location to implement strapdown INS systems thanks to the possibility of applying ZUPT corrections during the foot's stance phase, which reduces significantly the cumulative error. The foot-mounted navigation system used in this work is implemented through an unscented Kalman filter, as described in [216], and the stance phase detection is based on the proposal of Ruppelt *et al.* [217].

Pocket-mounted Navigation System

The upper thigh is, for several reasons, an attractive position to implement inertial PDR systems. Firstly, phases of the gait cycle can be clearly observed by tracking the motion of the leg. Secondly, walking in flat surfaces and walking up/down stairs can be detected by solely analyzing the thigh's inertial measurements. Finally, devices such as smartphones are often carried in the trousers' pocket. Thus, they can be used to implement such navigation systems.

The pocket-mounted navigation system in this work uses an IMU mounted on the user's upper thigh. Obviously, the SHS approach is used to estimate the user's position. The pitch angle of the upper thigh is used to detect steps by identifying its maximum peaks and the amplitude of the pitch angle estimation is related to the step length. A more detailed description can be found in [97].

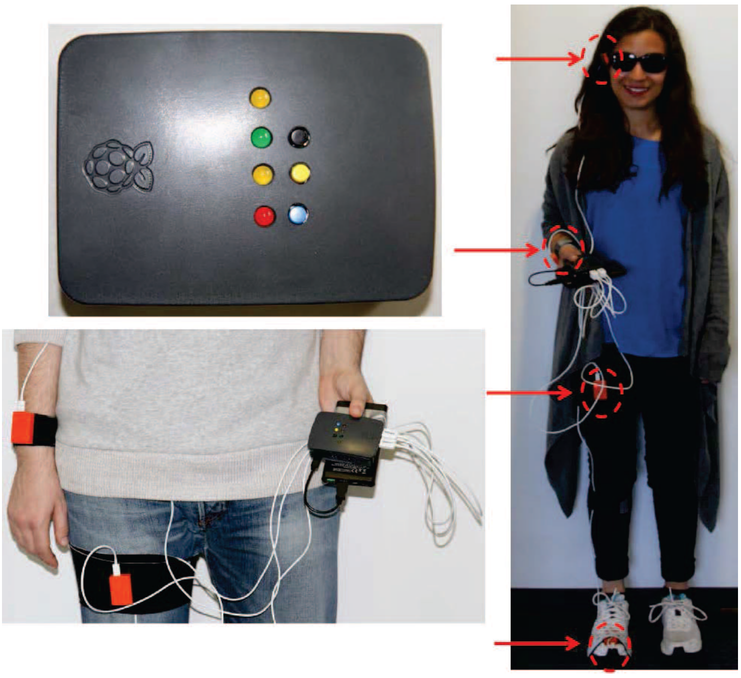

Figure 7.12: (Top left) Raspberry Pi module used to record the data from the IMUs. (Bottom left) From left to right, sensor on wrist and thigh and Raspberry Pi used to log the data and time stamps when the GTPs are crossed. (Right) Sensor set up on glasses, wrist, thigh and foot.

7.3.2 Experimental Method

7.3.2.1 Hardware Setup

The hardware setup consists of four IMUs placed on the glasses, the wrist, the upper thigh and the foot respectively, all of them in the right side of the user's body. The IMUs are connected by a cable to a Raspberry Pi that logs the IMUs measurements and the time stamp when a GTP is crossed. Although only the inertial measurements from the pocket-mounted, wrist-worn and foot-mounted IMU are used in this work, the sensor on the glasses is also included to collect more data and make it available to the public. The sensors' setup is shown in Figure 7.12.

Regarding the sensors, four MTw new generation manufactured by Xsens have been used. These devices include a 3D-accelerometer, a 3D-gyroscope, a 3D-magnetometer and they can also measure pressure and the sensor's temperature. The Allan variance analysis [44] has been run on the accelerometers and gyroscopes to guarantee that all IMUs have the same quality. This analysis is necessary to guarantee a fair comparison between INSs. The random walk and bias stability of each axis of each accelerometer and gyroscope have been estimated. The results showed that all sensors have the same quality. Nevertheless, the tables with the values of the random walk and bias stability are skipped for the sake of simplicity.

In order to use the ground truth system, a program was implemented to run on a Raspberry Pi. The program logs both the data from multiple IMUs, including an absolute time stamp, and stores an absolute time stamp when a GTP is crossed. In order to signal that a GPT is crossed, a board with multiple buttons and LED indicators is developed and attached to the Raspberry Pi (see Figure 7.12). There are several advantages about using the Raspberry Pi. The Raspberry is easy to use, it is portable and the design modifications allow a practical recording of the visited GTPs.

The data from the IMUs have been recorded at a frequency of 100Hz and the following information is recorded for each sensor in each walk: an absolute time stamp, a sequence number, 3D-acceleration, 3D-turn rate, 3D-magnetic field. Additionally, a list of time stamps, that indicate when the user passed a GTP, is also stored for each walk.

7.3.2.2 **Ground Truth Definition**

The experiments were conducted at the German Aerospace Center (DLR) site at Oberpfaffenhofen, close to Munich, Germany. In one part of these installations, a series of GTPs were installed in order to define different evaluation paths through their visit. The GTPs are indicated by nails that were hammered in the ground for the purpose of this work (see Figure 7.13a).

Once the GTPs are indicated by the nails, the next step is to measure their position. For this purpose, the Leica tachymeter was used to create a local frame. Figure 7.13b shows the Leica tachymeter and the prism located on top of a GTP. The origin and orientation of the local frame must be indicated to the tachymeter. In this case, we have set the origin and direction of the x-y axis as indicated in Figure 7.14. In the end, the ground truth system created in this work comprises 69 GTPs whose location is known with centimeter accuracy distributed in an area of 14380 m^2 (see Figure 7.14). In the latter, the GTPs are indicated by yellow pins.

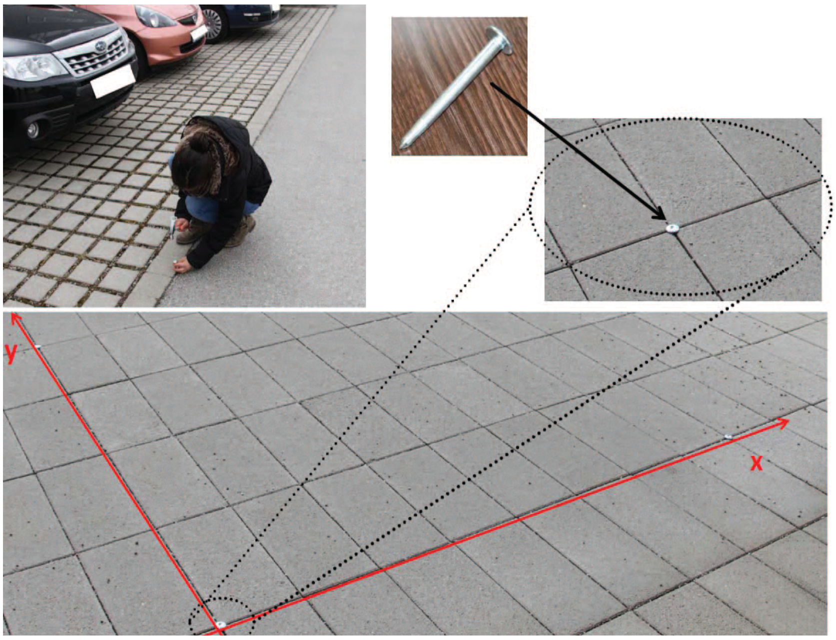

(a) Origin of coordinates and hammering of the nails in the ground

(b) (Left) Leica tachymeter. (Right) 360°prism located on top of a GTP.

Figure 7.13: GTPs installation.

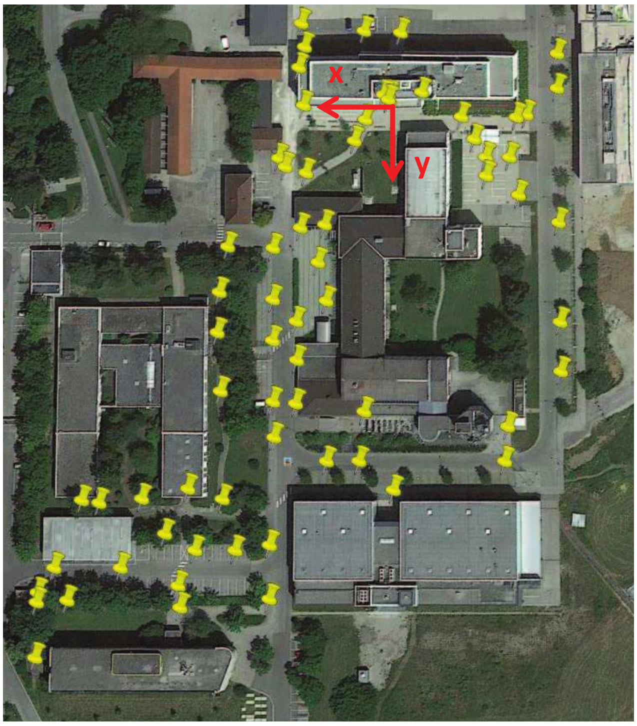

Figure 7.14: GTPs distributed in the test area of 14380 m^2 approximately. The map of the area was taken from Google Earth.

7.3.2.3 **Data Collection**

Regarding the walks, the GTPs to visit in each walk were decided prior to performing the walk. Eight evaluation paths of different shapes and lengths were defined, ranging from 0.2 km to 1.9 km, approximately.

During the experiments, the right wrist, that is, the one on which the IMU was mounted, was mainly swinging. Nevertheless, when indoor and outdoor areas were combined in a single walk, the users opened the doors with the hand where the wrist IMU was located, which increases the risk of outliers. The users were allowed to move the head freely during the walks.

Whenever the users walked over a GTP, the time stamp is recorded by pressing the blue button of the Raspberry Pi, which was held in the left hand. The users were indicated, prior to performing the walks, not stop on top of the GTPs when pressing the button. The reason was to favor natural walks.

Five different users (2 women and 3 men) took part in the data collection, generating 29 walks through 995 GTPs, equivalent to about 20 km traveled and almost five hours of duration.

7.3.2.4 Data Processing and Evaluation

The raw data from the corresponding sensors were processed by the three pedestrian navigation systems described in Section 7.3.1. Although the position estimation was done offline, no technique was applied during post-processing that could improve or smooth the results.

Subsequently, the error is computed as the difference between the estimated and true positions at each GTP. The error is then normalized with respect to the time elapsed in order to be able to more fairly aggregate the results obtained at the different GTPs and from the different paths and users. It also makes it possible to compare possible speed differences more fairly, since the heading error depends on the elapsed time and this error is then propagated to the position error. Another option would be to normalize by the traveled distance but it cannot be ensured that all users have followed the same path between successive GTPs. Therefore, the error metric (e_P) is defined, for the time instant k, as follows:

$$e_P(k) = \frac{|P^{GT}(k) - \hat{P}(k)|}{t_k} \tag{7.3}$$

where ($P^{GT}(k)$) denotes the true position vector of the GTP visited at the k-th time, ($\hat{P}(k)$) denotes the estimated position vector of the GTP visited at the k-th time, $|\cdot|$ denotes the norm of a vector and t_k denotes the elapsed time at the k-th time.

The number of gait cycle events, i.e. steps or strides, detected by each of the systems will also be compared.

7.3.3 Results

7.3.3.1 Systems Comparison

There are some differences between the three systems to be taken into account when comparing their performance. First, the foot-mounted system, being an INS, updates the position estimation at the same rate as the sensors offer their measurements. In this case, at 100 Hz. In contrast, the other two are PDR systems, which update their position estimation more slowly, after each detected step. This could have some small effect on the position error if it were the case that many GTPs were recorded while a step was being taken. Second, the foot-mounted and pocket-mounted systems detect strides, while the wrist-worn system detects steps. Therefore, for comparing the accuracy of detection of these gait events, it is assumed that a stride corresponds to two steps.

	Pocket-mounted	**Wrist-worn**	**Foot-mounted**
e_P [m/s]	0.19±0.15	0.30±0.70	0.19±0.21
Steps detected	27760	23195	29744

Table 7.4: Position error and steps/strides detected by each pedestrian navigation system. Mean (μ) and standard deviation (σ), written as $\mu \pm \sigma$, of the position error e_P of 29 walks with a total of 995 GTPs. The number of steps detected is also shown.

Step Detection

With regard to the number of steps detected, the results obtained by each system do not coincide, as can be seen in the Table 7.4. The stride detector of the pocket-mounted system has proven to be very accurate [97, 214] since the pitch angle of the upper thigh signal has a very characteristic and clear shape when walking and is highly unlikely to be generated by any other activity than walking. Therefore, its estimate will be taken as the true number of steps. According to this criterion, the foot-mounted system overestimated the number of steps because they are counted from the detected foot's stance phases and, as can be seen in Figure 7.15a, it can happen that a stance phase is divided into two. This problem seems plausible since many stance detection methods are based on checking that the accelerations and angular velocities do not exceed certain thresholds, so these errors can arise from small bounces. In contrast, the wrist-worn system underestimated the number of steps taken. These mis-detections are caused by undetected steps, false negatives, as the shadowed area in Figure 7.15b shows. This result makes sense because, since in these experiments the pedestrians are actually walking, it is more likely to miss steps when making irregular hand movements, such as opening a door, than to overcount steps, which is more common when the user is really still.

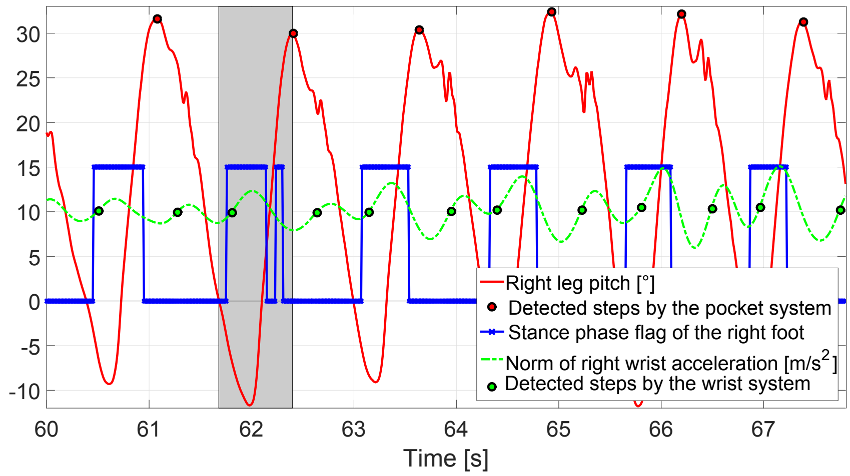

(a) Foot-mounted system detecting two stance phases instead of one

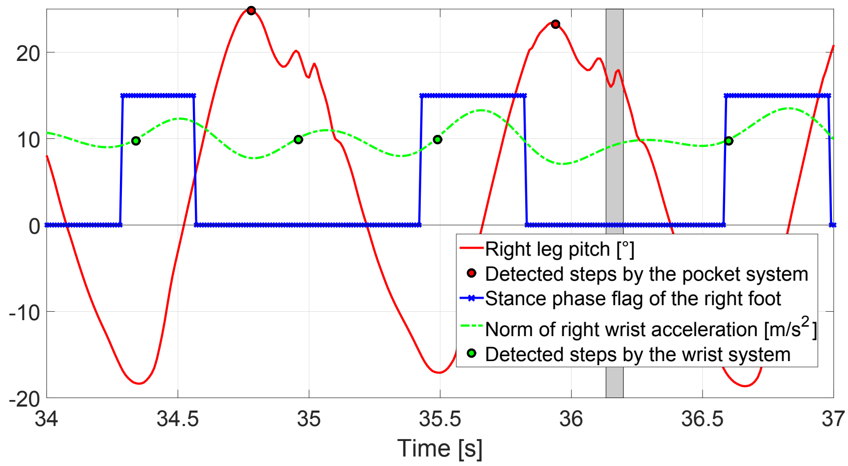

(b) Wrist-worn system missing one step

Figure 7.15: Comparison of the signals that each pedestrian navigation system uses to either detect strides (pocket), steps (wrist), or detect stance phases (foot). The shadowed area indicates an over-detected step by the foot-mounted system (a) and an undetected step by the wrist-worn system (b).

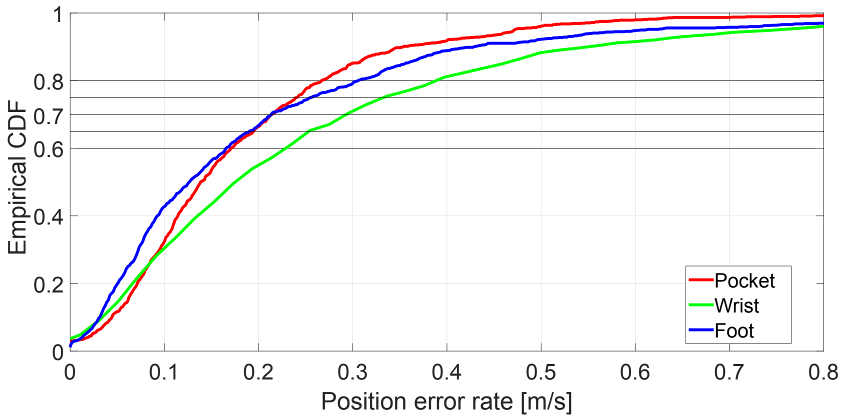

Figure 7.16: Empirical CDF of the position error of each pedestrian navigation system

Position Estimation

Figure 7.16 presents the empirical CDF of the position error rate in equation (7.3). It shows that, for around the 70% of the GTPs evaluated, the foot-mounted system achieves the lowest error accumulation rates. However, from that point on, the pocket-mounted gets lower error levels. In addition, as can be seen in Table 7.4, the pocket-mounted has the same mean error as the foot-mounted systems have the same average error and a lower standard deviation. One possible reason is that the foot-mounted system, when implemented as an INS, does not depend on any model to calculate the traveled distance and is capable of achieving lower error rates most of the time. However, it appears that it has suffered a greater number of outliers, possibly due to the fact that the evaluation paths have been run outside, including some sections with uneven terrain, which could have impacted on the performance of the ZUPT. By contrast, the pocket system, by using the signal of the thigh's pitch angle, gets less accurate but somewhat more precise estimations.

Regarding the wrist-worn system, the empirical CDF and the statistics confirm the distance between the wrist-worn system and the other two systems in terms of performance. This was expected after checking the number of steps that were not detected, since that error propagates directly to the position error. In addition, both the SD and SLE blocks may be affected the way each user walks and swings the arm while walking.

The fact that the CDFs are crossed and the statistics are so similar exemplifies the current difficulty of convincingly evaluating and comparing the performance of DR-based positioning systems. From the mean and standard deviation, it would not be entirely clear which system offers the least error. Following the criteria of the IPIN 2016 competition, that is, the third quartile of the position error, according to Figure 7.16 the pocket-mounted system would be more accurate than the foot-mounted system, when the latter is really capable of achieving better results for most of the time. The same problems arise with other evaluation metrics such as the final position error or the qualitative checking of the path on the map, especially if only one evaluation path is evaluated. Figure 7.17a presents one of the evaluation paths and the results obtained by the three pedestrian navigation systems for one user. The evaluation path definition is approximate because the users were indicated only which GTPs to visit, and not the exact path to follow. The position error rate metric of this walk is presented in Figure 7.17b. As can be seen, the wrist-worn system has the highest position error rate for most of the walk. However, because the shape of the path (it ends at the starting point but has little surface area) and because the system tends to miss steps and underestimate the traveled distance, it gets the lowest error rates at the last GTPs. This example shows the clear need to search for evaluation metrics that are capable of characterizing the performance of DR-based navigation systems in a comprehensive manner and independent of the shape of the evaluation path.

7.3.3.2 **Wrist-worn PDR System over Users**

The three main blocks of PDR systems (i.e. SD, SLE and SHE) may vary in performance depending on the user of the system. To get an overview of the wrist-worn PDR system's adaptability level to different users, the Figure 7.18 shows the step detection and traveled distance estimation errors for each path made by each user. Since the ground truth length of each individual step is not available, it is easier to use the traveled distance. Both errors are compared simultaneously using a scatter diagram. In this way, since errors in step detection directly affect the traveled distance estimation, the performance of the SLE block can be identified. First of all,

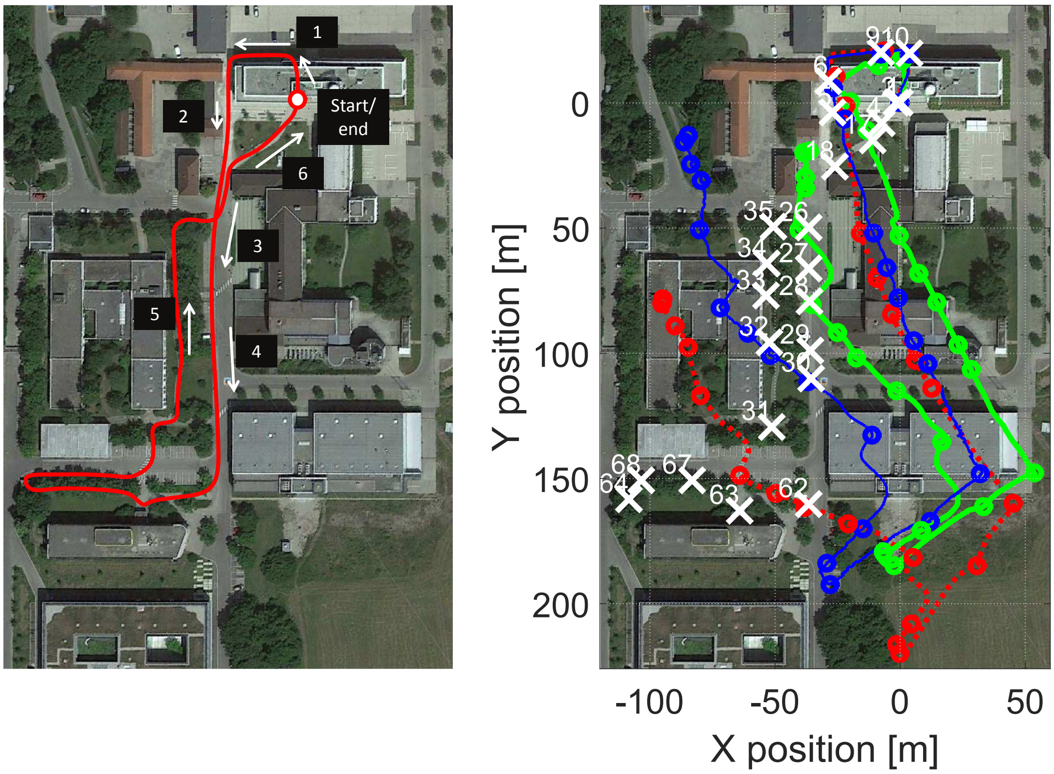

(a) Evaluation path (left) and trajectories estimated (right) by the pocket-mounted (red-dotted line), the wrist-worn (green-thick-solid line) and the foot-mounted systems (blue-thin-solid line). The x-marks indicate the true position of the GTPs and the circle marks the estimated ones.

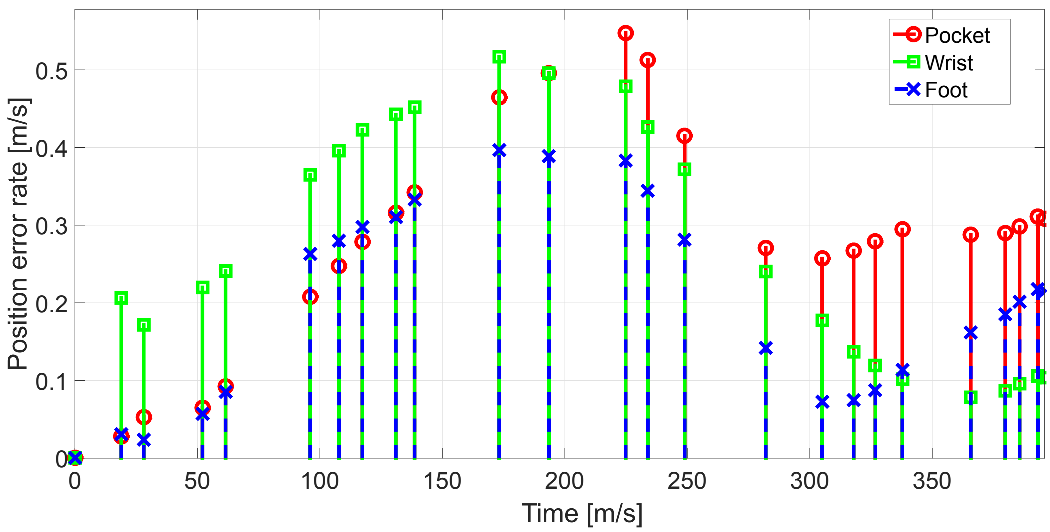

(b) Position error rate over time

Figure 7.17: Visualization of the trajectories estimated by the three pedestrian navigation systems for one of the evaluation paths

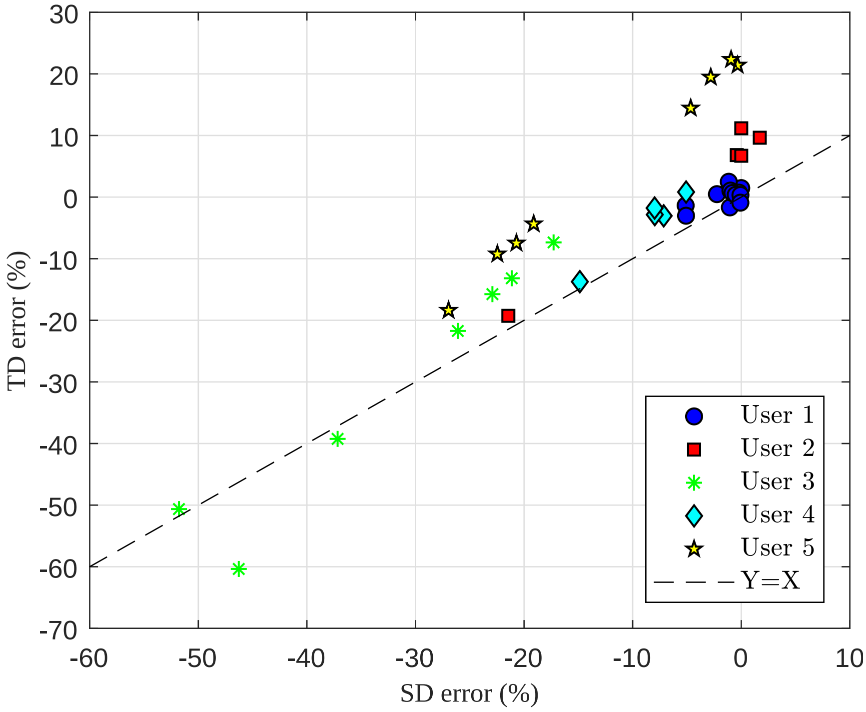

Figure 7.18: SD and TD errors of the wrist-worn inertial PDR system for each user

user 1 is the one for whom the system was calibrated in the Section 7.1 and thus clearly gets the best performance. With regard to the performance of the SD block, as noted above, there is a clear trend towards mis-detecting steps. It is mainly due to the existence of outliers when making movements not contemplated with the arm but it can also be appreciated how some users (users 3 and 5) present significantly worse results than the rest.

As for the SLE block, the fact that most results are above the $Y = X$ line indicates a clear tendency to overestimate the length of the steps. Again, users 3 and 5 have bigger errors than the rest, as their samples are farther away from the line $Y = X$. However, the fact that each user's samples are fairly well aligned indicates that the SLE error is mainly an offset.

In summary, it can be seen that the tested wrist-worn PDR system presents an important variability in terms of its performance over different users. More effort is therefore needed to design more flexible algorithms and to define calibration processes.

7.4 Conclusions

This chapter has focused on presenting two evaluation stages to which a state-of-the-art wrist-worn inertial PDR system has been subjected. The first one corresponded to the IPIN Indoor Localization Competition 2016 held during that year's IPIN conference, whose main characteristic is its challenging multi-floor long evaluation paths. However, the different participating navigation systems were not evaluated simultaneously and were carried by only one user, who was different for each system. A fair comparison of systems must be performed under the same conditions, i.e. same sensors, paths and users. For this reason, a second evaluation stage focused on the comparison of different inertial pedestrian navigation systems simultaneously carried and evaluated for a set of pedestrians. Table 7.5 shows the main characteristics of both evaluation stages.

	IPIN 2016 Competition	**Simultaneous Evaluation**
Evaluation Paths	1	8
Trials	2	1
Path Length	674 m	200 m - 1900 m
GTPs	57	13 - 79
Scenario	Indoor&Outdoor	Outdoor
Users	One different per system	5 (2W+3M)
Tested Navigation Systems	6	3
Simultaneous Test	No	Yes
Position Estimation	2.5D	2D
Error definition	Position error [m]	Normalized position error [m/s]
Evaluation Metric	3rd Quartile	Empirical CDF
SD Evaluation	No	Yes
Public datasets	No	Yes

Table 7.5: Comparison of the characteristics of the two evaluation stages

First, it was described the wrist-worn inertial PDR system that was selected from the existing literature to be implemented and tested during the evaluation stages. This system was extended to estimate 2.5D positions using a barometer and simple MC and FE algorithms. In addition, during the calibration process, it was verified that the inertial sensors must work at a sampling rate of at least 25 Hz to facilitate the detection of steps. Similarly, it was found that it is advisable to filter the acceleration signals to eliminate frequencies higher than the step walking rate.

During the two evaluation stages it has been observed that the performance of the wrist-worn inertial PDR system is generally worse than that of other systems with sensors mounted on other parts of the body, especially on the foot. Improvement measures should address three main issues:

1. The first one is the adaptability of the system to different users. It has been proven that the results obtained for the user for whom the PDR system was calibrated are significantly better than for different users. For this reason, more adaptive algorithms and calibration processes should be defined to alleviate this problem.

2. The second one is the drift in the heading estimation. If the PDR system is well calibrated to the user's characteristics, this is the main source of error. As could be seen in the IPIN competition, magnetometers are not reliable indoors and, therefore, gyro error accumulates over time in the form of heading drift, which is a general problem for all inertial systems. In addition, in the specific case of wrist-worn systems, the freedom of movement of the upper limbs when walking can generate additional heading errors due to misalignment with respect to travel direction.

3. The third one is the correct detection of steps. Wrist-worn inertial systems have two difficulties in this regard. On the one hand, when the pedestrian is stationary, the SD may suffer false positive steps if the upper extremities make movements that generate signals similar to those produced when walking. On the other hand, when the pedestrian is walking, it can also happen that some steps are not detected (false negatives). The latter problem has emerged during the evaluation as an underestimate of the number of steps. These difficulties in detecting the steps represent the current major limitation of wrist-worn systems compared to systems mounted on other parts of the body.

The SLE block also showed a tendency to over-estimate but, since its impact on the traveled distance is subject to the correct step detection, this problem is considered to be of lower priority.

Another general problem with DR-based positioning systems is the lack of a standard testing and evaluation methodology specific to this type of system that allows characterizing their performance and, therefore, predicting with some confidence their error levels in new scenarios. As discussed in Section 5.7.2, the ISO/IEC 18305 standard "Test and evaluation of localization and tracking systems" is more oriented to systems based on the position fixing localization method and the use of RF anchors. For example, the criterion used in the IPIN 2016 competition (the third quartile of the position error along an evaluation path) fits better with position fixing bases systems, since the errors in successive GTPs are independent, which allows characterizing the system and predicting its performance in similar future scenarios (LOS/NLOS, types of obstacles, materials, etc.). On the other hand, the position error in DR-based systems accumulates over time and, therefore, their value in successive GTPs are not independent observations but depend on past values. Therefore, the path followed and the possible error outliers make it difficult to characterize the performance of DR systems.

Finally, it should be noted that both evaluation stages have only evaluated the swinging mode, as it is considered to be the most common carrying mode during long walks and easier to process than the quasi-static modes such as texting or phoning. However, in order to achieve wrist-worn systems that are useful in indoor environments such as offices or homes, it will also be necessary to include different activities done by the upper extremities simultaneously when walking.

All things are difficult before they are easy.

Dr. Thomas Fuller

CHAPTER

8

Adaptation of the Heuristic Method iHDE for PDR Systems

Heading drift is currently one of the main problems for pedestrian localization systems based on inertial sensors, as the integration of the gyroscopes' measurements causes the heading error to accumulate over time. This problem is especially severe indoors because, as seen in the previous chapter, magnetometers are not reliable for obtaining the actual heading because of the magnetic disturbances. In order to mitigate this limitation, there exists a set of heuristic methods that use some prior information about the building in which the walk takes place. They assume that the majority of the buildings are composed of parallel and perpendicular straight corridors, oriented towards a small set of directions, known as dominant directions.

Both Borenstein *et al.* with the method HDE [61] and Abdulrahim *et al.* with a method known as *Cardinal Heading Aided Inertial Navigation* (CHAIN) [62] used this assumption but implemented their methods in different ways. Later, Jiménez *et al.* [63] proposed a method known as iHDE, in which they mitigate some common limitations of the previous methods. However, their proposal is designed as an integrated block of a foot-mounted INS systems. This led to the definition of the *specific objective 4*, which seeks to adapt the heuristic method iHDE so that it can be used in PDR systems. This chapter describes this adaptation and a brief evaluation of iHDE's ability to reduce the heading drift error, including synthetically generated experimental data as well as real data from a wrist-worn inertial PDR system.

The rest of the chapter is as follows: Section 8.1 describes briefly the existing heuristics. The proposed adaptation is described in Section 8.2 and the experimental results are described in Section 8.3. Finally, conclusions are drawn in Section 8.4.

8.1 Description of the Existing Heuristic Methods

8.1.1 Heuristic Drift Elimination (HDE)

Boreinstein and Ojeda initially proposed the heuristic method HDR which, assuming that people usually walk along a straight line, tries to estimate the bias associated with the heading drift and compensate for it [56]. This technique reduces the rate at which the heading error accumulates but cannot eliminate it completely because the actual heading is not observable.

Subsequently, the same authors proposed the heuristic method HDE, in which they use the observation that in most buildings the corridors are straight and either parallel or orthogonal to each other and to the peripheral walls [61]. Assuming that it is possible to know these dominant directions, they propose an algorithm based on a closed-loop controller that corrects the angular rate provided by a vertical gyroscope. The feedback loop is a binary I-controller that tracks the value needed for the correction using as input the sign of the difference between the estimated heading and the building's closest dominant direction. This way, the controller compensates gradually the accumulated gyroscopes' errors until the heading error is eliminated. Therefore, they make the heading error to be observable.

This method can be applied without actually having a vertically aligned gyroscope. To do this, a "virtual" gyroscope is corrected using the angular velocities associated with the change of heading calculated from the position estimates.

The main benefit of HDE is that reduces the heading error to near-zero in steady state and corrects already incurred heading errors. However, it only works properly when the user walks along the defined dominant directions. During curved paths or non-dominant direction oriented straight paths, HDE cannot correct the heading error and, in fact, if HDE is not deactivated during these paths, it may even introduce an additional error. Since it is sometimes not easy to clearly identify these scenarios, attenuators based on the step length and the mangnitude of the angular rate are applied to deactivate or reduce the correction of HDE.

Another sensitive issue is the selection of the value of the binary I-controller's fixed increment. A high value can get the steady state faster, but the estimation of the gyroscope bias can be less accurate, leading to transform a straight path into a zigzag. Moreover, the damage in the non-compliant segments could be larger as well. In contrast, a low value obtains a better gyroscope bias estimation, tolerates longer non-compliant segments but gets the steady state slower, generating some irrecoverable positioning errors.

8.1.2 Cardinal Heading Aided Inertial Navigation (CHAIN)

Almost at the same time as Boreinstein's HDE, Abdulrahim *et al.* proposed the CHAIN method, which is based on the same concept of dominant directions but it is implemented in an alternative way [62]. Their proposal is designed for a foot-mounted INS system and is integrated into the error-state KF. Their method works directly on the heading error: a measurement of the heading error is computed as the difference between each step's heading angle and the closest dominant direction of the building. Thus, this measurement is fed into the error-state KF with a constant covariance matrix. Additionally, they only apply this correction when the stride length is larger than 0.3 m.

The benefit of this implementation is that the speed of tracking of the gyroscope bias is not limited by a fixed value, as in the case of HDE. However, since they do not check if the pedestrian is actually walking straight, this method suffers the same problems in paths with non-compliant segments as HDE does.

8.1.3 Improved Heuristic Drift Elimination (iHDE)

Based on the two previous methods, Jiménez *et al.* proposed an improved version that tries to mitigate the limitations during the curved paths and the non-dominant direction oriented straight paths [63]. Their method is also designed for a foot-mounted INS system and integrated into the error-state KF. The improvement that they introduced is the use of a set of attenuators that adapt the confidence on the heading error measurement and, therefore, restrict the corrections depending on the type of path:

- Step Size (SS) is a binary attenuator that deactivates the correction if the length of the step is shorter than a certain threshold;
- Straight Line Path (SLP) is another binary attenuator that deactivates the correction when it is detected that the user is not walking along a straight line. To make that decision, they check whether the dispersion of the last 5 steps' heading is below a certain threshold.
- Finally, the confidence on heading error measurement will be inversely proportional to its value. This way, when there is a large uncertainty about whether the heading error is produced by the gyroscope bias or by a non-dominant oriented straight segment, the magnitude of the correction is decreased.

8.2 Adaptation of the Method iHDE

The aim of this work is to adapt the iHDE method so that it can be applied to PDR systems, such as a wrist-worn inertial PDR system, while preserving its improvements with respect to HDE and CHAIN. The strategy followed is to create a closed-loop controller that corrects the steps' heading angles provided by the PDR system, in a similar way as HDE does, but in an adaptive way, just like iHDE does. The block diagram is shown in Figure 8.1.

In the same way as iHDE, the heading error is estimated by a complementary KF in which the standard deviation of the measurement is not constant but adaptive.

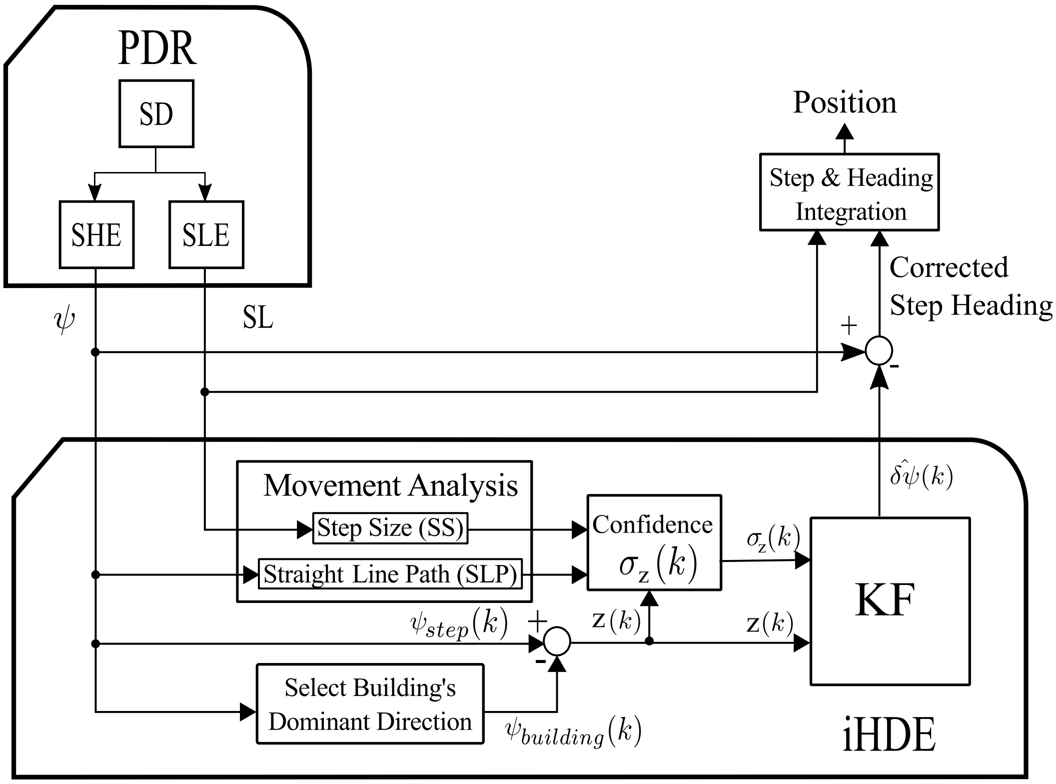

Figure 8.1: Block diagram of the adaptation of iHDE method for PDR systems

The process model is simplified as follows:

$$\delta\psi(k+1) = \delta\psi(k) + w(k) \tag{8.1}$$

where $\delta\psi(k)$ is the heading error at the step k and $w(k)$ is the process noise with covariance matrix $Q(k) = E(w(k)w^T(k))$.

The measurement of the heading error is obtained as the difference between the step's heading angle, obtained in this case as a direct output of the PDR, and the closest dominant direction of the building:

$$z(k) = \psi_{step}(k) - \psi_{building}(k) = \delta\psi(k) \tag{8.2}$$

The confidence of the measurement of the heading error will be computed in the same way as iHDE: its standard deviation variation is adapted by the SS and SLP attenuators and the value of the heading error measurement:

$$\sigma_z(k) = \frac{\sigma_{HDE}}{SLP \cdot SS \cdot e^{\alpha|z(k)|/\triangle}} \tag{8.3}$$

where σ_{HDE} is the maximum possible confidence assumed for any measurement, α is a negative value that manages the growing rate of the standard deviation when the heading error grows, and $\triangle$ is the least angular difference between the dominant directions of the building.

Due to this simple process model and the reset of the state vector after each measurement update, the estimation of the heading error can be expressed as:

$$\hat{\delta\psi}(k) = \frac{P^{-}(k)}{P^{-}(k) + R(k)} \cdot z(k) \tag{8.4}$$

where $P^{-}(k)$ is the estimation error covariance matrix after the time prediction, with the form $P^{-}(k) = P(k-1) + Q(k-1)$, and R is the measurement error covariance matrix computed for each step using the previous expression of $\sigma_z(k)$. Therefore, it can be seen that this simplified KF is just a proportional controller whose correction is inversely proportional to the absolute value of the heading error. When the heading error is low, it will be more likely that the drift is due to the gyroscope bias. In contrast, when the heading error is high, the uncertainty of whether it was produced by a non-dominant oriented straight path is also high, so the correction rate will be decreased.

8.3 Experimental Evaluation

The adaptation of the iHDE method will be evaluated by comparing the heading correction it introduces against a PDR system without heuristic methods and against one with built-in HDE. The experimentation includes both synthetically generated data and real data from a wrist-worn inertial PDR system.

8.3.1 Evaluation using synthetically generated data

The aim of using synthetically generated data is twofold. On the one hand, it facilitates the search for an optimal configuration of the different parameters of each method; on the other hand, it allows to test, in a more easy way, different paths and scenarios.

First, a set of test paths have been synthetically generated, including characteristics as dominant oriented straight segments, non-dominant oriented straight segments, turns, curved segments or several loops to a closed path. Then, each test path's ground truth has been obtained by expressing its length as a multiple of a constant step length and assigning to each step the desired step's heading angle. From the ground truth data, the PDR output is generated adding some angular bias to each step's heading angle. In this study, the heading bias followed a Gaussian random variable with mean 0.1°/s and standard deviation 0.8°/s.

In order to compare the performance of HDE and iHDE, the configuration of each algorithm that provides the best average correction over the set of test scenarios previously defined was sought. Table 8.1 collects the values of the parameters of HDE and iHDE methods for both the synthetically generated data and real data scenarios.

Algorithm	Parameter	Value
Both	Dominant direction ($\triangle$)	90°
	Angular rate threshold	6°/s
	Step length threshold	0.7 m
HDE	Filter time constant	0.9 s
	Integrator constant	0.2°/s
iHDE	# Steps straight path	5
	σ_{HDE}	0.25°/s
	α	10

Table 8.1: Configuration values of the HDE and iHDE methods.

As evaluation metric, the *Average Heading Error* (AHE) over the different steps' heading of the test path was used. Other frequent evaluation metrics are the *Distance-to-Origin* (DTO) or the *Final Heading Error* (FHE), but AHE is more convenient for any kind of scenario. DTO only makes sense for closed paths and FHE does not give a vision of the performance over the whole path.

Table 8.2 presents the results of the AHR and DTO metrics and the relative improvement with respect to the plain PDR system for three basic scenarios: four loops to a square path; a path composed by two dominant oriented straight segments joined by a middle segment oriented 30° away from a dominant direction; and a closed path composed by a dominant oriented straight segment and a circular

Scenarios	Path Length	PDR		PDR+HDE		PDR+iHDE	
		AHE	DTO	AHE	DTO	AHE	DTO
Square path	256 m	12.73°	5.86 m	0.86° (93.28%)	0.57 m (90.22%)	0.78° (93.88%)	0.73 m (87.6%)
Non-dominant segment	60 m	3.47°	-	30.08° (-767.52%)	-	0.74° (78.57%)	-
Curved segment	128 m	11.89°	8.86 m	13.19° (-10.94%)	20.31 m (-129.34%)	7.97° (32.93%)	6.76 m (23.67%)

Table 8.2: Results for synthetically generated data of a plain PDR system, one including HDE and one including iHDE.

path. Figures 8.2, 8.3 and 8.4 show the estimated trajectories by the three system for each scenarios, respectively. Each detected step is represented by a marker (square, circle or diamond), whose interior is colored when a heading correction has been applied.

Although these results cannot been taken as a definitive performance measure, they do give a good vision of the strengths and weaknesses of each heuristic. It can be seen that both HDE and iHDE correct almost all the heading error in scenarios with only dominant oriented segments, as it is the case of the square path (Figure 8.2). However, HDE suffers in scenarios with non-dominant oriented segments (Figure 8.3) or with curved paths (Figure 8.4). In fact, according to the AHE and DTO metrics, HDE can even worse the performance of the plain PDR, as indicates the negative improvement percentages.

As can be seen in Figure 8.3, although both HDE and iHDE methods correct the heading during the non-dominant segment, HDE does it in a stronger way, leading to introduce additional error. In a similar way, Figure 8.4 shows that HDE does not get disable during the curved segment, while iHDE does it in most of it. This makes iHDE to obtain better results.

8.3.2 Evaluation using real data

The wrist-worn inertial PDR systems corrected after the IPIN 2016 competition, as described in Section 7.2.2, was used for performing the real experiments. Then, the HDE and iHDE heuristics were integrated on the PDR's output, using the same configuration values than in the synthetically generated data section (Table 8.1).

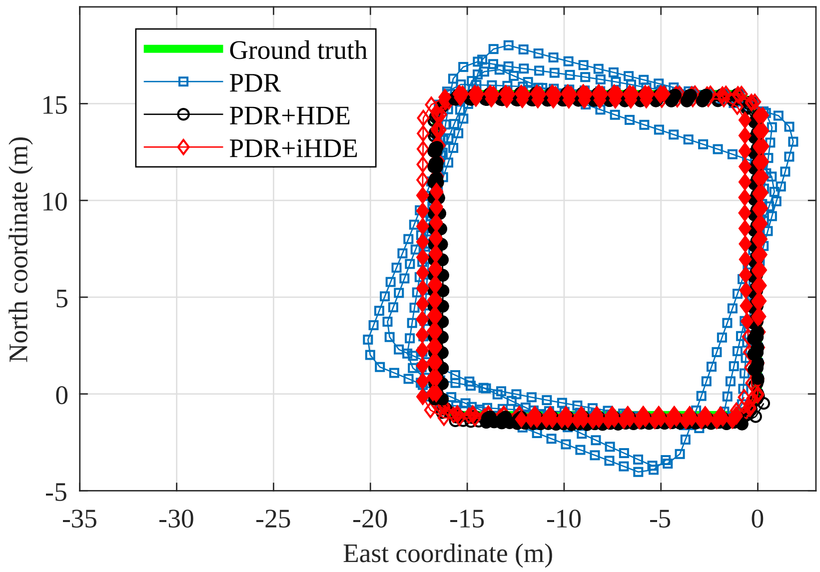

Figure 8.2: Correction of HDE and iHDE heuristics in a synthetic generated squared scenario.

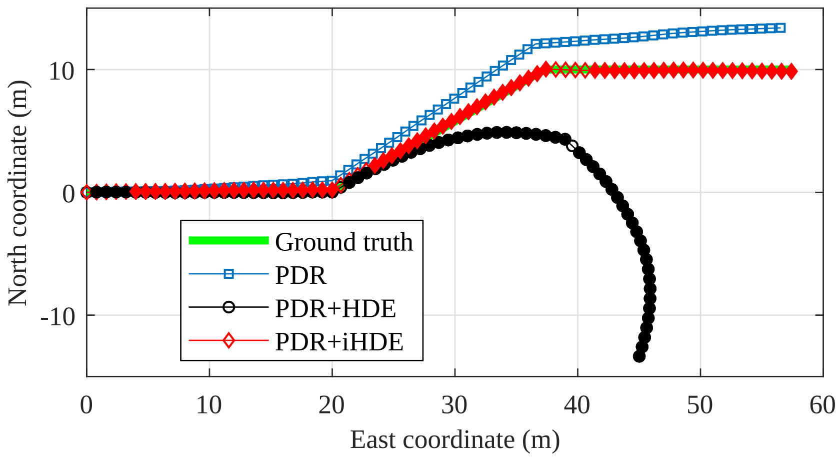

Figure 8.3: Correction of HDE and iHDE heuristics in a synthetic generated scenario with a non-dominant segment.

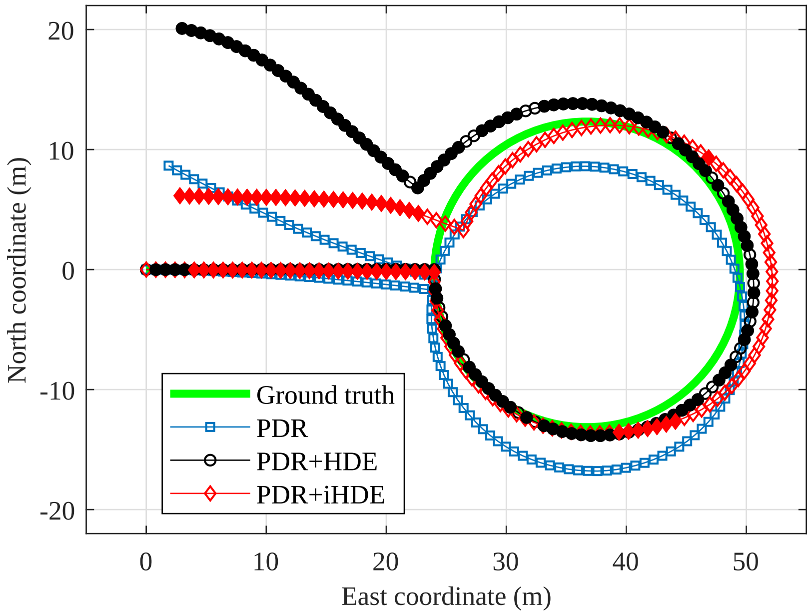

Figure 8.4: Correction of HDE and iHDE heuristics in a synthetic generated scenario with a curved segment.

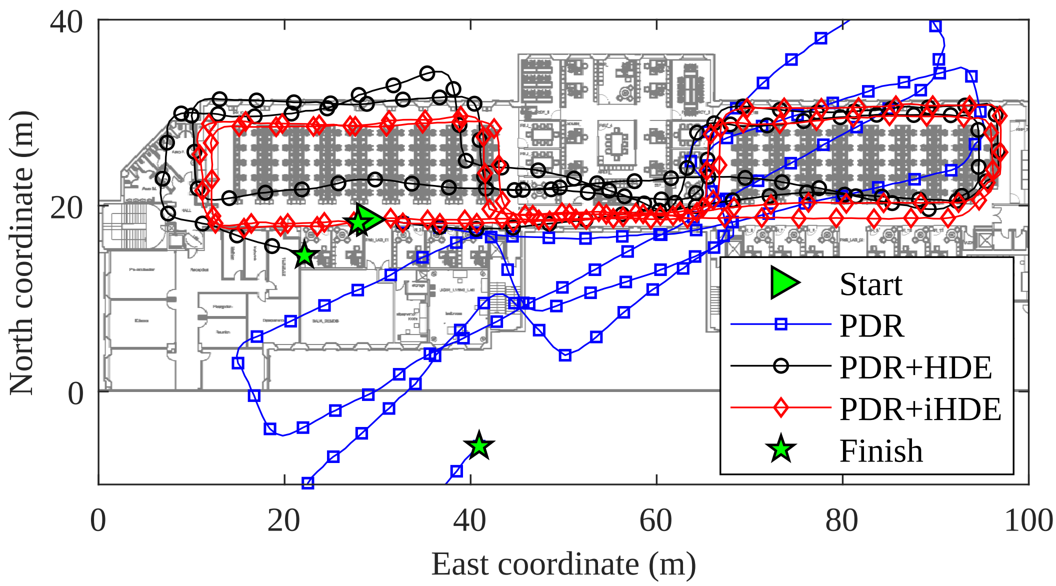

Figure 8.5: Correction of HDE and iHDE heuristics in a real scenario.

Figure 8.5 represents the output of the plain wrist-worn PDR system and the corrections of HDE and iHDE to a real indoor walk in which two loops were taken in the fourth floor of DeustoTech building, at the University of Deusto. Firstly, it can be seen how the plain PDR is not able to keep the right heading after a few dozens of meters, showing that heading drift is a real problem for PDR systems. Both HDE and iHDE help to correct the heading drift but, since the HDE method is less conservative when performing correction and also updates the correction value in constant increments, it can slightly distort the shape of the paths, limiting their correction capability. Meanwhile, iHDE is able to reduce or disable the correction, obtaining better results. After a path of 408 m long, the plain PDR system got a DTO error of 27.22 m, while the PDR with the iHDE method got 0.97 m. In contrast, the HDE method only got to reduce the DTO error to 7.7 m.

8.4 Conclusions

In this chapter the adaptation of the heuristic method iHDE to be used in PDR systems has been presented. It has been proven that the adaptation maintains the improvements that iHDE incorporates with respect to other methods such as HDE. In particular, HDE is only able to correct the heading drift properly when the scenario is close to the idealize assumption of straight segments. In contrast, iHDE can adapt its correction, although not perfectly, to a broader range of scenarios.

In addition, it has been proven that these types of heuristic methods are of great help in alleviating the problem of heading drift suffered by pedestrian localization systems based on inertial sensors. For this purpose, an experiment was carried out on a real indoor scenario using a wrist-worn inertial PDR system.

There's a fine line between fishing and just standing on the shore like an idiot.

Steven Wright

CHAPTER 9

Conclusions and Future Work

At the beginning of this thesis it was presented that, although GNSS systems are currently the main source of location information, due to the need for LOS with satellites, it is not possible to use them continuously. This is especially true for pedestrians, as most of their time is spent in indoor environments. The development of new LBS and systems under new paradigms such as ubiquitous computing requires seamless localization systems. To this end, the role of DR-based localization systems was seen as key because they do not need additional infrastructure to be installed in the environment.

In this context, thanks to the current availability of smart devices for the wrist, such as smartwatches and smartbands, the technical capabilities they usually include, and the convenience they offer to the user, wrist-worn inertial PDR systems seem to be a great opportunity to make further progress towards seamless pedestrian localization systems. However, despite their potential for developing pedestrian LBS, wrist-worn inertial PDR systems remain an open challenge. And the existing literature was not enough to provide a complete overview of the operation and performance of this type of localization systems. This indicated that there was a need to address wrist-worn inertial PDR systems in a specific and comprehensive manner. This was precisely the main goal of this thesis: to contribute to both the understanding and the improvement of the performance of wrist-worn inertial PDR systems. After the revision of the state of the art literature about inertial PDR systems in general, and wrist-worn in particular, four specific objectives were defined for this research work, which were presented in the final section of Chapter 3. This set of objectives was defined in such a way as to provide a global vision of the different blocks that make up a PDR system and this final chapter summarizes the conclusions and results obtained.

In this way, the Section 9.1 presents the main conclusions reached during this doctoral thesis. Subsequently, the Section 9.2 proposes the main lines of future research in this field. Finally, the Section 9.3 lists the articles that have been published in relation to the results of this thesis.

9.1 Conclusions

The research work began with a deep analysis of the characteristics of the signals coming from different types of wrist-worn sensors and their variability with respect to factors such as the type of carrying mode, the walking speed or different users. This analysis, presented in Chapter 4 and that is related to the *specific objective 1*, aims to gain a more detailed knowledge about the characteristics of the existing patterns in the wrist-worn inertial signals, to understand what implications they may have when designing a PDR system and, therefore, to assess the feasibility to do it. The different signals from sensors coupled to the pedestrian's COM when walking have been quite studied and used in the PDR field. In contrast, little is known about the origins, motives and characteristics of the swinging of the arms when walking with them free. Usually, PDR systems that consider swinging carrying mode assume an ideal swing and do not deepen their characteristics. Therefore, one of the contributions of this analysis is the confirmation that different users or walking speeds strongly influence the patterns of the different signals, due, especially, to the variation of both the amplitude and the direction in which the arms swing. Even quasi-static carrying modes also showed some variability depending on the user and, especially, on the walking speed. The main conclusion of this analysis, and therefore of Chapter 4, is that the presence of clear patterns related to the human walking on different types of signals during the main use cases confirms the feasibility of designing PDR systems on the wrist. However, it was also shown the need to design highly adaptive algorithms in all PDR blocks and, additionally, to define calibration processes that help to adjust these algorithms to each user or scenario.

During the review of the state of the art, a large number of SLE methods based on inertial sensors were found to exist, but it was difficult to obtain a clear and comparative view of the performance, strengths and weaknesses of each of them. In addition to the lack of a methodology to guide the evaluation and testing of these methods, no review work was found to provide a complete overview of this field, which is applicable in several areas other than PDR systems. Therefore, *specific objective 2* was defined and Chapter 5 presented a systematic and complete review that covered the whole workflow involved in the design, test, and evaluation of SLE methods based on inertial sensors. The main conclusion offered by this review work is that the field of SLE methods is still in the research stage due to two main reasons. On the one hand, the lack of a standard testing and evaluation methodology that marks a common way of working for all researchers in the field and, on the other hand, the lack of availability of public datasets or competitions that facilitate the comparison of the different proposals in a fair and reliable way. This work is, to the knowledge of the author, the first one in this field that offers a global vision and tries to serve as a starting point for the definition of future methodologies, to which we tried to contribute by offering a series of reflections on the matter.

One of the conclusions drawn in the previous Chapter 5 was the important role that the ground truth source plays in the calibration, testing and evaluation of SLE methods based on inertial sensors. Nevertheless, the technologies that are commonly used as ground truth do not offer a good balance between accuracy and coverage area. On the one hand, technologies such as optical systems can achieve millimeter accuracies of the lengths of each step or stride. Unfortunately, due to LOS requirements, its use is limited to very small areas, which makes it difficult to collect data associated with realistic day-to-day activities. On the other hand, other technologies that can be used in larger and outdoor areas are not able to measure the length of each individual step but the average after a walk. Motivated by these facts, the UWB technology was identified as a possible candidate to be used as a ground truth source in the field of SLE. This technology offers only decimeter-level ranging accuracy but provides larger coverage areas than optical or ultrasound systems, which can be useful for the training and evaluating PDR systems. Therefore, in Chapter 6, a preliminary evaluation of the accuracy of UWB technology as a ground truth source for SLE related tasks was presented. Four different methods were tested and, after analyzing their performances of the different SLE methods, a first observation can be highlighted: since the step is a relative measure between the foot positions, the use of inter-feet ranges has proven to be essential when it comes to reducing the estimation error. The first results indicate that it is possible to obtain errors below 10 cm for more than 50% of the steps, which makes us optimistic about the use of UWB as ground truth since it is possible to improve those results easily by installing a greater number of anchors to minimize NLOS situations and the use of filtering techniques for outliers ranges. This exploratory work therefore supports future work on assessing whether the combination of the accuracy and coverage provided by UWB is really useful for SLE training of inertial PDR systems, especially in comparison to the use of the average step length as ground truth.

The main advantage of wrist-worn inertial PDR systems over systems mounted on other parts of the body is the comfort and convenience offered by this body location to the users. At the same time, this comfort must be accompanied by a position estimation accuracy that, although a priori worse than that of systems in other parts of the body, can offer a good tradeoff. However, the evaluations available in the literature did not provide a clear picture of the performance of this type of systems. For this reason, and in line with the *specific objective 3*, the Chapter 7 presents the results obtained by the implementation of a wrist-worn system described in the literature during two evaluation processes. The first one corresponds to the IPIN Indoor Localization Competition 2016 held during that year's IPIN conference, whose main characteristic is its challenging evaluation paths. In order to participate, the PDR system had to be extended to provide 2.5D positioning. The second evaluation stage focused on the comparison of different inertial pedestrian navigation systems simultaneously carried on the wrist, pocket and foot, and evaluated for several users. In this way, an attempt was made to obtain a broader vision than that obtained in the competition, since in that competition each system was evaluated independently and by a single user, who was also different for each system. The results of both evaluation stages show that, although the wrist-worn system implemented achieves worse performance than other types of systems, especially foot-mounted INS systems, the distance is not excessive and has even managed to outperform systems that, a priori, should be more accurate. Specifically, the results obtained in the competition show that, once the error of using magnetometers in indoor environments has been corrected, the estimate of the trajectory obtained is quite acceptable. In the second evaluation, however, two of the current weaknesses of the wrist-worn system became more visible: the detection of false positive steps and the difficulty of offering similar performances for different users, both with regard to the detection of steps and the estimation of their length. These are the main conclusions of this evaluation chapter and will undoubtedly set the direction for future work.

The accumulation of heading drift is a problem that affects all localization systems that use gyroscopes to estimate the direction of travel. With the aim of trying to mitigate this problem, the *specific objective 4* was defined for trying to adapt the iHDE heading reduction method so that can be used in PDR systems. That adaptation was presented and tested in Chapter 8. The advantage of this type of heuristic methods is that they need to know very little information about the building. This facilitates its availability compared to other map-matching-based solutions, for which it is not always easy to obtain such information due to security, privacy or information formatting problems. The results of the experimentation carried out show that the adaptation maintains the same corrective characteristics as the original iHDE and that it fits perfectly into a wrist-worn inertial PDR system.

The main goal defined at the beginning of this thesis was to contribute to a better understanding of the wrist-worn inertial PDR systems and to try to provide proposals to improve their performance. Through the specific objectives that were defined, these are the main contributions:

- An in-depth analysis of the characteristics of the signals coming from different types of wrist-worn sensors and their variability with respect to factors such as the type of carrying mode, the walking speed or the different users.

- A complete and systematic review of the SLE methods based on inertial sensors was presented. The lack of public datasets and a standard methodology for testing and evaluation were identified as important reasons that keep this field is still in the research phase.

- The use of UWB technology as a source of step length ground truth has been proposed and evaluated. The balance between accuracy and coverage offered by UWB has been identified as useful for calibrating and validating PDR systems.

- The performance of a wrist-worn inertial PDR system has been evaluated in realistic scenarios and compared to other state-of-the-art inertial pedestrian navigation systems.

- A heading drift reduction method originally designed for foot-mounted INS systems has been adapted for PDR systems, obtaining a reduction in the heading drift error.

After carrying out the tasks associated with this thesis, the main conclusion that has been drawn is that the wrist-worn inertial PDR system is an option that is still considered to have great potential to be a fundamental part of seamless pedestrian localization systems. Clearly, the further away the inertial sensors are from the feet, the more complicated it is to design robust PDR systems as it increases the possibility of spurious signals and motions uncoupled to the walking. However, the results obtained throughout the thesis indicate that the distance, in terms of estimation accuracy, with respect to systems in other parts of the body is not too great and, furthermore, there is still room for improvement. The most important lines of future work are presented in the next section.

9.2 Future Research Work

In the specific field of wrist-worn inertial PDR systems, two main problems have been identified which should be addressed first:

- More robust SD methods: The arms are used for many activities that can be performed both when the person is still and when walking. These situations generate signal shapes that can make the SD over-count (false positive) or miss (false negative) steps, significantly reducing the accuracy of position estimation. Designing SD methods that offer better performance in these scenarios is key to developing wrist-worn inertial PDR systems that can be useful in real scenarios. Otherwise, they will always be very limited by this problem. Furthermore, the resolution of this problem is interesting for applications other than positioning, such as sport activity monitoring, energy consumption assessment, or prediction of human health status.

- User calibration: Even when the user moves the arms in an expected way, it has been observed that the step patterns vary considerably due to factors such as different users, the pose of the arm or the walking speed. This indicates the need to design highly adaptive algorithms for all PDR blocks and the definition of calibration processes that help to adjust those algorithms to each user characteristics.

For the resolution of these problems and, in general, of any related to wrist-worn systems, a possible source of further improvement may come from making use of the mechanical structure nature of the human body. Since the sensor is on a fixed and known position of that structure, which also can be known and modeled, this information may be useful to design new detection and estimation algorithms.

Finally, a general problem for all positioning systems based on DR is the lack of public available datasets and standard methodologies that guide the testing and evaluation. Such methodologies should be specific to the characteristics of DR-based systems, for example, taking into account the effect of the trajectory on error metrics or considering testing and evaluation at both the system and PDR block levels. In addition, new experimentation procedures and evaluation metrics should be define in order to provide a performance description of the tested system so that it would be possible to predict with some confidence the performance of a system in new scenario. This kind of actions helps a research area to move forward reliably and to turn research prototypes into commercial products.

9.3 Publications

This section presents the different research works of this thesis that has been published in international journals and conferences.

International Journals

- L. E. Díez, A. Bahillo, J. Otegui, and T. Otim, "Suitability Analysis of Wrist-Worn Sensors for Implementing Pedestrian Dead Reckoning Systems," *IEEE Sensors Journal*, vol. 18, no. 12, pp. 5098–5114, May 2018.
- L. E. Díez, A. Bahillo, J. Otegui, and T. Otim, "Step Length Estimation Methods Based on Inertial Sensors: A Review," *IEEE Sensors Journal*, vol. 18, no. 17, pp. 6908–6926, Sep. 2018.

International Conferences

- L. E. Díez, A. Bahillo, A. D. Masegosa, A. Perallos, L. Azpilicueta, F. Falcone, J. J. Astrain, and J. Villadangos, "Signal processing requirements for step detection using wrist-worn IMU," in *2015 International Conference on Electromagnetics in Advanced Applications (ICEAA)*, Turin, Italy, Sep. 2015, pp. 1032–1035.
- L. E. Díez, A. Bahillo, S. Bataineh, A. D. Masegosa, and A. Perallos, "Enhancing improved heuristic drift elimination for step-and-heading based pedestrian dead-reckoning systems," in *2016 38th Annual International Conference of the IEEE Engineering in Medicine and Biology Society (EMBC)*, Aug. 2016, pp. 4415–4418.
- L. E. Diez, A. Bahillo, S. Bataineh, A. D. Masegosa, and A. Perallos, "Enhancing Improved Heuristic Drift Elimination for Wrist-Worn PDR Systems in Buildings," in *2016 IEEE 84th Vehicular Technology Conference (VTC-Fall)*, Montreal, Canada, Sep. 2016, pp. 1–5.
- D. Bousdar, L. E. Díez, and E. Munoz Diaz, "Performance comparison of wearable-based pedestrian navigation systems in large areas," in *2017 International Conference on Indoor Positioning and Indoor Navigation (IPIN)*, Sapporo, Japan, Sep. 2017, pp. 1–7.

- L. E. Díez, A. Bahillo, J. Otegui, and T. Otim, "Step Length Estimation using UWB Technology: A Preliminary Evaluation," in *2018 International Conference on Indoor Positioning and Indoor Navigation (IPIN)*, Nantes, France, Sep. 2018.

Other publications related to localization techniques and systems, belonging to works carried out in the research group to which I belong, are also presented below:

Other Publications

- A. Bahillo, L. E. Díez, A. Perallos, and F. Falcone, "Enabling Seamless Positioning for Smartphones," in *XXX Simposium Nacional de la Unión Científica Internacional de Radio, URSI 2015*, Pamplona, Spain, Sep. 2015.
- S. Bataineh, A. Bahillo, L. E. Díez, E. Onieva, and I. Bataineh, "Conditional Random Field-Based Offline Map Matching for Indoor Environments," *Sensors*, vol. 16, no. 8, p. 1302, Aug. 2016.
- A. Bahillo, L. E. Díez, and A. Arambarri, "BLUE Care: A Cooperative Location Network for Handicapped Persons," *Procedia Engineering*, vol. 178, no. Supplement C, pp. 67–75, 2017.
- S. Bataineh, A. Bahillo, and L. E. Díez, "Using of behavioral information for enhancing Conditional Random Field-based map matching," in *2017 European Navigation Conference (ENC)*. Lausanne, Switzerland, May 2017, pp. 206–212.
- J. Otegui, A. Bahillo, I. Lopetegi, and L. E. Díez, "A Survey of Train Positioning Solutions," *IEEE Sensors Journal*, vol. 17, no. 20, pp. 6788–6797, Oct. 2017.
- J. Otegui, A. Bahillo, I. Lopetegi, and L. E. Díez, "Evaluation of Experimental GNSS and 10-DOF MEMS IMU Measurements for Train Positioning," *IEEE Transactions on Instrumentation and Measurement*, pp. 1–11, Jun. 2018.

Bibliography

[1] "Horizon 2020 - European Commission." [Online]. Available: https://ec.europa.eu/programmes/horizon2020/

[2] G. D. Abowd, A. K. Dey, P. J. Brown, N. Davies, M. Smith, and P. Steggles, "Towards a Better Understanding of Context and Context-Awareness," in *Proceedings of the 1st International Symposium on Handheld and Ubiquitous Computing (HUC '99).* Karlsruhe, Germany: Springer-Verlag, Sep. 1999, pp. 304–307. [Online]. Available: https://www.cc.gatech.edu/fce/contexttoolkit/chiws/Dey.pdf

[3] European GNSS Agency, "GNSS Market Report, Issue 5," Tech. Rep., 2017. [Online]. Available: https://www.gsa.europa.eu/system/files/reports/gnss_mr_2017.pdf

[4] United Nations, *The World's Cities in 2016: Data Booklet.* New York, NY, USA: United Nations, Department of Economic and Social Affairs, Population Division, 2016. [Online]. Available: http://www.un.org/en/development/desa/population/publications/pdf/urbanization/the_worlds_cities_in_2016_data_booklet.pdf

[5] N. E. Klepeis, W. C. Nelson, W. R. Ott, J. P. Robinson, A. M. Tsang, P. Switzer, J. V. Behar, S. C. Hern, and W. H. Engelmann, "The National Human Activity Pattern Survey (NHAPS): A resource for assessing exposure to environmental pollutants," *Journal of Exposure Analysis and Environmental Epidemiology*, vol. 11, no. 3, pp. 231–252, Jun. 2001.

[6] B. L. Diffey, “An overview analysis of the time people spend outdoors,” *The British Journal of Dermatology*, vol. 164, no. 4, pp. 848–854, Apr. 2011.

[7] Z. Yang, C. Wu, Z. Zhou, X. Zhang, X. Wang, and Y. Liu, “Mobility Increases Localizability: A Survey on Wireless Indoor Localization Using Inertial Sensors,” *ACM Computing Surveys*, vol. 47, no. 3, pp. 54:1–54:34, Apr. 2015.

[8] D. Dardari, P. Closas, and P. M. Djurić, “Indoor Tracking: Theory, Methods, and Technologies,” *IEEE Transactions on Vehicular Technology*, vol. 64, no. 4, pp. 1263–1278, Apr. 2015.

[9] H. S. Maghdid, I. A. Lami, K. Z. Ghafoor, and J. Lloret, “Seamless Outdoors-Indoors Localization Solutions on Smartphones: Implementation and Challenges,” *ACM Computing Surveys*, vol. 48, no. 4, pp. 53:1–53:34, Feb. 2016.

[10] P. Davidson and R. Piche, “A Survey of Selected Indoor Positioning Methods for Smartphones,” *IEEE Communications Surveys & Tutorials*, vol. 19, no. 2, pp. 1347–1370, May 2017.

[11] R. F. Brena, J. P. García-Vázquez, C. E. Galván-Tejada, D. Muñoz-Rodriguez, C. Vargas-Rosales, and J. Fangmeyer, “Evolution of Indoor Positioning Technologies: A Survey,” *Journal of Sensors*, vol. 2017, pp. 1–21, 2017.

[12] A. F. G. Ferreira, D. M. A. Fernandes, A. P. Catarino, and J. L. Monteiro, “Localization and Positioning Systems for Emergency Responders: A Survey,” *IEEE Communications Surveys Tutorials*, vol. 19, no. 4, pp. 2836–2870, May 2017.

[13] D. Lymberopoulos, J. Liu, X. Yang, R. R. Choudhury, V. Handziski, and S. Sen, “A Realistic Evaluation and Comparison of Indoor Location Technologies: Experiences and Lessons Learned,” in *Proceedings of the 14th International Conference on Information Processing in Sensor Networks*, ser. IPSN ’15. New York, USA: ACM, Apr. 2015, pp. 178–189.

[14] D. Lymberopoulos and J. Liu, "The Microsoft Indoor Localization Competition: Experiences and Lessons Learned," *IEEE Signal Processing Magazine*, vol. 34, no. 5, pp. 125–140, Sep. 2017.

[15] D. H. Titterton and J. L. Weston, *Strapdown Inertial Navigation Technology*. Stevenage: Institution of Electrical Engineers, 2004.

[16] P. D. Groves, "Navigation using inertial sensors [Tutorial]," *IEEE Aerospace and Electronic Systems Magazine*, vol. 30, no. 2, pp. 42–69, Feb. 2015.

[17] ——, *Principles of GNSS, Inertial, and Multisensor Integrated Navigation Systems*. Artech House, 2008.

[18] E. Foxlin, "Pedestrian tracking with shoe-mounted inertial sensors," *Computer Graphics and Applications, IEEE*, vol. 25, no. 6, pp. 38–46, Nov. 2005.

[19] A. R. Jiménez, F. Seco, J. C. Prieto, and J. Guevara, "Indoor Pedestrian Navigation using an INS/EKF framework for Yaw Drift Reduction and a Foot-mounted IMU," in *Proceeding of the 7th Workshop on Positioning Navigation and Communication (WPNC'10)*, Dresden, Germany, Mar. 2010, pp. 135–143. [Online]. Available: http://digital.csic.es/bitstream/10261/32215/1/Indoor.pdf

[20] R. Harle, "A Survey of Indoor Inertial Positioning Systems for Pedestrians," *IEEE Communications Surveys & Tutorials*, vol. 15, no. 3, pp. 1281–1293, Jul. 2013.

[21] F. de Arriba-Pérez, M. Caeiro-Rodríguez, and J. M. Santos-Gago, "Collection and Processing of Data from Wrist Wearable Devices in Heterogeneous and Multiple-User Scenarios," *Sensors*, vol. 16, no. 9, p. 1538, Sep. 2016. [Online]. Available: http://www.mdpi.com/1424-8220/16/9/1538

[22] K. Van Laerhoven, M. Borazio, and J. H. Burdinski, "Wear is Your Mobile? Investigating Phone Carrying and Use Habits with a Wearable Device," *Frontiers in ICT*, vol. 2, pp. 1–10, May 2015. [Online]. Available: http://journal.frontiersin.org/article/10.3389/fict.2015.00010/abstract

[23] F. Ichikawa, J. Chipchase, and R. Grignani, “Where’s The Phone? A Study of Mobile Phone Location in Public Spaces,” in *2005 2nd Asia Pacific Conference on Mobile Technology, Applications and Systems*, Nov. 2005, pp. 1–8.

[24] “Wearable Technology Database | Vandrico Inc,” accessed: June 11, 2018. [Online]. Available: http://vandrico.com/wearables/

[25] M. Hassani, M. Kivimaki, A. Elbaz, M. Shipley, A. Singh-Manoux, and S. Sabia, “Non-Consent to a Wrist-Worn Accelerometer in Older Adults: The Role of Socio-Demographic, Behavioural and Health Factors,” *PLOS ONE*, vol. 9, no. 10, Oct. 2014. [Online]. Available: http://journals.plos.org/plosone/article?id=10.1371/journal.pone.0110816

[26] A. Kamišalić, I. Fister, M. Turkanović, and S. Karakatič, “Sensors and Functionalities of Non-Invasive Wrist-Wearable Devices: A Review,” *Sensors*, vol. 18, no. 6, p. 1714, May 2018. [Online]. Available: http://www.mdpi.com/1424-8220/18/6/1714

[27] B. Mortazavi, E. Nemati, K. VanderWall, H. G. Flores-Rodriguez, J. Y. J. Cai, J. Lucier, A. Naeim, and M. Sarrafzadeh, “Can Smartwatches Replace Smartphones for Posture Tracking?” *Sensors*, vol. 15, no. 10, pp. 26 783–26 800, Oct. 2015. [Online]. Available: http://www.mdpi.com/1424-8220/15/10/26783

[28] G. M. Weiss, J. L. Timko, C. M. Gallagher, K. Yoneda, and A. J. Schreiber, “Smartwatch-based activity recognition: A machine learning approach,” in *2016 IEEE-EMBS International Conference on Biomedical and Health Informatics (BHI)*, Las Vegas, USA, Apr. 2016, pp. 426–429.

[29] J. Hernandez, D. McDuff, and R. W. Picard, “BioWatch: Estimation of Heart and Breathing Rates from Wrist Motions,” in *Proceedings of the 9th International Conference on Pervasive Computing Technologies for Healthcare*, Brussels, Belgium, May 2015, pp. 169–176.

[30] W.-W. Kao, C.-K. Chen, and J.-S. Lin, “Step-length Estimation Using Wrist-worn Accelerometer and GPS,” in *Proceedings of the 24th International Technical Meeting of The Satellite Division of the Institute of Navigation (ION GNSS 2011)*, Portland, OR, USA, Sep. 2011, pp. 3274 – 3280.

[31] J. Qian, J. Ma, L. Xu, R. Ying, W. Yu, and P. Liu, “Investigating the use of MEMS Based Wrist-worn IMU for Pedestrian Navigation Application,” in *Proceedings of the 26th International Technical Meeting of The Satellite Division of the Institute of Navigation (ION GNSS+ 2013)*, Nashville, TN, USA, Sep. 2013, pp. 1057 – 1064.

[32] H. T. Duong and Y. S. Suh, “Walking Parameters Estimation Based on a Wrist-Mounted Inertial Sensor for a Walker User,” *IEEE Sensors Journal*, vol. 17, no. 7, pp. 2100–2108, Jan. 2017.

[33] Y. Jiang, Z. Li, and J. Wang, “PTrack: Enhancing the Applicability of Pedestrian Tracking with Wearables,” in *2017 IEEE 37th International Conference on Distributed Computing Systems (ICDCS)*, Atlanta, GA, USA, Jun. 2017, pp. 2193–2199.

[34] N. Bowditch (originally by), *American Practical Navigator*, 53rd ed. National Geospatial-Intelligence Agency, Jun. 2017.

[35] H. Bray, *You Are Here: From the Compass to GPS, the History and Future of How We Find Ourselves*. Hachette UK, Apr. 2014.

[36] M. S. Grewal, L. R. Weill, and A. P. Andrews, *Global positioning systems, inertial navigation, and integration*. New York: John Wiley, 2001.

[37] P. L. Walter, “The History of the Accelerometer,” *Sound & Vibration Magazine*, p. 9, Jan. 2007.

[38] Mautz, Rainer, “Indoor Positioning Technologies,” Habilitation Thesis, ETH Zurich, Department of Civil, Environmental and Geomatic Engineering, Institute of Geodesy and Photogrammetry, Zurich, Switzerland, 2012. [Online]. Available: http://dx.doi.org/10.3929/ethz-a-007313554

[39] F. Gustafsson and F. Gunnarsson, “Mobile positioning using wireless networks: possibilities and fundamental limitations based on available wireless network measurements,” *IEEE Signal Processing Magazine*, vol. 22, no. 4, pp. 41–53, Jul. 2005.

[40] F. Seco, A. R. Jimenez, C. Prieto, J. Roa, and K. Koutsou, “A survey of mathematical methods for indoor localization,” in *2009 IEEE International Symposium on Intelligent Signal Processing*, Aug. 2009, pp. 9–14.

[41] S. A. Zekavat and R. M. Buehrer, Eds., *Handbook of Position Location: Theory, Practice and Advances.* Hoboken, N.J: Wiley-IEEE Press, 2012.

[42] *COST Action TU1302. SaPPART White paper: Better use of Global Navigation Satellite Systems for safer and greener transport*, ser. techniques et méthodes, TMI 1. Ifsttar, 2015.

[43] M. Quinion, “World Wide Words: Dead reckoning,” Aug. 2007. [Online]. Available: http://www.worldwidewords.org/qa/qa-dea7.htm

[44] O. J. Woodman, “An introduction to inertial navigation,” Technical report, Aug. 2007.

[45] M. D. Shuster, “Survey of attitude representations,” *Journal of the Astronautical Sciences*, vol. 41, pp. 439–517, Oct. 1993.

[46] J. R. Huddle, “Trends in inertial systems technology for high accuracy AUV navigation,” in *Proceedings of the 1998 Workshop on Autonomous Underwater Vehicles (Cat. No.98CH36290)*, Aug. 1998, pp. 63–73.

[47] A. G. Ledroz, E. Pecht, D. Cramer, and M. P. Mintchev, “FOG-based navigation in downhole environment during horizontal drilling utilizing a complete inertial measurement unit: directional measurement-while-drilling surveying,” *IEEE Transactions on Instrumentation and Measurement*, vol. 54, no. 5, pp. 1997–2006, Oct. 2005.

[48] D. A. Grejner-Brzezinska, Y. Yi, and C. K. Toth, “Bridging GPS Gaps in Urban Canyons: The Benefits of ZUPTs,” *NAVIGATION: Journal of The Institute of Navigation*, vol. 48, no. 4, pp. 216–226, 2001.

[49] T. Stöckel, R. Jacksteit, M. Behrens, R. Skripitz, R. Bader, and A. Mau-Moeller, "The mental representation of the human gait in young and older adults," *Frontiers in Psychology*, vol. 6, Jul. 2015. [Online]. Available: https://www.frontiersin.org/articles/10.3389/fpsyg.2015.00943/full

[50] F. Zampella, "Localización de personas mediante sensores inerciales y su fusión con otras tecnologías," Ph.D. dissertation, Universidad de Alcalá, 2017.

[51] Q. Wang, X. Zhang, X. Chen, R. Chen, W. Chen, and Y. Chen, "A novel pedestrian dead reckoning algorithm using wearable EMG sensors to measure walking strides," in *2010 Ubiquitous Positioning Indoor Navigation and Location Based Service*, Oct. 2010, pp. 1–8.

[52] J. Saarinen, J. Suomela, S. Heikkila, M. Elomaa, and A. Halme, "Personal navigation system," in *2004 IEEE/RSJ International Conference on Intelligent Robots and Systems (IROS) (IEEE Cat. No.04CH37566)*, vol. 1, Sep. 2004, pp. 212–217 vol.1.

[53] S.-y. Yeh, K.-h. Chang, C.-i. Wu, H.-h. Chu, and J. Y.-j. Hsu, "GETA sandals: a footstep location tracking system," *Personal and Ubiquitous Computing*, vol. 11, no. 6, pp. 451–463, Aug. 2007.

[54] G. V. Prateek, R. Girisha, K. V. S. Hari, and P. Händel, "Data Fusion of Dual Foot-Mounted INS to Reduce the Systematic Heading Drift," in *Modelling and Simulation 2013 4th International Conference on Intelligent Systems*, Jan. 2013, pp. 208–213.

[55] D. Bousdar Ahmed and E. Munoz Diaz, "Loose Coupling of Wearable-Based INSs with Automatic Heading Evaluation," *Sensors*, vol. 17, no. 11, p. 2534, Nov. 2017. [Online]. Available: http://www.mdpi.com/1424-8220/17/11/2534

[56] J. Borenstein, L. Ojeda, and S. Kwanmuang, "Heuristic Reduction of Gyro Drift for Personnel Tracking Systems," *The Journal of Navigation*, vol. 62, no. 01, pp. 41–58, Jan. 2009. [Online]. Available: http://journals.cambridge.org/article_S0373463308005043

[57] O. Woodman and R. Harle, "Pedestrian localisation for indoor environments," in *Proceedings of the 10th international conference on Ubiquitous computing*. ACM, Sep. 2008, pp. 114–123. [Online]. Available: http://www.cl.cam.ac.uk/research/dtg/www/publications/public/ojw28/Main-PersonalRedist.pdf

[58] Z. Xiao, H. Wen, A. Markham, and N. Trigoni, "Lightweight map matching for indoor localisation using conditional random fields," in *Proceedings of the 13th international symposium on Information processing in sensor networks*. IEEE Press, Apr. 2014, pp. 131–142. [Online]. Available: https://www.cs.ox.ac.uk/files/6677/MapCraftPublishedIPSN14.pdf

[59] S. Bataineh, A. Bahillo, L. E. Díez, E. Onieva, and I. Bataineh, "Conditional Random Field-Based Offline Map Matching for Indoor Environments," *Sensors*, vol. 16, no. 8, p. 1302, Aug. 2016. [Online]. Available: http://www.mdpi.com/1424-8220/16/8/1302

[60] A. R. Jiménez, F. Seco, F. Zampella, J. C. Prieto, and J. Guevara, "PDR with a Foot-Mounted IMU and Ramp Detection," *Sensors*, vol. 11, no. 10, pp. 9393–9410, Sep. 2011. [Online]. Available: http://www.mdpi.com/1424-8220/11/10/9393

[61] J. Borenstein and L. Ojeda, "Heuristic Drift Elimination for Personnel Tracking Systems," *Journal of Navigation*, vol. 63, no. 04, pp. 591–606, Oct. 2010. [Online]. Available: http://www.journals.cambridge.org/abstract_S0373463310000184

[62] K. Abdulrahim, C. Hide, T. Moore, and C. Hill, "Aiding MEMS IMU with building heading for indoor pedestrian navigation," in *Ubiquitous Positioning Indoor Navigation and Location Based Service (UPINLBS), 2010*. IEEE, Oct. 2010, pp. 1–6.

[63] A. R. Jiménez, F. Seco, F. Zampella, J. C. Prieto, and J. Guevara, "Improved Heuristic Drift Elimination (iHDE) for pedestrian navigation in complex buildings," in *Indoor Positioning and Indoor Navigation (IPIN), 2011 International Conference on*, Guimaraes, Portugal, Sep. 2011, pp. 1–8.

[64] ——, “Improved heuristic drift elimination with magnetically-aided dominant directions (MiHDE) for pedestrian navigation in complex buildings,” *Journal of Location Based Services*, vol. 6, no. 3, pp. 186–210, Sep. 2012. [Online]. Available: http://oa.upm.es/21258/1/INVE_MEM_2012_144174.pdf

[65] H. Durrant-Whyte and T. Bailey, “Simultaneous localization and mapping: part I,” *IEEE Robotics Automation Magazine*, vol. 13, no. 2, pp. 99–110, Jun. 2006.

[66] R. E. Kalman, “A new approach to linear filtering and prediction problems,” *Journal of Fluids Engineering*, vol. 82, no. 1, pp. 35–45, 1960. [Online]. Available: https://www.cs.unc.edu/~welch/kalman/media/pdf/Kalman1960.pdf

[67] G. Bishop and G. Welch, “An introduction to the kalman filter,” in *Proc of SIGGRAPH, Course 8*, Los Angeles, Aug. 2001, p. 41. [Online]. Available: http://old.shahed.ac.ir/references/kalman_filter_notes.pdf

[68] S. J. Julier and J. K. Uhlmann, “A new extension of the Kalman filter to nonlinear systems,” in *Int. symp. aerospace/defense sensing, simul. and controls*, vol. 3. Orlando, FL, 1997, pp. 3–2. [Online]. Available: http://www.control.auc.dk/~tb/ESIF/julier97new.pdf

[69] Arnaud, Doucet, and Johansen, “A Tutorial on Particle Filtering and Smoothing: Fifteen years Later,” Tech. Rep., 2008. [Online]. Available: http://www.cs.ubc.ca/~arnaud/doucet_johansen_tutorialPF.pdf

[70] D. Fox, J. Hightower, L. Liao, D. Schulz, and G. Borriello, “Bayesian filtering for location estimation,” *IEEE pervasive computing*, vol. 2, no. 3, pp. 24–33, 2003.

[71] R. Mahony, T. Hamel, and J.-M. Pflimlin, “Nonlinear Complementary Filters on the Special Orthogonal Group,” *IEEE Transactions on Automatic Control*, vol. 53, no. 5, pp. 1203–1218, Jun. 2008.

[72] S. O. Madgwick, "An efficient orientation filter for inertial and inertial/magnetic sensor arrays," Tech. Rep., Apr. 2010. [Online]. Available: https://www.samba.org/tridge/UAV/madgwick_internal_report.pdf

[73] E. Munoz Diaz, F. de Ponte Müller, and J. J. García Domínguez, "Use of the Magnetic Field for Improving Gyroscopes' Biases Estimation," *Sensors*, vol. 17, no. 4, p. 832, Apr. 2017. [Online]. Available: http://www.mdpi.com/1424-8220/17/4/832

[74] "IEEE Standard for Inertial Systems Terminology," *IEEE Std 1559-2009*, pp. c1–30, Aug. 2009.

[75] H. Wymeersch, J. Lien, and M. Z. Win, "Cooperative Localization in Wireless Networks," *Proceedings of the IEEE*, vol. 97, no. 2, pp. 427–450, Feb. 2009.

[76] D. Alvarez, R. C. González, A. López, and J. C. Alvarez, "Comparison of step length estimators from weareable accelerometer devices," in *2006 International Conference of the IEEE Engineering in Medicine and Biology Society*. New York, NY, USA: IEEE, Aug. 2006, pp. 5964–5967.

[77] R. W. Levi and T. Judd, "Dead reckoning navigational system using accelerometer to measure foot impacts," U.S. Patent US5 583 776 A, Dec., 1996. [Online]. Available: http://www.google.es/patents/US5583776

[78] C. Tom Judd, "A Personal Dead Reckoning Module," in *Proceedings of the 10th International Technical Meeting of the Satellite Division of The Institute of Navigation (ION GPS 1997)*, Kansas City, MO, USA, Sep. 1997, pp. 47–51.

[79] H. Weinberg, "Using the ADXL202 in pedometer and personal navigation applications," 2002, accessed: June 11, 2018. [Online]. Available: http://www.analog.com/media/en/technical-documentation/application-notes/513772624AN602.pdf

[80] W. Zijlstra and A. L. Hof, "Assessment of spatio-temporal gait parameters from trunk accelerations during human walking," *Gait & Posture*, vol. 18, no. 2, pp. 1–10, Oct. 2003.

[81] J. Scarlett, "Enhancing the performance of pedometers using a single accelerometer," Mar. 2007, accessed: June 11, 2018. [Online]. Available: http://www.analog.com/media/en/technical-documentation/application-notes/47076299220991AN_900.pdf

[82] Q. Ladetto, "On foot navigation: continuous step calibration using both complementary recursive prediction and adaptive Kalman filtering," in *Proceedings of the 13th International Technical Meeting of the Satellite Division of The Institute of Navigation (ION GPS 2000)*, vol. 2000, Salt Lake City, UT, Sep. 2000, pp. 1735–1740.

[83] S. H. Shin, C. G. Park, J. W. Kim, H. S. Hong, and J. M. Lee, "Adaptive Step Length Estimation Algorithm Using Low-Cost MEMS Inertial Sensors," in *2007 IEEE Sensors Applications Symposium*, Feb. 2007, pp. 1–5.

[84] M. Basso, M. Galanti, G. Innocenti, and D. Miceli, "Pedestrian Dead Reckoning Based on Frequency Self-Synchronization and Body Kinematics," *IEEE Sensors Journal*, vol. 17, no. 2, pp. 534–545, Jan. 2017.

[85] J. C. Alvarez, D. Alvarez, A. López, and R. C. González, "Pedestrian Navigation Based on a Waist-Worn Inertial Sensor," *Sensors*, vol. 12, no. 8, pp. 10 536–10 549, Aug. 2012. [Online]. Available: http://www.mdpi.com/1424-8220/12/8/10536

[86] S. Beauregard, "A Helmet-Mounted Pedestrian Dead Reckoning System," in *3rd International Forum on Applied Wearable Computing 2006*, Mar. 2006, pp. 1–11.

[87] Y. Zhu, R. Zhang, W. Xia, Z. Jia, and L. Shen, "A hybrid step model and new azimuth estimation method for pedestrian dead reckoning," in *2014 Sixth International Conference on Wireless Communications and Signal Processing (WCSP)*, Oct. 2014, pp. 1–5.

[88] M. Omr, “Portable Navigation Utilizing Sensor Technologies in Wearable and Portable Devices,” Ph.D. dissertation, Queen’s University, Department of Electrical and Computer Engineering, Kingston, Ontario, Canada, Aug. 2015. [Online]. Available: http://qspace.library.queensu.ca/handle/1974/12804

[89] D. Loh, S. Zihajehzadeh, R. Hoskinson, H. Abdollahi, and E. J. Park, “Pedestrian Dead Reckoning With Smartglasses and Smartwatch,” *IEEE Sensors Journal*, vol. 16, no. 22, pp. 8132–8141, Sep. 2016.

[90] J. W. Kim, H. J. Jang, D.-H. Hwang, and C. Park, “A Step, Stride and Heading Determination for the Pedestrian Navigation System,” *Journal of Global Positioning Systems*, vol. 03, no. 1-2, pp. 273–279, Dec. 2004. [Online]. Available: http://www.scirp.org/journal/PaperInformation.aspx?PaperID=282

[91] S. Godha, G. Lachapelle, and M. E. Cannon, “Integrated GPS/INS system for pedestrian navigation in a signal degraded environment,” in *ION GNSS*, vol. 2006, Sep. 2006.

[92] A. R. Jimenez, F. Seco, C. Prieto, and J. Guevara, “A comparison of pedestrian dead-reckoning algorithms using a low-cost MEMS IMU,” in *Intelligent Signal Processing, 2009. WISP 2009. IEEE International Symposium on*. IEEE, Aug. 2009, pp. 37–42.

[93] D. Gusenbauer, C. Isert, and J. Krosche, “Self-contained indoor positioning on off-the-shelf mobile devices,” in *Indoor Positioning and Indoor Navigation (IPIN), 2010 International Conference on*. Zürich, Switzerland: IEEE, Sep. 2010, pp. 1–9.

[94] W. Kang and Y. Han, “SmartPDR: Smartphone-Based Pedestrian Dead Reckoning for Indoor Localization,” *IEEE Sensors Journal*, vol. 15, no. 5, pp. 2906–2916, May 2015.

[95] I. Bylemans, M. Weyn, and M. Klepal, “Mobile Phone-Based Displacement Estimation for Opportunistic Localisation Systems,” in *2009 Third International Conference on Mobile Ubiquitous Computing, Systems, Services and Technologies*, Oct. 2009, pp. 113–118.

[96] U. Steinhoff and B. Schiele, “Dead reckoning from the pocket - An experimental study,” in *2010 IEEE International Conference on Pervasive Computing and Communications (PerCom)*, Mar. 2010, pp. 162–170.

[97] E. Diaz, “Inertial Pocket Navigation System: Unaided 3d Positioning,” *Sensors*, vol. 15, no. 4, pp. 9156–9178, Apr. 2015. [Online]. Available: http://www.mdpi.com/1424-8220/15/4/9156/

[98] E. M. Diaz, “Inertial Pocket Navigation System for Pedestrians,” Ph.D. dissertation, Universidad de Alcalá, Department of Electronics, Alcalá de Henares, Spain, Jul. 2016.

[99] A. Mikov, A. Moschevikin, A. Fedorov, and A. Sikora, “A localization system using inertial measurement units from wireless commercial hand-held devices,” in *International Conference on Indoor Positioning and Indoor Navigation*, Oct. 2013, pp. 1–7.

[100] M. Khedr and N. El-Sheimy, “A Smartphone Step Counter Using IMU and Magnetometer for Navigation and Health Monitoring Applications,” *Sensors*, vol. 17, no. 11, p. 2573, Nov. 2017. [Online]. Available: http://www.mdpi.com/1424-8220/17/11/2573

[101] M. Susi, V. Renaudin, and G. Lachapelle, “Motion Mode Recognition and Step Detection Algorithms for Mobile Phone Users,” *Sensors*, vol. 13, no. 2, pp. 1539–1562, Jan. 2013. [Online]. Available: http://www.mdpi.com/1424-8220/13/2/1539/

[102] Z. Xiao, H. Wen, A. Markham, and N. Trigoni, “Robust pedestrian dead reckoning (R-PDR) for arbitrary mobile device placement,” in *International Conference on Indoor Positioning and Indoor Navigation*, vol. 27, Oct. 2014, p. 30.

[103] Q. Tian, Z. Salcic, K. I. K. Wang, and Y. Pan, "A Multi-Mode Dead Reckoning System for Pedestrian Tracking Using Smartphones," *IEEE Sensors Journal*, vol. 16, no. 7, pp. 2079–2093, Apr. 2016.

[104] S. H. Shin, M. S. Lee, C. G. Park, and H. S. Hong, "Pedestrian dead reckoning system with phone location awareness algorithm," in *IEEE/ION Position, Location and Navigation Symposium*, May 2010, pp. 97–101.

[105] J. Qian, L. Pei, J. Ma, R. Ying, and P. Liu, "Vector Graph Assisted Pedestrian Dead Reckoning Using an Unconstrained Smartphone," *Sensors*, vol. 15, no. 3, pp. 5032–5057, Mar. 2015. [Online]. Available: http://www.mdpi.com/1424-8220/15/3/5032

[106] M. Elhoushi, J. Georgy, A. Noureldin, and M. J. Korenberg, "Motion Mode Recognition for Indoor Pedestrian Navigation Using Portable Devices," *IEEE Transactions on Instrumentation and Measurement*, vol. 65, no. 1, pp. 208–221, Jan. 2016.

[107] V. Renaudin, V. Demeule, and M. Ortiz, "Adaptative pedestrian displacement estimation with a smartphone," in *Indoor Positioning and Indoor Navigation (IPIN), 2013 International Conference on*. IEEE, Oct. 2013, pp. 1–9.

[108] A. Correa, E. Munoz Diaz, D. Bousdar Ahmed, A. Morell, and J. Lopez Vicario, "Advanced Pedestrian Positioning System to Smartphones and Smartwatches," *Sensors*, vol. 16, no. 11, p. 1903, Nov. 2016. [Online]. Available: http://www.mdpi.com/1424-8220/16/11/1903

[109] J. Qian, J. Ma, R. Ying, P. Liu, and L. Pei, "An improved indoor localization method using smartphone inertial sensors," in *Indoor Positioning and Indoor Navigation (IPIN), 2013 International Conference on*. IEEE, Oct. 2013, pp. 1–7.

[110] J. Qian, J. Ma, R. Ying, and P. Liu, "RPNOS: Reliable Pedestrian Navigation on a Smartphone," in *Proceedings of the International Conference on Geo-Informatics in Resource Management and Sustainable Ecosystem (GRMSE)*,

ser. Communications in Computer and Information Science. Wuhan, China: Springer Berlin Heidelberg, Nov. 2013, pp. 188–199.

[111] "LOPSI-CAR-CSIC-UPM research group." [Online]. Available: http://lopsi.weebly.com

[112] A. Brajdic and R. Harle, "Walk Detection and Step Counting on Unconstrained Smartphones," in *Proceedings of the 2013 ACM International Joint Conference on Pervasive and Ubiquitous Computing*, ser. UbiComp '13. New York, NY, USA: ACM, Sep. 2013, pp. 225–234.

[113] F. Li, C. Zhao, G. Ding, J. Gong, C. Liu, and F. Zhao, "A reliable and accurate indoor localization method using phone inertial sensors," in *Proceedings of the 2012 ACM Conference on Ubiquitous Computing*. ACM, Sep. 2012, pp. 421–430.

[114] S. Kammoun, J.-B. Pothin, and J.-C. Cousin, "An efficient fuzzy logic step detection algorithm for unconstrained smartphones," in *Personal, Indoor, and Mobile Radio Communications (PIMRC), 2015 IEEE 26th Annual International Symposium on*. IEEE, Sep. 2015, pp. 2110–2114.

[115] Y. R. Modi, "Wrist Pedometer Step Detection," U.S. Patent US20 140 074 431 A1, Mar., 2014, u.S. Classification 702/160; International Classification G06F15/00; Cooperative Classification G01C22/006. [Online]. Available: http://www.google.ch/patents/US20140074431

[116] H. Zhang, Weizheng Yuan, Qiang Shen, Tai Li, and Honglong Chang, "A Handheld Inertial Pedestrian Navigation System With Accurate Step Modes and Device Poses Recognition," *IEEE Sensors Journal*, vol. 15, no. 3, pp. 1421–1429, Mar. 2015.

[117] H.-h. Lee, S. Choi, and M.-j. Lee, "Step Detection Robust against the Dynamics of Smartphones," *Sensors*, vol. 15, no. 10, pp. 27 230–27 250, Oct. 2015. [Online]. Available: http://www.mdpi.com/1424-8220/15/10/27230/

[118] Y. Cho, H. Cho, and C. M. Kyung, "Design and Implementation of Practical Step Detection Algorithm for Wrist-Worn Devices," *IEEE Sensors Journal*, vol. 16, no. 21, pp. 7720–7730, Nov. 2016.

[119] Z. Xiao, H. Wen, A. Markham, and N. Trigoni, "Robust Indoor Positioning With Lifelong Learning," *IEEE Journal on Selected Areas in Communications*, vol. 33, no. 11, pp. 2287–2301, Nov. 2015.

[120] W. Zijlstra and A. L. Hof, "Displacement of the pelvis during human walking: experimental data and model predictions," *Gait & Posture*, vol. 6, no. 3, pp. 249–262, Dec. 1997.

[121] J. E. Bertram and A. Ruina, "Multiple Walking Speed–frequency Relations are Predicted by Constrained Optimization," *Journal of Theoretical Biology*, vol. 209, no. 4, pp. 445–453, Feb. 2001.

[122] M. Omr, J. Georgy, and A. Noureldin, "Using multiple portable/wearable devices for enhanced misalignment estimation in portable navigation," *GPS Solutions*, vol. 21, no. 2, pp. 393–404, Apr. 2017. [Online]. Available: https://link.springer.com/article/10.1007/s10291-016-0531-3

[123] T. Michel, H. Fourati, P. Genevès, and N. Layaïda, "A Comparative Analysis of Attitude Estimation for Pedestrian Navigation with Smartphones," in *Indoor Positioning and Indoor Navigation (IPIN), 2015 International Conference on*, vol. 2015 International Conference on Indoor Positioning and Indoor Navigation, Oct. 2015, p. 10. [Online]. Available: https://hal.inria.fr/hal-01194811/document

[124] P. Meyns, S. M. Bruijn, and J. Duysens, "The how and why of arm swing during human walking," *Gait & Posture*, vol. 38, no. 4, pp. 555–562, Sep. 2013.

[125] A. Mirelman, H. Bernad-Elazari, T. Nobel, A. Thaler, A. Peruzzi, M. Plotnik, N. Giladi, and J. M. Hausdorff, "Effects of Aging on Arm Swing during Gait: The Role of Gait Speed and Dual Tasking," *PLOS ONE*, vol. 10, no. 8, p. e0136043, Aug. 2015. [Online]. Available: http://journals.plos.org/plosone/article?id=10.1371/journal.pone.0136043

[126] I. Carpinella, P. Crenna, M. Rabuffetti, and M. Ferrarin, “Coordination between upper- and lower-limb movements is different during overground and treadmill walking,” *European Journal of Applied Physiology*, vol. 108, no. 1, pp. 71–82, Jan. 2010. [Online]. Available: http://link.springer.com/article/10.1007/s00421-009-1168-5

[127] Edoarado, “Anatomical Planes and Axis,” Nov. 2011. [Online]. Available: https://commons.wikimedia.org/wiki/File:Anatomical_Planes-en.svg

[128] A. Martinelli, H. Gao, P. D. Groves, and S. Morosi, “Probabilistic Context-aware Step Length Estimation for Pedestrian Dead Reckoning,” *IEEE Sensors Journal*, vol. 18, no. 4, pp. 1600–1611, Feb. 2018.

[129] BOSCH, “BMP180 Digital Pressure Sensor,” May 2015. [Online]. Available: https://ae-bst.resource.bosch.com/media/_tech/media/datasheets/BST-BMP180-DS000-121.pdf

[130] Infineon, “DPS310 - Digital Pressure Sensor,” Sep. 2016, accessed: June 11, 2018. [Online]. Available: https://www.infineon.com/dgdl/Infineon-DPS310-DS-v01_00-EN.pdf?fileId=5546d462576f34750157750826c42242

[131] L. E. Díez, A. Bahillo, A. D. Masegosa, A. Perallos, L. Azpilicueta, F. Falcone, J. J. Astrain, and J. Villadangos, “Signal processing requirements for step detection using wrist-worn IMU,” in *2015 International Conference on Electromagnetics in Advanced Applications (ICEAA)*, Turin, Italy, Sep. 2015, pp. 1032–1035.

[132] V. Renaudin, M. Susi, and G. Lachapelle, “Step Length Estimation Using Handheld Inertial Sensors,” *Sensors*, vol. 12, no. 7, pp. 8507–8525, Jun. 2012. [Online]. Available: http://www.mdpi.com/1424-8220/12/7/8507

[133] A. Köse, A. Cereatti, and U. Della Croce, “Bilateral step length estimation using a single inertial measurement unit attached to the pelvis,” *Journal of Neuroengineering and Rehabilitation*, vol. 9, p. 9, Feb. 2012.

[134] S. Yang and Q. Li, “Inertial Sensor-Based Methods in Walking Speed Estimation: A Systematic Review,” *Sensors*, vol. 12, no. 5, pp. 6102–6116, May 2012. [Online]. Available: http://www.mdpi.com/1424-8220/12/5/6102

[135] F. Huxham, J. Gong, R. Baker, M. Morris, and R. Iansek, “Defining spatial parameters for non-linear walking,” *Gait & Posture*, vol. 23, no. 2, pp. 159–163, Feb. 2006.

[136] J. Hannink, T. Kautz, C. F. Pasluosta, J. Barth, S. Schülein, K. G. Gaßmann, J. Klucken, and B. M. Eskofier, “Mobile Stride Length Estimation With Deep Convolutional Neural Networks,” *IEEE Journal of Biomedical and Health Informatics*, vol. 22, no. 2, pp. 354–362, Mar. 2018.

[137] S. Miyazaki, “Long-term unrestrained measurement of stride length and walking velocity utilizing a piezoelectric gyroscope,” *IEEE Transactions on Biomedical Engineering*, vol. 44, no. 8, pp. 753–759, Aug. 1997.

[138] S.-W. Lee and K. Mase, “Recognition of walking behaviors for pedestrian navigation,” in *Proceedings of the 2001 IEEE International Conference on Control Applications, 2001. (CCA ’01)*, Mexico City, Mexico, Sep. 2001, pp. 1152–1155.

[139] R. C. Gonzalez, D. Alvarez, A. M. Lopez, and J. C. Alvarez, “Modified Pendulum Model for Mean Step Length Estimation,” in *2007 29th Annual International Conference of the IEEE Engineering in Medicine and Biology Society*, Aug. 2007, pp. 1371–1374.

[140] Y. Song, S. Shin, S. Kim, D. Lee, and K. H. Lee, “Speed Estimation From a Tri-axial Accelerometer Using Neural Networks,” in *2007 29th Annual International Conference of the IEEE Engineering in Medicine and Biology Society*, Aug. 2007, pp. 3224–3227.

[141] A. M. Lopez, D. Alvarez, R. C. Gonzalez, and J. C. Alvarez, “Estimation of displacement along level straight paths through body center of mass accelerations,” in *2007 3rd IET International Conference on Intelligent Environments*, Ulm, Germany, Sep. 2007, pp. 354–360.

[142] Z. Sun, X. Mao, W. Tian, and X. Zhang, “Activity classification and dead reckoning for pedestrian navigation with wearable sensors,” *Measurement Science and Technology*, vol. 20, no. 1, p. 015203, Nov. 2008.

[143] H. Vathsangam, A. Emken, D. Spruijt-Metz, and G. S. Sukhatme, “Toward free-living walking speed estimation using Gaussian Process-based Regression with on-body accelerometers and gyroscopes,” in *2010 4th International Conference on Pervasive Computing Technologies for Healthcare*, Mar. 2010, pp. 1–8.

[144] Q. Li, M. Young, V. Naing, and J. M. Donelan, “Walking speed estimation using a shank-mounted inertial measurement unit,” *Journal of Biomechanics*, vol. 43, no. 8, pp. 1640–1643, May 2010.

[145] S. Yang and Q. Li, “Ambulatory walking speed estimation under different step lengths and frequencies,” in *2010 IEEE/ASME International Conference on Advanced Intelligent Mechatronics*, Jul. 2010, pp. 658–663.

[146] J. Jahn, U. Batzer, J. Seitz, L. Patino-Studencka, and J. Gutiérrez Boronat, “Comparison and evaluation of acceleration based step length estimators for handheld devices,” in *Indoor Positioning and Indoor Navigation (IPIN), 2010 International Conference on*. IEEE, Sep. 2010, pp. 1–6.

[147] S. H. Shin and C. G. Park, “Adaptive step length estimation algorithm using optimal parameters and movement status awareness,” *Medical Engineering & Physics*, vol. 33, no. 9, pp. 1064–1071, Nov. 2011.

[148] J.-g. Park, A. Patel, D. Curtis, S. Teller, and J. Ledlie, “Online Pose Classification and Walking Speed Estimation Using Handheld Devices,” in *Proceedings of the 2012 ACM Conference on Ubiquitous Computing*, ser. UbiComp ’12. New York, NY, USA: ACM, Sep. 2012, pp. 113–122. [Online]. Available: http://doi.acm.org/10.1145/2370216.2370235

[149] J. S. Hu, K. C. Sun, and C. Y. Cheng, “A Kinematic Human-Walking Model for the Normal-Gait-Speed Estimation Using Tri-Axial Acceleration Signals at Waist Location,” *IEEE Transactions on Biomedical Engineering*, vol. 60, no. 8, pp. 2271–2279, Aug. 2013.

[150] A. Wahdan, M. Omr, J. Georgy, and A. Noureldin, "Varying Step Length Estimation Using Nonlinear System Identification," in *Proceedings of the 26th International Technical Meeting of The Satellite Division of the Institute of Navigation (ION GNSS+ 2013)*, Nashville, Tennessee, Sep. 2013.

[151] J. Qian, L. Pei, D. Zou, K. Qian, and P. Liu, "Optical flow based step length estimation for indoor pedestrian navigation on a smartphone," in *Position, Location and Navigation Symposium - PLANS 2014, 2014 IEEE/ION*, May 2014, pp. 205–211.

[152] E. M. Diaz and A. L. M. Gonzalez, "Step detector and step length estimator for an inertial pocket navigation system," in *Indoor Positioning and Indoor Navigation (IPIN), 2014 International Conference on*. IEEE, Oct. 2014, pp. 105–110.

[153] M. Bertschi, P. Celka, R. Delgado-Gonzalo, M. Lemay, E. M. Calvo, O. Grossenbacher, and P. Renevey, "Accurate walking and running speed estimation using wrist inertial data," in *2015 37th Annual International Conference of the IEEE Engineering in Medicine and Biology Society (EMBC)*, Aug. 2015, pp. 8083–8086.

[154] C. Li, J. Zheng, Z. Jiang, X. Liu, Y. Yang, and B. Zhang, "A Novel Fuzzy Pedestrian Dead Reckoning System for Indoor Positioning Using Smartphone," in *Vehicular Technology Conference (VTC Fall), 2015 IEEE 82nd*, Sep. 2015, pp. 1–5.

[155] S. Yang, H. Zhu, G. Xue, and M. Li, "DiSen: Ranging Indoor Casual Walks with Smartphones," in *2015 11th International Conference on Mobile Ad-hoc and Sensor Networks (MSN)*, Dec. 2015, pp. 178–185.

[156] Y.-C. Lai, C.-C. Chang, C.-M. Tsai, S.-C. Huang, and K.-W. Chiang, "A Knowledge-Based Step Length Estimation Method Based on Fuzzy Logic and Multi-Sensor Fusion Algorithms for a Pedestrian Dead Reckoning System," *ISPRS International Journal of Geo-Information*, vol. 5, no. 5, p. 70, May 2016. [Online]. Available: http://www.mdpi.com/2220-9964/5/5/70

[157] Y. S. Suh, E. Nemati, and M. Sarrafzadeh, “Kalman-Filter-Based Walking Distance Estimation for a Smart-Watch,” in *2016 IEEE First International Conference on Connected Health: Applications, Systems and Engineering Technologies (CHASE)*, Jun. 2016, pp. 150–156.

[158] S. Zihajehzadeh and E. J. Park, “Experimental evaluation of regression model-based walking speed estimation using lower body-mounted IMU,” in *2016 38th Annual International Conference of the IEEE Engineering in Medicine and Biology Society (EMBC)*, Aug. 2016, pp. 243–246.

[159] ——, “Regression Model-Based Walking Speed Estimation Using Wrist-Worn Inertial Sensor,” *PLOS ONE*, vol. 11, no. 10, Oct. 2016. [Online]. Available: http://journals.plos.org/plosone/article?id=10.1371/journal.pone.0165211

[160] T. N. Do, R. Liu, C. Yuen, M. Zhang, and U. X. Tan, “Personal Dead Reckoning Using IMU Mounted on Upper Torso and Inverted Pendulum Model,” *IEEE Sensors Journal*, vol. 16, no. 21, pp. 7600–7608, Nov. 2016.

[161] S. Zihajehzadeh and E. J. Park, “A Gaussian process regression model for walking speed estimation using a head-worn IMU,” in *2017 39th Annual International Conference of the IEEE Engineering in Medicine and Biology Society (EMBC)*, Jul. 2017, pp. 2345–2348.

[162] B. Fasel, C. Duc, F. Dadashi, F. Bardyn, M. Savary, P.-A. Farine, and K. Aminian, “A wrist sensor and algorithm to determine instantaneous walking cadence and speed in daily life walking,” *Medical & Biological Engineering & Computing*, vol. 55, no. 10, pp. 1773–1785, Oct. 2017. [Online]. Available: https://link.springer.com/article/10.1007/s11517-017-1621-2

[163] G. A. Cavagna, H. Thys, and A. Zamboni, “The sources of external work in level walking and running,” *The Journal of Physiology*, vol. 262, no. 3, pp. 639–657, Nov. 1976.

[164] T. R. Han, N. J. Paik, and M. S. Im, “Quantification of the path of center of pressure (COP) using an F-scan in-shoe transducer,” *Gait &*

Posture, vol. 10, no. 3, pp. 248–254, Dec. 1999. [Online]. Available: http://www.sciencedirect.com/science/article/pii/S0966636299000405

[165] M. Schmid, G. Beltrami, D. Zambarbieri, and G. Verni, "Centre of pressure displacements in trans-femoral amputees during gait," *Gait & Posture*, vol. 21, no. 3, pp. 255–262, Apr. 2005.

[166] C. R. Lee and C. T. Farley, "Determinants of the center of mass trajectory in human walking and running," *The Journal of Experimental Biology*, vol. 201, no. Pt 21, pp. 2935–2944, Nov. 1998.

[167] S. A. Gard and D. S. Childress, "What Determines the Vertical Displacement of the Body during Normal Walking?" *Journal of Prosthetics and Orthotics*, vol. 13, no. 3, pp. 64–67, 2001. [Online]. Available: https://www.scholars.northwestern.edu/en/publications/what-determines-the-vertical-displacement-of-the-body-during-norm

[168] S. H. Collins, "Dynamic walking principles applied to human gait," Ph.D. dissertation, University of Michigan, 2008. [Online]. Available: https://deepblue.lib.umich.edu/bitstream/handle/2027.42/60646/shc_1.pdf?sequence=1

[169] H. Sato and K. Ishizu, "Gait patterns of Japanese pedestrians," *Journal of Human Ergology*, vol. 19, no. 1, pp. 13–22, Jun. 1990.

[170] A. D. Kuo, "A Simple Model of Bipedal Walking Predicts the Preferred Speed–Step Length Relationship," *Journal of Biomechanical Engineering*, vol. 123, no. 3, p. 264, Jun. 2001. [Online]. Available: http://Biomechanical.asmedigitalcollection.asme.org/article.aspx?articleid=1405720

[171] J. Sun, M. Walters, N. Svensson, and D. Lloyd, "The influence of surface slope on human gait characteristics: a study of urban pedestrians walking on an inclined surface," *Ergonomics*, vol. 39, no. 4, pp. 677–692, Mar. 1996. [Online]. Available: http://www.tandfonline.com/doi/abs/10.1080/00140139608964489

[172] P. Kasebzadeh, G. Hendeby, C. Fritsche, F. Gunnarsson, and F. Gustafsson, "IMU dataset for motion and device mode classification," in *2017 International Conference on Indoor Positioning and Indoor Navigation (IPIN)*, Sep. 2017, pp. 1–8.

[173] B. Bruno, F. Mastrogiovanni, and A. Sgorbissa, "Wearable Inertial Sensors: Applications, Challenges, and Public Test Benches," *IEEE Robotics & Automation Magazine*, vol. 22, no. 3, pp. 116–124, Sep. 2015. [Online]. Available: http://ieeexplore.ieee.org/lpdocs/epic03/wrapper.htm?arnumber=7214233

[174] G. H. Flores and R. Manduchi, "WeAllWalk: An Annotated Data Set of Inertial Sensor Time Series from Blind Walkers," in *Proceedings of the 18th International ACM SIGACCESS Conference on Computers and Accessibility*, ser. ASSETS '16. New York, NY, USA: ACM, Oct. 2016, pp. 141–150. [Online]. Available: http://doi.acm.org/10.1145/2982142.2982179

[175] M. Angermann, A. Friese, M. Khider, B. Krach, K. Krack, P. Robertson, and others, "A reference measurement data set for multisensor pedestrian navigation with accurate ground truth," in *Proc. European Navigation Conference (ENC-GNSS 2009), Naples, Italy*, 2009. [Online]. Available: http://www.dlr.de/kn/en/Portaldata/27/Resources/dokumente/04_abteilungen_fs/kooperative_systeme/AngermannEtAl_ENC-GNSS_2009.pdf

[176] M. Angermann, P. Robertson, T. Kemptner, and M. Khider, "A high precision reference data set for pedestrian navigation using foot-mounted inertial sensors," in *Indoor Positioning and Indoor Navigation (IPIN), 2010 International Conference on*. IEEE, Sep. 2010, pp. 1–6. [Online]. Available: http://ieeexplore.ieee.org/xpls/abs_all.jsp?arnumber=5646839

[177] D. Hanley, A. B. Faustino, S. D. Zelman, D. A. Degenhardt, and T. Bretl, "MagPIE: A dataset for indoor positioning with magnetic anomalies," in *2017 International Conference on Indoor Positioning and Indoor Navigation (IPIN)*, Sep. 2017, pp. 1–8.

[178] D. Bousdar, L. E. Díez, and E. Munoz Diaz, "Performance comparison of wearable-based pedestrian navigation systems in large areas," in *2017 International Conference on Indoor Positioning and Indoor Navigation (IPIN)*, Sapporo, Japan, Sep. 2017, pp. 1–7.

[179] "Kaggle: Your Home for Data Science," accessed: June 11, 2018. [Online]. Available: https://www.kaggle.com/

[180] "OU-ISIR Biometric Database," accessed: June 11, 2018. [Online]. Available: http://www.am.sanken.osaka-u.ac.jp/BiometricDB/index.html

[181] "UCI Machine Learning Repository," accessed: June 11, 2018. [Online]. Available: https://archive.ics.uci.edu/ml/index.php

[182] Computer Vision and Multimodal Computing, "Max-Planck-Institut für Informatik: Software and Datasets," accessed: June 11, 2018. [Online]. Available: https://www.mpi-inf.mpg.de/departments/computer-vision-and-multimodal-computing/software-and-datasets/

[183] Friedrich-Alexander-University Erlangen-Nuremberg, Machine Learning and Data Analytics Lab, "ActivityNet Project," accessed: June 11, 2018. [Online]. Available: https://www.mad.tf.fau.de/research/activitynet/

[184] O. Beauchet, G. Allali, H. Sekhon, J. Verghese, S. Guilain, J.-P. Steinmetz, R. W. Kressig, J. M. Barden, T. Szturm, C. P. Launay, S. Grenier, L. Bherer, T. Liu-Ambrose, V. L. Chester, M. L. Callisaya, V. Srikanth, G. Léonard, A.-M. De Cock, R. Sawa, G. Duque, R. Camicioli, and J. L. Helbostad, "Guidelines for Assessment of Gait and Reference Values for Spatiotemporal Gait Parameters in Older Adults: The Biomathics and Canadian Gait Consortiums Initiative," *Frontiers in Human Neuroscience*, vol. 11, no. 353, Aug. 2017. [Online]. Available: https://www.frontiersin.org/articles/10.3389/fnhum.2017.00353/full

[185] "ISO/IEC 18305:2016 - Information technology – Real time locating systems – Test and evaluation of localization and tracking systems," 2016, accessed: June 11, 2018. [Online]. Available: https://www.iso.org/standard/62090.html

[186] "Evaluating AAL Systems," accessed: June 11, 2018. [Online]. Available: http://evaal.aaloa.org/

[187] "IPIN 2018 Indoor Localization Competition." accessed: June 11, 2018. [Online]. Available: http://ipin2018.ifsttar.fr/competition/about/

[188] J. Torres-Sospedra, A. R. Jiménez, A. Moreira, T. Lungenstrass, W.-C. Lu, S. Knauth, G. M. Mendoza-Silva, F. Seco, A. Pérez-Navarro, M. J. Nicolau, A. Costa, F. Meneses, J. Farina, J. P. Morales, W.-C. Lu, H.-T. Cheng, S.-S. Yang, S.-H. Fang, Y.-R. Chien, and Y. Tsao, "Off-Line Evaluation of Mobile-Centric Indoor Positioning Systems: The Experiences from the 2017 IPIN Competition," *Sensors*, vol. 18, no. 2, p. 487, Feb. 2018. [Online]. Available: http://www.mdpi.com/1424-8220/18/2/487

[189] "PerfLoc: Performance Evaluation of Smartphone Indoor Localization Apps," accessed: June 11, 2018. [Online]. Available: https://perfloc.nist.gov/

[190] "Geo IoT World Indoor Location Testbed." accessed: June 11, 2018. [Online]. Available: https://www.geoiotworld.com/emea/testbed

[191] A. Muro-de-la Herran, B. Garcia-Zapirain, and A. Mendez-Zorrilla, "Gait Analysis Methods: An Overview of Wearable and Non-Wearable Systems, Highlighting Clinical Applications," *Sensors*, vol. 14, no. 2, pp. 3362–3394, Feb. 2014. [Online]. Available: http://www.mdpi.com/1424-8220/14/2/3362

[192] A. R. Jiménez and F. Seco, "Comparing Decawave and Bespoon UWB location systems: Indoor/outdoor performance analysis," in *2016 International Conference on Indoor Positioning and Indoor Navigation (IPIN)*, Oct. 2016, pp. 1–8.

[193] L. Yao, Y. W. A. Wu, L. Yao, and Z. Z. Liao, "An integrated IMU and UWB sensor based indoor positioning system," in *2017 International Conference on Indoor Positioning and Indoor Navigation (IPIN)*, Sapporo, Japan, Sep. 2017, pp. 1–8.

[194] A. R. Jiménez and F. Seco, "Finding objects using UWB or BLE localization technology: A museum-like use case," in *2017 International Conference on Indoor Positioning and Indoor Navigation (IPIN)*, Sapporo, Japan, Sep. 2017, pp. 1–8.

[195] D. Knobloch, "Practical challenges of particle filter based UWB localization in vehicular environments," in *2017 International Conference on Indoor Positioning and Indoor Navigation (IPIN)*, Sapporo, Japan, Sep. 2017, pp. 1–5.

[196] A. Jiménez and F. Seco, "Comparing Ubisense, BeSpoon, and DecaWave UWB Location Systems: Indoor Performance Analysis," *IEEE Transactions on Instrumentation and Measurement*, vol. 66, no. 8, pp. 2106–2117, Aug. 2017.

[197] B. Perrat, M. J. Smith, B. S. Mason, J. M. Rhodes, and V. L. Goosey-Tolfrey, "Quality assessment of an Ultra-Wide Band positioning system for indoor wheelchair court sports," *Proceedings of the Institution of Mechanical Engineers, Part P: Journal of Sports Engineering and Technology*, vol. 229, no. 2, pp. 81–91, Jun. 2015. [Online]. Available: http://pip.sagepub.com/content/229/2/81

[198] R. Maalek and F. Sadeghpour, "Accuracy assessment of ultra-wide band technology in locating dynamic resources in indoor scenarios," *Automation in Construction*, vol. 63, pp. 12–26, Mar. 2016.

[199] M. Ridolfi, S. Vandermeeren, J. Defraye, H. Steendam, J. Gerlo, D. De Clercq, J. Hoebeke, and E. De Poorter, "Experimental Evaluation of UWB Indoor Positioning for Sport Postures," *Sensors*, vol. 18, no. 1, p. 168, Jan. 2018. [Online]. Available: http://www.mdpi.com/1424-8220/18/1/168

[200] H. A. Shaban, M. A. El-Nasr, and R. M. Buehrer, "Toward a Highly Accurate Ambulatory System for Clinical Gait Analysis via UWB Radios," *IEEE Transactions on Information Technology in Biomedicine*, vol. 14, no. 2, pp. 284–291, Mar. 2010.

[201] R. B. Huitema, A. L. Hof, and K. Postema, "Ultrasonic motion analysis system—measurement of temporal and spatial gait parameters," *Journal of Biomechanics*, vol. 35, no. 6, pp. 837–842, Jun. 2002. [Online]. Available: https://pure.rug.nl/ws/files/6666881/Huitema_2002_Journal_of_Biomechanics.pdf

[202] Y. Qi, C. B. Soh, E. Gunawan, K.-S. Low, and R. Thomas, "Estimation of Spatial-Temporal Gait Parameters Using a Low-Cost Ultrasonic Motion Analysis System," *Sensors*, vol. 14, no. 8, pp. 15 434–15 457, Aug. 2014. [Online]. Available: http://www.mdpi.com/1424-8220/14/8/15434

[203] T. Brand and R. Phillips, "Foot-to-Foot Range Measurement as an Aid to Personal Navigation," in *Proceedings of the 59th Annual Meeting of The Institute of Navigation and CIGTF 22nd Guidance Test Symposium (2003)*, Albuquerque, NM, Jun. 2003, pp. 113–121.

[204] T. N. Hung and Y. S. Suh, "Inertial Sensor-Based Two Feet Motion Tracking for Gait Analysis," *Sensors*, vol. 13, no. 5, pp. 5614–5629, Apr. 2013. [Online]. Available: http://www.mdpi.com/1424-8220/13/5/5614

[205] D. Weenk, D. Roetenberg, B. J. J. F. v. Beijnum, H. J. Hermens, and P. H. Veltink, "Ambulatory Estimation of Relative Foot Positions by Fusing Ultrasound and Inertial Sensor Data," *IEEE Transactions on Neural Systems and Rehabilitation Engineering*, vol. 23, no. 5, pp. 817–826, Sep. 2015.

[206] "Barometric formula," Apr. 2018, page Version ID: 838719040. [Online]. Available: https://en.wikipedia.org/w/index.php?title=Barometric_formula&oldid=838719040

[207] Xsens, "MTw Awinda User Manual," May 2016, document MW0502P, Revision J.

[208] "IPIN 2016 : Indoor Positioning and Indoor Navigation conference." [Online]. Available: http://www3.uah.es/ipin2016/index.php

[209] "Calculate distance and bearing between two Latitude/Longitude points using haversine formula in JavaScript." [Online]. Available: http://www.movable-type.co.uk/scripts/latlong.html

[210] "WGS 84 / Pseudo-Mercator - Spherical Mercator, Google Maps, OpenStreetMap, Bing, ArcGIS, ESRI - EPSG:3857." [Online]. Available: https://epsg.io/3857

[211] "EPSG 4326 vs EPSG 3857 (projections, datums, coordinate systems, and more!) – Victory Formation." [Online]. Available: http://lyzidiamond.com/posts/4326-vs-3857

[212] "coordinate system - How can EPSG:3857 be in meters?" [Online]. Available: https://gis.stackexchange.com/questions/242545/how-can-epsg3857-be-in-meters

[213] D. Finker, J. Kocjan, J. Rutkowski, and R. Cai, "Evaluation of an autonomous navigation and positioning system for IAEA safeguards inspectors," in *2014 Ubiquitous Positioning Indoor Navigation and Location Based Service (UPINLBS)*, Nov. 2014, pp. 111–119.

[214] D. Bousdar, E. Munoz Diaz, and S. Kaiser, "Performance comparison of foot- and pocket-mounted inertial navigation systems," in *2016 International Conference on Indoor Positioning and Indoor Navigation (IPIN)*, Oct. 2016, pp. 1–7.

[215] "Data set of walks in a large area," May 2017, user name for access: PDR Walks LargeAreas guest, password: xU4nVwuz, port numbers: 20-21. [Online]. Available: ftp.dlr.de

[216] F. Zampella, M. Khider, P. Robertson, and A. Jiménez, "Unscented Kalman filter and Magnetic Angular Rate Update (MARU) for an improved Pedestrian Dead-Reckoning," in *Proceedings of the 2012 IEEE/ION Position, Location and Navigation Symposium*, Apr. 2012, pp. 129–139.

[217] J. Ruppelt, N. Kronenwett, G. Scholz, and G. F. Trommer, "High-precision and robust indoor localization based on foot-mounted inertial sensors," in *2016 IEEE/ION Position, Location and Navigation Symposium (PLANS)*, Apr. 2016, pp. 67–75.